


https://researchcommons.waikato.ac.nz/

Research Commons at the University of Waikato

Copyright Statement:

The digital copy of this thesis is protected by the Copyright Act 1994 (New Zealand).

The thesis may be consulted by you, provided you comply with the provisions of the Act and the following conditions of use:

- Any use you make of these documents or images must be for research or private study purposes only, and you may not make them available to any other person.
- Authors control the copyright of their thesis. You will recognise the author's right to be identified as the author of the thesis, and due acknowledgement will be made to the author where appropriate.
- You will obtain the author's permission before publishing any material from the thesis.

# Within-vine variability in kiwifruit qualities and carbohydrate reserves

A thesis submitted in partial fulfilment of

the requirements for the degree of

Doctor of Philosophy

in

Plant Physiology

at

The University of Waikato

by

Kris R. Kramer-Walter




THE UNIVERSITY OF
WAIKATO
*Te Whare Wānanga o Waikato*

2026

# Abstract

Minimising variability in fruit quality is a key objective for the New Zealand kiwifruit industry, as variability in fruit fresh weight (FW) and dry matter content (DM) can lead to grading losses, storage disorders, and inconsistent eating quality for consumers. Although variability occurs across seasons, regions, orchards, and vines, a substantial proportion arises within individual vines. Understanding the drivers of within-vine variability is therefore critical for improving fruit quality outcomes.

In this thesis, the major drivers of within-vine variability in fruit FW and DM were identified and quantified using whole-vine fruit population datasets. Entire fruit populations (approximately 10,000 fruit in total) were harvested from nine 'Zesy002' vines grown under three canopy management systems with contrasting shoot management and winter pruning practices (conventional, strung, and spur). Fruit- and shoot-level predictors were recorded throughout the season and analysed using linear mixed-effects models to assess their relative influence on fruit FW and DM.

Across all canopy management systems, the strongest predictors of fruit FW were position within the shoot, timing of individual flower anthesis, and shoot basal diameter. Larger fruit developed from mid-shoot positions, earlier-opening flowers, and on thicker shoots, factors that likely reflect higher sink strength and greater access to non-structural carbohydrates (NSC) during early cell division and expansion. Predictors of DM differed more between management systems, with shoot length and position within shoot being the most influential overall. Distal fruit on each shoot generally had lower DM, as did fruit borne on short shoots (i.e. shoots that self-terminated early or were pruned to a short length). In conventional and strung canopies, distance from the cordon also strongly influenced DM, likely reflecting spatial gradients in shoot length, leaf area and photoassimilate translocation; this pattern was not observed in spur-managed vines where shoot length was more uniformly constrained across the canopy via management.

Given the strong association between fruit development and NSC reserve availability, subsequent experiments examined reserve storage and mobilisation in kiwifruit canes. During winter dormancy, high-vigour canes had lower total non-structural carbohydrate (TNC) concentrations but higher TNC per unit length than low-vigour canes, indicating greater overall reserve storage capacity. Despite these differences, spring mobilisation patterns were similar across cane types, with all canes approaching starch depletion by anthesis. There were slight

differences in TNC storage and mobilisation between cultivars, however the general pattern was consistent. These results suggest that larger cane internodes may be able to supply more NSC to growing shoots and flowers, and may therefore be useful to maximise fruit growth potential.

Finally, experiments were conducted to test whether NSC availability could be increased via injections of exogenous sucrose in late autumn or winter. Sucrose injected into the xylem of dormant excised canes appeared to be rapidly cleaved and absorbed, and dose-dependent increases in starch and/or soluble sugars were observed in both bark and wood tissues. However, sucrose injections to both excised canes and intact vines did not consistently affect budbreak or flower production, and effects on subsequent shoot and fruit growth were not assessed.

Together, these findings demonstrate that within-vine variability in kiwifruit FW and DM is strongly influenced by developmental timing, shoot architecture, and spatio-temporal differences in NSC availability. While NSC reserves are clearly important for early growth, further work is required to understand how different reserve pools, including those of individual buds, ultimately contribute to spring growth, flower production, and fruit development.

# Acknowledgements

I owe a great deal of thanks to my supervisors, Mike Clearwater, Annette Richardson, and Nick Gould for all the valuable advice and support they have given me during my study. I also have many more colleagues and collaborators who have supported me on this journey. I would like to thank Jill Stanley, Mark McSherry, and Alex Batt for establishing the mentoring program that got this ball rolling over seven years ago. Thank you to Bill Snelgar for giving me an opportunity to grow and develop as a young scientist. To Patrick Snelgar, Peter Blattmann, Michael Kramer, Rachelle Anderson, Brydie Terry, Nico Fromont, Emma Todd, James Hickman, and Zoe Battershill, thank you for all your assistance in the field and for chats to take my mind off kiwifruit. I thank Helen Boldingh, Trisha Pereira, Ingrid Lindeman, Revati Vispute, Weiwen Qiu, and Darienne Voyle for their invaluable service in preparing and analysing my many samples for carbohydrate analysis. I thank Catherine McKenzie for her analysis suggestions and statistical advice. I thank Juanita Dunn and Yvette Jones for taking care of business and for all their support and encouragement. I would like to thank Mary Black, Tim Lowe, Monica Campbell, Sara Fraser-McKenzie and all Zespri collaborators who have helped focus and fund the research projects that went into this thesis. I give a huge thank you to Karen and Graeme McKenzie for hosting the trial from Chapter 2 on their orchard and to Phil Young for his impeccable orchard management and adaptability to our experimental needs. I likewise thank Steve Owen, Paul Adelman, Craig Maxwell, Stephen Wigley, Jamie Walker, and Gavin Schmidt for their excellent management of the Te Puke research orchard. I thank Jane Wilson for expertly sourcing all the obscure articles I sought. I also need to give a huge thank you to Bev Thwaites, Jeni Pearson, Sachet Sharma and all the FAST staff for organising and assessing tens of thousands of fruit over the last few years, a task made no easier by COVID social distancing requirements! I am also deeply gratefully to my family, friends, and all the pets who have supported me through this rollercoaster journey. Finally, I cannot thank my partner Cat enough for all her love, support, and encouragement over the last six and a half years. I simply couldn't have done it without you.

My study was graciously supported by The New Zealand Strategic Science Investment Fund, which funded my part-time study, consumables and orchard fees. I also received the 2023 NZIAHS Postgraduate Award, which funded travel to the 7th International Plant Dormancy Symposium in Perth. Data for Chapter 3 of this thesis were collected as part of Zespri project GP1835, and data collected for Chapter 4 were funded by project GP23235.

# Table of Contents

Abstract ..... II
Acknowledgements ..... IV
Table of Contents ..... V
List of Figures ..... VII
List of Tables ..... X
List of Abbreviations ..... XII
Chapter 1: Introduction, literature review and thesis aims ..... 1
1.1 Industry context and the problem of fruit variability ..... 1
1.1.1 A brief history of kiwifruit cultivation in New Zealand ..... 1
1.1.2 Marketing, industry standards and fruit variability ..... 2
1.1.3 Previous studies on variability ..... 4
1.2 Kiwifruit developmental biology ..... 6
1.2.1 Axillary bud formation and structure ..... 6
1.2.2 Dormancy, winter chilling, and budbreak ..... 7
1.2.3 Shoot and leaf growth ..... 11
1.2.4 Flower development ..... 13
1.2.5 Anthesis and pollination ..... 14
1.2.6 Fruit growth and maturation ..... 15
1.3 Carbohydrate dynamics ..... 19
1.3.1 Seasonality of carbohydrate balance ..... 19
1.3.2 Influences on reserve accumulation ..... 22
1.3.3 Sink strength, competition and proximity to reserves ..... 23
1.3.4 Photoassimilate distribution ..... 24
1.4 Summary ..... 26
1.5 Thesis aim and objectives ..... 27
1.5.1 Research objectives ..... 27
1.5.2 Thesis structure ..... 28
Chapter 2: Within-vine drivers of fruit variability ..... 29
2.1 Introduction ..... 29
2.2 Methods ..... 30
2.2.1 Orchard details ..... 30
2.2.2 Experimental design ..... 30
2.2.3 Vine management ..... 30
2.2.4 Shoot-level predictors ..... 32
2.2.5 Fruit-level predictors ..... 32
2.2.6 Fruit harvests ..... 32
2.2.7 Statistical analyses ..... 38
2.3 Results ..... 41
2.3.1 Drivers of fruit fresh weight ..... 41
2.3.2 Drivers of fruit dry matter content ..... 49
2.3.3 Correlations between predictors ..... 58
2.4 Discussion ..... 62
2.4.1 Effects of position within shoot reflect meristem size and phyllotaxy ..... 62
2.4.2 Early carbohydrate availability influences shoot growth and FW variability ..... 64
2.4.3 Local photoassimilate availability drives variability in dry matter content ..... 66
2.5 Conclusions ..... 69
Chapter 3: Cane carbohydrate reserves and mobilisation ..... 70
3.1 Introduction ..... 70
3.2 Methods ..... 71

3.2.1 Plant material ... 71
3.2.2 Dormant sampling ... 72
3.2.3 Carbohydrate analysis ... 72
3.2.4 Anatomical measurements ... 73
3.2.5 Spring sampling ... 74
3.2.6 Statistical analysis ... 75
3.3 Results ... 76
3.3.1 Dormant cane TNC reserves ... 76
3.3.2 TNC reserves and morpho-anatomical trait correlations ... 79
3.3.3 Morpho-anatomical differences ... 80
3.3.4 Spring mobilisation ... 85
3.4 Discussion ... 90
3.4.1 Drivers of winter NSC reserve pools ... 90
3.4.2 Internode anatomy ... 91
3.4.3 Spring mobilisation patterns ... 93
3.5 Conclusions ... 95
Chapter 4: Exogenous sucrose uptake and effects on growth ... 96
4.1 Introduction ... 96
4.2 Methods: ... 98
4.2.1 Experiment 1: Sucrose uptake in excised canes ... 98
4.2.2 Experiment 2: Sucrose concentration effects on excised canes ... 101
4.2.3 Experiment 3: Defoliation × sucrose injection of intact vines ... 104
4.2.4 Statistical analyses ... 107
4.3 Results ... 107
4.3.1 Experiment 1: Sucrose uptake rate ... 107
4.3.2 Experiment 2: Sucrose concentration effects ... 107
4.3.3 Experiment 3: Whole vine injection × defoliation ... 111
4.4 Discussion ... 116
4.4.1 Exogenous sucrose injections can increase cane NSC pools ... 116
4.4.2 Trunk sucrose injections increased cane soluble sugar but not starch ... 118
4.4.3 Exogenous sucrose did not increase spring growth ... 119
4.5 Conclusions ... 121
Chapter 5: Conclusions and future directions ... 122
5.1 Thesis overview ... 122
5.2 Chapter summaries ... 122
5.2.1 Chapter 2: Within-vine drivers of fruit variability ... 122
5.2.2 Chapter 3: Cane carbohydrate reserves and mobilisation ... 123
5.2.3 Chapter 4: Testing carbohydrate availability using exogenous sucrose ... 123
5.3 Synthesis ... 124
5.3.1 Integration of Chapters 2 and 3 ... 124
5.3.2 Integration of Chapter 4 ... 126
5.4 Practical industry applications and future research priorities ... 130
5.4.1 Targeted fruit thinning ... 130
5.4.2 Cane selection ... 131
5.4.3 Bud isolation and carbohydrate mobility ... 131
5.4.4 Theoretical effects of increased carbohydrate availability ... 132
5.5 Concluding remarks ... 134
Chapter 6: References ... 135
Appendix A ... 164
Appendix B ... 179
Appendix C ... 185

# List of Figures

Figure 1.1. Kiwifruit phenological sequence over two seasons. ..... 8

Figure 1.2. Structure of mature first order axillary buds (FOABs) from *Actinidia chinensis* var. *deliciosa* 'Hayward' vines, adapted from Walton et al. (1997). ..... 9

Figure 1.3. Progression of *Actinidia chinensis* var. *chinensis* 'Zesy002' buds from dormancy to shoot extension. .....12

Figure 1.4. Three stages of *Actinidia chinensis* var *deliciosa* 'Monty' fruit growth, adapted from Hopping (1976). .....17

Figure 1.5. Fruit fresh weight and dry matter growth from anthesis for three kiwifruit cultivars. .....18

Figure 1.6. Seasonal dynamics of starch concentrations in different organs of *Actinidia chinensis* var *deliciosa* 'Hayward' kiwifruit vines, adapted from Smith et al. (1992). .....21

Figure 2.1. Examples of A) conventional and B) strung canopies in summer. ..... 34

Figure 2.2. Examples of canopy structure following winter pruning for conventional, strung and spur canopy mangement treatment vines. ..... 35

Figure 2.3. Examples of shoot types prior to winter pruning on spur treatment vines..... 36

Figure 2.4. Shoot-level measurements..... 37

Figure 2.5. Fruit-level measurements. ..... 37

Figure 2.6. Trays of uniquely labelled *Actinidia chinensis* var. *chinensis* 'Zesy002' fruit..... 38

Figure 2.7. Distribution of anthesis timing and model-estimated effects on fruit relative fresh weight in *Actinidia chinensis* var. *chinensis* 'Zesy002'..... 46

Figure 2.8. Distribution and model-estimated effects of shoot basal diameter on fruit relative fresh weight in *Actinidia chinensis* var. *chinensis* 'Zesy002'..... 47

Figure 2.9. Distribution and model-estimated effect of fruit position within the canopy along the east–west axis on fruit relative fresh weight in *Actinidia chinensis* var. *chinensis* 'Zesy002'..... 48

Figure 2.10. Distribution and model-estimated effect of fruit position within the canopy along the east–west axis on fruit relative dry matter content in *Actinidia chinensis* var. *chinensis* 'Zesy002'..... 54

Figure 2.11. Distribution and model-estimated effect of fruit position within the canopy along the north–south axis on fruit relative dry matter content in *Actinidia chinensis* var. *chinensis* 'Zesy002'..... 55

Figure 2.12. Distribution and model-estimated effect of shoot length on fruit relative dry matter content in *Actinidia chinensis* var. *chinensis* 'Zesy002'. ..... 56

Figure 2.13. Distribution of relative height in the canopy and model-estimated effects on fruit relative dry matter content in *Actinidia chinensis* var. *chinensis* 'Zesy002'. ..... 57

Figure 2.14. Correlation matrix of shoot- and fruit-level predictor variables. ..... 59

Figure 2.15. Relationships between total leaf number, leaf area, shoot length, and shoot basal diameter for intact *Actinidia chinensis* var. *chinensis* 'Zesy002' shoots measured in late summer. .....61

Figure 3.1. Examples of cane vigour types from *Actinidia deliciosa* 'Hayward' vines..... 72

Figure 3.2. Kiwifruit cane tissue layers. ..... 74

Figure 3.3. Total non-structural carbohydrate (TNC) concentrations in dormant kiwifruit cane internodes. ..... 77

Figure 3.4. Total non-structural carbohydrate (TNC) per unit length in dormant kiwifruit cane internodes. ..... 78

Figure 3.5. Correlation matrix for cane internode total non-structural carbohydrate (TNC) concentration and TNC per unit length vs morpho-anatomical traits. ..... 80

Figure 3.6. Internode diameters of kiwifruit canes. ..... 82

Figure 3.7. Peri-medullary zone (PMZ) to wood area ratios of kiwifruit canes. ..... 83

Figure 3.8. Kiwifruit cane internodes showing higher starch concentrations. ..... 84

Figure 3.9. Kiwifruit cane internodes showing lower starch concentrations. ..... 85

Figure 3.10. Soluble sugar concentrations of kiwifruit cane internodes across spring. ..... 87

Figure 3.11. Starch concentrations of kiwifruit cane internodes across spring. ..... 88

Figure 3.12. Total non-structural carbohydrates (TNC) per unit length of kiwifruit cane internodes across spring. ..... 89

Figure 4.1. Methods used for exogenous sucrose uptake experiment 1. ..... 100

Figure 4.2. Methods used for exogenous sucrose injections on excised canes. ..... 103

Figure 4.3. Methods used for defoliation and sucrose injections in experiment 3 on *Actinidia chinensis var. chinensis* 'Zesy002' vines..... 106

Figure 4.4. Change in xylem sap sugar concentrations over time for *Actinidia chinensis* var. *deliciosa* 'Hayward' canes injected with water or a 5% w/v (50 mg $ml^{-1}$) sucrose solution. ..... 108

Figure 4.5. Changes in cane bark (A–C) and wood (D–F) carbohydrate concentration following injections of sucrose. ..... 109

Figure 4.6. Effects of sucrose injection treatments on A) budbreak percent; B) floral shoot percent; and C) inflorescences per axillary bud. ..... 110

Figure 4.7. A) pH; B) soluble solids concentration of exudate dripping from cane ends at the start and finish of the injection period. ..... 112

Figure 4.8. Examples of leaf phytotoxicity and damage following trunk injections of 10% (w/v) sucrose in experiment 3. ..... 112

Figure 4.9. Effects of defoliation and trunk injection on soluble sugar concentrations in the bark (A–C) and wood (D–F) of *Actinidia chinensis* var. *chinensis* 'Zesy002' shoots. ..... 113

Figure 4.10. Effects of defoliation and trunk injection on starch concentrations in the bark (A–C) and wood (D–F) of *Actinidia chinensis* var. *chinensis* 'Zesy002' shoots. ..... 114

Figure 4.11. Effects of defoliation and trunk injection on total non-structural carbohydrate (TNC) concentrations in the bark (A–C) and wood (D–F) of *Actinidia chinensis* var. *chinensis* 'Zesy002' shoots. ..... 115

Figure 4.12. Effects of trunk injection and defoliation on budbreak percentage, floral shoot percentage and inflorescences per bud of *Actinidia chinensis* 'Zesy002' canes. ..... 116

Figure 5.1. Conceptual model of seasonal carbohydrate availability and effects on fruit fresh weight and dry matter content. ....129

Figure 5.2. Hypothetical effects of increasing resource availability on within-vine fruit populations....133

Figure A1: Orchard plan for *Actinidia chinensis* 'Zesy002' vines used in Chapter 2. ....164

Figure A2. Distribution of fruit per shoot and model-estimated effects on fruit fresh weight in *Actinidia chinensis* 'Zesy002'....166

Figure A3. Distribution and model-estimated effect of internode diameter on fruit fresh weight in *Actinidia chinensis* 'Zesy002'. ....167

Figure A4. Distribution and model-estimated effect of shoot length on fruit fresh weight in *Actinidia chinensis* 'Zesy002'.... 168

Figure A5. Distribution of relative height in the canopy and model-estimated effects on fruit relative fresh weight in *Actinidia chinensis* 'Zesy002'....169

Figure A6. Distribution and model-estimated effect of fruit position along the north–south axis on fruit relative fresh weight in *Actinidia chinensis* 'Zesy002'....170

Figure A7. Distribution of anthesis timing and model-estimated effects on fruit relative dry matter content in *Actinidia chinensis* 'Zesy002'.... 171

Figure A8. Distribution of fruit per shoot and model-estimated effects on fruit relative dry matter content in *Actinidia chinensis* 'Zesy002'....172

Figure A9. Distribution and model-estimated effect of shoot basal diameter on fruit relative dry matter content in *Actinidia chinensis* 'Zesy002'....173

Figure A10. Distribution and model-estimated effect of internode diameter on fruit relative dry matter content in *Actinidia chinensis* 'Zesy002'....174

Figure A11. Correlations and linear regressions between fruit relative fresh weight and predictor variables. ....175

Figure A12. Correlations and linear regressions between fruit relative dry matter content and predictor variables. ....176

Figure A13. Bar plot of timing of anthesis by fruit position within shoots, number of fruit per shoot and by canopy management treatment....177

Figure A14. Seed count and seed mass regressions. ....178

Figure B1. Correlation matrix for cane internode diameter and total tissue layer areas....182

Figure B2. Individual sugar concentrations by cultivar for dormant kiwifruit canes and over spring sampling time points ....183

Figure B3. Starch and total soluble sugar concentrations by cultivar for dormant canes and over spring sampling time points .... 184

# List of Tables

Table 1.1. Kiwifruit count sizes and fresh weight bands. ..... 4

Table 1.2. Taste Zespri Grades (TZG) and corresponding dry matter (DM) bands. ..... 4

Table 2.1. Shoot and fruit replicate numbers by treatment. ..... 39

Table 2.3. Type III ANOVA results by treatment from linear mixed-effects models predicting fruit relative fresh weight (vine-mean centred) at harvest in *Actinidia chinensis* var. *chinensis* 'Zesy002' vines. ..... 43

Table 2.4. Type III ANOVA results from a linear mixed-effects model predicting fruit relative fresh weight (vine-mean-centred) at harvest in *Actinidia chinensis* var. *chinensis* 'Zesy002' ..... 44

Table 2.5. Effects of fruit position within shoots on fruit relative fresh weight in *Actinidia chinensis* var. *chinensis* 'Zesy002', within each fruit per shoot category. ..... 45

Table 2.6. Type III ANOVA results by treatment from linear mixed-effects models predicting relative fruit dry matter content (vine-mean centred) at harvest in *Actinidia chinensis* var. *chinensis* 'Zesy002' vines. ..... 51

Table 2.7. Type III ANOVA results from a linear mixed-effects model predicting fruit relative dry matter content (vine-mean centred) at harvest in *Actinidia chinensis* var. *chinensis* 'Zesy002' ..... 52

Table 2.8 Effects of fruit position within shoots on fruit relative dry matter content in *Actinidia chinensis* var. *chinensis* 'Zesy002', within each fruit per shoot category. ..... 53

Table 3.1. Phenological stages and dates of carbohydrate sampling of kiwifruit cane internodes during winter dormancy and spring growth. ..... 74

Table A1. Harvest dates and summary statistics for nine whole-vine fruit populations of 'Zesy002' kiwifruit from three canopy management treatments ..... 165

Table B1. Fixed-effect tests from linear mixed-effects model (Wald F tests) summary table for modelled effects on total non-structural carbohydrate concentration of dormant kiwifruit cane internodes. ..... 179

Table B2. Fixed-effect tests from linear mixed-effects model (Wald F tests) summary table for modelled effects on total non-structural carbohydrate per unit length of dormant kiwifruit cane internodes. ..... 179

Table B3. Fixed-effect tests from linear mixed-effects model (Wald F tests) summary table for modelled effects on internode diameter of dormant kiwifruit cane internodes. ..... 179

Table B4. Fixed-effect tests from linear mixed-effects model (Wald F tests) summary table for modelled effects on peri-medullary zone to wood area ratio of dormant kiwifruit cane internodes. ..... 180

Table B5. Fixed-effect tests from linear mixed-effects model (Wald F tests) summary table for modelled effects on soluble sugar concentrations of kiwifruit cane internodes during spring growth. ..... 180

Table B6. Fixed-effect tests from linear mixed-effects model (Wald F tests) summary table for modelled effects on starch concentrations of kiwifruit cane internodes during spring growth. ..... 180

Table B7. Fixed-effect tests from linear mixed-effects model (Wald F tests) summary table for modelled effects on total non-structural carbohydrate per unit length of kiwifruit cane internodes during spring growth. ..... 181

Table C1. Summary of heteroscedasticity-robust Wald tests for timing effects for each treatment and analyte in experiment 1. ..... 185

Table C2. Type II ANOVA table for each tissue and analyte in experiment 2. ..... 185

Table C3. Type II ANOVA summary table for budbreak percentage, floral shoot percentage and inflorescences per bud in experiment 2. ..... 186

Table C4. Mean ± standard error values (mg $g^{-1}$ DW) for individual carbohydrates in bark samples from experiment 2. ..... 187

Table C5. Mean ± standard error values (mg $g^{-1}$ DW) for individual carbohydrates in wood samples from experiment 2. ..... 188

Table C6. Type III ANOVA summary table for soluble sugars in experiment 3. ..... 189

Table C7. Type III ANOVA summary table for starch concentrations in experiment 3. ..... 190

Table C8. Type III ANOVA summary table for total non-structural carbohydrate concentrations (sum of sucrose, glucose, fructose, planteose, raffinose, stachyose and starch) in experiment 3. ..... 191

Table C9. Type III ANOVA summary table for budbreak percentage, floral shoot percentage and inflorescences per bud in experiment 3. ..... 192

Table C10. Mean ± standard error values for individual carbohydrate concentrations (mg $g^{-1}$ DW) in bark samples from experiment 3. ..... 193

Table C11. Mean ± standard error values for individual carbohydrate concentrations (mg $g^{-1}$ DW) in wood samples from experiment 3. ..... 194

# List of Abbreviations

| | |
|---|---|
| ABA | Abscisic acid |
| DAA | Days after anthesis |
| DABB | Days after budbreak |
| DM | Fruit dry matter content (%) |
| DW | Dry weight (g) |
| FOAB | First-order axillary bud |
| FW | Fruit fresh weight (g) |
| L:F | Leaf-to-fruit ratio |
| NSC | Non-structural carbohydrate |
| PAR | Photosynthetically active radiation |
| PMZ | Peri-medullary zone |
| PPFD | Photosynthetic photon flux density |
| Psa | *Pseudomonas syringae* pv. *actinidiae* |
| RAP | Ray and axial parenchyma |
| RFO | Raffinose family oligosaccharides |
| SAM | Shoot apical meristem |
| SDSM | Simple, dome-shaped meristem |
| SSC | Soluble solids content (°Brix) |
| TNC | Total non-structural carbohydrate (mg $g^{-1}$ DW) |
| TZG | Taste Zespri grade |
| VAC | Vessel associated cells |

# Chapter 1: Introduction, literature review and thesis aims

## 1.1 Industry context and the problem of fruit variability

The production of high-quality kiwifruit for export requires a high degree of consistency within fruit inventories to maximise storage potential and deliver a premium product to consumers. Biological variability in fruit development and quality challenges this consistency and potential sources of variability have been widely documented. This section provides the industry context for New Zealand kiwifruit production and reviews prior studies describing patterns of fruit variability.

### 1.1.1 A brief history of kiwifruit cultivation in New Zealand

A perennial deciduous vine native to the hills and mountains of southern and central China (Ferguson, 1984), kiwifruit (then known as Chinese gooseberry) was introduced to New Zealand in 1904 (Ferguson, 2004). Early New Zealand plantings were centred in Whanganui, where small-scale commercial orchards were established in the first decades of the 20$^{th}$ century (Ferguson et al., 2023b). From these humble beginnings, kiwifruit production has grown to become New Zealand's single largest horticultural industry, making up 45% of horticultural export value in the 2024–2025 season (Stats NZ, 2025), with total exports valued at nearly NZD 4.5 billion (Ministry for Primary Industries, 2025). As of 2024, the majority of kiwifruit production area was in the Bay of Plenty (approximately 80%), with orchards also located in Northland, Auckland, Waikato, Te Tairāwhiti and Nelson (New Zealand Kiwifruit Growers Incorporated, 2024).

Several cultivars have played important roles in the evolution of the New Zealand kiwifruit industry over time. By 1975, a single cultivar (*Actinidia chinensis* var. *deliciosa* [A Chev] CF Liang et AR Ferguson 'Hayward') had grown to dominate New Zealand production for export (Ferguson et al., 2023b), owing in part to its ability to maintain desirable flavour and texture over long-term cold-storage (Cotter et al., 1991). A domestic kiwifruit breeding program was established in 1977, and produced a new cultivar for commercial release in 1997 (*A. chinensis* var. *chinensis* Planch 'Hort16A', marketed as Zespri™ Gold™) (Ferguson, 1999). 'Hort16A' differed from 'Hayward' in terms of its distinct stylar 'beak', yellow flesh and sweeter flavour profile (Jaeger et al., 2003; Patterson et al., 2003), but proved highly susceptible to *Pseudomonas syringae* pv. *actinidiae* (Psa), leading to large-scale canopy removal in 2012 (Ministry for Primary Industries, 2012; Vanneste, 2012). At this time, another yellow-fleshed cultivar (*A. chinensis* var. *chinensis* Planch 'Zesy002', marketed as Zespri™ SunGold™) had

recently been commercially released from the domestic breeding program and proved to be more resilient to Psa (Horner & Manning, 2012). In 2019, a new red-fleshed variety was commercially released (*A. chinensis* var. *chinensis* Planch 'Zes008', marketed as Zespri™ RubyRed™), characterised by its naturally smaller size profile, red inner and outer pericarp, and berry-like flavour notes (New Zealand Kiwifruit Growers Incorporated, 2024).

As the New Zealand kiwifruit industry recovered from and adapted to Psa, 'Zesy002' proved to be a truly golden cultivar, finding favour with growers due to its Psa tolerance, productivity and profitability (Zespri Group Limited, 2025), and with consumers for its sweet taste, balanced acidity, and high nutrient density (New Zealand Kiwifruit Growers Incorporated, 2024). Seasonal volumes of 'Zesy002' fruit production have grown almost every year since 2013, surpassing volumes of 'Hayward' for the first time in 2019 (New Zealand Kiwifruit Growers Incorporated, 2025). Of the approximately 193 million trays of New Zealand grown kiwifruit in 2025, approximately 65% of the total volume was comprised of 'Zesy002' fruit (Zespri Group Limited, 2025). While this success reflects strong cultivar performance and demand from markets, it also places increasing pressure on understanding and managing sources of biological variation in fruit quality across commercial production systems.

### 1.1.2 Marketing, industry standards and fruit variability

Kiwifruit exported under the Zespri™ brand must maintain high standards of quality to ensure fruit reach consumers in optimal condition and deliver consistent and enjoyable eating experiences, despite New Zealand's geographical distance from major world markets. This focus on consistently high quality has proved successful, with recent reporting by Kantar Brand Power ranking Zespri™ as the number one fruit brand across its core 15 markets (New Zealand Kiwifruit Growers Incorporated, 2024). This brand recognition allows Zespri™ to drive demand through repeat purchasing (Mowat & Collins, 2000), maintain premium pricing in markets, and maximise returns to growers (New Zealand Kiwifruit Growers Incorporated, 2024).

In order to maintain this high level of quality, fruit are routinely tested prior to harvest. Random samples of fruit are collected from each orchard maturity area (a designated orchard area anticipated to have similar maturity and therefore harvest timing) and quantified for fresh weight (FW) and dry matter content (DM), typically calculated as the dry weight (DW) of an equatorial slice divided by the fresh weight. These fruit quality metrics are necessary for efficient packing, directing fruit to appropriate markets and maintaining taste standards, and also strongly influence monetary returns to growers. Fruit are graded into count sizes based on FW

bands (Table 1.1), which represent the number of fruit required to sum to approximately 3.5 kg per tray. Fruit DM is a strong predictor of ripe soluble solids content (SSC) (Jordan et al., 2000), and as DM and ripe SSC increase, so too do sweetness, flavour intensity and consumer liking scores (Burdon et al., 2004; Mitchell et al., 1992). While ripe SSC alone is a strong driver of consumer eating experience, the sugar to acid ratio also contributes to taste perception (Marsh et al., 2004; Rossiter et al., 2000), and overall sweetness can interact with perceptions of volatile flavour compounds (Marsh et al., 2006). For these reasons, and given its relative ease of measurement, DM has become an industry standard proxy for ripe SSC and ripe taste, with Taste Zespri Grade (TZG) thresholds used to incentivise the production of high DM fruit (Table 1.2), which can then be directed to premium markets. In 'Zesy002', heavier fruit tend to also have higher DM at harvest (Richardson et al., 2019), and to account for this relationship TZG scores are calculated separately for each count size band.

Depending on cultivar, additional maturity metrics such as flesh hue angle, firmness, and seed colour are also quantified for sampled fruit, alongside SSC. These attributes change during physiological maturity and are used to infer likely post-harvest performance. Fruit with higher DM at harvest typically also have higher SSC and retain greater firmness after extended cold storage (Famiani et al., 2012; Velemis et al., 1997). Similarly, higher DM/SSC and lower flesh hue angle at harvest are associated with reduced susceptibility to post-harvest disorders, including chilling injury, skin pitting and rots (Clark et al., 2004; Spadaro et al., 2010). Higher SSC at harvest can also reduce rates of physiological storage disorders (Burdon et al., 2007). As a result of these relationships, a minimum SSC of 6.2 °Bx at harvest has been used as a standard indicator of physiological maturity for several decades (Harman, 1981). However, more recent research has indicated that the rate of change, rather than absolute value of SSC, is a better indicator of the true physiological state of fruit and their subsequent storage behaviour (Burdon et al., 2013; Burdon et al., 2016).

Variability in kiwifruit FW and DM can lead to inefficiencies and wastage at multiple points in the supply chain from orchard to consumer. Growers will often thin (deliberately remove flowers/fruit) to set a desired crop load (fruit per m²) and will typically target flowers with aberrant shape or visibly smaller fruit before further resources are wasted on their development. Another round of thinning is often done shortly before harvest to remove clearly undersized fruit, as well as fruit with excessive blemishes or other defects. Consumer preference is for 'mid-sized' kiwifruit (Jaeger et al., 2011), therefore fruit in the smallest and largest weight ranges are often considered 'non-standard supply' and may be directed to lower value markets, depending

on cultivar and season. Fruit with very high DM may also have correspondingly high SSC at the time of picking (Velemis et al., 1997), potentially leading to early ripening and ethylene emission in storage (Park et al., 2006), with knock-on effects for neighbouring fruit. Similarly, fruit with low DM at harvest may also have lower than ideal SSC, increasing the risk of post-harvest disorders. Together, these examples illustrate how biological variation in fruit FW and DM translates into economic risk, highlighting the importance of understanding the sources of this variability within kiwifruit populations.

Table 1.1. Kiwifruit count sizes and fresh weight bands. Depending on cultivar and season, the highest and lowest count sizes are often considered non-standard supply and may not necessarily be accepted for export. In the 2025 harvest, 'Zesy002' fruit in count size 14, 39 and 42 were non-standard supply, as were 'Hayward' fruit in count sizes 14 and 46.

| **Count size (fruit per tray)** | 14 | 16 | 18 | 22 | 25 | 27 | 30 | 33 | 36 | 39 | 42 | 46 |
|---|---|---|---|---|---|---|---|---|---|---|---|---|
| **Upper weight limit (g)** | <270 | <240 | <210 | <180 | <151 | <138 | <128 | <118 | <106 | <91 | <82 | <74 |
| **Lower weight limit (g)** | ≥240 | ≥210 | ≥180 | ≥151 | ≥138 | ≥128 | ≥118 | ≥106 | ≥91 | ≥82 | ≥74 | ≥72 |

Table 1.2. Taste Zespri Grades (TZG) and corresponding dry matter (DM) bands. TZG bands allow fruit of differing DM to be segregated for storage and export, with TZG band Y fruit having the highest export value and TZG band M the lowest. For *Actinidia chinensis* var. *chinensis* 'Zesy002', TZG is calculated for each count size of fruit within a maturity area, while for *A. chinensis* var. *deliciosa* 'Hayward' the fruit population of the maturity area is graded collectively. MTS = minimum taste standard. Fruit with DM below the MTS will not be accepted for export.

| **TZG** | **DM (%)** | |
|---|---|---|
| | **'Hayward'** | **'Zesy002'** |
| Y | ≥16.6 | ≥17.9 |
| T | ≥16.3 <16.6 | ≥17.4 <17.9 |
| R | ≥16.1 <16.3 | ≥17.1 <17.4 |
| M | ≥15.5 <16.1 | ≥16.1 <17.1 |
| MTS | 15.5 | 16.1 |

### 1.1.3 Previous studies on variability

Variability in kiwifruit quality occurs across multiple scales. Between-orchard variability can be driven by a range of factors including soil properties, climate and vine management (Mowat & Kay, 2007; Pailly et al., 1995, 1997). Variability at this level is largely managed via maturity testing to determine appropriate harvest times, as well as post-harvest grading to segregate fruit into FW and DM bands for export. While significant variation exists between orchards, multiple studies have shown that the majority of variation in fruit quality arises within orchards, and

particularly, within individual vines (Woodward, 2006). Between-vine differences in crop load have repeatedly been shown to strongly influence fruit quality (Antognozzi et al., 1992; Burge et al., 1987; Cooper & Marshall, 1992; Famiani et al., 2012; Richardson & McAneney, 1990). Differences in canopy density between vines can also influence fruit quality (Praat et al., 2006; Snelgar et al., 1998), while microclimatic factors such as proximity to shelter belts do not appear to affect fruit quality directly, but can reduce total flower numbers and yield (Snelgar et al., 1992b). These factors highlight the sensitivity of fruit quality to vine-level management practices, and the potential for substantial variation to arise even within a single orchard block.

Studies on both 'Hayward' and 'Hort16A' support the notion that the majority of variability in fruit quality originates within, rather than between vines (Boyd et al., 2008b; Woodward, 2006). Several studies have examined the structure of this within-vine variability. On 'Hayward' vines grown on T-bar supports, Miles et al. (1996) showed that most within-vine variation in FW occurred within rather than between canopy zones. In agreement, both Smith et al. (1994) and De Silva and Ball (1997) attributed the highest proportion of variance of FW to differences between fruit within individual shoots, followed by shoots within canes, then canes within vines, with only a small proportion attributed to between-vine differences. Smith et al. (1994) also reported similar structuring of within-vine variance for DM, although reported in text as its reciprocal, weight ratio (FW/DW). Collectively, these studies demonstrate that fruit-to-fruit differences within individual shoots and canes represent the dominant source of variation in both FW and DM.

Several studies have identified spatial patterns in fruit FW and DM within kiwifruit vines, although the direction and magnitude of these effects are not always consistent across training systems and cultivars. In 'Hayward' vines trained on T-bar and pergola systems, higher FW has been associated with increasing distance from the trunk along the cordon (N/S direction), as well as with increasing distance along canes (E/W direction), although opposing trends have also been reported (De Silva & Ball, 1997; Smith et al., 1994). Patterns in DM have generally been weaker, with some studies reporting modest declines with increasing canopy distance from the trunk or cordon (Smith et al., 1994). Similar spatial trends have been observed in 'Hort16A', where fruit located further E/W from the cordon tended to have higher FW but lower DM, while fruit closer to the cordon were smaller but with higher DM (Boyd et al., 2008b).

Despite the clear spatial structuring of within-vine variability, relatively few studies have successfully linked these patterns to underlying physiological drivers. In 'Hayward', Smith et al.

(1994) note that the pattern of higher FW with increasing distance E/W in the canopy correlated well with the timing of anthesis, where larger fruit often developed from earlier opening flowers near the ends of canes. In contrast, the spatial pattern of FW observed by Boyd et al. (2008a) in 'Hort16A' was not well associated with timing of anthesis, as they observed that flowers closer to the leader zone were more likely to open earlier, but fruit from this zone were not necessarily larger at harvest. Instead, Boyd et al. (2008a) suggest that canopy density was a better predictor of fruit size, with higher FW in denser canopy zones. Together, these findings suggest that spatial patterns in fruit quality may arise from multiple, interacting drivers, including phenology, local source–sink balance, and canopy position, the relative importance of which remains unresolved.

Together, these studies demonstrate that variability in fruit quality is strongly expressed at both fine and broad spatial scales within kiwifruit vines, and that this variability is structured rather than random. While several biological drivers of these patterns have been proposed, including flowering phenology and canopy architecture, the physiological mechanisms linking vine structure, resource availability, and individual fruit development remain incompletely understood. Addressing these relationships requires an understanding of kiwifruit phenology, shoot and fruit development, and seasonal patterns of carbohydrate dynamics, which are reviewed in the following sections.

## 1.2 Kiwifruit developmental biology

The full developmental process of kiwifruit spans two growing seasons, beginning with the formation of axillary buds in the first season (Figure 1.1 A), and development of shoots (Figure 1.1 B), flowers (Figure 1.1 C), and fruit (Figure 1.1 D) in the second season. The following sections detail both the phenological stages of kiwifruit development and the influence of biotic and abiotic factors on growth at each stage. The majority of developmental research on kiwifruit has been conducted on 'Hayward'; other cultivars are assumed here to share broadly similar phenological and morphological traits, except for where data exists to the contrary.

### 1.2.1 Axillary bud formation and structure

In the first season of development, first-order axillary buds (FOABs) are formed in the leaf axils of growing shoots (Figure 1.2 A). As FOABs mature over the remainder the season they progressively develop bud scales, leaf primordia, and second-order axillary structures. These structures are arranged at approximately 137.5° intervals (Figure 1.2 B), producing either clockwise or anti-clockwise spirals and establishing a 2/5 phyllotaxy (Ferguson, 1984). From

formation, FOABs take approximately 125 days to develop a full cohort of leaf primordia and second-order axillary structures (Walton et al., 1997). FOABs nearer to the base of shoots form earlier in the season and reach maturity early, while buds further from the base are correspondingly delayed in their development (Snowball, 1995). By the time of winter dormancy, FOABs can contain up to 22 pre-formed nodes consisting of bud scales and basal buds (nodes 1–4), or leaf primordia and simple, dome-shaped meristems (SDSMs, nodes ≥5) (Brundell, 1975b; Walton et al., 1997). Basal buds (second-order axillary buds) can also contain third-order axillary meristems (Figure 1.2 C) (Walton et al., 1997).

During late spring and summer of the first season, a subset of SDSMs can undergo floral evocation, correlated with distinct changes in gene expression within buds (Walton et al., 2001), although no morphological differentiation is apparent until the following spring (Brundell, 1975c; Polito & Grant, 1984). Manipulating carbohydrate availability via girdling, shading or defoliation can influence the number of nodes able to form flowers in the following season, and differential effects of such manipulations throughout the season were thought to relate to the timing of floral evocation (Snelgar & Manson, 1992; Snowball, 1996). However, later experiments has shown that leaf-derived signals including FLOWERING LOCUS T (FT) proteins are more fundamental to floral evocation (Varkonyi-Gasic, 2018), but are in practice difficult to disentangle experimentally from carbohydrate availability and accumulation of reserves required for sustained floral growth in the following spring (Richardson, 2015).

In 'Hayward' FOABs there are nodal positions that are more likely to develop into floral structures in the following season (Figure 1.2 C), which may relate to the size of SDSMs and subtending leaf primordia (Brundell, 1975c). While all axillary structures are discernible by 125 days after bud formation, SDSMs in certain nodes appear to undergo further expansion until much later in the season (Walton et al., 1997). As a result of this growth, SDSMs in nodes 6–10 have the largest cross-sectional areas at winter dormancy (Figure 1.2 D) and are more likely to form floral structures, while node 5 and nodes ≥12 are substantially smaller and are less likely to form floral structures (Walton et al., 1997). SDSMs that are not evoked to form floral structures in season 2 will gradually develop their own cohort of leaf primordia and SDSMs throughout the growing season to form mature FOABs.

### 1.2.2 Dormancy, winter chilling, and budbreak

Using an established framework of dormancy terminology (Faust et al., 1997; Lang, 1987), kiwifruit FOABs have three distinct dormancy states: paradormancy, endodormancy, and

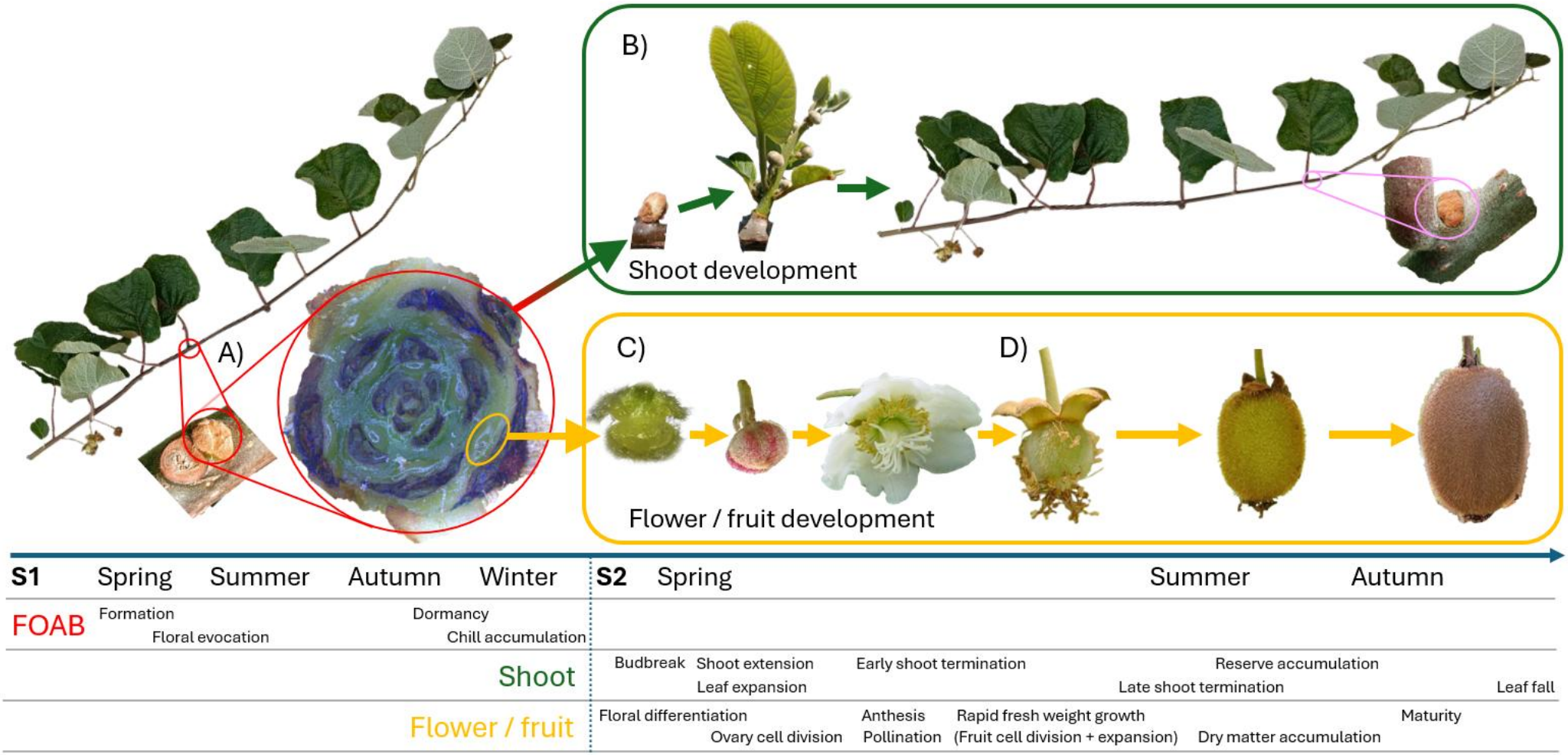


Figure 1.1. Kiwifruit phenological sequence over two seasons. A) In the first season (S1), first-order axillary buds (FOABs, circled in red) develop a number of leaf primordia (stained with Alcian blue in a dissected bud with trichomes and outer bud scales removed) and simple dome-shaped meristems (SDSMs, e.g. circled in yellow). Floral evocation of SDSMs occurs shortly after FOABs form in season 1. After winter dormancy, budbreak occurs in the spring of season 2 (S2). B) FOAB grow into shoots (green box) by elongation of internodes and expansion of leaves. Shoots may terminate in spring without forming any additional nodes from the apical meristem, or may continuing growing until terminating later in summer. In late summer and autumn, shoots accumulate non-structural carbohydrate reserves and lignify, becoming canes at leaf fall. C) Flowers develop from SDSMs within FOABs (yellow box), and from bud swell to anthesis subsequent whorls of floral structures differentiate from the floral meristem. D) Fruit development begins at pollination, and undergoes a period of rapid fresh weight growth driven by cell division and expansion. Approximately 2 months after anthesis, fruit begin to accumulate starch, steadily increasing their dry matter content. A new cohort of FOABs also form on shoots in season 2 (pink circle), which in turn develop into shoots and flowers in the subsequent season. Labelled phenological events show the relative sequence of developmental events, rather than absolute timings.

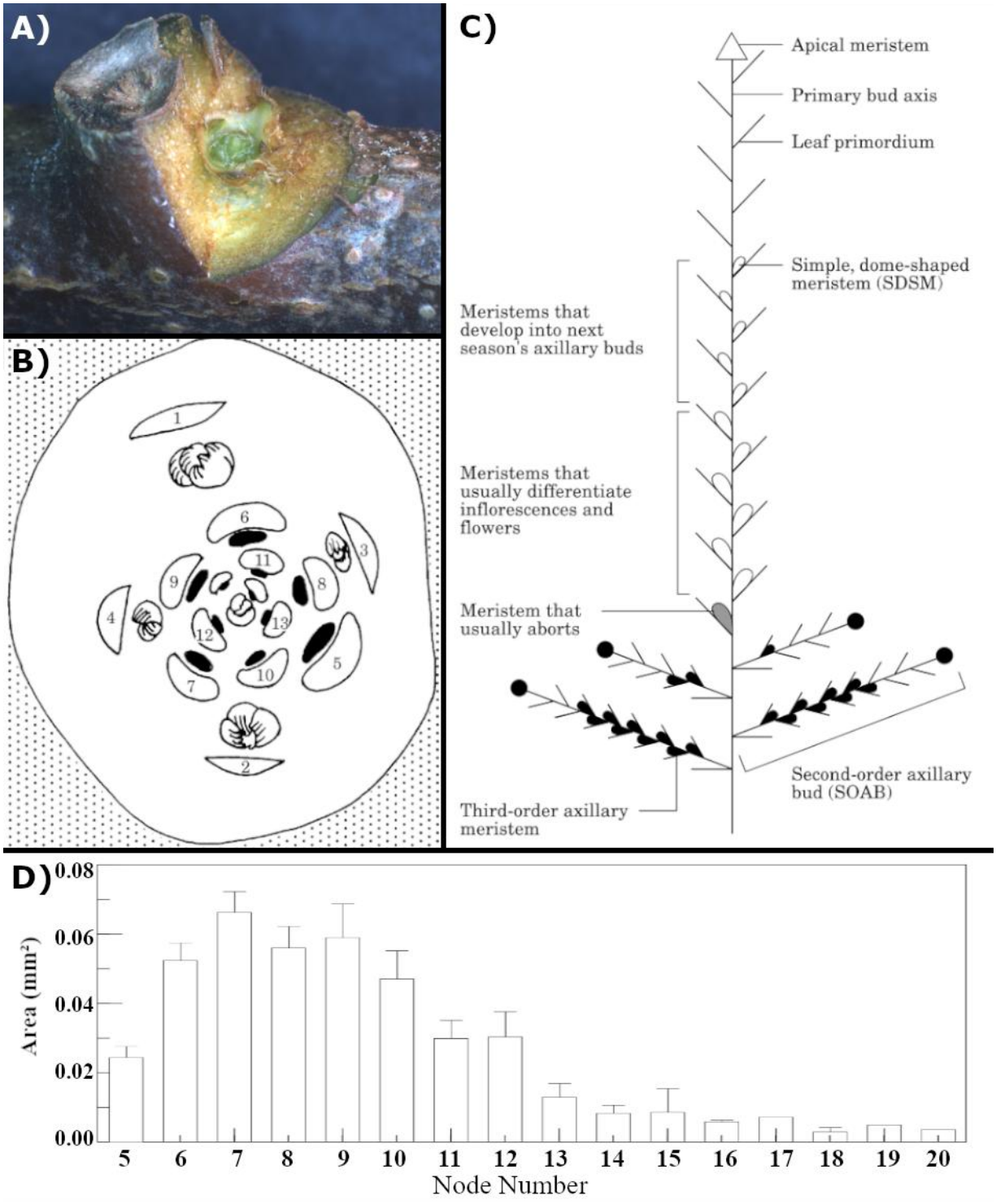


Figure 1.2. Structure of mature first order axillary buds (FOABs) from *Actinidia chinensis* var. *deliciosa* 'Hayward' vines, adapted from Walton et al. (1997). A) FOAB with bud cover and trichomes removed, revealing green leaf primordia and meristems. B) Top-down view of a dormant FOAB showing bud scales and second order axillary buds (SOABs) in basal nodes 1–4, then true leaf primordia subtending simple dome-shaped meristems (SDSMs) in nodes ≥5. Nodes are arranged in a spiral approximately 137.5° apart, forming a 2/5 phyllotaxy. C) Side-on schematic view of FOAB structure. SDSMs in nodes 5–12 may develop into either floral primordia or FOABs in the following spring. D) Mean transverse-sectional areas of SDSMs within FOABs taken from node 15 of canes, 334 days after budbreak. Vertical bars are standard error.

ecodormancy. From their formation in spring/summer, FOAB are paradormant and capable of eventual outgrowth, but are inhibited by endogenous signals. This paradormancy can be released if the shoot apical meristem (SAM) is damaged or removed (Minchin et al., 2010), a response that has been shown in other species to be facilitated by both reduced auxin concentrations and increased carbohydrate availability (Bertheloot et al., 2020; Cao et al., 2023; Mason et al., 2014).

During the autumn of season 1, FOAB transition into an endodormant state, responding to short day conditions and associated with an accumulation of abscisic acid (ABA) in the bud cover (Lionakis & Schwabe, 1984a). The depth and duration of this endodormancy in kiwifruit remain somewhat unclear, as do the exact timing and environmental conditions required to release endodormancy. A period of cool winter temperatures may not be absolutely necessary to release endodormancy, as even single bud cuttings collected late autumn were largely able to eventually break bud (Brundell, 1976; Guerriero et al., 1992). However, accumulation of either natural or artificial chilling hours significantly decreases the time required to break bud and increases total number of flowers produced in single bud cuttings (Brundell, 1976; Guerriero et al., 1992), effects that are likely related to the increased expression of FT in dormant buds with increased chill accumulation (Varkonyi-Gasic et al., 2013). In contrast, experiments with potted vines demonstrate that significant chill accumulation is required to increase budbreak above 10%, even when placed into warm, budbreak forcing conditions (Guerriero et al., 1990). Similarly, in experiments with excised canes, lower mean monthly air temperatures from May to July largely accelerated budbreak, increased budbreak percentage, and increased flower production (Snelgar et al., 1997). These contrasting observations suggest that kiwifruit bud endodormancy may only be maintained by endogenous mechanisms for a relatively short period, signalling a transition to ecodormancy and ability for individual buds to grow once environmental conditions are conducive. Once budbreak begins, early-breaking buds (particularly those nearer to the apex of canes) can effectively suppress outgrowth of buds from later and/or more basal buds (Guerriero et al., 1990). Modelling work suggests that increased chill accumulation and/or use of hydrogen cyanamide can effectively reduce the spread of budbreak within canes, reducing correlative inhibition effects between buds and improving total budbreak (Austin et al., 2002).

Bud dormancy and release are also associated with changes to carbohydrate pools and metabolism. Bud sucrose and hexose concentrations reach minimums near the end of autumn, then begin increasing throughout winter (Richardson et al., 2010). Approximately 10–20 days before budbreak, sucrose concentration sharply decreases while hexose concentrations increase

(Richardson et al., 2010), closely aligned with sharp increases to bud respiration (McPherson et al., 1997b). These metabolic shifts also align well with visible bud swelling and the beginning of morphological changes within buds (see sections 1.2.3 and 1.2.4).

Budbreak occurs in spring of season two, however the precise timing of budbreak can differ substantially by cultivar and climate. In a trial near Auckland, New Zealand 'Zesy002' broke bud 19 days earlier than co-located 'Hayward' (Hernández et al., 2015), although depending on season and orchard the difference in budbreak between these cultivars can vary from 1–3 weeks (Zespri Group, 2025). In a warmer climate (Kerikeri, New Zealand), 'Hayward' budbreak typically occurs in early October, but in cooler New Zealand regions such as Riwaka and Hawke's Bay budbreak can occur closer to mid-September (McPherson et al., 1994; Salinger et al., 1993).

### 1.2.3 Shoot and leaf growth

As buds emerge from dormancy (Figure 1.3 A), they begin to visibly swell as shoot internodes begin to elongate and leaf primordia begin to expand (Figure 1.3 B). This process accelerates from budbreak (Figure 1.3 C), with shoots progressing through several stages as detailed in Brundell (1975b). Shoots reach 'open cluster' stage (Figure 1.3 D) approximately 10 days after budbreak (DABB), and 'advanced open cluster' stage (Figure 1.3 E) approximately 15 DABB. During these open cluster stages leaves begin to unfurl and separate from the shoot axis. Shoot extension can then occur rapidly: by 20 DABB shoots may be 15–20 cm long (Figure 1.3 F), and 40–50 cm long by 50 DABB.

Warmer temperatures and longer day lengths can increase rates of shoot elongation and leaf expansion, as well as the total area of fully expanded leaves (Greer et al., 2003; Greer et al., 2004; Morgan et al., 1985a; Morgan et al., 1985b; Seleznyova & Greer, 2001). Low rates of internode expansion during early shoot growth can lead to shoot tip termination, with many kiwifruit shoots ceasing extension growth within the first few weeks following budbreak (Foster et al., 2007). Restricted access to carbohydrate reserves, competition between shoots, and high crop loads have been associated with reduced shoot growth rates and increased rates of shoot termination (Clearwater et al., 2006; Piller et al., 1998; Xiloyannis et al., 1997). Terminated shoots are composed of only pre-formed phytomers (node, internode, axillary bud and leaf) and typically reach final lengths of less than 50 cm (Seleznyova et al., 2002; Snowball, 1997b). Very early shoot tip termination often results in some of the pre-formed phytomers aborting development and necrotising. Because of this, two categories of terminated shoots have been

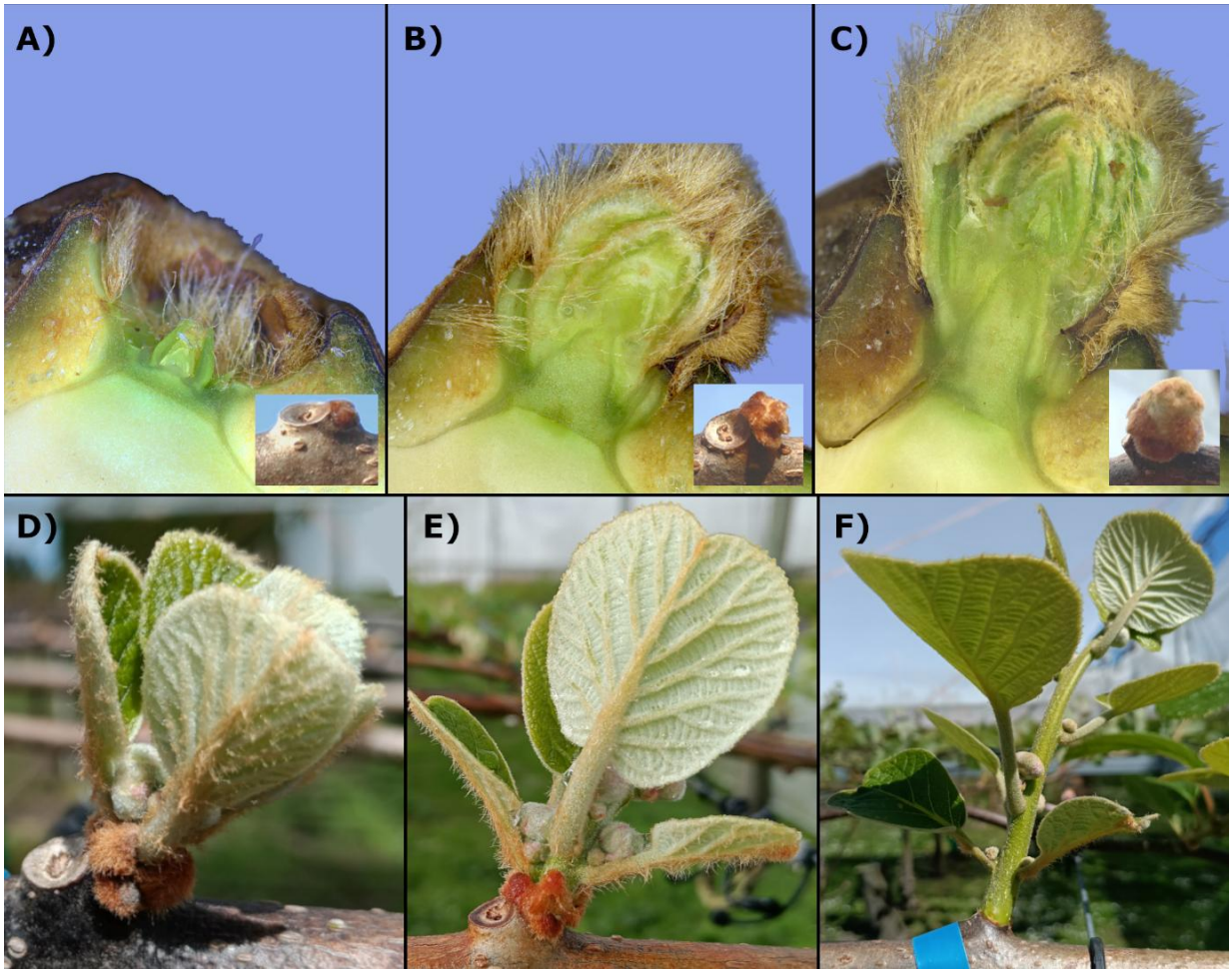


Figure 1.3. Progression of *Actinidia chinensis* var. *chinensis* 'Zesy002' buds from dormancy to shoot extension. A) Bisected dormant bud. N.B. outer bud scales and most trichomes have been removed. B) Bisected bud at bud swell stage. C) Bisected bud at budbreak stage. Inset images in panels A–C show external bud appearance. D) Shoot at open cluster stage. E) Advanced open cluster stage. F) Shoot extension stage. Photos in panels A–C credited to Brydie Terry.

defined for kiwifruit. Short shoots are defined as having nine or less nodes, and medium shoots as having at least nine nodes, but no neoformed nodes (Seleznyova et al., 2002).

In addition to terminated shoots, a minority of shoots will continue to elongate by producing additional neo-formed phytomers from the SAM. This cohort of long shoots may reach several metres in length, with extension growth continuing into late spring or summer before eventual termination (Richardson et al., 2021; Snowball, 1997b; Snowball, 1995). Long shoots tend to develop near either the base or tip of the parent cane, although the orientation of the cane in the previous season can influence this pattern (Costa et al., 1991). Average internode lengths can also be used to differentiate shoot types, with values of 9, 27 and 47 mm for short, medium and long shoots, respectively (Seleznyova et al., 2002).

The final, fully expanded areas of individual leaves are strongly influenced by their position within shoots, as detailed by Seleznyova and Greer (2001). In 'Hayward', the first eight true leaves (i.e. excluding bud scales) on a non-terminated shoot progressively increase in final leaf area. The next nine leaves reach similar high final areas (approximately 400–600 $cm^2$), then final area trends downward for subsequent leaves. Temperature during development also affects rates of leaf expansion. Under controlled day/night temperatures of 22 °C day/17 °C night, only the first 15 leaves reached full expansion within 70 days of growth (Greer, 1996). The pattern and maximum area of leaves along shoots also varies by cultivar and can be influenced by rootstock. For 'Zes008' vines, leaves in positions 4–7 reached the maximum leaf area, with sharp declines in final leaf area at lower and higher nodes (Richardson et al., 2021). In the same study, the overall pattern of leaf area within shoots was similar between vines grown on *A. chinensis* var. *deliciosa* 'Bruno' or *A. macrosperma* rootstocks, but the maximum leaf area on long shoots was 50% higher on 'Bruno' rootstocks.

The dynamics of both leaf and shoot growth strongly influence their net carbon balance in spring and subsequent ability to produce photoassimilates for fruit growth and reserve accumulation. These carbohydrate dynamics will be further detailed in section 1.3.1.

### 1.2.4 Flower development

Under favourable conditions, 'Hayward' shoots can produce up to nine inflorescences (Walton & Fowke, 1993). However, a proportion of floral structures typically fail to develop or abort during spring morphogenesis between bud swell and anthesis (Walton & Fowke, 1993). Flower abortion can occur in response to internal signals such as insufficient carbohydrate and/or nutrient availability (Jean & Lapointe, 2001; Keller & Koblet, 1994; Li et al., 2022), as well as external factors such as Psa bud rot (Kabir et al., 2019), extreme temperatures or physical damage (Stephenson, 1981).

Kiwifruit inflorescences are structured as a compound dichasium (Brundell, 1975c). The terminal flower in the inflorescence is colloquially known as the king flower, while flowers that branch inferiorly from the peduncle are termed lateral flowers (Richardson et al., 2022). Kiwifruit vines are dioecious plants with separate male (staminate) and female (pistillate) plants. Female cultivars rarely produce more than 3 flowers in an inflorescence, while male cultivars may produce more than six flowers per inflorescence (Brundell, 1975d). In over 90% of 'Hayward' inflorescences, both lateral flowers abort during floral differentiation, leaving only the king flower (Brundell, 1975d). Rates of lateral flower abortion are lower than 'Hayward' in

both ‘Zesy002’ and ‘Zes008’ (Richardson et al., 2025; Zespri Group, 2025). During development, lateral flowers can also fuse with king flowers and produce fruit with aberrant shape, occurring more commonly on nodes at the base of the shoot (Engin et al., 2011; Watson & Gould, 1994). Under commercial production, lateral flowers are typically removed prior to anthesis as they can compete for resources, reduce pollination efficacy, and produce substandard fruit (Ferguson et al., 2023a; New Zealand Kiwifruit Growers Incorporated, 2024).

Microscopic observations of floral differentiation of king flowers of female and male cultivars have been described by Brundell (1975c), Gökbayrak et al. (2010) and Caporali et al. (2019). Floral differentiation begins during bud swell in evoked SDSMs, during which floral structures progressively differentiate from the floral meristem. Differentiation of bracts, sepals and petals occurs by budbreak, with stamens and stigma differentiated by 10 DABB. Male and female flower development diverge shortly after this time, with gynoecial development halting in male flowers, but continuing in female flowers to form a superior ovary at approximately 18 DABB. Female flowers develop filaments and anthers, but do not produce viable pollen grains (Hopping, 1990). Ovary expansion continues steadily, and ovule differentiation occurs at approximately 45 DABB. Cell division in the ovary is rapid, and by anthesis ovaries may already contain approximately 60–65% of the total cell number of a mature fruit (Cruz-Castillo et al., 2002; Hopping, 1976).

In ‘Hayward’, flowers reach anthesis approximately 60 days after budbreak, however warmer conditions can accelerate this development (McPherson et al., 1992; Salinger et al., 1993). Lateral flowers follow a similar but delayed sequence of development, reaching anthesis 4–7 days after king flowers (Ferguson, 1984; Richardson et al., 2019; Richardson et al., 2001; Watson & Gould, 1994).

### 1.2.5 Anthesis and pollination

The spread of anthesis is approximately 1–3 weeks (Richardson et al., 2019; Smith et al., 1994; Snelgar et al., 2002), but can be compressed by hydrogen cyanamide application (McPherson et al., 2001b). Within vines, flowers that reach anthesis earlier typically have a heavier DW as well as larger and heavier ovaries (Cruz-Castillo et al., 1991; Lai et al., 1990; Lawes et al., 1990; Richardson et al., 2019). Flowers that are lagging behind in development typically have conversely smaller ovaries, and may even abort before reaching anthesis, probably a result of an inability to compete for carbohydrates (Richardson et al., 2022; Stephenson, 1981; Walton &

Fowke, 1993). Brundell (1975c) notes that for 'Hayward', the most distal flower bud within each shoot is typically the first to reach anthesis.

Effective pollination can be challenging due to kiwifruit's dioecious nature, requiring separate male plants with synchronous timing of anthesis and compatible pollen (Chen et al., 2019; Snelgar et al., 2002). Multiple male cultivars with staggered anthesis timings are often planted in orchards to ensure that male flowers are open throughout female anthesis (Abbate et al., 2023; Gonzalez et al., 1994). The most commonly used pollinator is the western honey bee (*Apis mellifera*), although bumble bees (*Bombus* spp.) are also employed (Broussard & Pattemore, 2023; Cutting et al., 2018). The degree of pollination can strongly influence subsequent fruit growth, although pollination requirements for full seed set also differ by cultivar. Maximum fruit size strongly correlates to seed count in 'Hayward', with growth plateauing above 1500 seeds per fruit (Costa et al., 1993; Lai et al., 1989c). In contrast, both 'Hort16A' and 'Zesy002' appear to require only 600–800 seeds per fruit to maximise fruit growth potential (Broussard et al., 2021; Goodwin et al., 2013; Seal & McKenzie, 2025).

### 1.2.6 Fruit growth and maturation

After anthesis and adequate pollination, kiwifruit undergo distinct stages of growth. Pratt and Reid (1974) described the volume growth of 'Hayward' as triple-sigmoid shaped, while Hopping (1976) described the FW growth of *A. chinensis* var. *deliciosa* 'Monty', as double-sigmoid shaped with three discrete growth stages (Figure 1.4 A). Maximum rates of cell division occur early within stage I, during the first 0–58 days after anthesis (DAA; Figure 1.4 B). Rapid cell expansion occurs slightly later in stage I, with additional cell expansion in the inner pericarp continuing during stages II and III (Figure 1.4 C). Subsequent authors have described two distinct FW growth phases, with an initial period of rapid FW growth starting at pollination and continuing until 50–60 days after anthesis, followed by a period of slower growth which lasts until fruit maturation. (Bebbington et al., 2009; Gallego et al., 1997; Hall et al., 1996).

This two-stage fruit growth model also aligns well with DM dynamics. Fruit DM drops during early growth, reaching a minimum between 40–60 DAA, depending on cultivar (Hall et al., 2013; Le Lievre et al., 2021; Richardson et al., 2011) (Figure 1.5 A–C). From this minimum, DM accumulates rapidly, although the rate of accumulation gradually slows over time (Figure 1.5 A–C). Until approximately 140 DAA, increases in DM largely correlate with accumulation of starch in the fruit, which may constitute 40–50% of the total DM at the peak (Gould et al., 2013; Nardozza et al., 2010; Okuse & Ryugo, 1981; Richardson et al., 1997). While commercial harvest

typically occurs between 160–200 DAA, fruit can continue to increase in DM until approximately 225 DAA (Richardson et al., 2011) (Figure 1.5 A), although this possibly reflects net loss of FW rather than continued DW accumulation (Bebbington et al., 2009; Clearwater et al., 2011).

During the early phase of rapid fruit FW growth, both xylem inflow and transpiration water losses are relatively high and gradually decline as the season progresses (Montanaro et al., 2012; Morandi et al., 2010). Fruit skin conductance decreases substantially by approximately 60 DAA, coinciding with progressive suberisation of outer cell layers and degeneration of surface hairs, contributing to reduced transpiration rates later in development (Hallett & Sutherland, 2005; Montanaro et al., 2012). Despite this reduction in skin conductance, under conditions of high vapour pressure deficit (e.g. 3.0 kPa), combined xylem and phloem sap flows may be insufficient to balance fruit transpiration losses, potentially causing visible shrivelling during late fruit development (Boini et al., 2025; Clearwater et al., 2011).

Phloem unloading in kiwifruit has been argued to be primarily apoplastic throughout fruit development, as evidenced by confinement of carboxyfluorescein to phloem strands, in combination with an apparent lack of plasmodesmata connecting sieve element–companion cell complexes to surrounding parenchyma (Chen et al., 2017). However, other authors have argued that the relatively high transcription of neutral invertase and sucrose synthase, combined with the lack of cell wall invertase activity, can be inferred as indirect evidence for symplastic phloem unloading in the fruit (Nardozza et al., 2013). Based on carboxyfluorescein movements and $^{14}C$-labelling experiments, it has also been claimed that the phloem unloading pathway is initially symplastic up to 91 DAA but may then become apoplastic (Morrison, 2012). Similarly, post-unloading transport to the outer pericarp appears to be largely symplastic during early fruit development, with potentially greater involvement of apoplastic transport later in fruit development as the symplastic connectivity declines (Gould et al., 2013).

Fruit maturation is associated with a plateau of starch accumulation and a subsequent increase in SSC as imported sugars accumulate (Burdon, 2022; Nardozza et al., 2013). Cooler autumn air temperatures can cause starch catabolism and accelerate the rise in SSC (Salinger et al., 1993; Seager et al., 1996), but are not strictly necessary for maturation (Burdon et al., 2016). The majority of accumulated sugars in the fruit are in the form of glucose and fructose, with a smaller fraction of sucrose, although there is some variability in these proportions between cultivars and seasons (Boldingh et al., 2000; Burdon et al., 2016; Mills et al., 2009; Reid et al., 1982). The

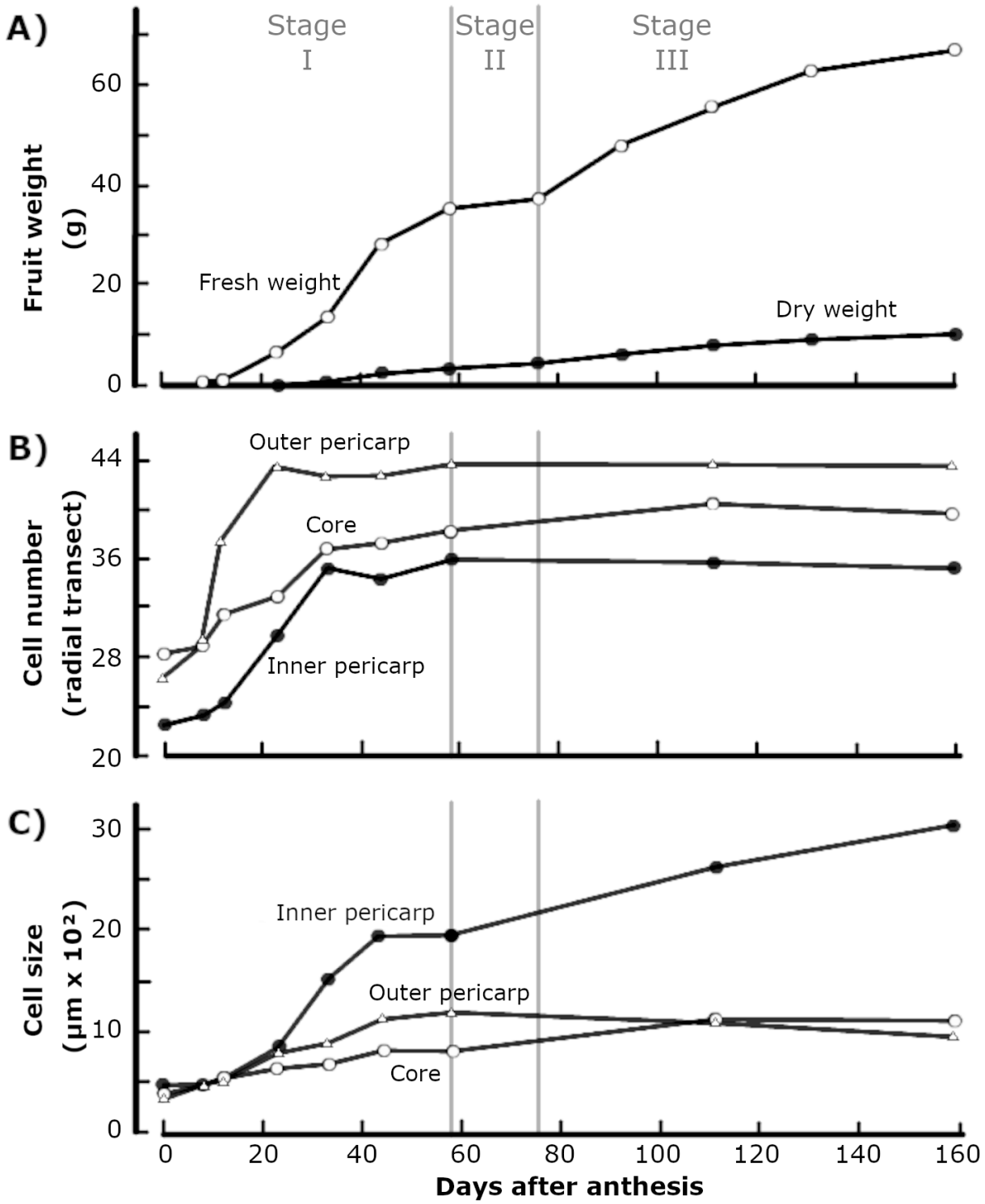


Figure 1.4. Three stages of *Actinidia chinensis* var *deliciosa* 'Monty' fruit growth, adapted from Hopping (1976). A) Fruit fresh weight and dry weight. B) Cell numbers of core, inner and outer pericarp, counted on radial transects of dissected fruit. C) Mean cell size of core, inner and outer pericarp.

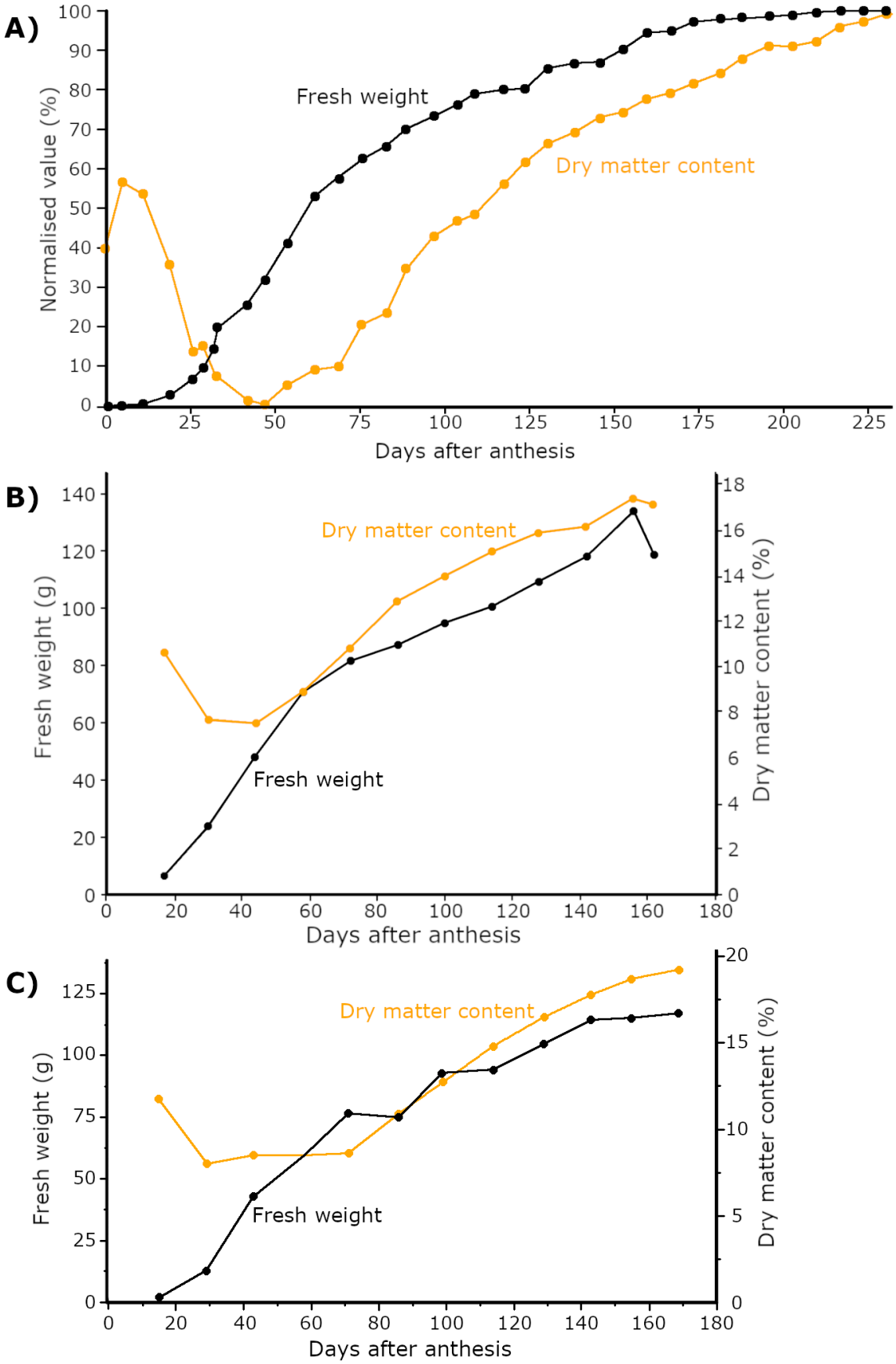


Figure 1.5. Fruit fresh weight and dry matter growth from anthesis for three kiwifruit cultivars. A) Normalised values for *Actinidia chinensis* var. *chinensis* 'Hort16A', adapted from Richardson et al. (2011). B) Absolute values for *Actinidia chinensis* var. *deliciosa* 'Hayward, adapted from Hall et al. (2013). C) Absolute values for *Actinidia chinensis* var. *chinensis* 'Zesy002', adapted from Le Lievre et al. (2021).

timing of maturity can vary by cultivar, climate, and season (Burdon et al., 2021; Hopkirk et al., 1989; Li et al., 2021), and can also be influenced by manipulating carbohydrate availability earlier in the growing season (Boyd & Barnett, 2011; Le Lievre et al., 2021; Lionakis et al., 1994; Seager et al., 1995).

The increase in SSC with fruit maturity is also typically followed by a reduction in fruit firmness, although this too is influenced by temperature and differs by cultivar (Burdon et al., 2021; Burdon et al., 2017). Similarly, in yellow-fleshed cultivars like 'Hort16A' and 'Zesy002', flesh hue begins to change from green to yellow at maturity (Burdon et al., 2021; Richardson et al., 2011), driven by degradation of flesh chlorophyll while retaining carotenoid pigments (McGhie & Ainge, 2002; Montefiori et al., 2009; Pilkington et al., 2012). In contrast, colour development in red-fleshed cultivars begins earlier with gradual accumulation of the anthocyanin pigments (starting approximately 84 DAA), and appears to be highly sensitive to carbohydrate availability and temperature (Chen et al., 2026; Nardozza et al., 2019; Nardozza et al., 2015; Richardson et al., 2021; Yu-Ping et al., 2015). While changes in SSC, firmness and hue roughly coincide at maturity, the regulation of each metric does not appear to be tightly coupled, as they can respond independently to endogenous and exogenous signals (Burdon et al., 2014).

## 1.3 Carbohydrate dynamics

As perennial deciduous plants, kiwifruit accumulate non-structural carbohydrate (NSC) reserves during the growing season and mobilise these reserves in the subsequent spring to produce new photosynthetic and reproductive tissues. Reserve pools must support budbreak, rapid shoot growth, and flower development before vines return to a net positive carbon balance, resulting in a period of intense competition for carbohydrates across multiple concurrently developing organs. In addition to temporal constraints on availability, the spatial organisation of vines and their vascular connections may further influence how carbohydrates are distributed among competing sinks. This section reviews the seasonal dynamics of carbohydrate balance in kiwifruit vines, as well as factors that can influence reserve accumulation, reserve availability between sinks, and distribution of newly fixed photoassimilates.

### 1.3.1 Seasonality of carbohydrate balance

As is common to many other woody perennial species (Dietze et al., 2014; Hoch et al., 2003), kiwifruit vines store NSC reserves primarily in the form of insoluble starch and the soluble sugars sucrose, glucose, and fructose (Boldingh et al., 2000). Consistent with other winter

deciduous species (Martínez-Vilalta et al., 2016), NSC reserves in kiwifruit are rapidly mobilised in spring between budbreak and anthesis (approximately 50–60 DABB), followed by a period of steady reserve accumulation after whole-vine carbon balance becomes positive, lasting through to leaf fall (Richardson et al., 2017; Smith et al., 1992). All perennial organs exhibit this seasonal pattern, although the timing and extent of mobilisation differ between reserve pools (Smith et al., 1992) (Figure 1.6). The majority of studies on seasonal carbohydrate dynamics in kiwifruit have been for 'Hayward'; however, there may be differences in other cultivars with differing phenology and/or productivity. These dynamics are governed by whole-vine carbon balance, which is determined by the supply of photoassimilates relative to whole-vine respiratory demand.

Kiwifruit leaves begin to export photoassimilate when they reach 50–60% of fully expanded area (Lai et al., 1988), with full expansion taking 40–70 days depending on shoot nodal position and ambient temperature (Greer, 1996; Seleznyova & Greer, 2001). The maximum assimilation rate and saturating photosynthetically active radiation (PAR) of leaves can also vary by timing of leaf emergence and leaf age (Buwalda et al., 1991). Due to these differences in timing of emergence and expansion, as well as final leaf area and assimilation rates, early emerging leaves may contribute almost half of shoot net carbon assimilation over the first 2–3 months (Greer, 1996). Light environments also strongly influence leaf function, with leaves in shaded parts of the canopy receiving much lower photosynthetic photon flux density (PPFD) and accordingly having substantially lower rates of photosynthesis (Grant & Ryugo, 1984b). Leaves grown in low PPFD conditions also have lower light saturation points and lower saturated assimilation rates than those grown in higher PPFD conditions (Greer & Halligan, 2001).

The transition of shoots from net carbon importers to exporters depends on temperature, shoot tip status, and whether they bear flowers/fruit. Under warm controlled conditions (28/22 °C, day/night), non-terminated shoots have a considerable negative daily carbon balance until 60 days after budbreak, but after this point their net carbon export steadily increases (Greer et al., 2003). In contrast, shoots growing at cooler temperatures (17/12 °C) experience a smaller initial carbon deficit and become net exporters by around 45 days after budbreak, but also export relatively less across a season, totalling only approximately 56% of that exported by shoots under warmer conditions (Greer et al., 2003). These dynamics were quantified for flower-bearing shoots, however in the absence of floral sinks the transition to net carbon export occurs earlier (Greer & Jeffares, 1998). Under field conditions, long shoots have a much larger early

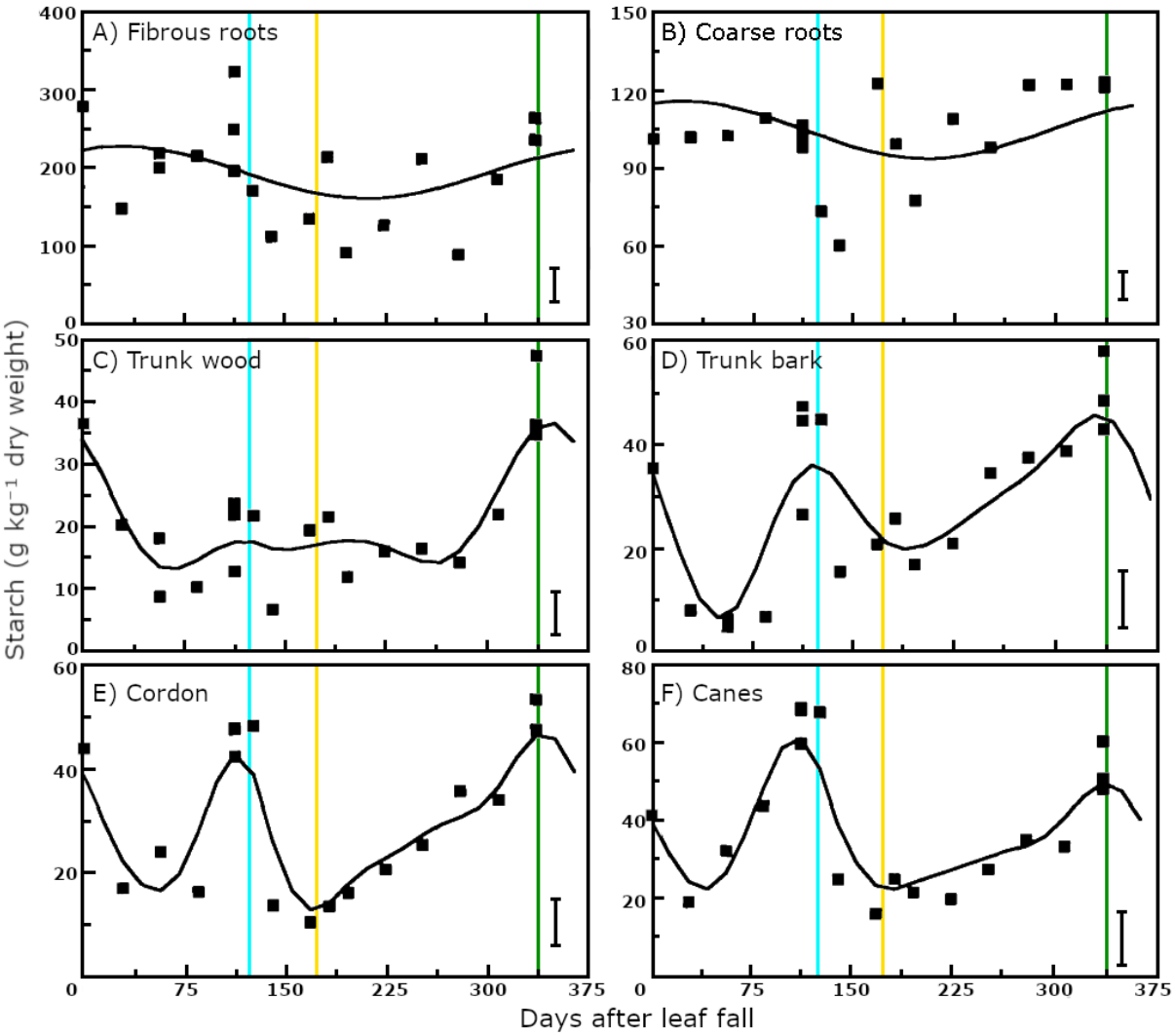


Figure 1.6. Seasonal dynamics of starch concentrations in different organs of *Actinidia chinensis* var *deliciosa* 'Hayward' kiwifruit vines, adapted from Smith et al. (1992). Blue, yellow, and green lines show budbreak, anthesis, and fruit harvest, respectively. Fitted curves are polynomial plus covariance function plus independent error, see Smith et al. (1992) for detail.

carbon deficit than short shoots (6–10-fold), but by anthesis the weekly carbon gain from long shoots can be over twice that of short shoots (Piller & Meekings, 1997).

As leaves expand and shoots elongate, whole-canopy photosynthetic capacity increases rapidly during the first approximately 30 days after budbreak (Greer et al., 2004). Measurements of canopy $CO_2$ exchange indicate that the daily net carbon balance of the canopy shifts from negative to positive between 25–35 DABB, reflecting the combined effects of increasing leaf area and respiratory costs early in the season (Buwalda, 1994). Whole-canopy photosynthetic capacity continues to increase more gradually until approximately 120 DABB, after which it declines slowly toward leaf senescence at approximately 240 DABB (Greer et al., 2004). Although photosynthetic capacity is high, daily fluctuations in environmental conditions can

strongly influence the actual carbon fixation, potentially producing a net negative canopy carbon balance on days with relatively low temperatures and PAR, even during summer (Buwalda et al., 1992). Because of this, seasonal variability in environmental conditions could significantly shift the timings of transitions in carbon balance.

Growth of fibrous roots occurs later in the season, after the period of peak competition with shoot and flower/fruit growth (Buwalda, 1991b). New fine root growth increases after anthesis, with peak growth and respiration demands occurring in summer and early autumn (Black, 2012; Richardson, 2015; von Bennewitz et al., 2019).

A mathematical model of carbon acquisition and utilisation of whole vines (i.e. including respiration, reserve replenishment, and root growth) was produced by Buwalda (1991a). This model predicts that reserve pools are rapidly depleted during the first 45 DABB. A brief period of reserve replenishment occurs at around anthesis, which coincides with an observed period of starch accumulation in leaves (Smith et al., 1992). Following fruit set, the reserve pool once again predominantly shrinks until approximately 100 DABB, when shoot biomass plateaus and the allocation of carbon to tissue growth is reduced. The reserve pool then rapidly replenishes until returning to baseline amounts at approximately 180 DABB. These modelled reserve dynamics appear to disagree somewhat with measurements by Smith et al. (1992), particularly where canes and cordon starch concentrations reached minimums near anthesis and then slowly replenish. However, Buwalda (1991a) modelled reserves as the total pool across organs, and therefore the post-anthesis period of reserve depletion could represent a slower and more sustained mobilisation from root pools, or depletion of non-starch carbohydrates.

### 1.3.2 Influences on reserve accumulation

Manipulating vine carbon balance and transport via shading, defoliation, and girdling can significantly affect NSC reserve accumulation throughout the plant. Shading or defoliating vines during autumn reduces NSC concentrations in roots, shoot internodes and buds (Kwack et al., 2014; Richardson, 2015). Conversely, girdling canes can increase internode NSC concentrations under both well-lit and partially shaded conditions (Richardson, 2015).

Although not all carbohydrate manipulation experiments have directly quantified effects on NSC reserves, there is abundant experimental evidence that shading and defoliation can reduce budbreak and flower production in the subsequent season (Buwalda & Smith, 1990; Grant & Ryugo, 1984a; Lionakis et al., 1994; Morgan et al., 1985a; Snelgar et al., 1991; Snelgar et al., 1992a). Similarly, high crop loads and/or low leaf-to-fruit ratio (L:F) in one season can also

reduce floral productivity in the next (Boyd & Barnett, 2011; Burge et al., 1987; Cooper & Marshall, 1992), suggesting that NSC reserve accumulation is compromised by excessive crop loads (Buwalda, 1991a; Xiloyannis et al., 1997).

Reserve accumulation is not homogenous within vines. When defoliation treatments are applied to a proportion of individual canes, flower production is globally reduced in the subsequent season; however, the effects are more severe on defoliated canes than on those that retained leaves (Buwalda & Smith, 1990; Tombesi et al., 1993).

### 1.3.3 Sink strength, competition and proximity to reserves

Because reserve pools are finite and competition is intense during spring growth, NSC availability has the potential to limit the development of different organs. The distribution of NSC between organs will depend on the relative strengths of sources and sinks, which are typically characterised as the product of their size (e.g. leaf area or cell number) and activity (i.e. ability to export or import sugars) (Marcelis, 1996; White et al., 2016). Due to competition between sinks and/or saturation of sink activity, the potential sink strength or absolute ability of a plant organ to import carbohydrates is typically not realised (Ho, 1988). The apparent sink strength, or realised ability to import carbohydrates, is a dynamic property of the network of sources and sinks, and can be expected to change as the system is perturbed (Ho, 1988; Minchin & Thorpe, 1996; Minchin et al., 1997).

During early shoot growth, leaves appear to be relatively strong sinks in comparison to flowers and shoot tips. When leaves are removed from single-node kiwifruit cuttings from budbreak, floral abortion is reduced and shoot extension is increased (Brundell, 1975a), mirroring experiments with grape cuttings by Mullins (1966). Grape inflorescence retention is further improved by removal of several basal leaves as well as the shoot tip (Mullins & Rajasekaran, 1981). Also in grapevines, cooling of individual inflorescences can be used to manipulate their apparent sink strength, with cooled inflorescences having reduced flower/fruit development rates and lower fruit set (Keller et al., 2022).

When NSC pools are increased by using larger or longer sections of kiwifruit cane, longer/heavier shoots are produced (Lawes, 1979; Snowball et al., 1996). On otherwise intact kiwifruit vines, cane girdling can similarly be used to restrict or enhance shoot access to NSC reserves. Severely restricting NSC availability by girdling canes 1 cm either side of a shoot base shortly after budbreak can significantly increase rates of floral abortion, and also reduce shoot and fruit growth rates (Piller et al., 1998). However, partial defoliation of shoots from two weeks

after budbreak does not affect floral abortion or fruitlet size after anthesis, suggesting that by this stage the removal of competing leaf sinks is balanced by the loss of photosynthetic potential (Piller et al., 1998).

At the level of whole vines, reducing competition by deliberate flower thinning can increase subsequent individual fruit growth potential, with larger effect size from earlier and/or more intense thinning (Antognozzi et al., 1992; Lahav et al., 1989). When shoots are similarly removed shortly after budbreak, the remaining shoots have increased growth rates and lower rates of self-termination (Clearwater et al., 2006), reflecting the substantial carbon deficit and reliance of reserves during early non-terminated shoot growth (Piller & Meekings, 1997).

Competition between shoots is also influenced by their relative proximity to cane NSC reserves. When girdles are used to provide paired shoots asymmetric access to cane reserve pools, shoots located more centrally to reserves grow significantly longer than shoots located further from reserves (Greaves et al., 1999). Even the slight tapering of internode diameter along the length of a cane may create a gradient of reserve accessibility, evidenced by shoots nearer to the base of girdled canes exhibiting more growth in spring (Greaves et al., 1999). Observational data of shoot growth patterns are generally consistent with modelled distributions of canopy NSC reserve availability, with the exception of apical shoots (Cieslak et al., 2011; Greaves et al., 1999; Seleznyova et al., 2002). To account for the more rapid growth of apical shoots, Greaves et al. (1999) incorporated additional model parameters including an earlier time of budbreak and an increased constant for 'vigour' of the apical shoot. These additional parameters likely reflect the interactions between NSC availability, phytohormones, and sink strength (Barbier et al., 2019; Bertheloot et al., 2020; Wardlaw, 1990), and how these factors combine to regulate bud/shoot growth.

### 1.3.4 Photoassimilate distribution

As the season progresses, sink development gradually depends less on imported reserves and more on newly fixed photoassimilates. Starch accumulation in leaves and depletion of canopy starch reserves suggest that this transition is likely to occur shortly prior to anthesis (Boldingh et al., 2000; Smith et al., 1992). Photoassimilate availability is also heterogenous within plants due to differences in local leaf area, photosynthetic capacity, and shading. The translocation of photoassimilates within plants is strongly influenced by sink strength and can also be influenced by vascular connectivity within shoots and proximity (i.e. pathway length) between shoots (Wardlaw, 1968; Watson & Casper, 1984).

In many plant species, movement of assimilates within individual shoots appears to be highly constrained by orthostichies, defined as the series of directly vascularly connected leaf traces that form along the stem (Kirchoff, 2008). Additional vascular connections between nodes (parastichies) can also result from lateral leaf traces (Kuhlemeier, 2007). These morphological constraints can strongly influence photoassimilate distribution to fruit. When kiwifruit leaves were supplied with $^{14}CO_2$ tracers after fruit set, Lai et al. (1988) found that fruit received 57–62% of the photoassimilates exported from their subtending leaf (node *n*) and also imported photoassimilates from leaves at nodes *n*+5 and *n*+8, but not from any other measured leaf positions. The import of carbohydrate from node *n*+5 is likely a result of the orthostichy between node *n* and n+5, while the import from node *n*+8 likely reflects parastichy connections, which have been described in *A. arguta* (Puławska, 1965). However, there is also evidence that these strict vascular connections in kiwifruit can be disrupted by pruning, following which fruit are able to import photoassimilates from all leaves on their parent shoot (Lai et al., 1988). Similar disruption to rigid patterns of assimilate translocation has been observed after leaf removal in sugar beet (Joy, 1964), and after branch phloem girdling in oak (De Schepper et al., 2013). As shoots develop, vascular systems may naturally become less confined to orthostichies as a result of secondary growth, increased lateral connectivity, and formation of vascular anastomoses (Aloni & Barnett, 1996; Kirchoff, 2008; Preston, 1998). The relatively free movement of $^{14}C$-labelled NSC between shoots on kiwifruit canes is consistent with such vascular development (Lai et al., 1989b); however, it is not currently clear when in shoot/cane development this transition naturally occurs.

A range of experimental manipulations demonstrate that competition for NSC within or between shoots after fruit set can strongly affect fruit development by redistributing photoassimilates among competing sinks. Targeted heating of individual fruit can increase their sink activity and ability to compete for photoassimilates, with large increases in FW observed when fruit are heated from 14–50 DAA, and large increases in DM occurring when fruit were heated from 101–150 DAA (Snelgar et al., 2005). Similarly, when fruit on girdled shoots were treated with plant growth regulators, they can have significantly higher FW and DW at harvest, indicating that they were able to attract a larger share of the parent shoot's photoassimilates (Famiani et al., 1995). In contrast, when fruit compete with vegetative regrowth on girdled shoots, early fruit growth rate is almost halved, and fruit FW at harvest can be reduced by up to 29% (Minchin et al., 2010; Snelgar et al., 2012). When shoots or entire canes with high L:F are isolated by girdling after anthesis, fruit FW and/or DM growth increases, indicating that some

photoassimilate export is occurring from intact shoots/canes and that fruit sink activity is not typically saturated (Le Lievre et al., 2021; Snelgar & Thorp, 1988). This observation is consistent with carbon balance calculations showing that in the first 130 DABB, approximately 30% of a fruit-bearing shoot's net assimilated carbon is exported, rather than being incorporated as fruit or shoot biomass (Greer et al., 2003).

A range of studies in kiwifruit have demonstrated that photoassimilates can translocate throughout the canopy to support the growth of fruit with relatively low local L:F, even when fruit are over 2 m from the nearest source leaves (Snelgar & Thorp, 1988; Snelgar et al., 1986; Tombesi et al., 1993). Similar effects have been observed in other species, including apples, olives and sweet cherry (Ayala & Lang, 2018; Hansen, 1969; Proietti et al., 2006). This indirect fruit growth evidence is supported by $^{14}C$ isotope studies that show that labelled photoassimilate can be translocated between shoots that are at least 7 nodes apart (Lai et al., 1989b). However, reduced photoassimilate availability or increased total crop load within a vine results in reduced translocation distance and increased reliance on local sources of photoassimilate. This can be seen in partial defoliation experiments, where reduced L:F in particular areas of vines reduces mean FW in all areas of the vine, but with more severe effects observed in the defoliated portions (Buwalda & Smith, 1990; Cruz-Castillo et al., 2010). Again, $^{14}C$ isotope studies support these field studies, showing that translocation from labelled shoots was greatest to adjacent shoots and declined considerably with increasing distance, particularly when other fruit-bearing shoots were present along the translocation pathway (Lai et al., 1989b). Similar patterns of reducing photoassimilate translocation with increasing distance and/or competition have been observed in apple, grape, peach, and tomato (Hansen, 1969; Khan & Sagar, 1966; Swanson & El-Shishiny, 1958; Wu et al., 2005; Yoshioka, 1986).

These observations of photoassimilate distribution within plants are also consistent with Münch pressure flow models of phloem transport. In such models, increasing pathway length increases hydraulic resistance between source and sink, while competing sinks along shared pathway segments can draw down the available pressure drop, reducing the driving force for more distal transport and lowering mass flow rates (Knoblauch et al., 2016; Minchin et al., 1993).

## 1.4 Summary

Kiwifruit exports make a major contribution to New Zealand's economy. The premium prices fruit can command in international markets depend on the production of consistently high-quality fruit that store well and reach consumers in excellent condition. Variability within fruit

populations can compromise fruit quality, and the largest proportion of overall variability arises within individual vines.

The development of individual kiwifruit is influenced by a range of factors acting across two growing seasons. In the first season, axillary buds and the floral meristems they contain are formed, and non-structural carbohydrate (NSC) reserves are accumulated throughout the vine for use in the following spring.

After winter dormancy, floral meristems begin to rapidly differentiate and grow, shortly prior to budbreak. Following budbreak, shoots begin to elongate, and leaves begin to expand. Intense competition for NSC at this stage can result in floral abortion, shoot tip termination, and reduced growth potential of individual flowers and fruit.

Following anthesis, fruit undergo periods of cell division and expansion, initiating a stage of rapid fresh weight (FW) growth. The net carbon assimilation of individual shoots becomes increasingly important for fruit growth at this time and is strongly influenced by earlier shoot growth and termination. From approximately two months post-anthesis, fruit enter a stage of steady starch and dry matter (DM) accumulation, coinciding with a reduced rate of FW growth. A plateau in starch accumulation and increase in soluble sugars typically occurs within 160–200 DAA, indicating that fruit have reached maturity.

Within vines, mobilised NSC can move long distances to support fruit growth, but this translocation is reduced with increasing competition and pathway distance and can also be constrained by shoot vasculature. Consequently, within-vine factors affecting access to both NSC reserves and recently fixed photoassimilates are expected to strongly influence fruit development, and ultimately FW and DM at harvest.

## 1.5 Thesis aim and objectives

Building on the patterns of variability and physiological mechanisms outlined in the preceding review, the primary aim of this thesis is to identify the major drivers of within-vine variability in fruit FW and DM, and how these can be influenced by canopy management systems.

Secondary aims are to investigate how cane type and cultivar influence carbohydrate reserve storage and mobilisation in spring; and whether NSC reserves and spring growth can be influenced with injections of exogenous sucrose.

### 1.5.1 Research objectives

Three specific research objectives contribute to these aims:

1. To identify the strongest fruit- and shoot-level predictors of within-vine variability in fruit FW and DM, and to link these predictors to underlying biological processes.
2. To characterise non-structural carbohydrate storage in dormant kiwifruit canes across cane types and cultivars, examine relationships with cane anatomical traits, and describe the patterns of NSC mobilisation during spring growth.
3. To experimentally test whether increasing NSC availability during dormancy alters subsequent spring growth, using injections of exogenous sucrose.

### 1.5.2 Thesis structure

Chapter 1 introduces the historical and commercial context of kiwifruit production in New Zealand, with a focus on the challenge of variability in fruit quality. Previous work describing patterns of variability is reviewed, followed by an overview of key aspects of kiwifruit biology relevant to axillary bud, shoot, leaf, flower, and fruit development.

Chapter 2 examines within-vine variability across commercial 'Zesy002' kiwifruit vines growing under three distinct canopy management methods, ranks individual fruit- and shoot-level predictors for their influence on fruit FW and DM, and explores how relationships between these predictors are influenced by canopy management.

Chapter 3 examines seasonal dynamics of NSC reserves in kiwifruit canes, comparing anatomical traits, carbohydrate storage, and patterns of mobilisation between cane types and cultivars.

Chapter 4 investigates whether exogenous sucrose injections during dormancy can bolster influence NSC reserves and affect spring budbreak and flower production.

Chapter 5 integrates findings across all chapters to develop a conceptual understanding of the drivers of within-vine variability in kiwifruit and discusses implications for orchard management and future fundamental research.

Chapter 6 is a full bibliography, and Appendices A, B, and C contain additional tables and figures relevant to Chapter 2, 3 and 4, respectively

# Chapter 2: Within-vine drivers of fruit variability

## 2.1 Introduction

Variability in fruit fresh weight (FW) and dry matter content (DM) within individual kiwifruit vines represents a major source of overall fruit variability and poses a persistent challenge for orchard management efficiency. While differences in fruit quality between orchards and between vines are well recognised, multiple studies have shown that a substantial proportion of variability arises within individual vines, among fruit borne on different shoots, canes, and canopy positions (Boyd et al., 2008b; Smith et al., 1994; Woodward, 2006).

Previous research has identified a range of factors associated with within-vine variability in fruit FW and DM, including timing of anthesis, pollination efficacy, shoot type, leaf-to-fruit ratio (L:F), canopy light environment, and cane characteristics (Broussard et al., 2021; Grant & Ryugo, 1984a; Lai et al., 1989a; Richardson et al., 2019; Richardson et al., 2021; Volz et al., 1992). These factors are often interrelated, and their effects on fruit development are mediated through local source–sink relationships and patterns of carbohydrate supply (Lai et al., 1989b; Minchin et al., 2010). As a result, the relative importance of individual drivers remains difficult to disentangle, particularly under commercial orchard conditions.

Canopy management practices influence vine architecture, light interception, shoot growth patterns, and the spatial distribution of carbohydrate sources and sinks within the vine (Clearwater et al., 2006; Greaves et al., 1999; Miller et al., 2001; Thorp et al., 2003). Differences in canopy structure therefore have the potential to modify both the magnitude of within-vine variability and the relationships between drivers of fruit FW and DM. However, few studies have explicitly examined within-vine variability across contrasting canopy management systems or assessed how management alters the strength and correlation of fruit- and shoot-level predictors.

In this chapter, within-vine variability in fruit FW and DM is examined across commercial ‘Zesy002’ kiwifruit vines grown under three distinct canopy management systems. Fruit- and shoot-level variables are evaluated to identify the strongest predictors of within-vine variability, assess how these relationships compare between canopy management treatments, and explore correlations among predictors. The results are interpreted in the context of reserve mobilisation, source–sink dynamics, and fruit developmental stages, providing insight into how canopy management influences fruit variability within kiwifruit vines.

## 2.2 Methods

### 2.2.1 Orchard details

The trial orchard was located near Paengaroa, Bay of Plenty, New Zealand (37.8070° S, 176.4101° E; approximately 19 m above sea level). The trial block consisted of female *A. chinensis* var. *chinensis* 'Zesy002' kiwifruit vines planted in rows with approximately 3 m between vines in a north-south direction, and bay widths of 3.2 m in an east-west direction. Vine canopies were trained onto horizontal pergola structures (Hopping et al., 1993). Rows of female vines were alternated with compact *A. chinensis* 'M33' and *A. chinensis* 'M91' male vines ('strip male' layout). Female canopy widths were approximately 5.6 m; male canopy widths were approximately 0.4 m. Female and male scions were grafted onto one-year-old seedling (i.e. non-clonal) *A. chinensis* var. *deliciosa* 'Bruno' rootstocks in 2011.

### 2.2.2 Experimental design

The vines used in this chapter were part of a longer running canopy management research trial. When the trial was established in 2017, vine replicates were statistically blocked into groups of three. Within each statistical block (Appendix Figure A1), vines were randomly assigned to one of three canopy management treatments: conventional replacement canes ('conventional'), strung replacement canes ('strung'), and spur pruned ('spur'). Descriptions of canopy management in these treatments are given in section 2.2.3. The work described in this chapter took place in the 2019–2020 growing season, when vines were in their third consecutive season under these management treatments. Nine vines (three statistical blocks) were selected based on having similar crop loads in the previous season and visible vine health. Predictor data were collected from these vines throughout the season, with replication for some predictors at the level of individual shoots (section 2.2.4) and for other predictors at the level of individual fruit (section 2.2.5).

### 2.2.3 Vine management

Canopy management differed substantially between treatments, particularly in the presence and training of replacement canes. On conventional treatment vines, long non-terminated shoots within 60 cm of the cordons and with suitable orientation were retained to form the next season's replacement canes (Figure 2.1 A), in accordance with established 'leader-pruning' methods (Miller et al., 2001; Patterson & Thorp, 2023). Shoots of this type typically continue elongation until January or February (Richardson et al., 2021; Vattiprolu et al., 2011). They can reach lengths of over 2.5 m and become pendulous under their own weight or twine around

adjacent shoots. On strung treatment vines, long shoots near the cordon were also retained, but were instead trained onto strings in late spring and early summer (Figure 2.1 B). The strings were attached at an approximate 45° angle to poles on adjacent rows (Patterson & Currie, 2011; Patterson & Thorp, 2023). This training results in long, relatively straight replacement canes that typically taper less along their length than conventional replacement canes (Figure 2.2 A, B). For both conventional and strung treatment vines, any non-terminated shoots more than ~60 cm from the cordon had the apical meristem gently squeezed to encourage termination of growth ('tip-crushing') (Patterson & Currie, 2011), with monitoring for non-terminated growth occurring four times during spring and early summer. Also, in both conventional and strung treatments, all excess high vigour shoots (i.e. excluding those suitable for replacement canes) in the leader zone were removed outright or pruned to remove all axillary buds distal to the floral nodes ('zero-leaf pruning') (Patterson & Currie, 2011).

Canopy management of spur treatment vines contrasted strongly with both conventional and strung treatments, principally in that no replacement canes were grown. In the first season of spur treatment, the supporting canopy structure was established from full length canes that had been trained onto strings in the previous season. Throughout the initial and subsequent seasons, the vines were monitored weekly during spring and summer for non-terminated shoot growth, which was managed via tip-crushing. Any secondary growth produced from current season's axillary buds was also removed. During winter pruning all shoots were pruned to 1–2 axillary buds (Figure 2.2 C). By the third year of spur management the canopy structure consisted of multiple seasons of growth with a range of vigour still apparent (Figure 2.3 A–C).

Prior to anthesis, all lateral and clearly misshapen flowers were thinned from the trial vines. After fruit set no further cosmetic or size thinning was done. All other vine management was performed according to standard orchard practices, including fertiliser applications and sprays for control of Psa. Fertiliser inputs included lime (1.5 t/ha) and NPK base mix fertiliser (1.1 t/ha) in winter, followed by compost (8 t/ha), calcium ammonium nitrate (0.35 t/ha), potassium sulphate (0.15 t/ha), and kieserite (0.15 t/ha) in the spring of each season. All vines were sprayed with hydrogen cyanamide for budbreak enhancement (McPherson et al., 2001b) on 14/08/2019, formulated as 6% active ingredient with 0.2% Driftstop™ at a water rate of 700 l/ha. Trunk girdles (Currie et al., 2018) were applied on 7/01/2020 and 8/02/2020. During flowering, 10 honeybee hives per hectare were stationed in the orchard block and no supplemental pollen was applied. Vine water supply was entirely rainfed.

### 2.2.4 Shoot-level predictors

Each shoot within the study vines was labelled with a unique identifier for subsequent data collection (Figure 2.4 A). The total number of fruit per shoot was recorded. Shoot position in the canopy was measured using a grid of bungee cords at 1 m spacing, with perpendicular coordinates measured by tape measure. Distances were recorded relative to the trunk in a north–south direction (distance N/S) and relative to the cordon in an east–west direction (distance E/W).

After harvest, the basal diameter and total length of each shoot were measured, along with the diameter of the cane internode immediately proximal to the shoot on the trunk side (Figure 2.4 B). Only primary growth was measured for shoot length (i.e. secondary growth from axillary buds formed in the current season was excluded). For very long shoots, length measurements were truncated at 500 cm. Shoot basal diameters were measured using digital vernier callipers (Sylvac, Switzerland) positioned on the first internode above the tapered section at shoot-cane junction. Internode diameters were measured in the middle of the internode directly prior to each shoot, proximal to the trunk.

Additional shoots were collected for destructive measurements in late summer (February 2020). Shoots were sourced from vines in the same orchard block, adjacent to the trial area. On these shoots the basal diameter and total length were measured, the total number of leaves was counted, and the total leaf area was measured with a LI-3100C leaf area meter (LI-COR Environmental, USA).

### 2.2.5 Fruit-level predictors

Throughout anthesis, newly open flowers were tagged at two-day intervals (27/10/2019–12/11/2019). Flowers were tagged with short lengths of coloured wire loosely attached around the pedicel, with a different colour used for each new two-day period (Figure 2.5 A). In January, each fruit was uniquely labelled by writing on the skin with permanent markers (Figure 2.5 B). The date anthesis of each fruit was recorded, as was the positional order of fruit from the base to the tip of each shoot. The height of individual fruit relative to the nearest pergola wire was measured, using 10 cm vertical height bands above or below the pergola wires.

### 2.2.6 Fruit harvests

Based on previous season's harvest dates, fruit harvests on all nine vines were originally planned for the first week of April 2020. Due to abrupt COVID-19 restrictions, one vine from each

treatment was harvested on 24/03/2020, prior to lockdown taking effect. These fruit were stored in plastic-lined trays in cool store for six weeks before being assessed. The remaining six vines were harvested between 29/04/2020 and 8/05/2020. These fruit were kept at room temperature overnight and assessed the following day. During picking, fruit were placed into pre-assigned tray positions to allow fruit data to be accurately cross-referenced (Figure 2.6 A).

Fruit FW was measured using a balance with 0.01 g precision (PG5002-S, Mettler Toledo). Fruit DM was measured by taking an approximately 3-mm wide slice from the equatorial region of the fruit using a double-bladed knife. The slice was transferred onto a pre-weighed petri dish and weighed (PG5002-S, Mettler Toledo), placed into a dehydrator (FD1000, Ezidry®) and dehydrated at 60°C for 24 ± 2 h to attain a constant dry weight. Immediately after removal from the dehydrator, the petri dish and slice were reweighed. The weight of the petri dish was subtracted to determine the fresh and dry weights, and percentage DM was calculated as dry weight divided by fresh weight. Fruit maturity metrics of SSC, flesh firmness, and hue angle were also measured for each fruit using standard protocols (Richardson et al., 2011), but due to influence of harvest date and cold storage on these metrics, the data are not presented here.

A random subset of fruit from each vine and from each flowering date were selected for seed count assessments. For these fruit, the equatorial slice for measuring DM was recovered and recombined with the remainder of the fruit. The inner pericarp of each fruit was extracted and combined with 2.5 g $L^{-1}$ of pectolytic enzyme (Lafazym®, Laffort®) in individual plastic specimen vials. After digestion for 2–7 days, the remaining pulp was separated from the seeds by washing through a sieve. Seeds were dried to constant dry weight (24 ± 2 h). The total dry weight of the seeds was measured, and a 50 seed subsample was counted and weighed. Total seed number was calculated as:

Total seed number = (seed subsample count × total seed weight) / seed subsample weight

Summary statistics for each vine are provided in Appendix Table A1, including harvest dates and total fruit counts, as well as means, standard deviations, skew and kurtosis scores for both FW and DM.




Figure 2.1. Examples of A) conventional and B) strung canopies in summer. In both conventional and strung treatments, high vigour shoots near the central cordon were retained in spring to form replacement canopies in the following season. Under conventional management, shoots were self supporting, while under strung treatment shoots were trained onto strings at approximately 45°. Non-terminated shoots that were located further from the central cordon were managed by crushing of the apical meristem, pruning axillary buds distal to the floral nodes, or complete removal. The pictured vines are representative of the trial canopy managements systems, but are not from the actual research trial.




Figure 2.2. Examples of canopy structure following winter pruning for conventional, strung and spur canopy mangement treatment vines. In both A) conventional and B) strung treatments, the previous year's fruiting canopy was removed and replacement canes originating near the cordon were trained down and clipped to support wires. C) In spur treatment vines the previous year's fruting canopy was retained, and all shoots grown in that season were pruned to 1–2 axillary buds. Panel C shows a spur canopy after the first season of growth and winter pruning. Data presented in this chapter were collected during the third season of repeated spur pruning, where up to three years of reccurent growth had been retained in the fruiting canopy (see Figure 2.3).

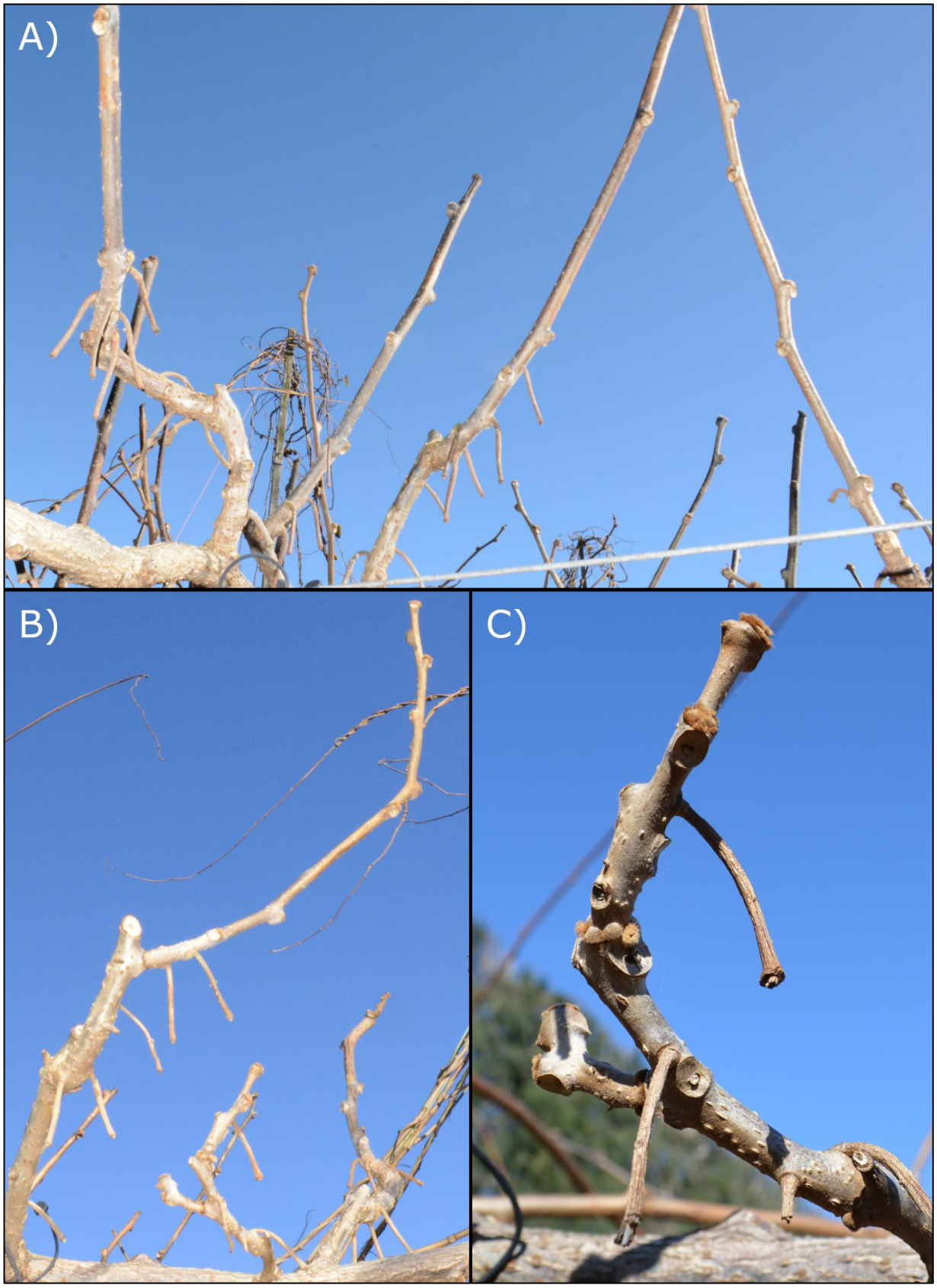


Figure 2.3. Examples of shoot types prior to winter pruning on spur treatment vines. A) Long, vigorous shoots typically grew near the cordon, did not self-terminate and often required tip-crushing or pruning and regular removal of secondary axillary growth. B) Medium shoots self-terminated before additional nodes were formed from the shoot apical meristem. C) Short shoots formed true spurs after self-terminating early in spring and had few axillary buds distal to fruit-bearing nodes.

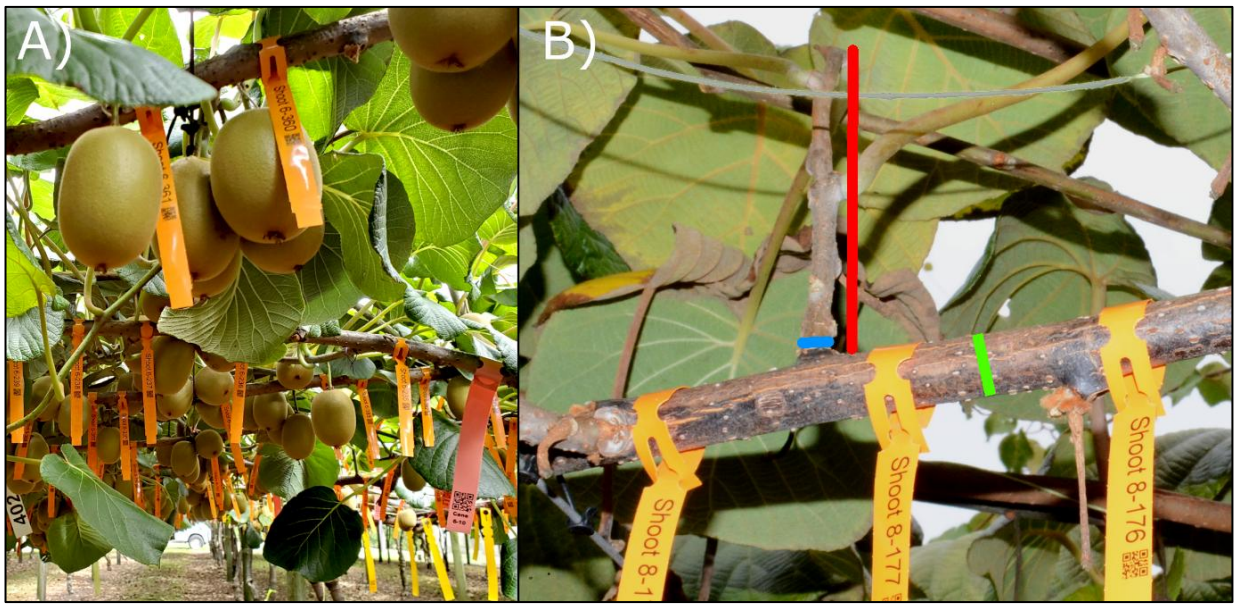


Figure 2.4. Shoot-level measurements. A) Every shoot within the studied vines was uniquely tagged and several aspects were measured. Prior to harvest, the number of fruit per shoot was recorded and the position of each shoot in the canopy was measured using east–west and north–south coordinates. B) After harvest, each shoot was assessed for basal diameter (blue), total length (red), and the diameter of the cane internode immediately proximal to the shoot on the trunk side (green).

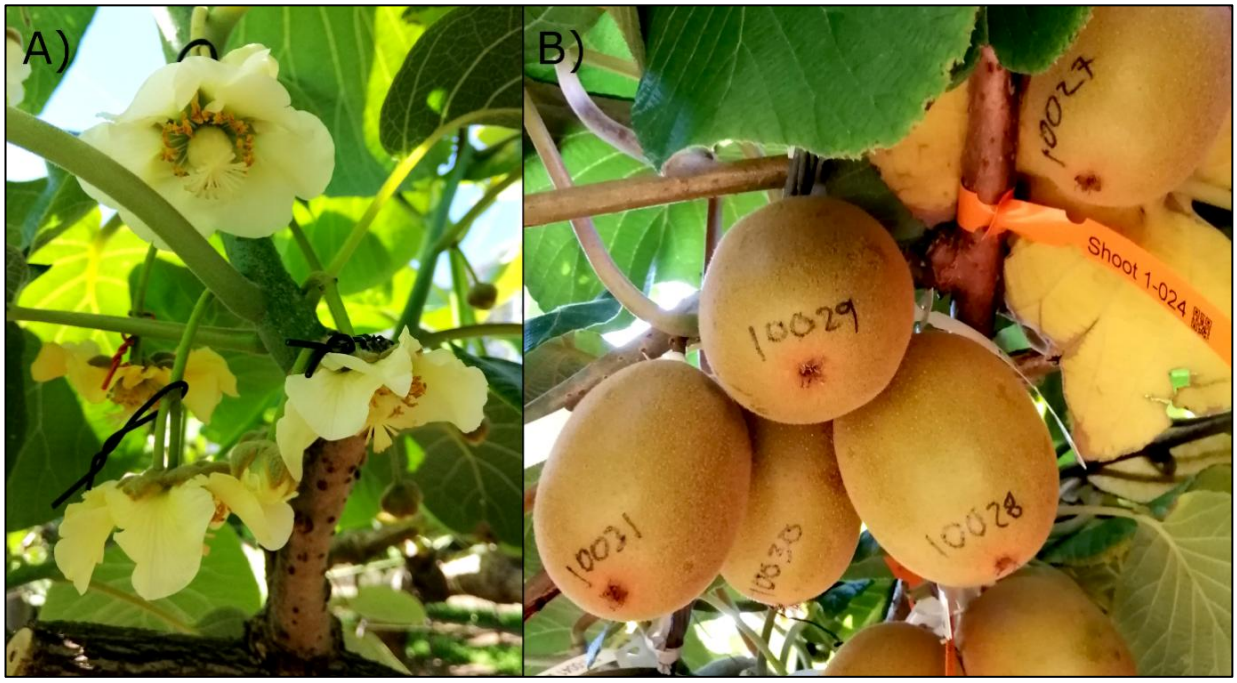


Figure 2.5. Fruit-level measurements. A) Flowers were tagged with coloured wire to indicate which 2-day interval anthesis occurred in. B) After fruit had been assigned unique identifiers, data were recorded for the timing of anthesis, fruit positional order within shoots, height band relative to canopy wires, and which shoot they were borne on.




Figure 2.6. Trays of uniquely labelled *Actinidia chinensis* var. *chinensis* 'Zesy002' fruit. Details including parent shoot ID, position on shoot, and date of anthesis were recorded. A) Each uniquely labelled fruit was picked and placed into pre-assigned positions in trays to ensure fruit data were correctly recorded and could be cross-referenced to other fruit- and shoot-level data. B) The same fruit after fresh weight measurement and removal of an equatorial slice for of dry matter content assessment. Fruit randomly sub-sampled for seed counts were recombined with their equatorial slice prior to digestion with pectolytic enzyme.

### 2.2.7 Statistical analyses

Fruit FW and DM data were mean-centred within vines by subtracting vine means from individual fruit values. This effectively removes between-vine variance from the data and allows the mean-relative effects of within-vine predictors to be directly quantified. Continuous predictor variables (shoot diameter; shoot length; internode diameter; distance E/W; distance N/S) were standardised and centred prior to analysis, and scarce levels of factorial predictors (timing of anthesis; fruit per shoot; position within shoot; relative height) were collapsed prior to analyses.

Linear mixed-effects models were fitted using restricted maximum likelihood (REML) to assess relationships between vine-mean centred fruit FW or DM and the predictor variables. Modelling required the exclusion of fruit with missing values for any modelled predictor. After these exclusions were made, final numbers of fruit and shoots included for modelling purposes are presented in Table 2.1.

Table 2.1. Shoot and fruit replicate numbers by treatment.

| Treatment | Shoot replicates | Fruit replicates |
|---|---|---|
| Conventional | 875 | 2846 |
| Strung | 997 | 3400 |
| Spur | 884 | 3468 |
| Total | 2756 | 9714 |

Models included a nesting structure accounting for fruit position within shoots, stratified by the number of fruit per shoot. Models were first fitted separately for each canopy management treatment, followed by a global model incorporating interaction terms between treatment and each predictor variable. Random intercepts were included for individual shoots nested within vines, accounting for the hierarchical structure of the data and clustering of fruit within shoots. Denominator degrees of freedom for hypothesis testing were estimated using the Kenward–Roger approximation.

Effect sizes (partial $\eta^2$) are reported to indicate the relative contribution of predictor variables and interactions to explained variance. Effect sizes were calculated as the sums of squares of the main effect or interaction divided by the total sums of squares. Significant differences between factor levels (within treatments), between treatments (for a given factor level), or between treatment slopes were assessed using post-hoc pairwise testing with Šidák correction to control the family-wise error rate. Slopes for continuous predictors were back transformed prior to plotting. To focus on biologically meaningful effects, only main effects or treatment interactions with an effect size >0.05 in the global model for FW or DM are included as plots in the main text. Plots for effects and interactions with an effect size of <0.05 are included in Appendix A.

To assess correlations between predictor variables, a pair-wise correlation matrix was generated. Pearson's r values are presented for the entire dataset and within individual treatments. Major axis regressions were fitted and plotted to visualise the linear relationships between variables.

For relationships between leaf area, leaf number, shoot length and shoot diameter of destructively harvested shoots, linear, quadratic and power models were fitted to the data. The best models for each comparison were selected based on Akaike information criterion (AIC) values and visual inspection of the fitted lines. Goodness of fit was calculated as:

$$\text{Pseudo } R^2 = 1 - (\text{Residual Sums of Squares} / \text{Total Sums of Squares})$$

All analyses and data visualisation were performed in R software version 4.3.3 (R Core Team, 2025). Data manipulation was handled using the *dplyr* package (Wickham et al., 2024). AIC values were calculated using the *stats* package (R Core Team, 2025). Linear mixed effect models were constructed and assessed using the *lme4* and *lmerTest* packages (Bates et al., 2015; Kuznetsova et al., 2017). Estimated marginal means and effect slopes were derived from models using the *emmeans* package (Lenth, 2024). Post-hoc tests and compact letter displays for statistical groupings were performed using the *multcomp* and *multcompView* packages (Graves et al., 2024; Hothorn et al., 2008). The correlation matrix was generated using the *GGally* package (Schloerke et al., 2024), and major axis regressions were fitted using *lmodel2* package (Legendre & Oksanen, 2025). Data were visualised using the *ggplot2* package (Wickham, 2016) and arranged with the *patchwork* package (Pedersen, 2025). Summary statistics for each vine are provided in Appendix Table A1, including harvest dates and total fruit counts, as well as means, standard deviations, skew and kurtosis scores for both FW and DM.

## 2.3 Results

### 2.3.1 Drivers of fruit fresh weight

Across all three treatments, the four strongest drivers of variability in fruit FW were fruit position within shoots, timing of anthesis, shoot diameter, and distance E/W. All four effects were highly significant ($p<0.001$; Table 2.3). The remaining predictors varied in their ranked importance between treatments, but each accounted for less than 5% of the total variability. In the global model, these same four factors were also the strongest predictors of FW. When the effect sizes for main effects and treatment interactions were combined, position within shoot accounted for 42% of the total variability; timing of anthesis accounted for 28%; shoot diameter, 14%; and distance E/W, 7.5% (Table 2.4). The only predictor that did not have a significant main effect was relative height ($p = 0.232$); however, there were also significant treatment interaction effects for position within shoot ($p<0.001$), distance N/S ($p<0.001$), timing of anthesis ($p<0.001$), relative height ($p<0.05$), and shoot diameter ($p<0.05$; Table 2.4).

**Position within shoot.** Fruit position within shoot had clear and relatively consistent effects on FW across treatments, with only minor but significant treatment-specific differences. Generally, for shoots with 2–4 fruit, those in the most distal position had significantly lower FW than fruit in more basal positions ($p<0.05$; Table 2.5). Across all treatments, for shoots bearing ≥5 fruit, fruit in the 1–2 most basal positions and the most distal position tended to have significantly lower FW than fruit in the central positions. The greatest difference in FW between fruit positions occurred in shoots with ≥7 fruit in all three treatments, with a difference of 14.1 g in strung vines, 18.2 g in spur vines, and 22.6 g in conventional vines. Treatment-specific deviations from this general pattern were limited. In spur vines, basal fruit on shoots bearing five or six fruit were significantly smaller than those in equivalent positions on conventional vines, with similar but weaker differences relative to strung vines. In contrast, only minor positional differences were observed between strung and conventional vines.

**Timing of anthesis.** Anthesis was highly condensed in spring 2019, with over 90% of flowers reaching anthesis within a four-day period in all three treatments (Figure 2.7 A–C). Despite this, there were still significant differences in FW depending on timing of anthesis, particularly between flowers that opened on days 7–8 and those that opened on days 9–10, which were significantly different in all three treatments ($p<0.05$; Figure 2.7 D–F). This two-day difference in the timing of anthesis resulted in a 7.5 g difference in FW at harvest in spur vines, an 8.2 g difference in strung vines, and an 8.8 g difference in conventional vines. Fruit from flowers that

opened on days 11–16 were significantly lower again in both conventional and strung vines ($p<0.05$, Figure 2.7 D, E), although fruit from these late flowers represented <5% of the total population in all treatments.

**Shoot basal diameter.** Distributions of shoot basal diameter were fairly similar between treatments, with the majority falling between 5–10 mm and a peak at approximately 7.5 mm (Figure 2.8 A, B, C). Shoot basal diameter was significantly and positively correlated with fruit FW in all three treatments ($p< 0.001$; Figure 2.8 D, E, F). The relationship between shoot basal diameter and FW was similar in conventional and strung vines, with FW increasing by 2.34 g $mm^{-1}$ and 2.47 g $mm^{-1}$, respectively. In spur vines this slope was significantly steeper, with FW increasing by 3.46 g $mm^{-1}$.

**Distance E/W.** Fruit were scarcest near the cordon and the distal edges of the vines but were otherwise distributed fairly similarly across treatments (Figure 2.9 A–C). For all three treatments, there was a significant and positive marginal effect of increasing distance E/W on FW (but see section 2.4.2.3). The slopes of this relationship were not significantly different between treatments and ranged from 4.29 g $m^{-1}$ in conventional vines, to 5.46 g $m^{-1}$ in spur vines (Figure 2.9 D–F).

Table 2.3. Type III ANOVA results by treatment from linear mixed-effects models predicting fruit relative fresh weight (vine-mean centred) at harvest in *Actinidia chinensis* var. *chinensis* 'Zesy002' vines. Separate models were fitted for each canopy management treatment (conventional, strung, spur). Continuous predictors included shoot diameter, shoot length, internode diameter, and distance from the vine centre in the east–west (E/W) and north–south (N/S) directions. Categorical predictors included timing of anthesis, relative height within the canopy, number of fruit per shoot, and fruit position within the shoot. Models incorporated random intercepts for individual shoots to account for clustering of fruit within shoots. Within each treatment, main effects are ranked by effect size ($\eta^2$), indicating their relative contribution to explained variance. Bolded terms were statistically significant ($p < 0.05$). Numerator degrees of freedom. *Fruit position within the shoot was nested within fruit per shoot.

| Fresh weight<br>Treatment and predictors | Sums of squares | DF | F value | P value | Effect size ($\eta^2$) |
|---|---|---|---|---|---|
| Conventional | | | | | |
| **Position within shoot*** | 39754 | 21 | 14.2 | <0.001 | 0.442 |
| **Timing of anthesis** | 27203 | 3 | 68.0 | <0.001 | 0.302 |
| **Shoot diameter** | 8610 | 1 | 64.5 | <0.001 | 0.096 |
| **Distance E/W** | 5292 | 1 | 39.7 | <0.001 | 0.059 |
| **Distance N/S** | 3302 | 1 | 24.7 | <0.001 | 0.037 |
| **Fruit per shoot** | 2997 | 6 | 3.7 | <0.01 | 0.033 |
| **Internode diameter** | 1646 | 1 | 12.3 | <0.001 | 0.018 |
| Relative height | 820 | 5 | 1.2 | 0.293 | 0.009 |
| Shoot length | 341 | 1 | 2.6 | 0.110 | 0.004 |
| Strung | | | | | |
| **Timing of anthesis** | 25665 | 3 | 65.6 | <0.001 | 0.345 |
| **Position within shoot*** | 25631 | 21 | 9.4 | <0.001 | 0.345 |
| **Shoot diameter** | 10148 | 1 | 77.8 | <0.001 | 0.137 |
| **Distance E/W** | 5801 | 1 | 44.5 | <0.001 | 0.078 |
| **Internode diameter** | 2374 | 1 | 18.2 | <0.001 | 0.032 |
| **Fruit per shoot** | 2056 | 6 | 2.6 | <0.05 | 0.028 |
| **Relative height** | 1574 | 5 | 2.4 | <0.05 | 0.021 |
| **Distance N/S** | 984 | 1 | 7.5 | <0.01 | 0.013 |
| Shoot length | 89 | 1 | 0.7 | 0.408 | 0.001 |
| Spur | | | | | |
| **Position within shoot*** | 45059 | 21 | 19.7 | <0.001 | 0.488 |
| **Timing of anthesis** | 16601 | 3 | 50.7 | <0.001 | 0.180 |
| **Shoot diameter** | 14985 | 1 | 137.4 | <0.001 | 0.162 |
| **Distance E/W** | 7645 | 1 | 70.1 | <0.001 | 0.083 |
| **Fruit per shoot** | 3551 | 6 | 5.4 | <0.001 | 0.038 |
| **Distance N/S** | 1850 | 1 | 17.0 | <0.001 | 0.020 |
| **Shoot length** | 1194 | 1 | 10.9 | <0.001 | 0.013 |
| Relative height | 906 | 6 | 1.4 | 0.217 | 0.010 |
| **Internode diameter** | 511 | 1 | 4.7 | <0.05 | 0.006 |

Table 2.4. Type III ANOVA results from a linear mixed-effects model predicting fruit relative fresh weight (vine-mean-centred) at harvest in *Actinidia chinensis* var. *chinensis* 'Zesy002'. Continuous predictors included shoot diameter, shoot length, internode diameter, and distance from the vine centre in the east–west (E/W) and north–south (N/S) directions. Categorical predictors included timing of anthesis, relative height within the canopy, number of fruit per shoot, and fruit position within the shoot. Interactions between each predictor and canopy management treatment (conventional, strung, spur) were also tested. The model incorporated random intercepts for individual shoots to account for clustering of fruit within shoots. Main effects and interactions are ranked by effect size ($\eta^2$), indicating their relative contribution to explained variance. Bolded terms were statistically significant ($p < 0.05$). DF = Numerator degrees of freedom. *Fruit position within the shoot was nested within fruit per shoot.

Relative fresh weight

| Predictor variables<br>Main effects | Sums of squares | DF | F value | P value | Effect size ($\eta^2$) |
|---|---|---|---|---|---|
| **Position within shoot*** | 89781 | 21 | 34.6 | <0.001 | 0.358 |
| **Timing of anthesis** | 66331 | 3 | 179.2 | <0.001 | 0.264 |
| **Shoot diameter** | 33669 | 1 | 272.9 | <0.001 | 0.134 |
| **Distance E/W** | 18627 | 1 | 151.0 | <0.001 | 0.074 |
| **Fruit per shoot** | 6341 | 6 | 8.6 | <0.001 | 0.025 |
| **Internode diameter** | 3907 | 1 | 31.7 | <0.001 | 0.016 |
| **Shoot length** | 1140 | 1 | 9.2 | <0.01 | 0.005 |
| Relative height | 690 | 4 | 1.4 | 0.232 | 0.003 |
| Treatment | 633 | 2 | 2.6 | 0.086 | 0.003 |
| **Distance N/S** | 480 | 1 | 3.9 | <0.05 | 0.002 |
| Interactions with treatment | | | | | |
| **Position within shoot* : Treatment** | 15862 | 42 | 3.1 | <0.001 | 0.063 |
| **Distance N/S : Treatment** | 5500 | 2 | 22.3 | <0.001 | 0.022 |
| **Timing of anthesis : Treatment** | 3049 | 6 | 4.1 | <0.001 | 0.012 |
| **Relative height : Treatment** | 2117 | 8 | 2.1 | <0.05 | 0.008 |
| Fruit per shoot : Treatment | 1396 | 12 | 0.9 | 0.502 | 0.006 |
| **Shoot diameter : Treatment** | 1045 | 2 | 4.2 | <0.05 | 0.004 |
| Distance E/W : Treatment | 240 | 2 | 1.0 | 0.379 | 0.001 |
| Shoot length : Treatment | 222 | 2 | 0.9 | 0.408 | 0.001 |
| Internode diameter : Treatment | 98 | 2 | 0.4 | 0.671 | 0.000 |

Table 2.5. Effects of fruit position within shoots on fruit relative fresh weight in *Actinidia chinensis* var. *chinensis* 'Zesy002', within each fruit per shoot category. Values represent the mean ± standard error of vine-mean centred fresh weight at harvest, estimated from a linear mixed-effects model that controlled for other measured covariates. Lowercase letters indicate significant differences between fruit positions within each row, while uppercase letters denote significant differences between treatments for each specific combination of fruit per shoot and position. Groups that do not share a letter differ significantly based on pairwise comparisons (Šidák adjusted α = 0.05). Fruit per shoot and position values ≥7 were pooled due to limited replication. Cell colours indicate the direction and magnitude of the estimated effect, with red indicating negative values and blue indicating positive values.

| **Relative fresh weight (g)** | | (basal) | | Position within shoot | | | | (distal) |
|---|---|---|---|---|---|---|---|---|
| | | 1 | 2 | 3 | 4 | 5 | 6 | ≥7 |
| | Fruit per shoot | | | | | | | |
| Conventional | 1 | -3.9 ± 1.4<br>A | | | | | | |
| | 2 | -0.1 ± 1.3<br>a<br>A | -5.1 ± 1.3<br>b<br>A | | | | | |
| | 3 | 3.0 ± 1.2<br>a<br>A | 1.0 ± 1.2<br>a<br>A | -4.6 ± 1.2<br>b<br>A | | | | |
| | 4 | 1.6 ± 1.3<br>a<br>A | 2.6 ± 1.3<br>a<br>A | -0.3 ± 1.3<br>a<br>A | -6.3 ± 1.3<br>b<br>A | | | |
| | 5 | 3.4 ± 1.4<br>bc<br>A | 5.1 ± 1.4<br>ab<br>A | 7.2 ± 1.3<br>a<br>A | 0.8 ± 1.3<br>c<br>A | -5.9 ± 1.3<br>d<br>B | | |
| | 6 | -1.5 ± 1.8<br>bc<br>A | 3.8 ± 1.8<br>ab<br>A | 6.4 ± 1.8<br>a<br>A | 5.8 ± 1.8<br>a<br>A | 1.8 ± 1.8<br>abc<br>A | -3.7 ± 1.8<br>c<br>A | |
| | ≥7 | -3.7 ± 4.2<br>c<br>A | -6.9 ± 4.0<br>c<br>A | 2.4 ± 4.0<br>bc<br>A | 10.9 ± 4.0<br>ab<br>A | 15.7 ± 4.0<br>a<br>A | 2.7 ± 4.0<br>bc<br>A | -4.7 ± 4.0<br>c<br>A |
| Strung | 1 | -2.0 ± 1.4<br>A | | | | | | |
| | 2 | 0.7 ± 1.3<br>a<br>A | -2.3 ± 1.3<br>b<br>A | | | | | |
| | 3 | 1.5 ± 1.2<br>a<br>A | 1.0 ± 1.2<br>a<br>A | -3.7 ± 1.2<br>b<br>A | | | | |
| | 4 | -0.4 ± 1.2<br>a<br>A | 1.7 ± 1.2<br>a<br>A | -0.2 ± 1.2<br>a<br>A | -5.6 ± 1.2<br>b<br>A | | | |
| | 5 | 0.8 ± 1.3<br>ab<br>AB | 1.1 ± 1.3<br>ab<br>A | 2.3 ± 1.3<br>a<br>B | -1.4 ± 1.3<br>bc<br>A | -4.0 ± 1.2<br>c<br>AB | | |
| | 6 | -1.6 ± 1.7<br>c<br>A | -0.2 ± 1.7<br>c<br>A | 6.0 ± 1.7<br>ab<br>A | 7.5 ± 1.7<br>a<br>A | 1.4 ± 1.7<br>bc<br>A | -2.2 ± 1.7<br>c<br>A | |
| | ≥7 | -8.2 ± 2.6<br>d<br>A | -4.2 ± 2.6<br>cd<br>A | 1.3 ± 2.6<br>abc<br>A | 3.5 ± 2.6<br>abc<br>A | 5.9 ± 2.6<br>a<br>A | 3.9 ± 2.6<br>ab<br>A | -1.9 ± 2.4<br>bcd<br>A |
| Spur | 1 | -5.7 ± 2.0<br>A | | | | | | |
| | 2 | -1.5 ± 1.6<br>a<br>A | -3.9 ± 1.6<br>a<br>A | | | | | |
| | 3 | 0.1 ± 1.3<br>a<br>A | -0.8 ± 1.3<br>a<br>A | -5.5 ± 1.3<br>b<br>A | | | | |
| | 4 | -1.1 ± 1.2<br>a<br>A | 1.9 ± 1.2<br>a<br>A | -0.2 ± 1.2<br>a<br>A | -4.5 ± 1.2<br>b<br>A | | | |
| | 5 | -2.4 ± 1.2<br>d<br>B | 4.7 ± 1.2<br>ab<br>A | 5.3 ± 1.2<br>a<br>AB | 1.4 ± 1.2<br>bc<br>A | -0.9 ± 1.2<br>cd<br>A | | |
| | 6 | -8.0 ± 1.5<br>c<br>B | 3.9 ± 1.5<br>ab<br>A | 7.4 ± 1.5<br>a<br>A | 4.9 ± 1.5<br>ab<br>A | 4.5 ± 1.5<br>ab<br>A | 1.0 ± 1.5<br>b<br>A | |
| | ≥7 | -8.4 ± 2.1<br>d<br>A | -1.5 ± 2.1<br>c<br>A | 4.2 ± 2.1<br>abc<br>A | 9.8 ± 2.1<br>a<br>A | 8.5 ± 2.1<br>a<br>A | 6.8 ± 2.1<br>ab<br>A | 2.1 ± 2.0<br>bc<br>A |

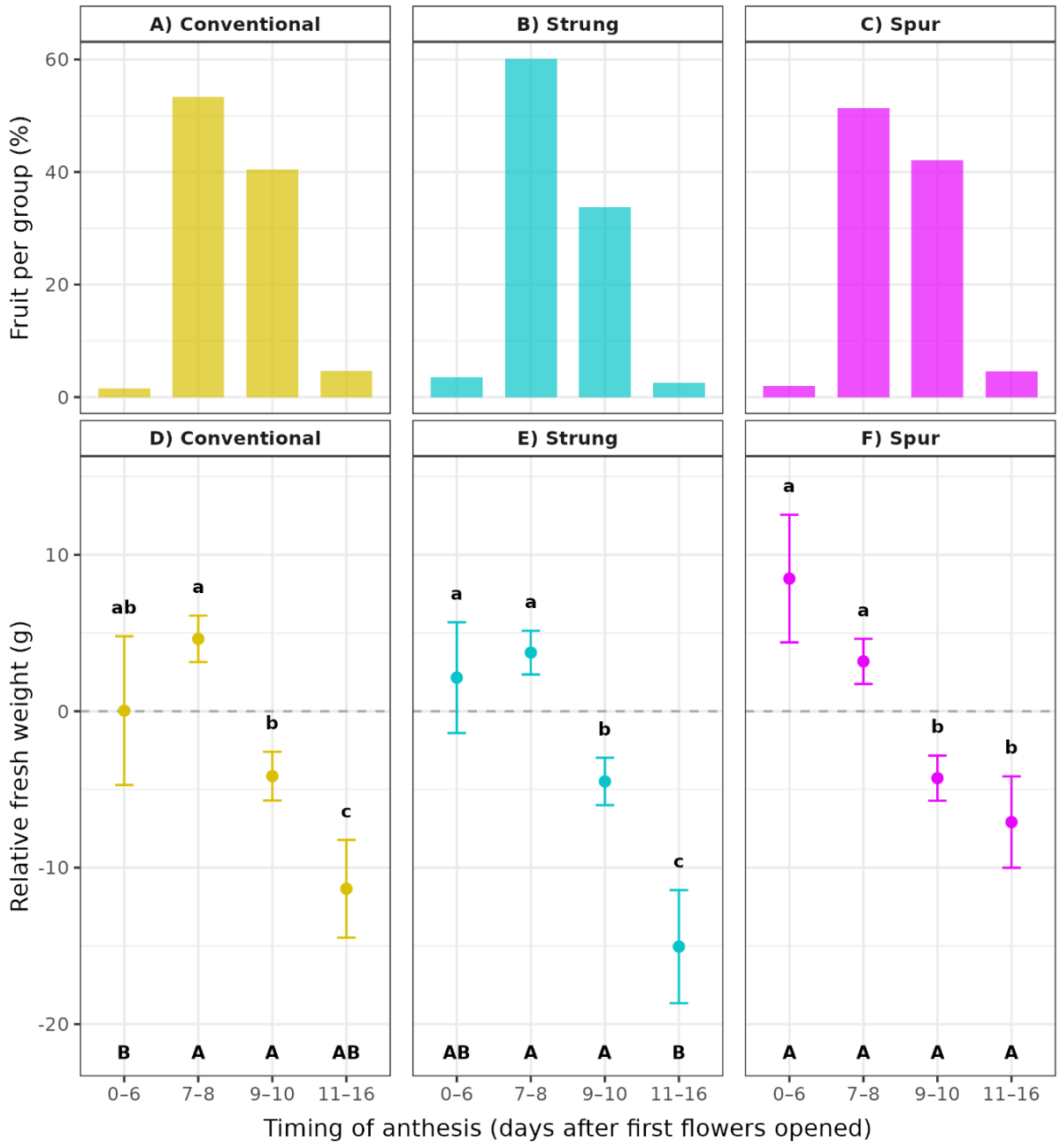


Figure 2.7. Distribution of anthesis timing and model-estimated effects on fruit relative fresh weight in *Actinidia chinensis* var. *chinensis* 'Zesy002'. Panels A–C show the distribution of anthesis timing grouped into four bands, expressed as the percentage of total fruit within each treatment. Panels D–F display estimated marginal means for fruit fresh weight (centred on the vine mean) at harvest, derived from a linear mixed-effects model controlling for other measured shoot- and fruit-level covariates. Lowercase letters above points denote groupings between anthesis timing bands within each treatment panel based on pairwise comparisons, and uppercase letters along the x-axis indicate groupings between treatments for a given anthesis band. Means that do not share a letter were significantly different (Šidák adjusted α = 0.05). Error bars represent 95% confidence intervals. Day 0 of anthesis was 27/11/2019.

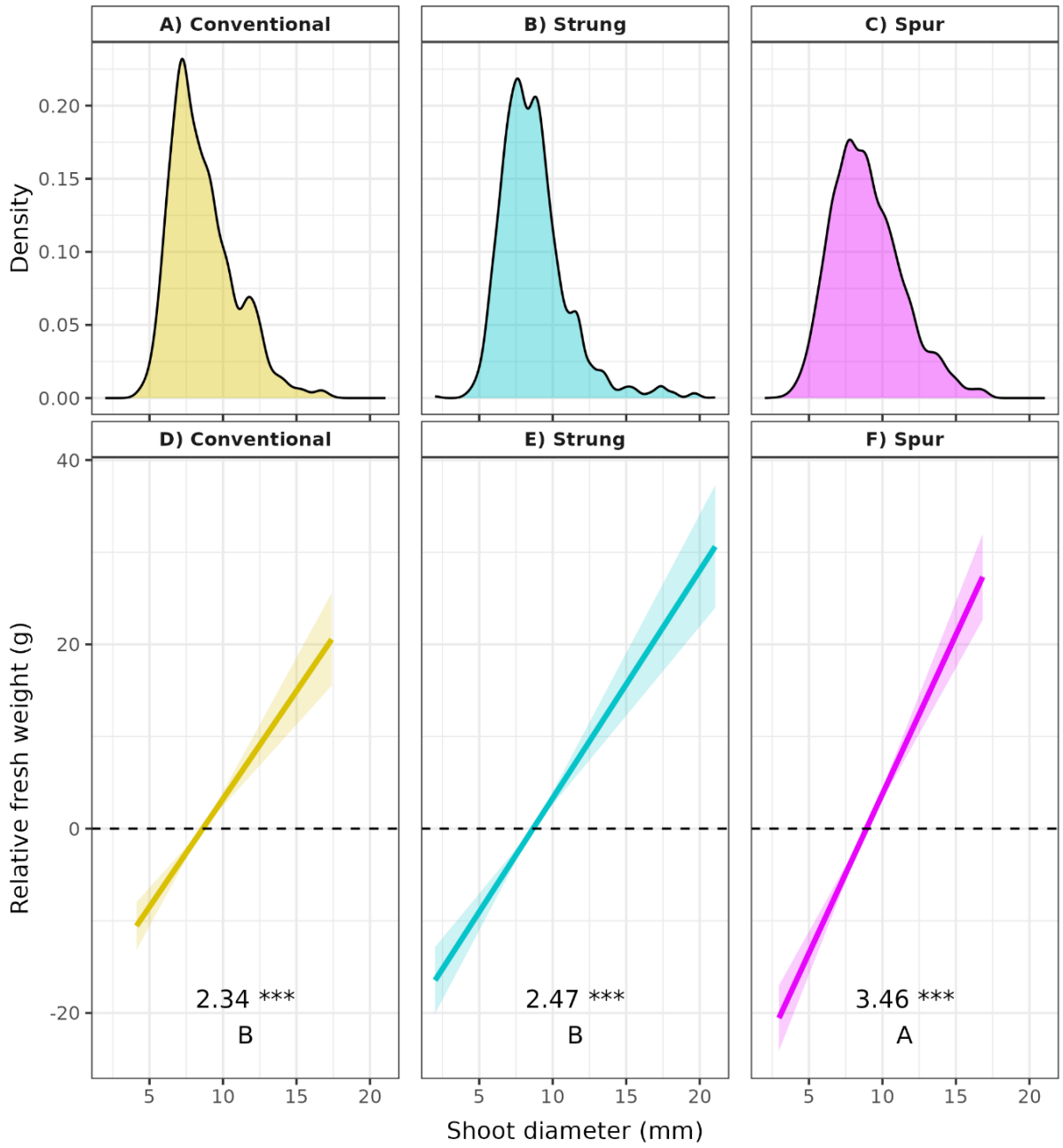


Figure 2.8. Distribution and model-estimated effects of shoot basal diameter on fruit relative fresh weight in *Actinidia chinensis* var. *chinensis* 'Zesy002'. Diameters were measured at the base of each shoot, immediately above the tapering region at the cane–shoot junction. Panels A–C show the distribution of shoot diameters for each canopy management treatment, expressed as kernel density plots of all measured shoots. Panels D–F display fitted relationships between shoot diameter and vine-mean centred fresh weight at harvest, based on estimated marginal trends from a linear mixed-effects model. Slopes represent the expected increase in fruit fresh weight per mm increase in shoot diameter, after controlling for other covariates in the model. Shaded ribbons indicate 95% confidence intervals. Numeric values within each panel indicate the estimated slope and its significance level (*** $p < 0.001$), and uppercase letters below the slope denote differences in the slope between treatments. Slopes that do not share a letter differ significantly based on pairwise comparisons (Šidák adjusted $\alpha = 0.05$).

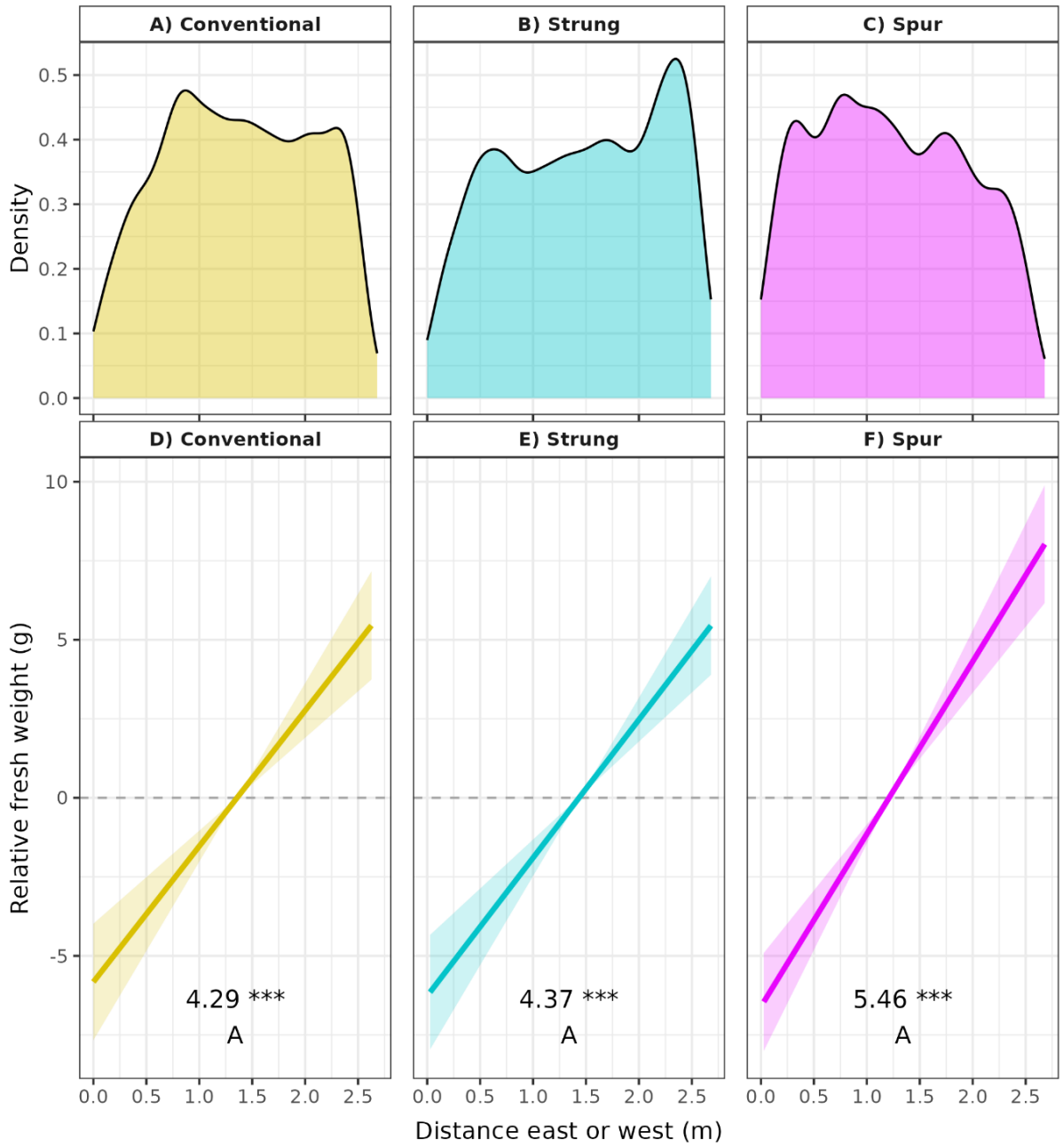


Figure 2.9. Distribution and model-estimated effect of fruit position within the canopy along the east–west axis on fruit relative fresh weight in *Actinidia chinensis* var. *chinensis* 'Zesy002'. Panels A–C show the distribution of fruit across the canopy for each management treatment, expressed as kernel density plots of all measured fruit. Panels D–F display fitted relationships between distance east or west from the cordon and fruit fresh weight (centred on the vine mean) at harvest, based on estimated marginal trends from a linear mixed-effects model. Slopes represent the expected increase in fresh weight per metre east or west from the cordon, controlling for other covariates in the model. Shaded ribbons indicate 95% confidence intervals. Numeric values within each panel indicate the estimated slope and its significance level (*** $p < 0.001$), while uppercase letters below the slope denote differences in the slope between treatments. Slopes that do not share a letter differ significantly based on pairwise comparisons (Šidák adjusted $\alpha = 0.05$).

### 2.3.2 Drivers of fruit dry matter content

The relative importance of predictors of fruit DM differed between treatments. Position within shoot and distance E/W were the most influential drivers for both conventional and strung vines (Table 2.6), whereas in spur vines position within ranked third, after shoot length and distance N/S (Table 2.6). When the effect sizes of main effects and treatment interactions in the global model were combined, there were five predictors that each accounted for over 5% of the total variability in DM. Position within shoot accounted for 37%; distance E/W, 17%; distance N/S, 16%; shoot length, 14%; and relative height, 5.9% (Table 2.7). The only predictor that did not have a significant main or treatment interaction effect was internode diameter (main effect, $p = 0.057$; interaction effect, $p = 0.571$). There were also no significant treatment interaction effects for timing of anthesis ($p = 0.584$), and fruit per shoot ($p = 0.978$).

**Position within shoot.** Fruit in the most distal positions on shoots tended to be lower in DM than those in more basal positions. This effect was strongest in strung vines, where on shoots with ≥3 fruit the most distal fruit was consistently significantly lower than at least one more basal fruit within the shoot ($p<0.05$, Table 2.8). On conventional vines, only shoots with 5 or 6 fruit had distal fruit with significantly lower DM than those from more basal positions ($p<0.05$). In spur vines only shoots with 3 fruit showed this effect, where the distal fruit was significantly lower in DM than the most basal fruit ($p<0.05$). The largest within shoot positional differences occurred in shoots with ≥7 fruit for conventional (0.44 DM%) and spur vines (0.22 DM%), whereas in strung vines the largest difference occurred on shoots with six fruit (0.57 DM%). The only significant difference between treatments was for fruit in the distal position on shoots with five fruit, which were significantly lower in strung vines than the equivalent fruit on spur vines ($p<0.05$).

**Distance E/W.** Increasing distance E/W was associated with a decrease in DM in all three treatments. The slope of this relationship was similar in both conventional and strung vines, where every metre of increasing distance from the cordon was associated with a 0.32 or 0.36 DM% decrease ($p<0.001$; Figure 2.10 D, E), while in spur vines the slope was shallower, with only a 0.1 DM% decrease per metre ($p<0.05$, Figure 2.10 F).

**Distance N/S.** The distribution of fruit along the north-south axis was similar between treatments within the first 1.5 m of the canopy, with peaks and troughs in conventional and strung vines likely reflecting the regular spacing of canes along this axis (Figure 2.11 A, B). In contrast, the more even distribution in spur vines is likely a result of the multiple years of spur

growth perpendicular to the original canes (see Figure 2.2). Additionally, one of the spur vines had a slightly longer-than-average cordon, which contributed to the elongated tail past 1.5 m (Figure 2.11 C). The effects of increasing distance N/S on DM contrasted between treatments. In conventional and strung vines, each metre further N/S from the trunk was associated with a 0.44 or 0.29 DM% increase, respectively ($p<0.001$, Figure 2.11 D, E), while in spur vines there was an inverse relationship where each metre further N/S was associated with a decrease in DM by 0.41 units ($p<0.001$; Figure 2.11 F).

**Shoot length.** Shoot length distributions were strongly right skewed in all three treatments (Figure 2.12 A, B, C). Spur vines had two peaks below 100 cm, likely representing naturally self-terminating true spurs and more vigorous shoots that had been tip-crushed or pruned. Both conventional and strung vines had more shoots >100 cm than spur vines, and both had a small peak at the right end of the distribution representing shoots ≥500 cm (i.e. replacement canes). Longer shoots were associated with higher DM, with slight differences between treatments. The strongest effect was in spur vines, where every additional metre of shoot length was associated with an increase of 0.3 DM% ($p<0.001$; Figure 2.12 F). Conventional vines had a significantly lower slope than spur vines ($p<0.05$), with an increase of only 0.1 DM% per metre of shoot length ($p<0.01$; Figure 2.12 D). Strung vines had a slope of 0.2 DM% per metre ($p<0.001$), which was not significantly different from that of either conventional or spur treatments (Figure 2.12 E).

**Relative height.** The distributions of relative height were similar between conventional and strung vines, with over 50% of fruit located in the first 10 cm above the canopy wire (Figure 2.13 A, B). In contrast, spur vines had a wider distribution of fruit relative heights, with over 10% of fruit located at least 10 cm below the canopy wires (Figure 2.13 C). Although relative height had a significant effect on DM in the global model ($p<0.001$; Table 2.7), only strung vines showed a significant effect in the treatment level models (Table 2.6). Within strung vines, fruit that were located below the canopy wire had significantly lower DM than those above the canopy wire (Figure 2.13 E).

Table 2.6. Type III ANOVA results by treatment from linear mixed-effects models predicting relative fruit dry matter content (vine-mean centred) at harvest in *Actinidia chinensis* var. *chinensis* 'Zesy002' vines. Separate models were fitted for each canopy management treatment (conventional, strung, spur). Continuous predictor variables included shoot diameter, shoot length, internode diameter, and distance from the vine centre in both east–west (E/W) and north–south (N/S) directions. Categorical predictors included timing of anthesis, relative height in the canopy, number of fruit per shoot, and fruit position within the shoot. Models incorporated random slopes for individual shoots to account for clustering of fruit within shoots. Within each treatment, predictors are ranked by effect size ($\eta^2$), indicating their relative contribution to explained variance. Bolded terms were statistically significant ($p < 0.05$). DF = Numerator degrees of freedom. *Fruit position within the shoot is nested within fruit per shoot.

| Relative dry matter content Treatment and predictors | Sums of squares | DF | F value | P value | Effect size ($\eta^2$) |
|---|---|---|---|---|---|
| Conventional | | | | | |
| **Distance E/W** | 16.72 | 1 | 76.07 | <0.001 | 0.305 |
| **Position within shoot*** | 14.71 | 21 | 3.19 | <0.001 | 0.268 |
| **Distance N/S** | 13.51 | 1 | 61.48 | <0.001 | 0.246 |
| **Shoot diameter** | 2.50 | 1 | 11.36 | <0.001 | 0.045 |
| **Shoot length** | 2.21 | 1 | 10.07 | <0.01 | 0.040 |
| Fruit per shoot | 2.16 | 6 | 1.64 | 0.132 | 0.039 |
| Timing of anthesis | 1.48 | 3 | 2.25 | 0.081 | 0.027 |
| Relative height | 1.48 | 5 | 1.34 | 0.243 | 0.027 |
| Internode diameter | 0.12 | 1 | 0.52 | 0.469 | 0.002 |
| Strung | | | | | |
| **Position within shoot*** | 40.31 | 21 | 6.49 | <0.001 | 0.447 |
| **Distance E/W** | 16.00 | 1 | 54.04 | <0.001 | 0.177 |
| **Relative height** | 9.49 | 5 | 6.41 | <0.001 | 0.105 |
| **Shoot length** | 8.74 | 1 | 29.54 | <0.001 | 0.097 |
| **Distance N/S** | 7.30 | 1 | 24.67 | <0.001 | 0.081 |
| **Shoot diameter** | 2.90 | 1 | 9.81 | <0.01 | 0.032 |
| Timing of anthesis | 2.30 | 3 | 2.59 | 0.051 | 0.026 |
| Fruit per shoot | 1.70 | 6 | 0.96 | 0.451 | 0.019 |
| **Internode diameter** | 1.37 | 1 | 4.61 | <0.05 | 0.015 |
| Spur | | | | | |
| **Shoot length** | 16.84 | 1 | 69.94 | <0.001 | 0.383 |
| **Distance N/S** | 9.00 | 1 | 37.38 | <0.001 | 0.205 |
| **Position within shoot*** | 8.27 | 21 | 1.64 | <0.05 | 0.188 |
| **Timing of anthesis** | 4.22 | 3 | 5.84 | <0.001 | 0.096 |
| Relative height | 2.84 | 6 | 1.97 | 0.067 | 0.065 |
| Fruit per shoot | 1.26 | 6 | 0.87 | 0.513 | 0.029 |
| **Distance E/W** | 1.19 | 1 | 4.94 | <0.05 | 0.027 |
| Shoot diameter | 0.23 | 1 | 0.96 | 0.329 | 0.005 |
| Internode diameter | 0.08 | 1 | 0.35 | 0.555 | 0.002 |

Table 2.7. Type III ANOVA results from a linear mixed-effects model predicting fruit relative dry matter content (vine-mean centred) at harvest in *Actinidia chinensis* var. *chinensis* 'Zesy002'. Continuous predictor variables included shoot diameter, shoot length, internode diameter, and distance from the vine centre in both east–west (E/W) and north–south (N/S) directions. Categorical predictors included timing of anthesis, relative height in the canopy, number of fruit per shoot, and fruit position within the shoot. Interactions between each predictor and canopy management treatment (conventional, strung, spur) were also tested. The model incorporated random slopes for individual shoots to account for clustering of fruit within shoots. Main effects and interactions are ranked by effect size ($\eta^2$), indicating their relative contribution to explained variance. Bolded terms were statistically significant ($p < 0.05$). DF = Numerator degrees of freedom. *Fruit position within the shoot is nested within fruit per shoot.

Relative dry matter content

| Predictor variables<br>Main effects | Sums of squares | DF | F value | P value | Effect size ($\eta^2$) |
|---|---|---|---|---|---|
| **Position within shoot*** | 45.33 | 21 | 8.5 | <0.001 | 0.248 |
| **Distance E/W** | 26.46 | 1 | 104.3 | <0.001 | 0.145 |
| **Shoot length** | 22.39 | 1 | 88.3 | <0.001 | 0.123 |
| **Timing of anthesis** | 6.79 | 3 | 8.9 | <0.001 | 0.037 |
| **Relative height** | 5.62 | 4 | 5.5 | <0.001 | 0.031 |
| **Fruit per shoot** | 3.57 | 6 | 2.3 | <0.05 | 0.020 |
| **Distance N/S** | 2.34 | 1 | 9.2 | <0.01 | 0.013 |
| **Shoot diameter** | 2.15 | 1 | 8.5 | <0.01 | 0.012 |
| Internode diameter | 0.92 | 1 | 3.6 | 0.057 | 0.005 |
| Treatment | 0.25 | 2 | 0.5 | 0.618 | 0.001 |
| Interactions with treatment | | | | | |
| **Distance N/S : Treatment** | 27.54 | 2 | 54.3 | <0.001 | 0.151 |
| **Position within shoot* : Treatment** | 21.30 | 42 | 2.0 | <0.001 | 0.117 |
| **Distance E/W : Treatment** | 5.09 | 2 | 10.0 | <0.001 | 0.028 |
| **Relative height : Treatment** | 5.05 | 8 | 2.5 | <0.05 | 0.028 |
| **Shoot diameter : Treatment** | 2.72 | 2 | 5.4 | <0.01 | 0.015 |
| **Shoot length : Treatment** | 2.49 | 2 | 4.9 | <0.01 | 0.014 |
| Timing of anthesis : Treatment | 1.19 | 6 | 0.8 | 0.584 | 0.007 |
| Fruit per shoot : Treatment | 1.09 | 12 | 0.4 | 0.978 | 0.006 |
| Internode diameter : Treatment | 0.28 | 2 | 0.6 | 0.571 | 0.002 |

Table 2.8 Effects of fruit position within shoots on fruit relative dry matter content in *Actinidia chinensis* var. *chinensis* 'Zesy002', within each fruit per shoot category. Values represent the mean ± standard error of vine-mean-centred fresh weight at harvest, estimated from a linear mixed-effects model that controlled for other measured covariates. Lowercase letters indicate significant differences between fruit positions within each row, while uppercase letters denote significant differences between treatments for each combination of fruit per shoot and position. Groups that do not share a letter differ significantly based on pairwise comparisons (Šidák adjusted α = 0.05). Fruit per shoot and position values ≥ were pooled due to limited replication. Cell colours indicate the direction and magnitude of the estimated effect, with red indicating negative values and blue indicating positive values.

| **Dry matter content (% units)** | | (basal) Position within shoot | | | | | | (distal) |
|---|---|---|---|---|---|---|---|---|
| | | 1 | 2 | 3 | 4 | 5 | 6 | ≥7 |
| | Fruit per shoot | | | | | | | |
| Conventional | 1 | -0.23 ± 0.08<br>A | | | | | | |
| | 2 | -0.05 ± 0.08<br>a<br>A | -0.11 ± 0.08<br>a<br>A | | | | | |
| | 3 | 0.04 ± 0.07<br>a<br>A | 0.03 ± 0.07<br>a<br>A | -0.05 ± 0.07<br>a<br>A | | | | |
| | 4 | 0.01 ± 0.07<br>a<br>A | 0.06 ± 0.07<br>a<br>A | 0.03 ± 0.07<br>a<br>A | -0.05 ± 0.07<br>a<br>A | | | |
| | 5 | 0.05 ± 0.08<br>a<br>A | 0.01 ± 0.08<br>ab<br>A | 0.14 ± 0.08<br>a<br>A | -0.01 ± 0.08<br>ab<br>A | -0.12 ± 0.08<br>b<br>AB | | |
| | 6 | 0.03 ± 0.11<br>a<br>A | 0.05 ± 0.11<br>a<br>A | 0.03 ± 0.11<br>a<br>A | 0.12 ± 0.11<br>a<br>A | -0.02 ± 0.11<br>ab<br>A | -0.24 ± 0.11<br>b<br>A | |
| | ≥7 | 0.09 ± 0.24<br>a<br>A | 0.12 ± 0.24<br>a<br>A | -0.11 ± 0.24<br>a<br>A | 0.33 ± 0.24<br>a<br>A | 0.21 ± 0.24<br>a<br>A | 0.33 ± 0.24<br>a<br>A | -0.05 ± 0.24<br>a<br>A |
| Strung | 1 | -0.10 ± 0.08<br>A | | | | | | |
| | 2 | 0.07 ± 0.07<br>a<br>A | -0.03 ± 0.08<br>a<br>A | | | | | |
| | 3 | 0.13 ± 0.07<br>a<br>A | 0.11 ± 0.07<br>a<br>A | -0.05 ± 0.07<br>b<br>A | | | | |
| | 4 | 0.03 ± 0.07<br>a<br>A | 0.01 ± 0.07<br>a<br>A | -0.03 ± 0.07<br>a<br>A | -0.19 ± 0.07<br>b<br>A | | | |
| | 5 | 0.00 ± 0.07<br>a<br>A | -0.07 ± 0.07<br>a<br>A | -0.03 ± 0.07<br>a<br>A | -0.16 ± 0.07<br>ab<br>A | -0.30 ± 0.07<br>b<br>B | | |
| | 6 | 0.10 ± 0.10<br>ab<br>A | 0.15 ± 0.10<br>ab<br>A | 0.24 ± 0.10<br>a<br>A | 0.15 ± 0.10<br>ab<br>A | -0.07 ± 0.10<br>b<br>A | -0.33 ± 0.10<br>c<br>A | |
| | ≥7 | 0.09 ± 0.15<br>ab<br>A | 0.20 ± 0.15<br>a<br>A | 0.12 ± 0.15<br>ab<br>A | 0.17 ± 0.15<br>a<br>A | 0.12 ± 0.15<br>ab<br>A | 0.01 ± 0.15<br>ab<br>A | -0.19 ± 0.15<br>b<br>A |
| Spur | 1 | -0.18 ± 0.12<br>A | | | | | | |
| | 2 | 0.01 ± 0.09<br>a<br>A | -0.08 ± 0.09<br>a<br>A | | | | | |
| | 3 | 0.04 ± 0.07<br>a<br>A | -0.02 ± 0.07<br>ab<br>A | -0.11 ± 0.08<br>b<br>A | | | | |
| | 4 | -0.01 ± 0.07<br>a<br>A | 0.01 ± 0.07<br>a<br>A | 0.00 ± 0.07<br>a<br>A | -0.10 ± 0.07<br>a<br>A | | | |
| | 5 | 0.05 ± 0.07<br>a<br>A | 0.09 ± 0.07<br>a<br>A | 0.04 ± 0.07<br>a<br>A | 0.06 ± 0.07<br>a<br>A | 0.02 ± 0.07<br>a<br>A | | |
| | 6 | -0.11 ± 0.09<br>a<br>A | -0.01 ± 0.09<br>a<br>A | 0.05 ± 0.09<br>a<br>A | 0.02 ± 0.09<br>a<br>A | 0.06 ± 0.09<br>a<br>A | -0.08 ± 0.09<br>a<br>A | |
| | ≥7 | 0.12 ± 0.13<br>a<br>A | 0.09 ± 0.13<br>a<br>A | 0.02 ± 0.13<br>a<br>A | 0.12 ± 0.13<br>a<br>A | 0.13 ± 0.13<br>a<br>A | 0.24 ± 0.13<br>a<br>A | 0.09 ± 0.12<br>a<br>A |

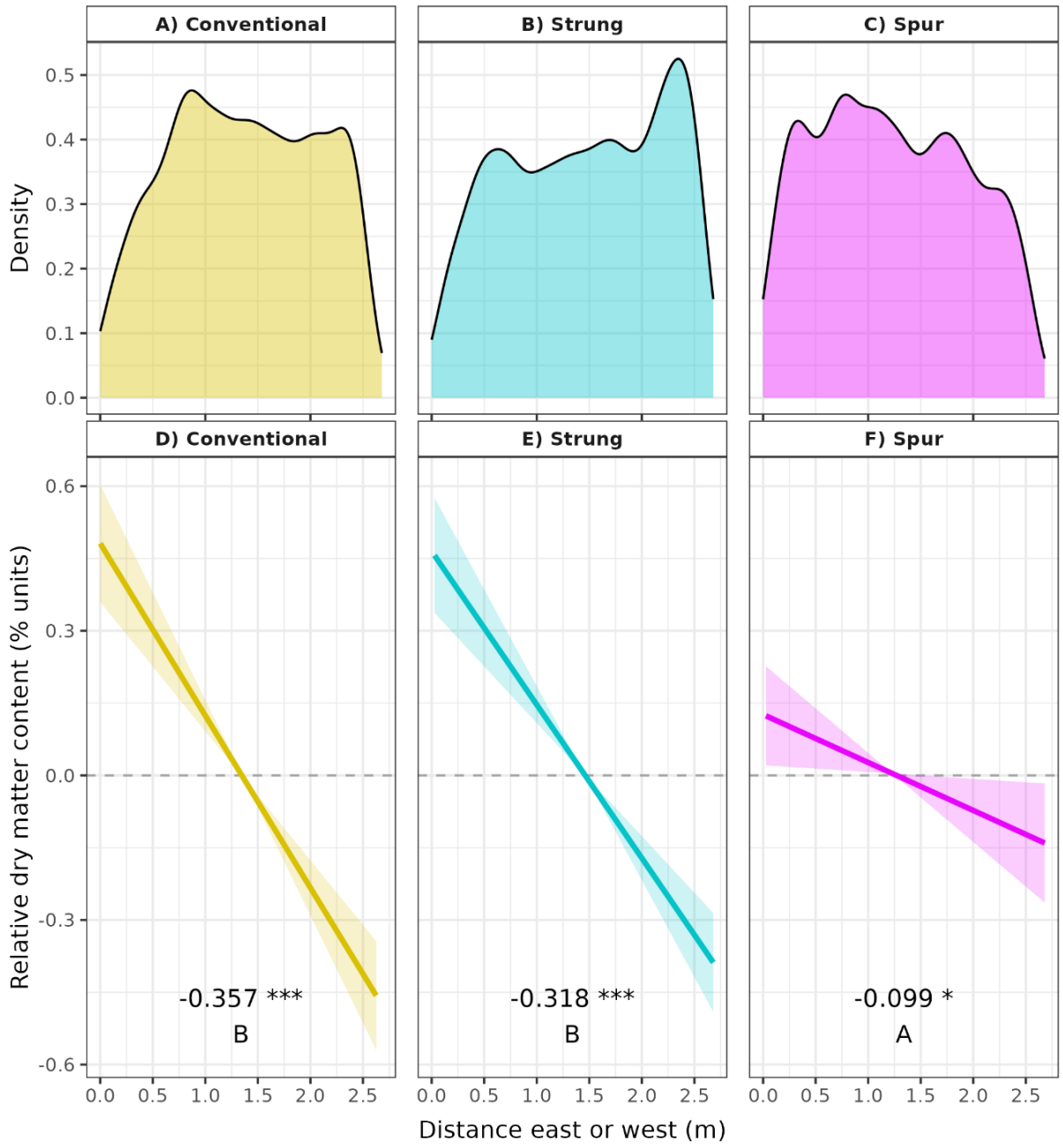


Figure 2.10. Distribution and model-estimated effect of fruit position within the canopy along the east–west axis on fruit relative dry matter content in *Actinidia chinensis* var. *chinensis* 'Zesy002'. Panels A–C show the distribution of fruit across the canopy for each management treatment, expressed as kernel density plots of all measured fruit. Panels D–F display fitted relationships between distance east or west from the cordon and fruit dry matter content (centred on the vine mean) at harvest, based on estimated marginal trends from a linear mixed-effects model. Slopes represent the expected increase in dry matter per metre east or west from the cordon, controlling for other covariates in the model. Shaded ribbons indicate 95% confidence intervals. Numeric values within each panel indicate the estimated slope and its significance level (*** $p < 0.001$), while uppercase letters below the slope denote differences in the slope between treatments. Slopes that do not share a letter differ significantly based on pairwise comparisons (Šidák adjusted $\alpha = 0.05$).

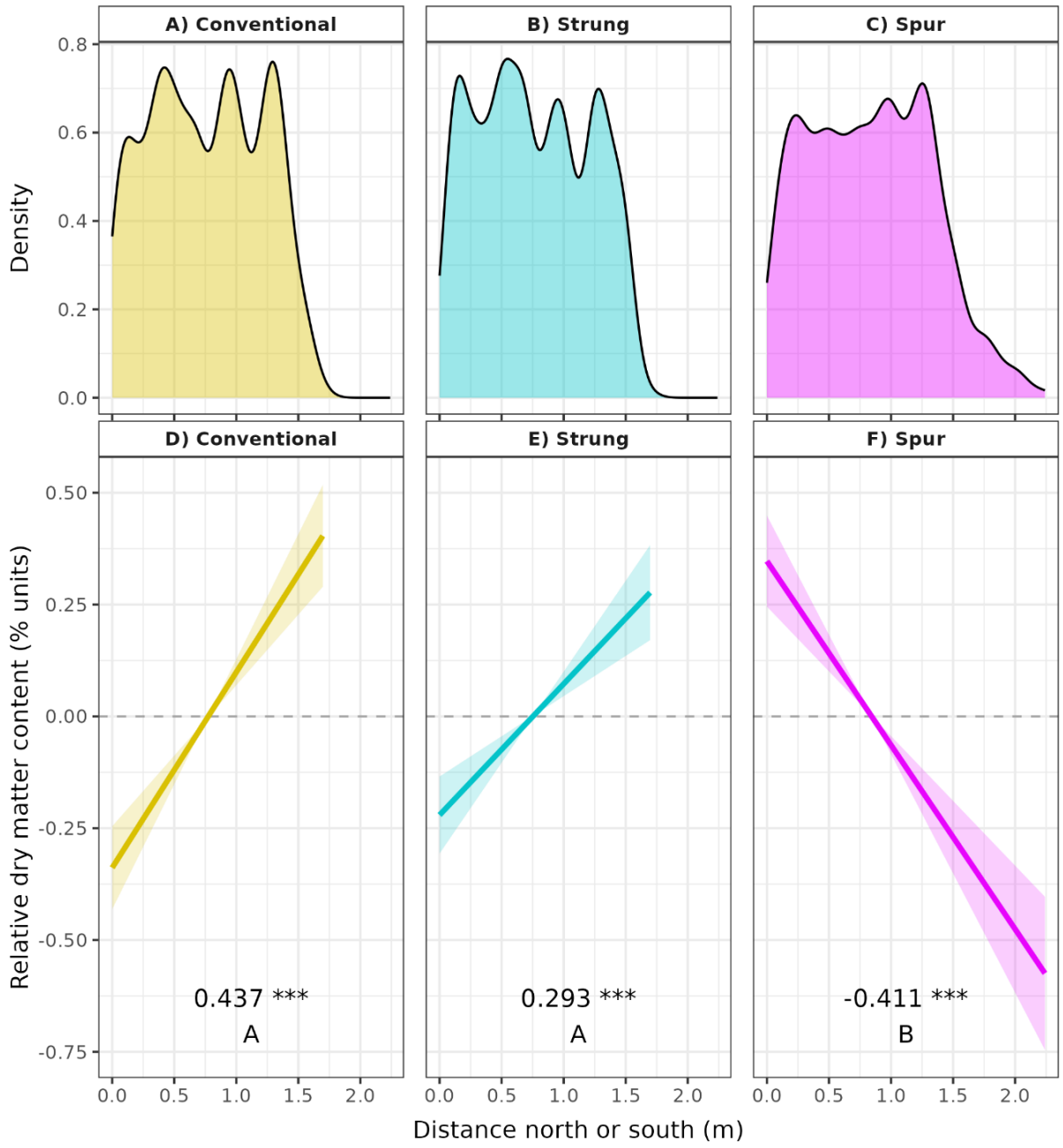


Figure 2.11. Distribution and model-estimated effect of fruit position within the canopy along the north–south axis on fruit relative dry matter content in *Actinidia chinensis* var. *chinensis* 'Zesy002'. Panels A–C show the distribution of fruit across the canopy for each management treatment (A: Conventional, B: Strung, C: Spur), expressed as kernel density plots of all measured fruit. Panels D–F display fitted relationships between distance north or south from the vine centre (in metres) and fruit dry matter content (centred on the vine mean) at harvest, based on estimated marginal trends from a linear mixed-effects model. Slopes represent the expected increase in dry matter content per metre north from the vine centre, after adjusting for other covariates in the model. Shaded ribbons indicate 95% confidence intervals. Numeric values within each panel indicate the estimated slope and its significance level (*** $p < 0.001$), while uppercase letters below the slope denote differences in the slope between treatments. Slopes that do not share a letter differ significantly based on pairwise comparisons (Šidák adjusted $\alpha = 0.05$).

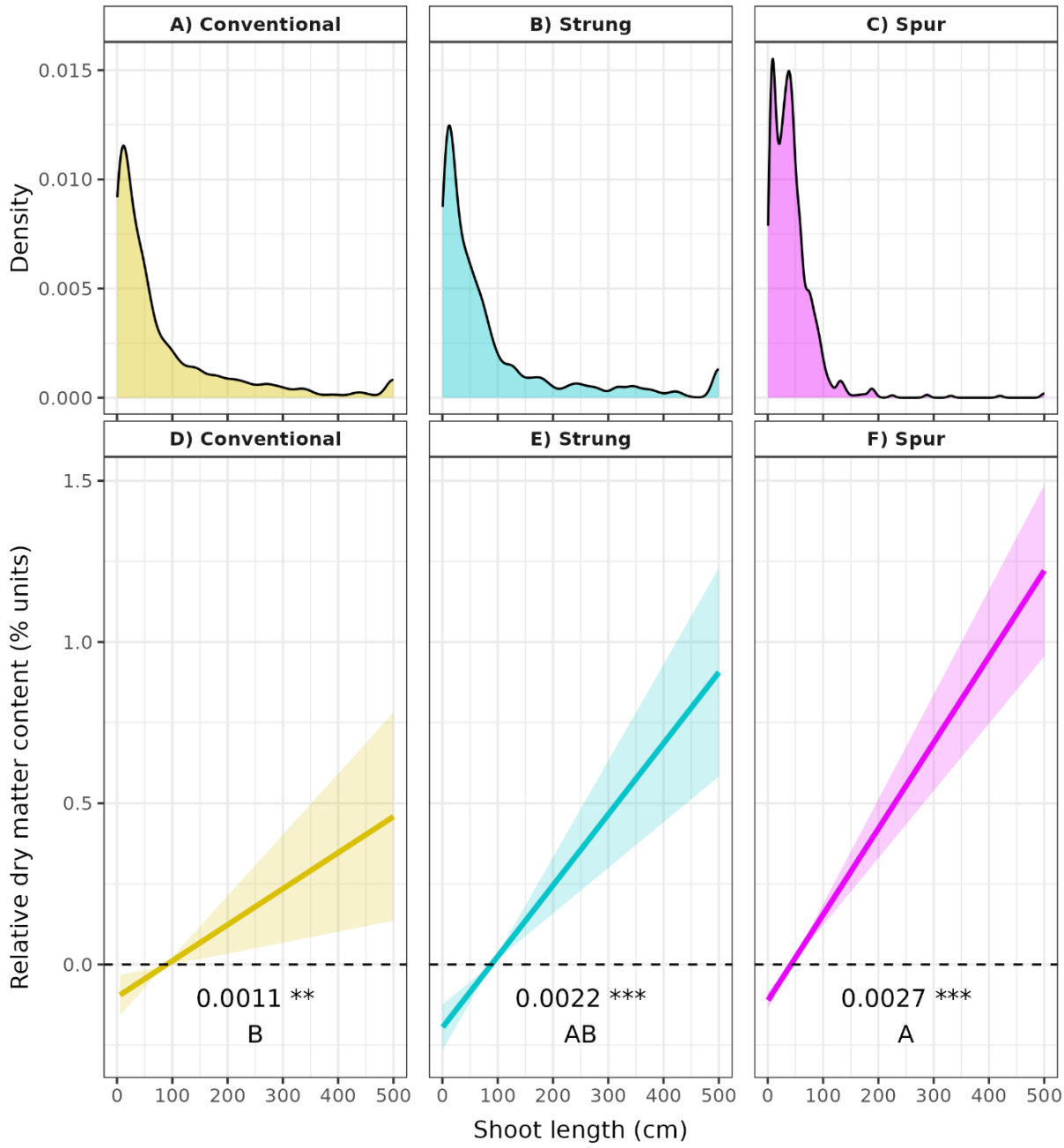


Figure 2.12. Distribution and model-estimated effect of shoot length on fruit relative dry matter content in *Actinidia chinensis* var. *chinensis* 'Zesy002'. Shoot length was measured after harvest and only includes the primary shoot axis (i.e. excludes secondary growth). Shoots lengths were truncated at 500 cm. Panels A–C show the distribution of shoot lengths for each canopy management treatment, expressed as kernel density plots of all measured shoots. Panels D–F display fitted relationships between shoot diameter (mm) and fruit dry matter content (centred on the vine mean) at harvest, based on estimated marginal trends from a linear mixed-effects model. Slopes represent the expected increase in dry matter content per centimetre increase in shoot length, after adjusting for other covariates in the model. Shaded ribbons indicate 95% confidence intervals. Numeric values within each panel indicate the estimated slope and its significance level (** $p < 0.01$; *** $p < 0.001$), while uppercase letters below the slope denote differences in the slope between treatments. Slopes that do not share a letter differ significantly based on pairwise comparisons (Šidák adjusted $\alpha = 0.05$).

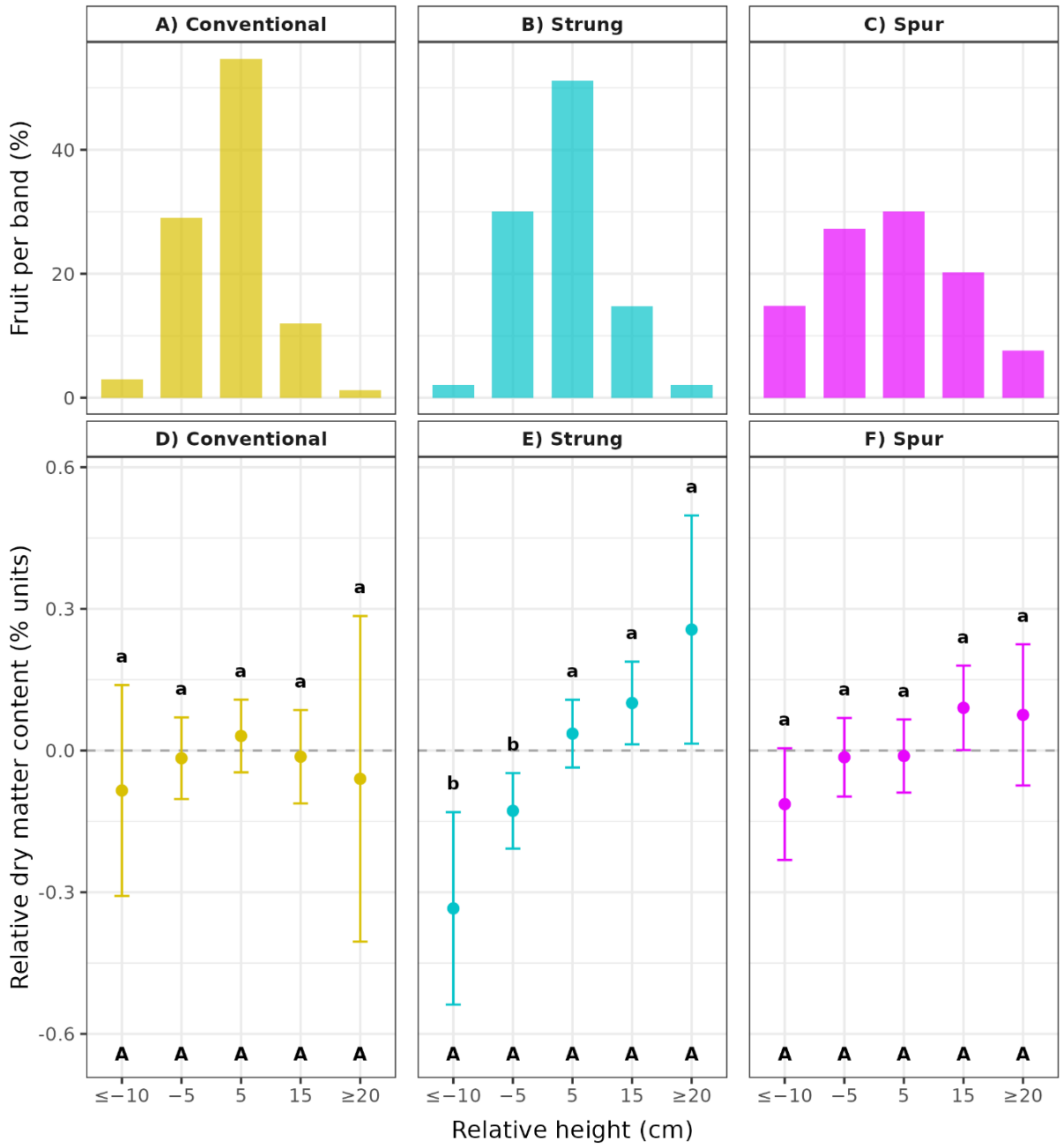


Figure 2.13. Distribution of relative height in the canopy and model-estimated effects on fruit relative dry matter content in *Actinidia chinensis* var. *chinensis* 'Zesy002'. Relative height was measured at the stylar end of the fruit and assigned to 10 cm bands (e.g. 5 cm = all fruit whose stylar ends were between 0 and 10 cm above the canopy wire). Due to limited replication, fruit more than 10 cm below the canopy wires have been combined, as have all fruit 20 cm above the canopy wires. Panels A–C show the distribution of relative height in the canopy, expressed as the percentage of total fruit within each treatment. Panels D–F display estimated marginal means for fruit dry matter content (centred on the vine mean) at harvest, derived from a linear mixed-effects model that accounts for other measured shoot- and fruit-level covariates. Lowercase letters above points denote groupings between relative height groups within each treatment panel, while uppercase letters along the x-axis indicate groupings across treatments for a given height. Means that do not share a letter differ significantly based on pairwise comparisons (Šidák adjusted $\alpha = 0.05$). Error bars represent 95% confidence intervals.

### 2.3.3 Correlations between predictors

Numerous correlations were observed among predictor variables, with several clear and treatment-specific patterns in both the strength and direction of these relationships (Figure 2.14). In particular, correlations differed between spatial position variables and shoot vigour traits, and were consistently weaker or altered in spur-managed vines compared with conventional and strung treatments

In all three treatments, distance E/W was moderately negatively correlated with shoot diameter, internode diameter, and relative height (Figure 2.14 AE–AG), indicating that fruit located further east or west from the vine centre tended to be associated with lower shoot vigour. This negative association with internode diameter was weaker in strung vines than in conventional and spur vines. Additionally, in both conventional and strung treatments, distance E/W was also negatively correlated with shoot length (Figure 2.14 AD). In contrast, correlations between distance N/S and other predictor variables were uniformly weak across treatments, with correlation coefficients generally ranging between −0.15 and 0.1 (Figure 2.14 BA–BH). This suggests that variation along the north–south axis contributed little to structured covariation among shoot or fruit attributes.

Timing of anthesis was most strongly correlated with the number of fruit per shoot, with shoots bearing more fruit tending to flower earlier and those with fewer fruit tending to flower later (Figure 2.14 CG). Weaker correlations were also observed between timing of anthesis and shoot vigour traits. In conventional and spur vines, thicker shoots showed a slight tendency to flower earlier (Figure 2.14 CE), whereas in strung vines internode diameter was weakly positively correlated with timing of anthesis (Figure 2.14 CF).

Strong intercorrelations were observed among shoot vigour traits in all treatments. Shoot length and shoot diameter were strongly correlated, particularly in conventional and strung vines, with spur vines showing a consistently weaker relationship (Figure 2.14 DE). Shoot length was also strongly correlated with internode diameter (Figure 2.14 DF) and moderately correlated with relative height in conventional and strung vines (Figure 2.14 DH). Together, these relationships indicate that longer shoots tended to have thicker diameters, originate from thicker internodes, and bear fruit higher in the canopy, although these associations were consistently weaker in spur vines.

Consistent with these patterns, shoot diameter was strongly positively correlated with internode diameter and relative height across treatments (Figure 2.14 EF, EH), and showed weaker

positive correlations with fruit number per shoot (Figure 2.14 EG). In general, thicker shoots tended to originate from thicker internodes, carry fruit higher in the canopy, and bear slightly more fruit per shoot.

In addition to its association with shoot diameter and shoot length, internode diameter was also positively correlated with relative height, most strongly in spur vines and to a moderate extent in conventional and strung vines (Figure 2.14 FH). In these cases, fruit borne on thicker internodes tended to be positioned higher within the canopy.

Relationships between fruit number per shoot and relative height differed between treatments. In both conventional and strung vines, fruit positioned lower in the canopy tended to be borne on shoots carrying more fruit (Figure 2.14 GH). In contrast, this relationship was reversed in spur vines, where fruit positioned higher in the canopy were more likely to originate from shoots with higher fruit numbers. Other correlations involving fruit number per shoot or relative height were weak and are described above.

Strong correlations were also observed among shoot length, shoot diameter, number of leaves, and total leaf area in destructively harvested intact shoots (Figure 2.15). Shoot length and number of leaves showed the strongest correlation, whereas shoot length and shoot diameter exhibited the weakest relationship among these traits.

Figure 2.14. Correlation matrix of shoot- and fruit-level predictor variables. *(Figure on next page)*. Variables are: A) distance from the cordon east or west (E/W, cm), B) distance from the trunk north or south (N/S, cm), C) timing of anthesis (days since flowering commenced), D) shoot length (cm), E) shoot basal diameter (mm), F) internode diameter (mm), G) fruit per shoot, and H) relative fruit height in the canopy (cm). Each point represents an individual fruit from three whole-vine populations per treatment. Lower-left panels show scatterplots and major-axis regression lines fitted to the full dataset (black dashed line) and separately by treatment (conventional = yellow; strung = cyan; spur = magenta). Diagonal panels show the distribution for each variable by treatment. Upper-right panels show Pearson correlation coefficients for each pairwise comparison calculated for the full dataset (black) and for each treatment individually (coloured text). Asterisks indicate the significance of each correlation under the null hypothesis of no linear relationship between variables: *$p < 0.05$; **$p < 0.01$; ***$p < 0.001$.

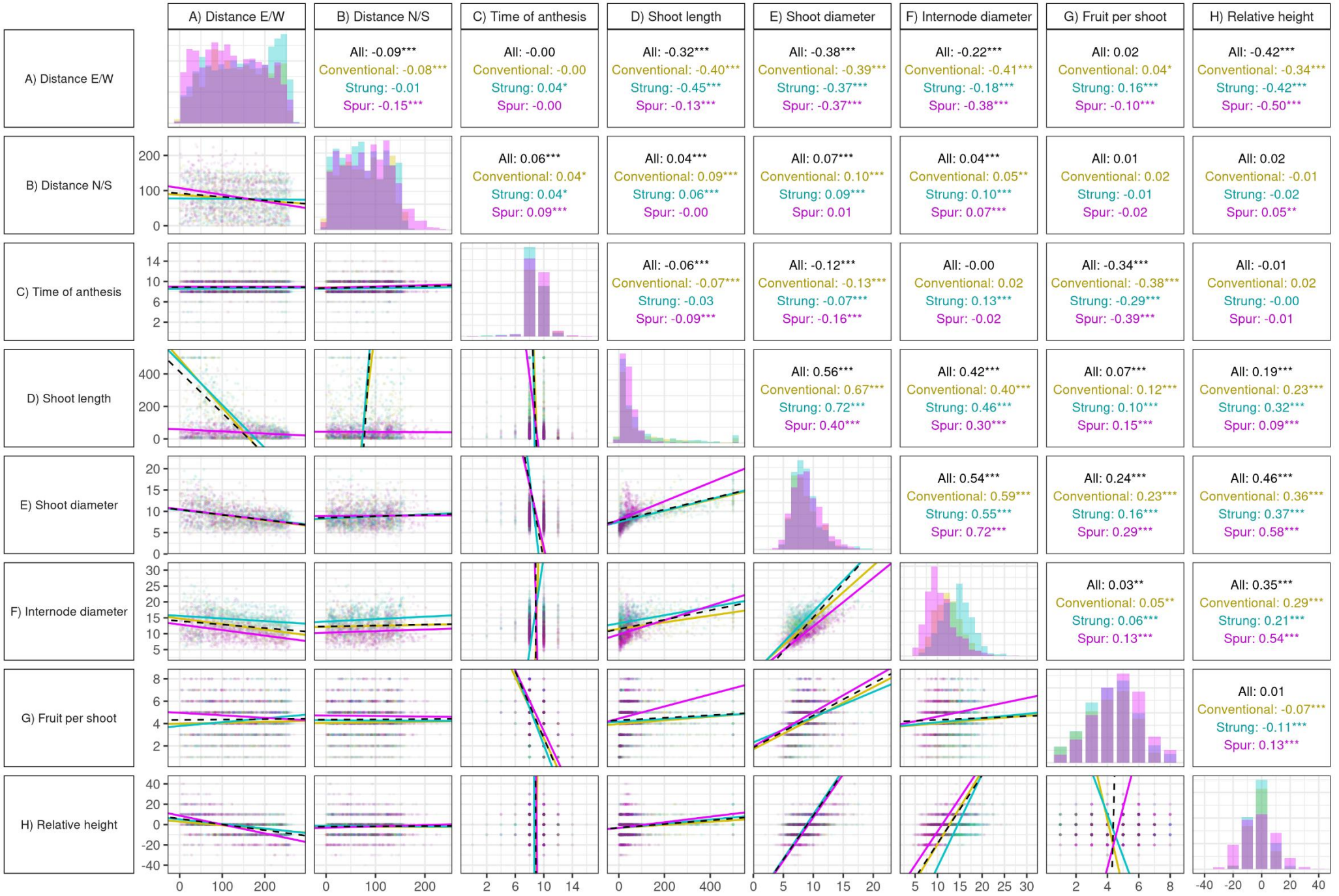
A) Distance E/W
B) Distance N/S
C) Time of anthesis
D) Shoot length
E) Shoot diameter
F) Internode diameter
G) Fruit per shoot
H) Relative height
All: -0.09***
Conventional: -0.08***
Strung: -0.01
Spur: -0.15***
All: -0.00
Conventional: -0.00
Strung: 0.04*
Spur: -0.00
All: -0.32***
Conventional: -0.40***
Strung: -0.45***
Spur: -0.13***
All: -0.38***
Conventional: -0.39***
Strung: -0.37***
Spur: -0.37***
All: -0.22***
Conventional: -0.41***
Strung: -0.18***
Spur: -0.38***
All: 0.02
Conventional: 0.04*
Strung: 0.16***
Spur: -0.10***
All: -0.42***
Conventional: -0.34***
Strung: -0.42***
Spur: -0.50***
All: 0.06***
Conventional: 0.04*
Strung: 0.04*
Spur: 0.09***
All: 0.04***
Conventional: 0.09***
Strung: 0.06***
Spur: -0.00
All: 0.07***
Conventional: 0.10***
Strung: 0.09***
Spur: 0.01
All: 0.04***
Conventional: 0.05**
Strung: 0.10***
Spur: 0.07***
All: 0.01
Conventional: 0.02
Strung: -0.01
Spur: -0.02
All: 0.02
Conventional: -0.01
Strung: -0.02
Spur: 0.05**
All: -0.06***
Conventional: -0.07***
Strung: -0.03
Spur: -0.09***
All: -0.12***
Conventional: -0.13***
Strung: -0.07***
Spur: -0.16***
All: -0.00
Conventional: 0.02
Strung: 0.13***
Spur: -0.02
All: -0.34***
Conventional: -0.38***
Strung: -0.29***
Spur: -0.39***
All: -0.01
Conventional: 0.02
Strung: -0.00
Spur: -0.01
All: 0.56***
Conventional: 0.67***
Strung: 0.72***
Spur: 0.40***
All: 0.42***
Conventional: 0.40***
Strung: 0.46***
Spur: 0.30***
All: 0.07***
Conventional: 0.12***
Strung: 0.10***
Spur: 0.15***
All: 0.19***
Conventional: 0.23***
Strung: 0.32***
Spur: 0.09***
All: 0.54***
Conventional: 0.59***
Strung: 0.55***
Spur: 0.72***
All: 0.24***
Conventional: 0.23***
Strung: 0.16***
Spur: 0.29***
All: 0.46***
Conventional: 0.36***
Strung: 0.37***
Spur: 0.58***
All: 0.03**
Conventional: 0.05**
Strung: 0.06***
Spur: 0.13***
All: 0.35***
Conventional: 0.29***
Strung: 0.21***
Spur: 0.54***
All: 0.01
Conventional: -0.07***
Strung: -0.11***
Spur: 0.13***

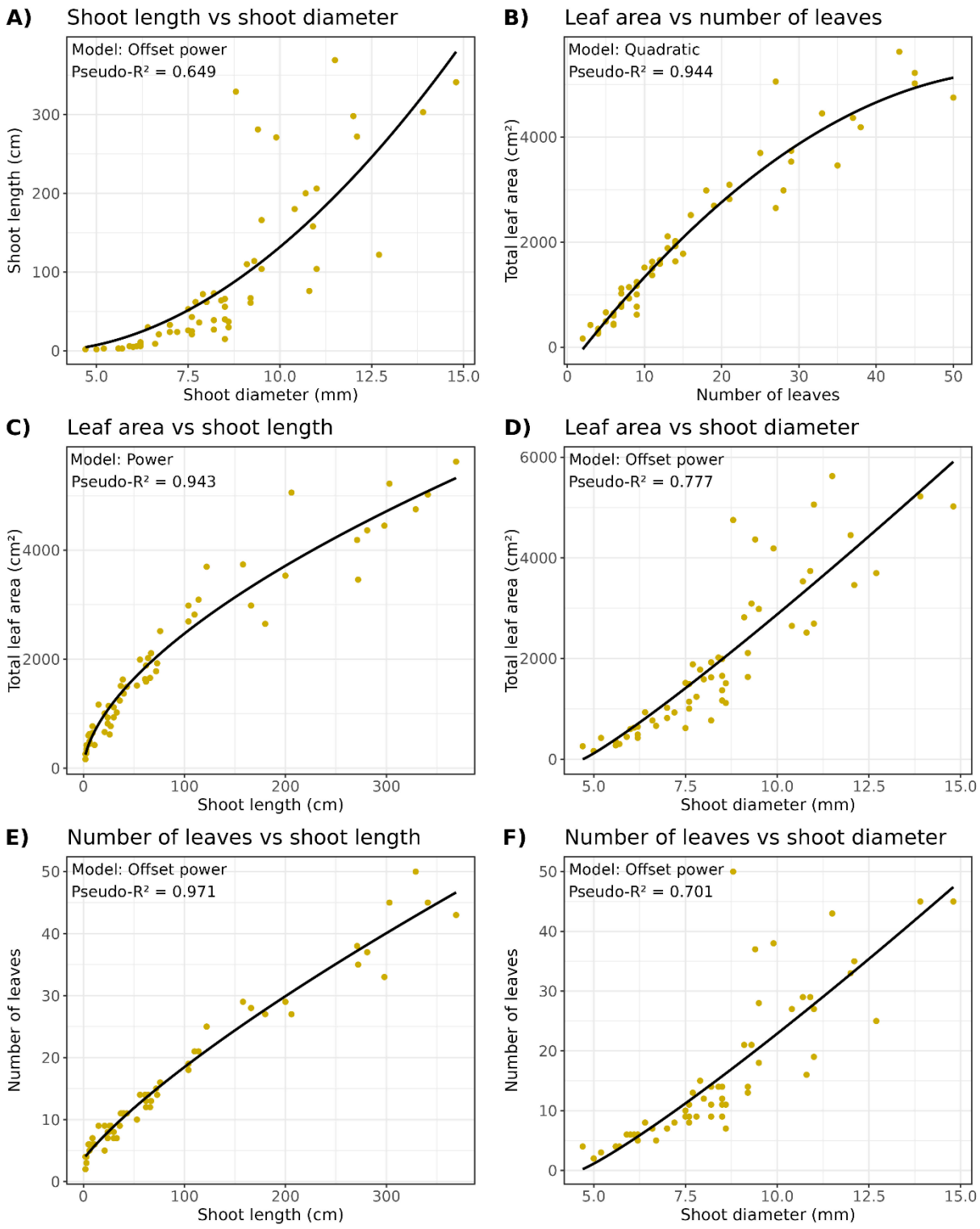


Figure 2.15. Relationships between total leaf number, leaf area, shoot length, and shoot basal diameter for intact *Actinidia chinensis* var. *chinensis* 'Zesy002' shoots measured in late summer. Shoots were sourced from vines adjacent to those studied for within-vine fruit variability. Linear, quadratic, or power models were fitted to the data; panels show the best fits selected based on Akaike information criterion values and visual inspection. Pseudo $R^2$ is a goodness-of-fit metric and represents the proportion of total variation in the data that is explained by the selected model.

## 2.4 Discussion

### 2.4.1 Effects of position within shoot reflect meristem size and phyllotaxy

Both FW and DM were influenced by the position of fruit within shoots, although the effects were stronger and more consistent across treatments for FW. Several physiological factors may contribute to these patterns, including variation in floral meristem size, phyllotactic organisation and vascular connectivity, subtending leaf size, and the timing of leaf expansion.

As detailed in section 1.2.1, floral meristems within dormant kiwifruit axillary buds vary in size and likelihood of developing into mature flowers, with both traits peaking in the middle of the potentially floral nodes and declining sharply on either side (Walton & Fowke, 1993; Walton et al., 1997). Although this pattern was described for 'Hayward' buds, it also closely aligns with the effects of position within shoots on fruit FW observed in 'Zesy002', particularly on shoots bearing five or more fruit where a fuller range of nodal positions can be compared. Floral meristem size prior to budbreak may therefore exert a residual influence on subsequent flower and fruit growth, potentially through increased sink strength associated with greater cell number or enhanced vascular connectivity.

Subtending leaf size is likely to strongly influence carbohydrate availability to flowers, particularly prior to anthesis when competition for NSCs among sinks is intense. When fully expanded, leaves subtending nodes in the middle of the potentially floral zone typically have larger lamina than those at more basal or distal nodes (Greer, 1996; Richardson et al., 2021; Snowball, 1995). Lai et al. (1988) demonstrated that approximately 60% of photoassimilate exported from a ^14C-labelled leaf is delivered directly to its subtending fruit, therefore the area and light interception of individual subtending leaves will strongly influence carbohydrate availability to flowers and fruits.

The timing of leaf expansion is also likely to contribute to positional differences in fruit growth. Although leaves at more basal nodes tend to be smaller, they reach full expansion earlier in spring (Seleznyova & Greer, 2001) and become net carbon exporters within weeks of budbreak (Greer, 1996). In contrast, leaves further along the shoot take longer to become net exporters, and may therefore contribute less photoassimilate to support floral development during early spring growth.

Phyllotactic arrangement and the resulting vascular connectivity between nodes are also intrinsically linked to the carbon balance of individual flowers and fruit. In addition to photoassimilate supplied by their subtending leaf (node $n$), kiwifruit fruit have been shown to

import substantial photoassimilate from leaves at nodes $n + 5$ and $n + 8$ (Lai et al., 1988). Consequently, flowers or fruit at basal floral nodes may partially compensate for smaller subtending leaves by receiving assimilates from larger leaves further along the shoot. However, as fruit number per shoot increases, the likelihood of multiple fruit sharing an orthostichy also increases, leading to direct competition for photoassimilate. Proximity to a source has been shown to be a strong determinant of assimilate allocation between competing sinks (Lai et al., 1989b; Wu et al., 2005). It is therefore likely that photoassimilate distribution among competing fruit within an orthostichy is largely governed by spatial proximity, although this remains poorly tested experimentally.

The combination of these factors may help to explain the FW patterns observed within shoots in this chapter. Smaller distal fruit may reflect delayed leaf expansion at more distal nodes and the resulting lag before these leaves become net carbon sources. The additional pattern of reduced FW in basal fruit on shoots with high fruit numbers may relate to the underlying distribution of floral meristem size within dormant axillary buds, as well as increased competition for photoassimilate with distal fruit within shared orthostichies.

The effect of fruit position within shoots on DM was weaker than for FW. Only the most distal one to two fruit showed significantly lower DM within shoots, a pattern that was most evident in strung vines and largely absent in spur vines. Because smaller fruit tend to have lower DM (Appendix Figure A12), phyllotaxy-related reductions in FW of distal fruit may also reduce sink strength (Marcelis, 1996), thereby reducing their ability to import photoassimilates during the dry matter accumulation stage of fruit growth.

If fruit FW were the sole within-shoot driver of DM, smaller basal fruit would also be expected to exhibit reduced DM, which was not observed. Although basal fruit are further from larger source leaves along the shoot, they are also closer to adjacent shoots that may have higher L:F. This proximity may facilitate access to imported carbohydrates sufficient to offset local source limitations (Lai et al., 1989b; Snelgar et al., 1986). As fruit DM accumulation accelerates approximately 60 days after anthesis (Clearwater et al., 2007; Le Lievre et al., 2021; Richardson et al., 2021), photoassimilate distribution may become increasingly integrated within and between shoots through the formation or activation of vascular connections between orthostichies (Aloni & Barnett, 1996; Aloni & Peterson, 1990; De Schepper et al., 2013; Lai et al., 1989b).

### 2.4.2 Early carbohydrate availability influences shoot growth and FW variability

Beyond positional effects within shoots, variability in FW was also strongly and consistently influenced by timing of anthesis, shoot diameter and distance E/W in the canopy. These factors can largely be interpreted in terms of their relationships to carbohydrate availability to individual shoots, flowers and fruit during early spring growth.

#### *2.4.2.1 Timing of anthesis*

The strong effect of timing of anthesis on FW is consistent with findings in a number of horticultural species including apples, cherries, peaches, persimmons and tomatoes (Bohner & Bangerth, 1988; Hasegawa & Nakajima, 1990; Patten et al., 1986; Spencer & Couvillon, 1975; Sullivan, 1965). In kiwifruit, differentiation of floral primordia can begin as early as bud swell, approximately 10 days prior to budbreak (Brundell, 1975c; Snowball & Considine, 1986). By flowering, differential developmental rates between flowers can manifest as differences in individual ovary size and timing of anthesis (Cruz-Castillo et al., 1991; Lai et al., 1990; Richardson et al., 2019), or as floral abortion as competition for resources intensifies (Linsley-Noakes & Allan, 1987; Snowball & Considine, 1986).

Flowers that open earlier and/or have larger ovaries typically exhibit faster growth following fruit set, resulting in larger fruit at harvest (Brantley et al., 2019; Cruz-Castillo et al., 2002; Nardozza et al., 2015; Patterson et al., 1999; Richardson et al., 2019; Smith et al., 1994). Over a wide flowering window, some of this FW difference could be fairly attributed to the lag in fruit development in later-opening flowers. However, in the current chapter the largest marginal effect (i.e. after controlling for other predictors) of anthesis timing was an 8.8 g difference in FW at harvest, arising from a two-day difference in anthesis. This difference is too large to be accounted for by a mere lag in fruit development and instead emphasises the intense competition for carbohydrates during early flower and fruit development, resulting in persistent effects on subsequent sink strength and fruit growth.

#### *2.4.2.2 Shoot basal diameter*

Shoot basal diameter was a consistent driver of harvest FW, ranking third in importance in all three treatments and explaining over 13% of the overall variability. The most likely causal mechanism underlying this relationship is the local availability of NSC reserves and photoassimilates during early shoot and flower growth.

As detailed in section 1.3.1, early shoot growth is highly influenced by the availability of local NSC reserves (Piller et al., 1998), and can strongly affect subsequent local carbon balance (Piller & Meekings, 1997). The strong correlations between shoot basal diameter, shoot length and internode diameter observed in this chapter support the notion that proximity to larger internode reserves facilitates early shoot growth, and this access to NSC reserves may also directly support early flower development. By the time of anthesis, vigorous, thicker shoots can also support rapid fruit growth via a larger abundance of photoassimilate availability.

The stronger predictive power of shoot basal diameter relative to shoot length reflects differences in their developmental timing and sensitivity to canopy management. Approximately 50% of a shoot's final diameter can be attained within two weeks of budbreak, whereas shoot elongation accelerates later and continues for longer (Richardson et al., 2017). Although shoot length and basal diameter are strongly correlated on unpruned shoots (Figure 2.15 A), management practices such as summer pruning and tip-crushing can decouple these traits by reducing shoot length and leaf area with minimal effect on basal diameter (Patterson & Currie, 2011). As shoot measurements were taken after harvest, basal diameter likely provides a more robust proxy for early-season growth conditions and local carbohydrate availability during flower and fruit development.

Previous studies have observed similar effects of shoot diameter on fruit FW (Dattola et al., 2024; Gullo et al., 2025), but others have not (Richardson et al., 2021). There are several reasons why the influence of shoot type on FW may not always be detected. The large number of fruit (>9,700) and shoot (>2,700) replicates in the current study provide a high degree of statistical sensitivity to effects on fruit quality. Further sensitivity is gained by utilising shoot basal diameter as a continuous variable, as opposed to grouping shoots into categories based on shoot length or vigour. The results presented in this chapter also demonstrate that there are multiple drivers of FW that may confound results if not accounted for. Finally, under conditions of intense competition, effects of NSC availability become more localised (Buwalda & Smith, 1990; Tombesi et al., 1993). The vines in this chapter carried a moderately high crop load (65 fruit/m² average), and therefore likely experienced intense competition for resources between shoots, particularly during early fruit growth. Under conditions of reduced competition, shoot-level effects on FW may be more difficult to detect.

#### *2.4.2.3 Distance east or west in the canopy*

Distance east–west within the canopy was a significant driver of FW across all treatments, explaining over 7% of total variability. Several physiological gradients vary along this spatial axis, including shoot length and shoot diameter. Internode diameter, a major determinant of local NSC storage capacity (see Chapter , Figure 3.4), also declined with increasing distance E/W in all treatments. In conventional and strung vines this largely reflects the tapering of canes from base to tip (see Figure 3.6), and in spur vines a similar spatial pattern persisted despite multiple seasons of low-vigour management. Shoots nearer to the cordon may also have greater access to trunk and root carbohydrate reserve pools, also potentially contributing to early shoot and fruit growth. Based on these relationships, a negative correlation between FW and distance E/W might be expected. However, no such relationship was evident in the raw data for any treatment (Appendix Figure A11). This indicates the presence of at least one opposing biological factor that counteracts the positive influence of shoot vigour on FW along the E/W axis.

Pollination efficacy and timing of anthesis are two plausible contributors. Although pollination efficacy can decline with distance from male vines (Testolin, 1991), no significant relationship was observed between distance E/W and seed number or total seed mass (Figure A14), suggesting relatively uniform pollination across the canopy. A within-vine variability study in 'Hayward' observed increasing FW with distance E/W, and attributed this to a spatial gradient in anthesis timing where earlier flowers were located near the ends of canes (Smith et al., 1994). In contrast, earlier flowers were more common nearer to the cordon in 'Hort16A', and were not associated with higher FW (Boyd et al., 2008a). In the current study, no strong association between distance E/W and timing of anthesis was detected; however, the compressed flowering window and bi-daily sampling may have limited detection of subtle spatial trends. Given the strong influence of timing of anthesis on FW, even small undetected gradients could plausibly generate the observed marginal effect of distance E/W.

### 2.4.3 Local photoassimilate availability drives variability in dry matter content

There were clear differences between treatments for the drivers of DM, which can largely be interpreted in terms of differences in canopy structure and the resulting effects on local photoassimilate availability during the dry matter accumulation phase of fruit growth.

#### *2.4.3.1 Shoot length and distance east or west in the canopy*

In both conventional and strung vines, DM was strongly influenced by distance E/W, where DM was highest near to the cordon and reduced along the length of canes. These spatial patterns of DM are similar to those observed within 'Hayward' and 'Hort16A' vines grown on pergolas

(Boyd et al., 2008a; Smith et al., 1994). In both conventional and strung treatments, long shoots were retained near the cordon to form the next season's replacement canes, driving the strong negative correlations between shoot length and distance E/W. Long, non-terminated shoots have previously been shown to produce higher DM fruit on 'Hayward' vines (Buxton, 2005), and long shoots were shown to have significantly higher L:F and leaf area per fruit than medium or spur shoots in 'Zesy002' (Gullo et al., 2025). However, in red-fleshed *A. chinensis* cultivars, shoot length appears to influence anthocyanin accumulation more strongly than DM (Nardozza et al., 2015; Richardson et al., 2021).

Notably, in both conventional and strung treatments the marginal effect of distance E/W on DM was stronger than the marginal effect of shoot length. This suggests that in these treatments the numerous long shoots near the cordon increased the local photoassimilate availability for not only the individual long shoots, but also other shoots in their proximity. As detailed in section 1.3.4, kiwifruit vines can translocate photoassimilates from shoots with high L:F to those with lower L:F; however, this translocation declines with distance and increasing competition (Lai et al., 1989b; Tombesi et al., 1993). As leaf area on non-terminated kiwifruit shoots continues to increase until mid-summer (Richardson et al., 2021), the resulting elevated photoassimilate availability near the cordon is likely to be particularly influential during the dry matter accumulation phase of fruit growth. Shoots of all lengths near the cordon may also have greater access to light due to the positioning and orientation of replacement cane shoots, which tend to form a V-shape away from the cordon (Figure 2.1), while shoots further from the cordon are more likely to be shaded by the long replacement shoots. Together, these patterns indicate that proximity to long, high L:F shoots near the cordon increases local photoassimilate availability during the dry matter accumulation phase, producing a strong spatial gradient in DM.

#### *2.4.3.2 Distance north or south in the canopy*

Distance N/S within the canopy also contributed to variability in DM, but the direction and magnitude of this effect differed markedly between treatments. In conventional and strung vines, DM increased with increasing distance N/S from the trunk, whereas in spur vines this relationship was inverted. In contrast to distance E/W, distance N/S was not strongly correlated with shoot length in any treatment, suggesting that this spatial pattern is not driven by differences in shoot vigour or leaf area distribution alone. The physiological basis of this effect is therefore less clear than for distance E/W, but may relate to proximity effects on the allocation and translocation of photoassimilates between shoots, structural wood, and reserve pools

After the mobilisation of starch reserves to support spring growth, trunk and root reserve pools are gradually replenished over the remainder of the growing season (Richardson et al., 2017; Smith et al., 1992)(Richardson et al., 2017; Smith et al., 1992). Shoots located closer to the trunk may therefore contribute a greater proportion of exported photoassimilates to reserve replenishment (Buwalda & Smith, 1990), potentially reducing the allocation of assimilates to fruit DM accumulation. This interpretation is consistent with the increase in DM observed with increasing distance north or south from the trunk in conventional and strung vines, and with similar patterns reported previously in 'Hayward' (Smith et al., 1994). In spur vines, the inversion of this spatial relationship suggests that canopy structure fundamentally alters the scale and pathways of carbohydrate distribution. The greater volume of multi-year structural wood retained under spur management may act as a more distributed canopy reserve pool, potentially reducing positional gradients in carbohydrate availability for fruit DM accumulation. However, there is currently a lack of direct experimental evidence to confirm these hypothesised patterns of carbohydrate reserve dynamics.

#### *2.4.3.3 Relative height*

In strung treatment vines, fruit that hung at least partially below the canopy wires had significantly lower DM than those positioned higher in the canopy. This pattern is consistent with observations in 'Hayward' vines, where DM declined sharply with decreasing fruit height under both pergola and T-bar systems Across all treatments, fruit height was also associated with other spatial and structural factors, with lower-hanging fruit more commonly borne on shoots with smaller basal diameters and at greater distances east or west from the cordon.

The most likely driver of this height-related effect on DM is variation in light environment and the resulting differences in local photosynthetic capacity. Fruit positioned below the canopy are more likely to be borne on shoots that are shaded by their neighbours, particularly during the dry matter accumulation phase, when fruit growth is strongly dependent on newly fixed photoassimilate supply. In strung vines, this effect is likely exacerbated by the dense shade cast by vigorous replacement canes trained vertically up strings, increasing self-shading within the canopy. In contrast, replacement canes on conventional vines tend to be less vigorous and more pendulous (Figure 2.1), which may reduce the degree of self-shading.

Although not directly quantified in this study, shoot orientation is also likely to contribute to variation in fruit height. Upward-facing buds are more likely to produce shoots in spring (Friend et al., 2014), but shoot orientation can change over the season due to wind exposure and

increasing fruit mass. Fruit on spur vines exhibited a wider distribution of heights, but the more intensive canopy management and lower overall shoot vigour under spur pruning may have reduced height-related shading effects, consistent with the weaker influence of relative height on DM in this treatment.

## 2.5 Conclusions

This chapter demonstrated that position within shoots, timing of anthesis and early shoot growth are strong drivers of variability in kiwifruit FW at harvest. These factors are strongly linked to floral meristem size, early carbohydrate availability and floral development, with subsequent effects on sink strength and fruit growth after anthesis. The three canopy management treatments were similarly influenced by these factors, suggesting bud meristem development and spatial patterns of carbohydrate reserves were not strongly affected by canopy management.

Drivers of variability in fruit DM reflected the influence of canopy management and structure on photoassimilate availability during the dry matter accumulation stage of fruit growth. Proximity to leaf area, as reflected by parent shoot length and canopy position, was a strong driver of DM in all three treatments. In strung and conventional vines, the high leaf area of long shoots concentrated near the cordon produced a strong east-west gradient in DM. The export of photoassimilates from these shoots likely also supports DM accumulation in nearby fruit. In spur treatment vines, shoot length was more uniform across the canopy, but additional shoot length and leaf area still strongly increased the DM of fruit borne on longer shoots. Gradients of DM with distance north or south from the trunk were contrasting between treatments and possibly relate to competition for photoassimilate between fruit and replenishing reserve pools. Fruit height may reflect patterns of self-shading within the canopy that can also influence local photoassimilate availability.

# Chapter 3: Cane carbohydrate reserves and mobilisation

## 3.1 Introduction

As deciduous plants, kiwifruit vines rely on the mobilisation of carbohydrate reserves to support shoot and flower development in spring, prior to returning to a net positive carbon balance (detailed in section 1.3.1). The size and availability of reserves strongly influence early shoot growth, with growth rates declining sharply when carbohydrate supply is limited (Piller et al., 1998; Piller & Meekings, 1997). Reduced carbohydrate availability can also lead to shoot tip termination (Foster et al., 2007), floral abortion, and smaller ovaries (Piller et al., 1998; Richardson, 2015), with downstream effects on the timing of anthesis (Lai et al., 1990) and subsequent fruit growth and quality. As shown in Chapter 2, early shoot growth and anthesis timing are major drivers of fruit fresh weight and dry matter at harvest. Carbohydrate reserves are therefore critical determinants of reproductive performance in kiwifruit. Reserve pools of one-year-old canes are of particular relevance as they represent the most proximal and management-responsive reserve pool for supporting early spring growth.

Kiwifruit vines produce a range of shoot types in spring, commonly classified as short, medium, or long based on node number and shoot tip termination (Seleznyova et al., 2002). In contrast, the classification of one-year-old canes has been inconsistent across studies, with criteria variously based on cane length, basal diameter, or shoot termination status. Despite this variability in classification, longer or thicker canes generally exhibit higher budbreak and floral production, although responses have differed between cultivars and studies (Thorp et al., 2018; Thorp et al., 2003; Volz et al., 1992; Wilson, 1989). These differences in cane vigour are likely linked to variation in carbohydrate reserves accumulated during the previous season and mobilised in spring. In other deciduous species, reserve storage capacity has been shown to depend on internode anatomy and volumetric storage capacity (Eltom et al., 2013; Jupa et al., 2021). However, few studies have explicitly examined anatomical differences among kiwifruit cane types or cultivars or linked these traits directly to carbohydrate reserve size.

Existing studies of cane carbohydrate dynamics have instead focused on seasonal patterns of starch and sugar accumulation and mobilisation, demonstrating peak non-structural carbohydrate concentrations at leaf fall followed by rapid depletion from budbreak to anthesis (Richardson et al., 2017; Richardson, 2015; Smith et al., 1992). In the study by Smith et al. (1992), entire vines were destructively harvested at each time point, with all one-year-old canes pooled prior to analysis. As a result, these data describe average reserve dynamics at the

whole-vine scale, rather than variation among individual canes or cane types. Similarly, internodes analysed by Richardson (2015) were sampled from distal cane positions, but without characterisation of cane vigour or dimensions. Although Greaves et al. (1999) modelled how cane tapering reduces starch pools toward the cane tip, the empirical data they present aggregates concentrations across entire dormant canes. Additionally, these studies have focused exclusively on *A. chinensis* var. *deliciosa* 'Hayward'.

Consequently, it remains unknown whether carbohydrate reserve concentrations and pool sizes differ systematically among cane vigour types, internode positions, or cultivars, or whether internode anatomical traits provide a useful proxy for reserve storage capacity. It is also unclear whether patterns of spring reserve mobilisation differ between cultivars or cane types, and whether such differences influence the minimum reserve levels reached near anthesis. This chapter addresses these gaps by characterising cane anatomy and carbohydrate reserve dynamics across kiwifruit cultivars, cane vigour types, and positions along one-year-old canes during winter and spring.

## 3.2 Methods

### 3.2.1 Plant material

Kiwifruit vines used in this study were located in a mixed-cultivar block at the Bioeconomy Science Institute research orchard, Te Puke, Bay of Plenty, New Zealand. Trial vines were selected based on visual assessment of health as well as quantity and diversity of cane vigour. Five vines were selected from each of three kiwifruit cultivars: *A. chinensis* var. *deliciosa* 'Hayward', *A. chinensis* var. *chinensis* 'Zesy002' and *A. chinensis* var. *chinensis* 'Zes008'. Rootstocks were *A. chinensis* var. *deliciosa* 'Bruno' seedlings planted in 2012, with scions grafted between 2012 and 2016 depending on cultivar. Vine management was typical of that described for conventional treatment vines in Chapter 2.

Vines were pruned in winter 2022 to retain at least six one-year-old canes per vine from each of three defined vigour classes (Figure 3.1 A). Cane types were defined as:

- low vigour: 0.5–1.0 m long and <14 mm basal diameter.
- medium vigour: 1.0–2.0 m long and <14 mm basal diameter.
- high vigour: >2.0 m long or >14 mm basal diameter.

All canes were dormant and had terminated shoot tips at sampling (Figure 3.1 B) although some shoot tips had been damaged or pruned during the season. All canes were determined to have

emerged during the spring flush (i.e. at budbreak) by the presence of flower stalks or aborted floral nodes (Figure 3.1 C).

### 3.2.2 Dormant sampling

During winter dormancy one cane of each vigour type per vine was removed for sampling (sampling dates in Table 3.1). Samples were taken from each cane at three distances from the cane base: 0.3, 0.4 and 0.5 m for low-vigour canes, and 0.3, 0.5 and 1.0 m for medium- and high-vigour canes (Figure 3.1 A). At each distance, the internode closest to the nominal sampling point was excised and divided into three sections for anatomical, dry weight and carbohydrate analyses.

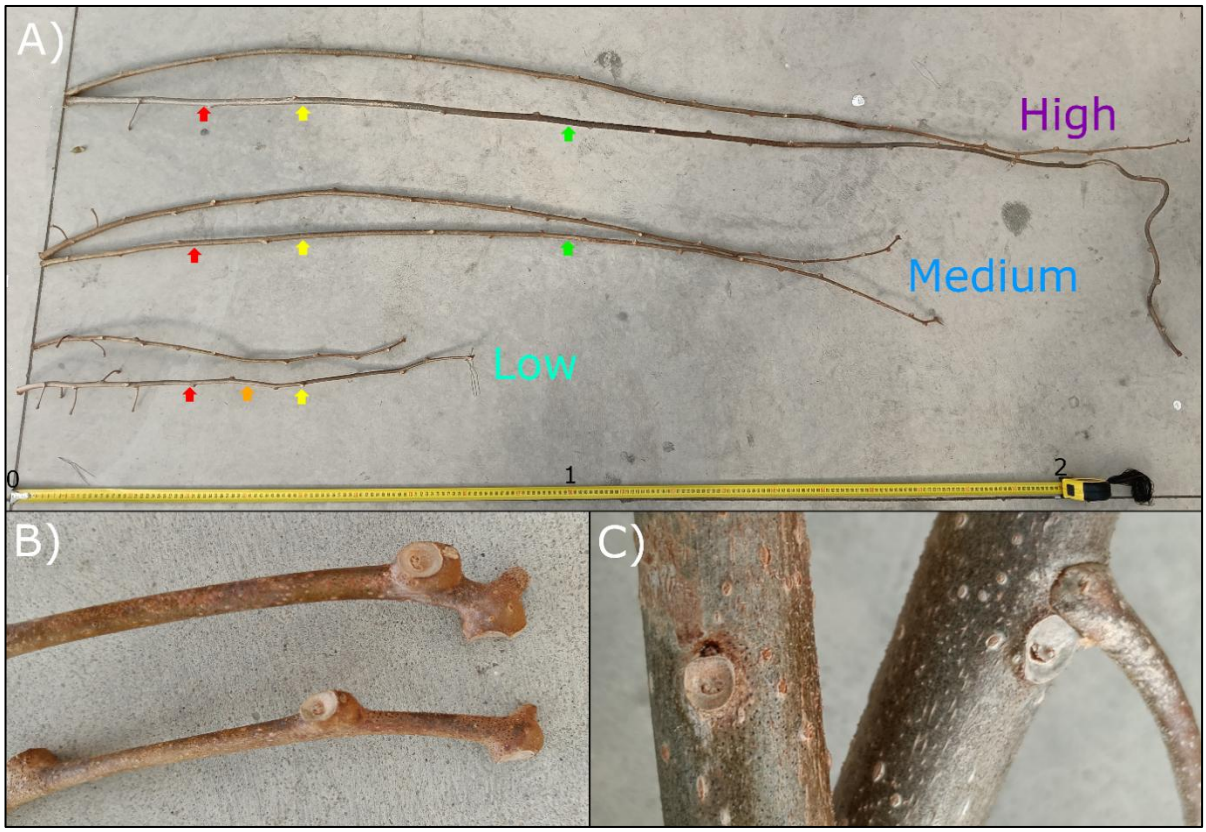


Figure 3.1. Examples of cane vigour types from *Actinidia deliciosa* 'Hayward' vines. A) Cane vigour was classified using the following criteria: low, 0.5–1.0 m length with basal diameter <14 mm; medium, 1.0–2.0 m with basal diameter <14 mm; high, >2.0 m or basal diameter ≥14 mm. Internodes were sampled for carbohydrate contents and anatomy at approximately 0.3 m (red arrows), 0.4 m (orange arrow), 0.5 m (yellow arrows) and 1.0 m (green arrows) from the cane base. B) Terminated cane tips. C) All canes were of similar age and grew during the spring flush, evidenced by the presence of aborted floral nodes (left) or fruit stalks (right).

### 3.2.3 Carbohydrate analysis

Internode samples for carbohydrate analysis were analysed intact (bark and wood combined). Approximately 1 cm lengths of internode were finely chopped and immediately snap-frozen in liquid nitrogen, stored at −80 °C, and lyophilised using a FreeZone Triad 74000 (LABCONCO,

Kansas City, MO, USA). Dried samples were ground using a Pulverisette 14 rotor mill (Fritsch, Idar-Oberstein, Germany). Soluble carbohydrates were extracted from 0.05 g of ground material using 80% (v/v) ethanol. Concentrations of glucose, fructose, sucrose, raffinose, stachyose and planteose were quantified by ion chromatography using a DIONEX ICS-5000 Reagent-Free™ IC system (Thermo Scientific, San Jose, CA, USA) equipped with an amino trap and CarboPac PA20 column. Starch content was determined by enzymatic digestion of the insoluble residue followed by colorimetric glucose quantification using a UV-160A spectrophotometer (Shimadzu, Kyoto, Japan).

To account for potential interconversion during winter, starch and soluble sugars from dormant cane samples were summed and expressed as total non-structural carbohydrate (TNC) concentration (mg $g^{-1}$ DW). A third section of each internode was measured for length and minimum and maximum diameter, weighed fresh, and dried at 60 °C until constant weight. Dry matter content (%) was calculated as dry weight / fresh weight. Dry weight per unit length (mg $mm^{-1}$) was calculated as dry weight / length. TNC per unit length (mg $mm^{-1}$) was calculated as TNC concentration × dry weight per unit length. Concentrations of individual sugars and for each sampling time point (averaged across cane vigour types) are presented in Appendix Figure B2, and starch and soluble sugar concentrations for each sampling time point are similarly presented in Appendix Figure B3.

### 3.2.4 Anatomical measurements

Internode samples for anatomical measurements were preserved in FAA fixative (38% formaldehyde, glacial acetic acid, 96% ethanol, and distilled water in a ratio of 10:5:50:35). Samples were removed from FAA after two weeks and transferred into 50% ethanol. Transverse sections were subsequently prepared using an SM2010 sliding microtome (Leica, Germany), and images of the cut surface were captured at 12.6× magnification using a MIchrome 20 microscope camera (Tucsen, China) (Figure 3.2 A). Five tissue layers were identified in each image: pith, peri-medullary zone (PMZ), secondary xylem (hereafter referred to as wood), phloem, and outer bark (including bast fibres, cortex and epidermis). Tissue areas were quantified using Fiji image analysis software (Fiji; Schindelin et al., 2012) was used to set a scale for the images, then tissue layers were outlined by hand and areas were calculated (Figure 3.2), and expressed as proportions of total cross-sectional area. For starch localisation, 40 µm transverse sections were stained in Lugol's solution for two minutes, rinsed, mounted, and imaged at 40× magnification.

Table 3.1. Phenological stages and dates of carbohydrate sampling of kiwifruit cane internodes during winter dormancy and spring growth. 'Hayward' = *Actinidia chinensis* var. *deliciosa;* 'Zesy002' and 'Zes008' = *A. chinensis* var. *chinensis*. DABB = days after budbreak.

| | Phenological stage and date of sampling | | | | | |
|---|---|---|---|---|---|---|
| Cultivar | Dormant | Budbreak (0 DABB) | Post-budbreak (15-17 DABB) | Pre-anthesis (34-35 DABB) | Anthesis (46-50 DABB) | Post-anthesis (59-67 DABB) |
| 'Hayward' | 04/09/2022 | 14/10/2022 | 31/10/2022 | 17/11/2022 | 30/11/2022 | 13/12/2022 |
| 'Zesy002' | 26/08/2022 | 03/10/2022 | 21/10/2022 | 7/11/2022 | 18/11/2022 | 01/12/2022 |
| 'Zes008' | 19/08/2022 | 01/09/2022 | 16/09/2022 | 05/10/2022 | 21/10/2022 | 07/11/2022 |

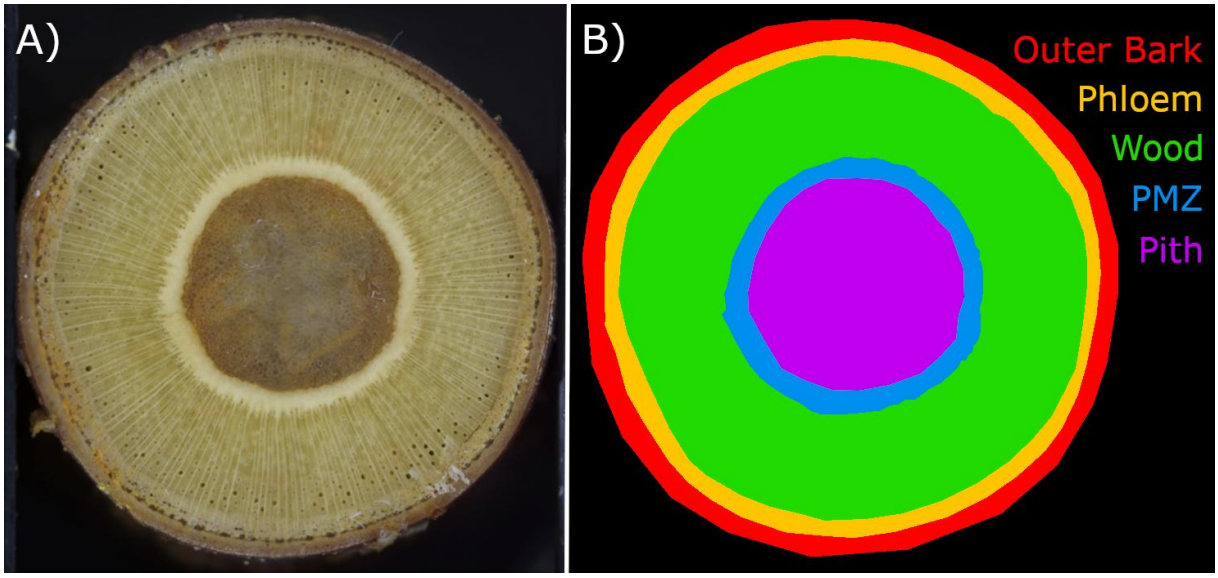


Figure 3.2. Kiwifruit cane tissue layers. A) Example kiwifruit cane cut in transverse section. B) the same cane colour-coded by each of five distinct tissue layers. The total area of each tissue layer was measured with Fiji image processing software and converted to proportions of the total cane area. Outer bark includes the epidermis, cortex and bast fibres. Wood = secondary xylem. PMZ = peri-medullary zone.

### 3.2.5 Spring sampling

Budbreak was deemed to have begun once approximately 5% of buds had visibly broken for each cultivar. From budbreak, internode samples were collected at ~2-week intervals until after anthesis. Spring sampling focused on temporal changes in carbohydrate mobilisation rather than spatial variation along canes.

At each sampling date, one cane per vigour type was removed from each vine, and internode samples were collected at approximately 30 cm from the cane base. This position was chosen to provide a consistent and biologically relevant reference point proximal to developing shoots and flowers while minimising confounding effects of cane tapering.

Five phenological time points were assigned for analysis: budbreak (0 DABB), post-budbreak (15–17 DABB), pre-anthesis (34–35 DABB), anthesis (46–50 DABB), and post-anthesis (59–67

DABB). There were slight differences in phenological timing and sampling between cultivars, sampling dates for each cultivar are presented in Table 3.1.

Internode samples were analysed for starch and soluble sugar concentrations as described in section 3.2.3. During spring, starch and soluble sugars were analysed separately, with TNC per unit length used as an integrated measure of reserve pool size.

### 3.2.6 Statistical analysis

All analyses and data visualisations were performed in R software version 4.3.3 (R Core Team, 2025). To assess relationships between dormant cane TNC concentration, TNC per unit length, and morpho-anatomical traits, data were pooled across cultivars, cane vigour types, and positions along canes. A correlation matrix between these variables was produced using the *corrplot* package (Wei & Simko, 2017).

Linear mixed-effects models were used to assess the effects of cultivar, cane vigour, and distance from the cane base on dormant cane internode TNC concentrations and TNC per unit length. Models were constructed using the *nlme* package (Pinheiro et al., 2023). Cultivar and cane vigour were modelled as fixed factors and distance from the cane base was a covariate. Models incorporated random intercepts for canes nested within vines. Distance from the cane base was centred to aid model convergence and interpretation, and back-transformed for plotting. Wald F test summary tables are included in Appendix B.

Spring starch and soluble sugar concentrations, and TNC per unit length, were analysed using mixed-effects models with variance structures to account for heteroscedasticity across sampling time points. Models were constructed using the *nlme* package (Pinheiro et al., 2023). Cultivar, cane vigour type, and sampling time point were included as fixed effects, with random intercepts fitted for vine. Interpretation of ANOVA results focusses on the interaction of cultivar and cane vigour with sampling time point, as comparing mobilisation patterns was the primary interest of this analysis. Wald F test summary tables are included in Appendix B.

For analysis of both dormant and spring datasets, estimated marginal means and slopes were obtained using the *emmeans* R package (Lenth, 2024), with pairwise comparisons adjusted using the Šidák correction to control family-wise error rates. Data visualisations were generated with the *ggplot2* package (Wickham, 2016), using the *ggeffects* package (Lüdecke, 2018) to generate predicted values from linear mixed-effects models.

## 3.3 Results

### 3.3.1 Dormant cane TNC reserves

**TNC concentrations.** The main effects of cultivar, cane vigour and distance from cane base all significantly affected TNC concentrations. 'Hayward' canes had significantly higher TNC concentrations than both 'Zesy002' and 'Zes008' canes ($p < 0.05$, Figure 3.3 A). Low vigour canes had significantly higher TNC concentrations than medium canes ($p < 0.001$, Figure 3.3 B). TNC concentration significantly increased with distance from the cane base ($p < 0.001$, Figure 3.3 C).

There was a significant interaction between cane vigour and distance from the base of canes, where the slope of this relationship was significantly steeper in low vigour canes than in both medium and high vigour canes (both $p < 0.001$, Figure 3.3 D).

**TNC per unit length.** TNC per unit length was also significantly affected by the main effects of cultivar, cane vigour and distance from cane base. 'Hayward' canes had significantly higher TNC per unit length than both 'Zesy002' and 'Zes008' ($p < 0.001$, Figure 3.4 A). TNC per unit length was significantly higher in high vigour canes than in both low and medium vigour canes ($p < 0.001$, Figure 3.4 B) and was significantly higher in medium vigour canes than in low vigour canes ($p < 0.01$, Figure 3.4 B). TNC per unit length decreased with increasing distance from the cane base ($p < 0.001$, Figure 3.4 C).

There were significant interaction effects for both cultivar and cane vigour with distance from the cane base on TNC per unit length. TNC per unit length fell more rapidly with increasing distance from the base in 'Hayward' canes than in 'Zes008' canes ($p < 0.01$, Figure 3.4 D). Similarly, TNC per unit length fell more rapidly with increasing distance from the base in high vigour canes in comparison to medium vigour canes ($p < 0.05$, Figure 3.4 E).

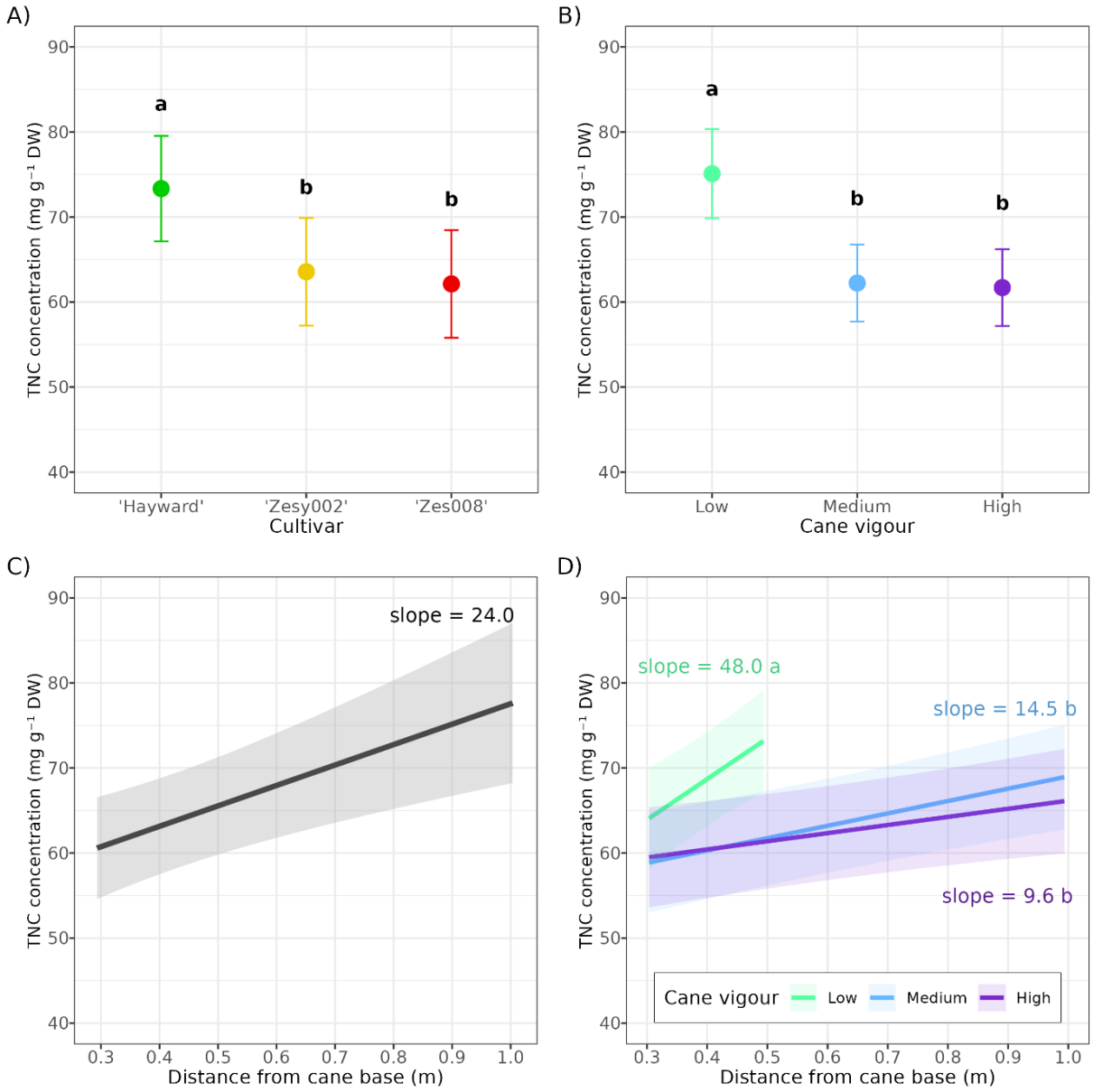


Figure 3.3. Total non-structural carbohydrate (TNC) concentrations in dormant kiwifruit cane internodes. Plots show TNC concentrations as affected by A) cultivar; B) cane vigour; C) distance from cane base; and D) the interaction of cane vigour and distance from cane base. Points are estimated marginal means from a mixed-effects model; error bars are 95% confidence intervals. Lines show model-predicted relationships controlling for other variables, ribbons are 95% confidence intervals. In panels A and B, differences between group means were assessed; in panel D, differences between slopes were assessed. Groups that do not share a letter are significantly different (Šidák adjusted $\alpha = 0.05$).

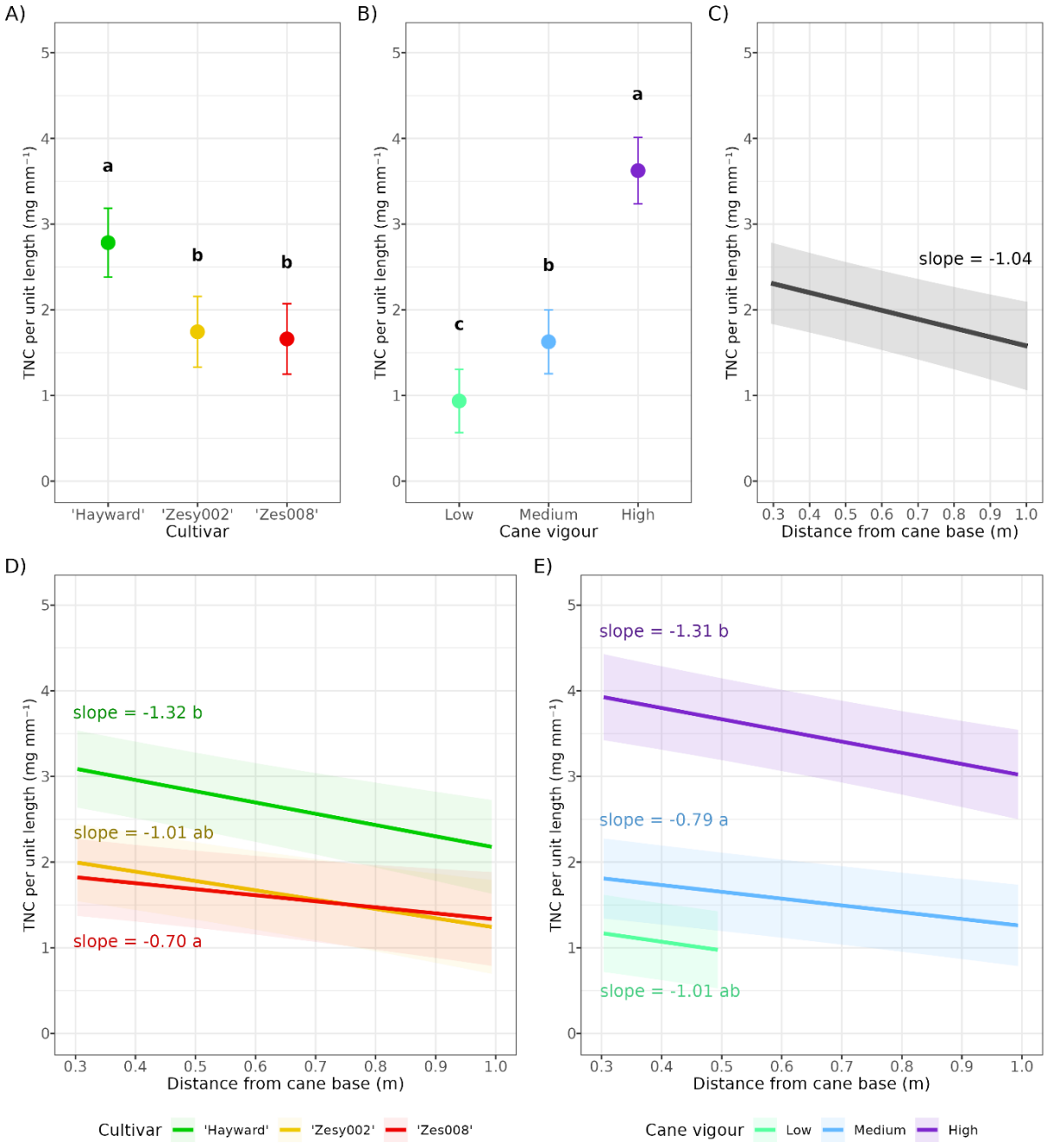


Figure 3.4. Total non-structural carbohydrate (TNC) per unit length in dormant kiwifruit cane internodes. Plots show TNC per unit length as affected by A) cultivar; B) cane vigour; C) distance from cane base; D) the interaction of cultivar and distance from cane base; and E) the interaction of cane vigour and distance from cane base. Points are estimated marginal means from a mixed-effects model; error bars are 95% confidence intervals. Lines show model-predicted relationships controlling for other variables, ribbons are 95% confidence intervals. In panels A and B, differences between group means were assessed; in panels D and E, differences between slopes were assessed. Groups that do not share a letter are significantly different (Šidák adjusted $\alpha = 0.05$).

### 3.3.2 TNC reserves and morpho-anatomical trait correlations

Correlations between TNC concentration and morpho-anatomical traits were generally weak (Figure 3.5). The strongest correlation was with PMZ to wood ratio (r = 0.34), which was slightly stronger than the correlations of either PMZ or wood proportions alone (r = 0.33, -0.33, respectively).

In contrast, several variables showed strong correlations with TNC per unit length. Internode diameter was strongly positively correlated (r = 0.82), and dry matter content was moderately positively correlated (r = 0.51). Among tissue proportions, outer bark proportion was strongly negatively correlated (r = −0.71), whereas wood proportion was moderately positively correlated (r = 0.53).

Correlations between morpho-anatomical traits also varied in strength. Outer bark proportion strongly decreased with diameter (r = −0.83). PMZ proportion decreased with diameter (r = −0.65), while wood proportion increased with internode diameter (r = 0.69). PMZ and wood proportions were strongly negatively correlated (r = −0.92), while correlations between internode diameter vs pith proportion (r = 0.07) and phloem vs PMZ proportions (r = 0.08) were weak. As expected, PMZ-to-wood ratio was strongly positively correlated with PMZ proportion (r = 0.90) and strongly negatively correlated with wood proportion (r = −0.94), reflecting the shared contribution of these tissues to both metrics.

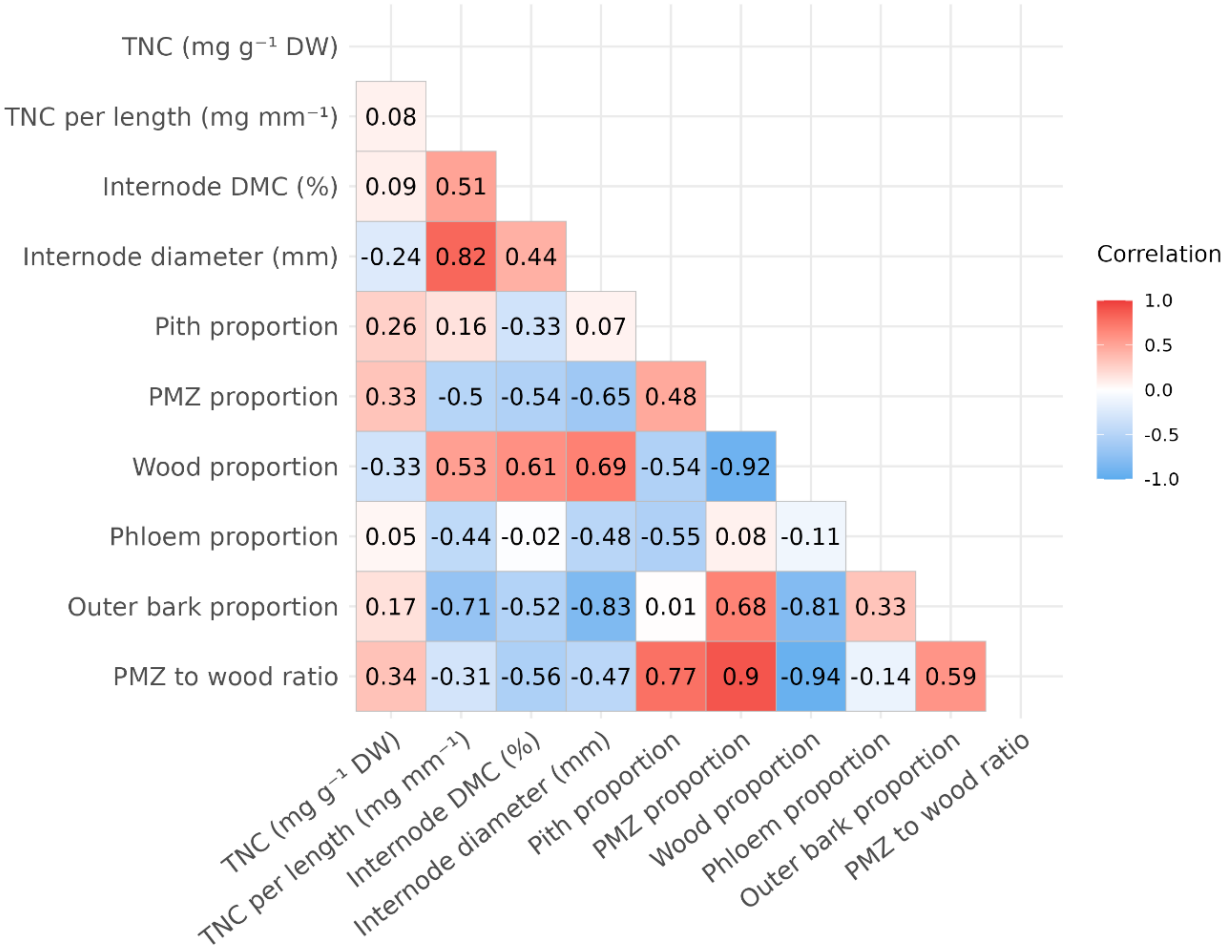


Figure 3.5. Correlation matrix for cane internode total non-structural carbohydrate (TNC) concentration and TNC per unit length vs morpho-anatomical traits. DMC = dry matter content, PMZ = peri-medullary zone, wood = secondary xylem, outer bark = bast fibres, cortex and epidermis. Cell values are Pearson's correlation coefficient (r); colour indicates magnitude and sign (red = positive, blue = negative). Correlations were computed on data pooled across cultivars, cane vigour, and internode positions.

### 3.3.3 Morpho-anatomical differences

**Internode diameter.** Internode diameters on 'Hayward' canes were significantly larger than those of both other cultivars ($p < 0.05$, Figure 3.6A). Internodes on high vigour canes were significantly thicker than those on medium vigour canes ($p < 0.001$), which in turn were significantly thicker than internodes on low vigour canes ($p < 0.001$, Figure 3.6B). Overall, internode diameters declined with increasing distance from the cane base ($p < 0.001$, Figure 3.6C). A significant cultivar × distance interaction was detected ($p < 0.001$, Appendix Table B3); however, pairwise comparisons indicated that differences among cultivar-specific slopes were not statistically significant (Figure 3.6D).

**PMZ to wood ratio.** Patterns in PMZ to wood ratio were primarily driven by cane vigour and distance from the cane base, with weaker effects between cultivars. Low vigour canes had a significantly higher PMZ to wood ratio than both medium and high vigour canes ($p < 0.001$,

Figure 3.7A). The ratio of PMZ to wood generally increased with increasing distance from the cane base ($p < 0.001$, Figure 3.7B), although the slope was significantly less steep in 'Hayward' canes in comparison to canes of both 'Zesy002' ($p < 0.05$) and 'Zes008' ($p < 0.01$, Figure 3.7C). The relationship between PMZ to wood ratio and distance from the cane base was also steeper in low vigour canes in comparison to both medium ($p < 0.01$) and high vigour canes ($p < 0.05$, Figure 3.7D). A significant three-way interaction was detected among cultivar, cane vigour, and distance from the cane base. In medium vigour canes, the increase in PMZ to wood ratio with distance was steeper in 'Zesy002' than in 'Zes008' ($p < 0.05$, Figure 3.7E). The slope was also particularly steep in low vigour 'Zes008' canes, which was greater than in medium or high vigour canes of both other cultivars ($p < 0.05$).

**Starch visualisation.** Stained sections of internodes showed that those with the highest starch concentrations tended to have ray and axillary parenchyma filled with starch, and very few parenchyma cells in the PMZ without starch granules (Figure 3.8). In contrast, internodes with the lowest starch concentrations frequently had portions of ray parenchyma that were devoid of starch, and numerous empty or poorly filled PMZ parenchyma cells (Figure 3.9).

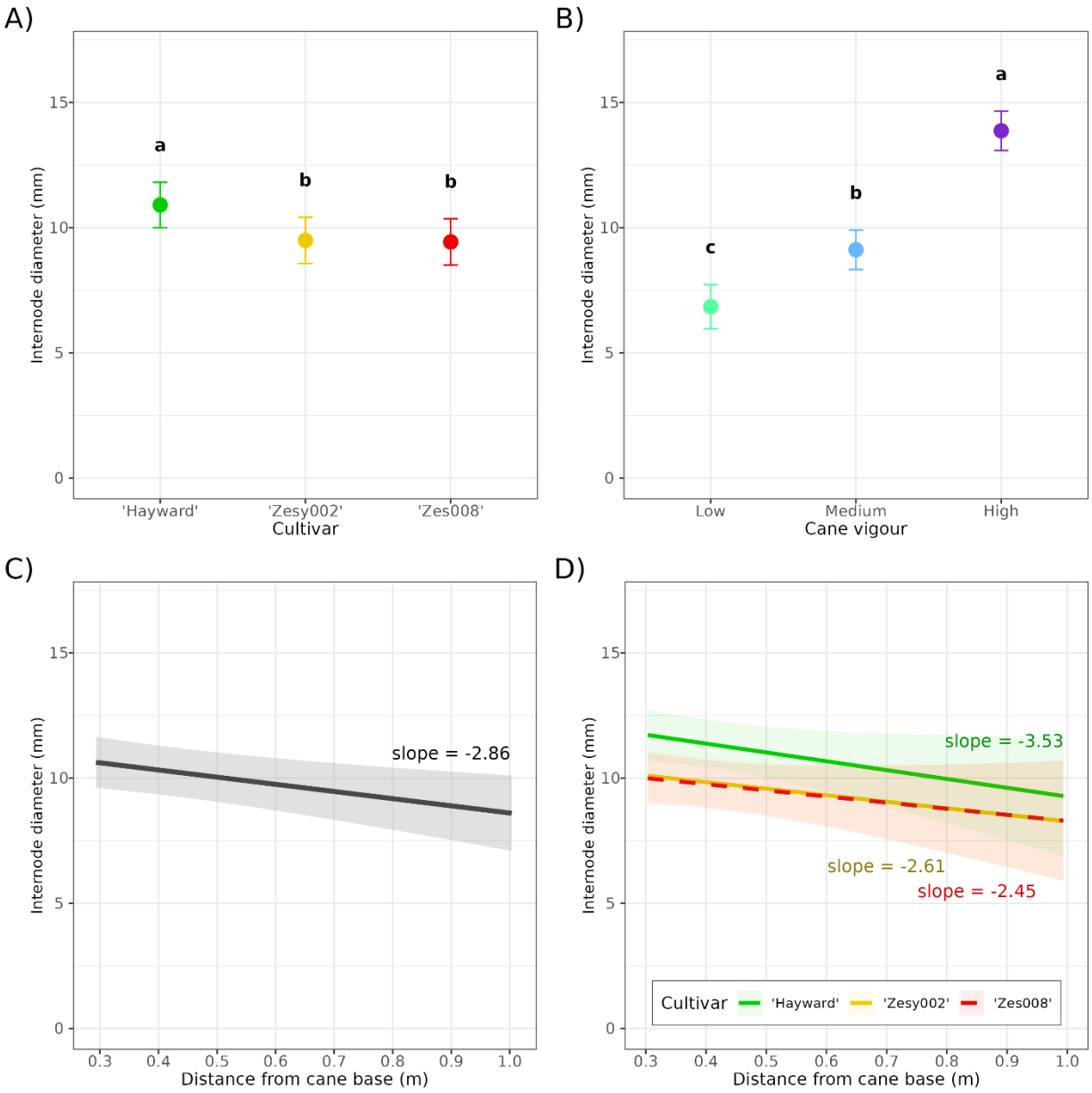


Figure 3.6. Internode diameters of kiwifruit canes. Canes from three cultivars were sampled during winter dormancy, these being: *Actinidia chinensis* var. *deliciosa* 'Hayward', *A. chinensis* var. *chinensis* 'Zesy002' and *A. chinensis* var. *chinensis* 'Zes008'. Linear mixed-effects models were used to assess the effects of cultivar, cane vigour and distance from the cane base on internode diameters, and only significant effects are plotted. These were: A) marginal effect of cultivar; B) marginal effect of cane vigour, C) marginal effect of distance from the cane base; D) interaction effect of cultivar and distance from the cane base. In panels A and B points are estimated marginal means, bars are 95% confidence intervals, and differences between group means were assessed. In panels C and D lines show model-predicted relationships controlling for other variables, ribbons are 95% confidence intervals. In panel D differences between slopes were assessed. Within each panel, groups that do not share a letter are significantly different (Šidák adjusted $\alpha = 0.05$).

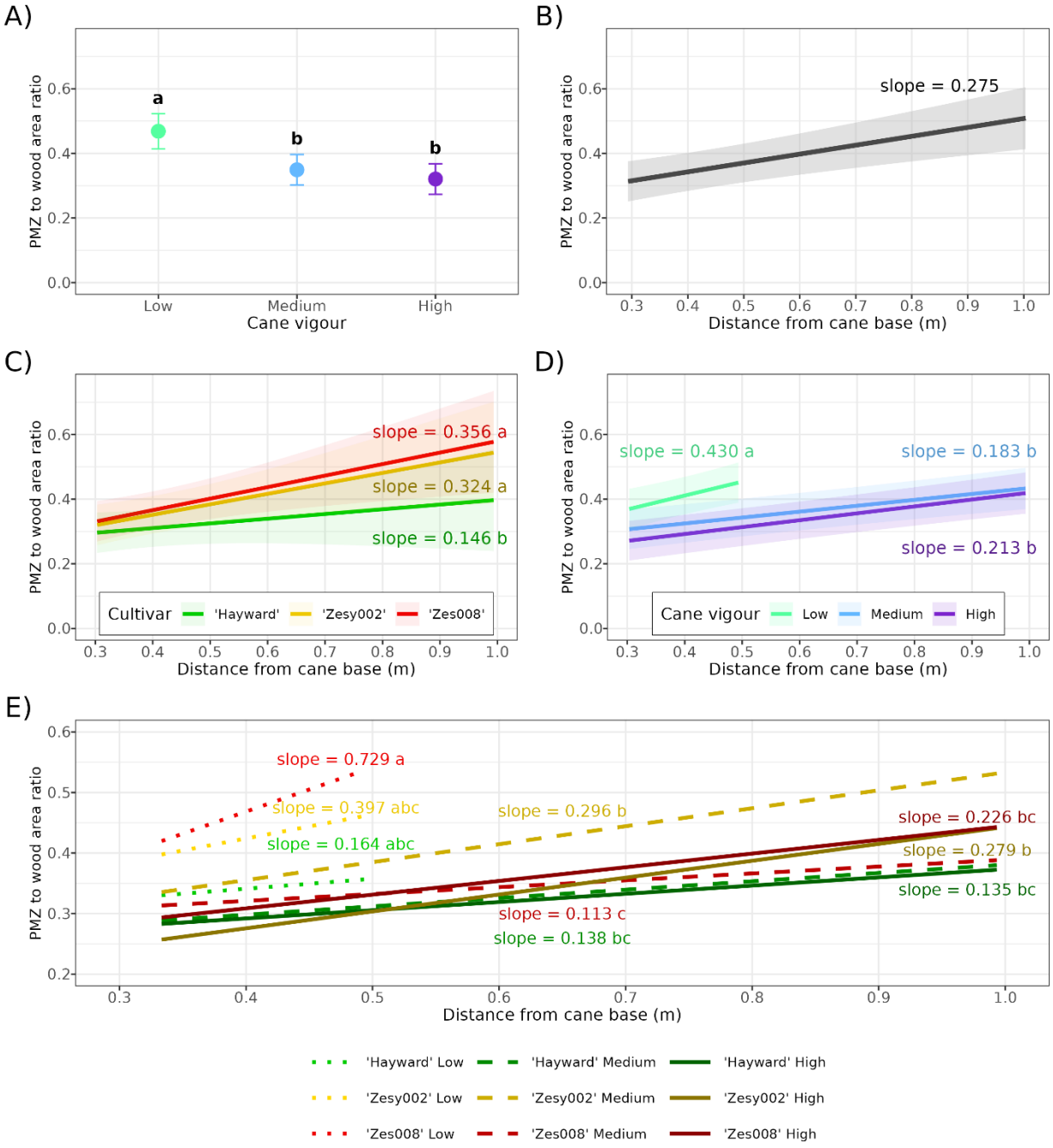


Figure 3.7. Peri-medullary zone (PMZ) to wood area ratios of kiwifruit canes. Canes from three cultivars were sampled during winter dormancy, these being: *Actinidia chinensis* var. *deliciosa* 'Hayward', *A. chinensis* var. *chinensis* 'Zesy002' and *A. chinensis* var. *chinensis* 'Zes008'. Linear mixed-effects models were used to assess main effects and interactions on PMZ to wood ratio, and only significant effects are plotted. These were: A) marginal effect of cane vigour; B) marginal effect of distance from the cane base; C) interaction effect of cultivar and distance from the cane base; D) interaction effect of cane vigour and distance from the cane base; E) three-way interaction effect of cultivar, cane vigour, and distance from base of cane. In panel A, points are estimated marginal means, bars are 95% confidence intervals, and differences between group means were assessed. In panels B, C, D and E, lines show model-predicted relationships controlling for other variables and ribbons are 95% confidence intervals (ribbons omitted in panel E for clarity). In panels C, D and E differences between slopes were assessed. Within each panel, groups that do not share a letter are significantly different (Šidák adjusted $\alpha = 0.05$).

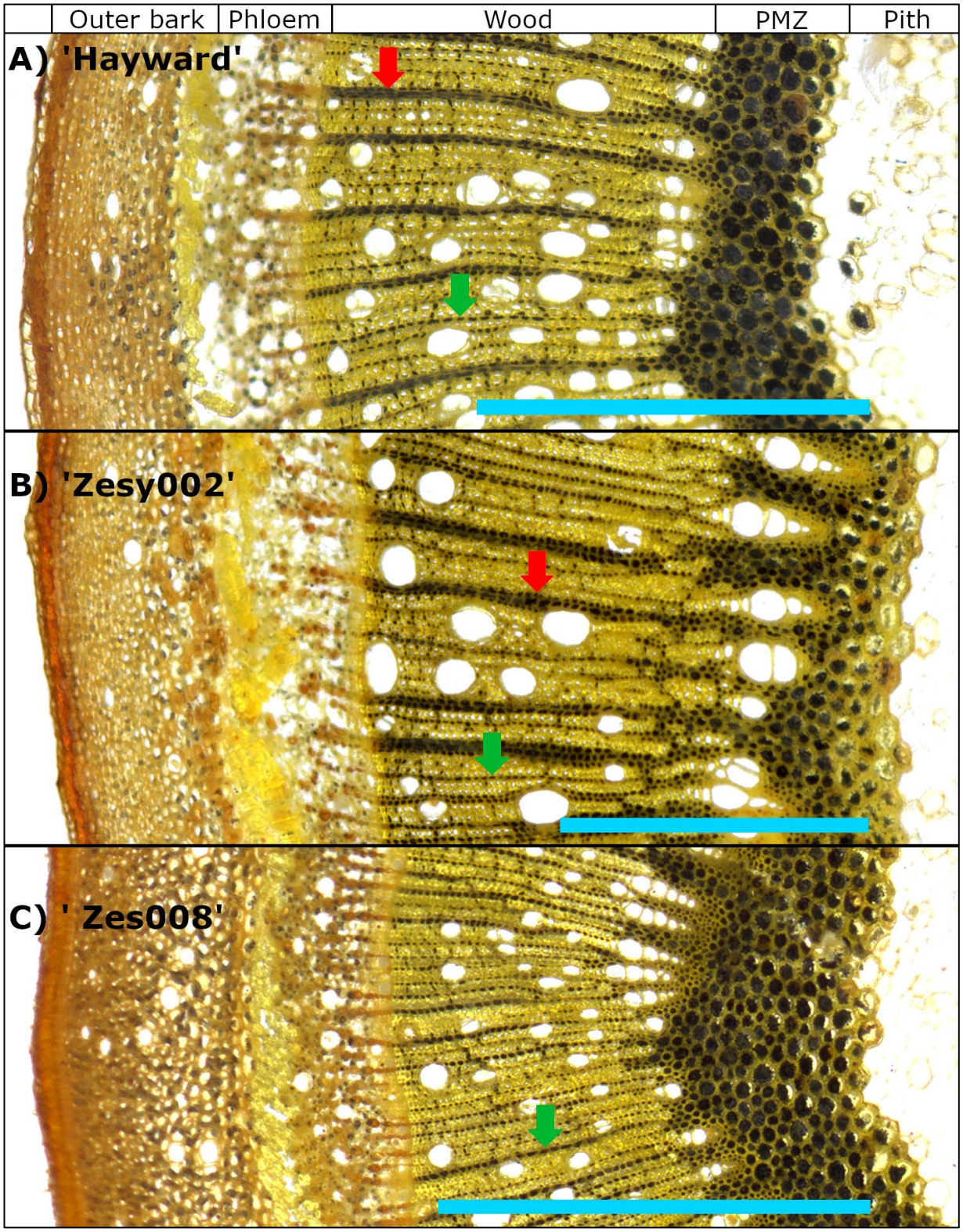


Figure 3.8. Kiwifruit cane internodes showing higher starch concentrations. Starch granules appear black after staining with Lugol's solution. Sections were taken from three cultivars during winter dormancy: A) *Actinidia chinensis var. deliciosa* 'Hayward'; B) *A. chinensis var.* chinensis 'Zesy002; C) *A. chinensis var. chinensis* 'Zes008'. Tissue layers are indicated at the top of figure A. Outer bark includes the epidermis, cortex and bast fibres. Starch accumulates mainly in the peri-medullary zone (PMZ) and the wood (secondary xylem) rays. Rays may be uniseriate (green arrows) or multiseriate (red arrows). The displayed sections were taken from the internodes with the highest starch concentrations measured per cultivar (A = 73.9 mg/g DW; B = 49.9 mg/g DW; C = 57.4 mg/g DW). Blue scale bars are 1 mm long.

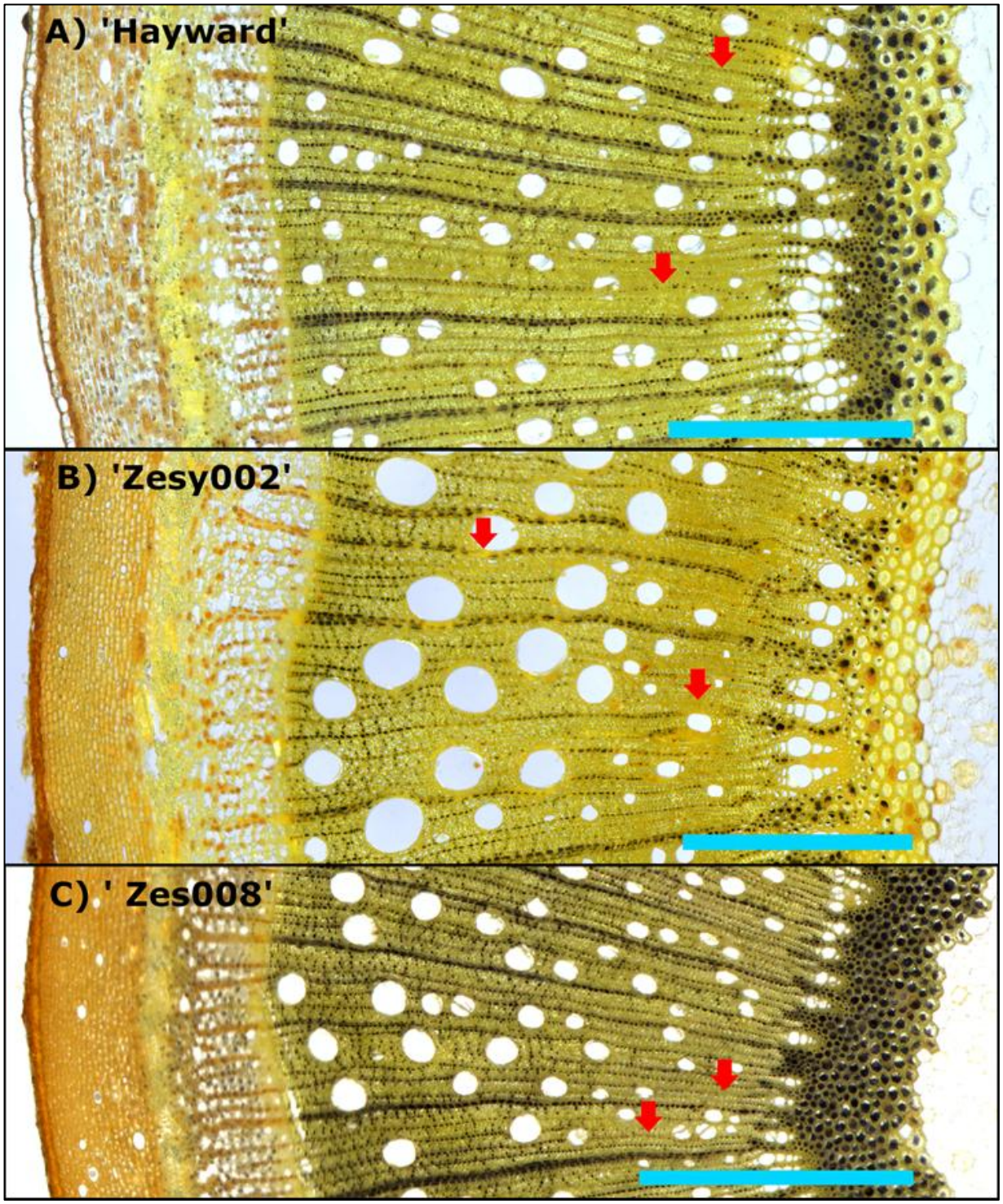


Figure 3.9. Kiwifruit cane internodes showing lower starch concentrations. Starch granules appear black after staining with Lugol's solution. Sections were taken from three cultivars during winter dormancy: A) *Actinidia chinensis var. deliciosa* 'Hayward'; B) *A. chinensis var.* chinensis 'Zesy002; C) *A. chinensis var. chinensis* 'Zes008'. The displayed sections were taken from the internodes with the lowest starch concentrations measured per cultivar (A = 29.7 mg/g DW; B = 16.3 mg/g DW; C = 32.1 mg/g DW). Red arrows highlight areas of ray parenchyma that have few starch granules. Blue scale bars are 1 mm long.

### 3.3.4 Spring mobilisation

**Soluble sugar concentration.** There was a significant interaction between cultivar and sample time point on internode soluble sugar concentration ($p < 0.001$, Figure 3.10). At

budbreak, internodes of ‘Zesy002’ had significantly higher soluble sugar concentration than those of both ‘Hayward’ and ‘Zes008’. Across all cultivars concentrations peaked at budbreak and declined sharply by 15–17 DABB. After budbreak the soluble sugar concentrations of all three cultivars were fairly stable, averaging approximately 10 mg $g^{-1}$ DW.

**Starch concentration.** The interaction between cultivar x time point on internode starch concentration was significant ($p < 0.001$, Figure 3.11 A). At budbreak, post-budbreak and pre-anthesis, ‘Zesy002’ internodes had lower starch concentrations than both ‘Hayward’ and ‘Zes008’. ‘Zesy002’ remained lower than ‘Hayward’ at anthesis and post-anthesis. ‘Hayward’ and ‘Zes008’ were broadly similar across time points, with both showing large declines from post-budbreak to pre-anthesis and again from pre-anthesis to anthesis, reaching minimums at anthesis (means: ‘Hayward’ 6.7 mg $g^{-1}$ DW, ‘Zesy002’ 0.9 mg $g^{-1}$ DW, ‘Zes008’ 3.0 mg $g^{-1}$ DW).

Within each time point (Figure 3.11 B), some cultivar × cane vigour pairwise contrasts were significant, but when cultivars were pooled there was no consistent main effect of cane vigour on starch concentration across time points ($p = 0.113$, Appendix Table B6).

**TNC per unit length.** There was a significant cultivar × time point interaction effect on TNC per unit length ($p < 0.001$, Figure 3.12 A). Across cultivars, TNC per unit length was highest at budbreak and declined to minimum values by anthesis or post-anthesis. At budbreak, ‘Hayward’ exceeded both ‘Zesy002’ and ‘Zes008’, and a similar pattern held at post-anthesis. At post-budbreak and pre-anthesis, ‘Hayward’ and ‘Zes008’ had similar values of TNC per unit length, and both exceeded ‘Zesy002’. At anthesis, cultivars did not differ significantly (Figure 3.12 A).

There was also a significant cane vigour × time point interaction effect on TNC per unit length ($p < 0.001$, Figure 3.12 B). High vigour canes had higher TNC per unit length than medium and low vigour canes at every time point. Medium vigour canes had higher TNC per unit length than low vigour canes at budbreak and anthesis but not at other time points.

Within time points, cultivar × cane vigour pairwise contrasts showed several significant differences (Figure 3.12 C). At budbreak and post-anthesis, high vigour ‘Hayward’ canes had higher TNC per unit length than high vigour canes of both other cultivars ($p < 0.05$). At pre-anthesis, the TNC per unit length of medium vigour ‘Hayward’ canes exceeded that of medium vigour ‘Zesy002’ canes ($p < 0.05$). At anthesis and post-anthesis, medium ‘Hayward’ had higher TNC per unit length than medium canes of both other cultivars ($p < 0.05$).

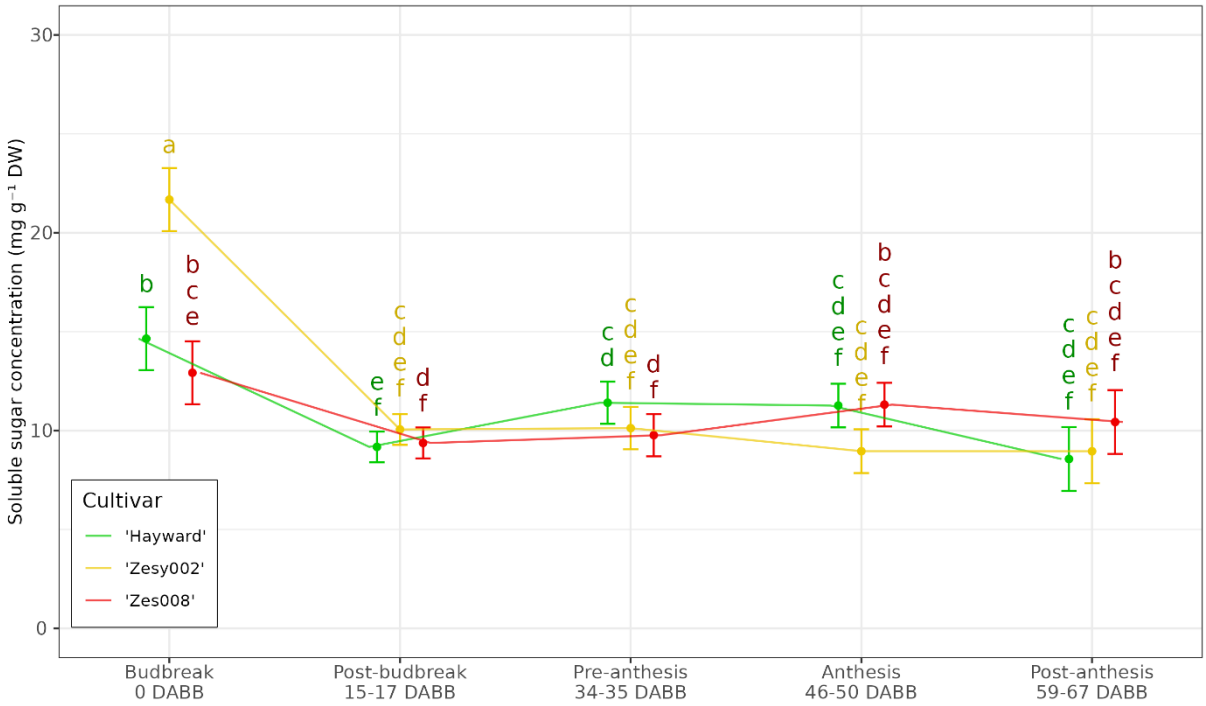


Figure 3.10. Soluble sugar concentrations of kiwifruit cane internodes across spring. Cultivars were *Actinidia chinensis var. deliciosa* 'Hayward' (green), *A. chinensis var. chinensis* 'Zesy002' (yellow), and *A. chinensis var. chinensis* 'Zes008' (red). Points show estimated marginal means from a mixed effect mode; bars are 95% confidence intervals. The cultivar x time point interaction is shown; letters denote pairwise differences across all cultivar x time point combinations (Šidák adjusted α = 0.05). DABB = days after budbreak.

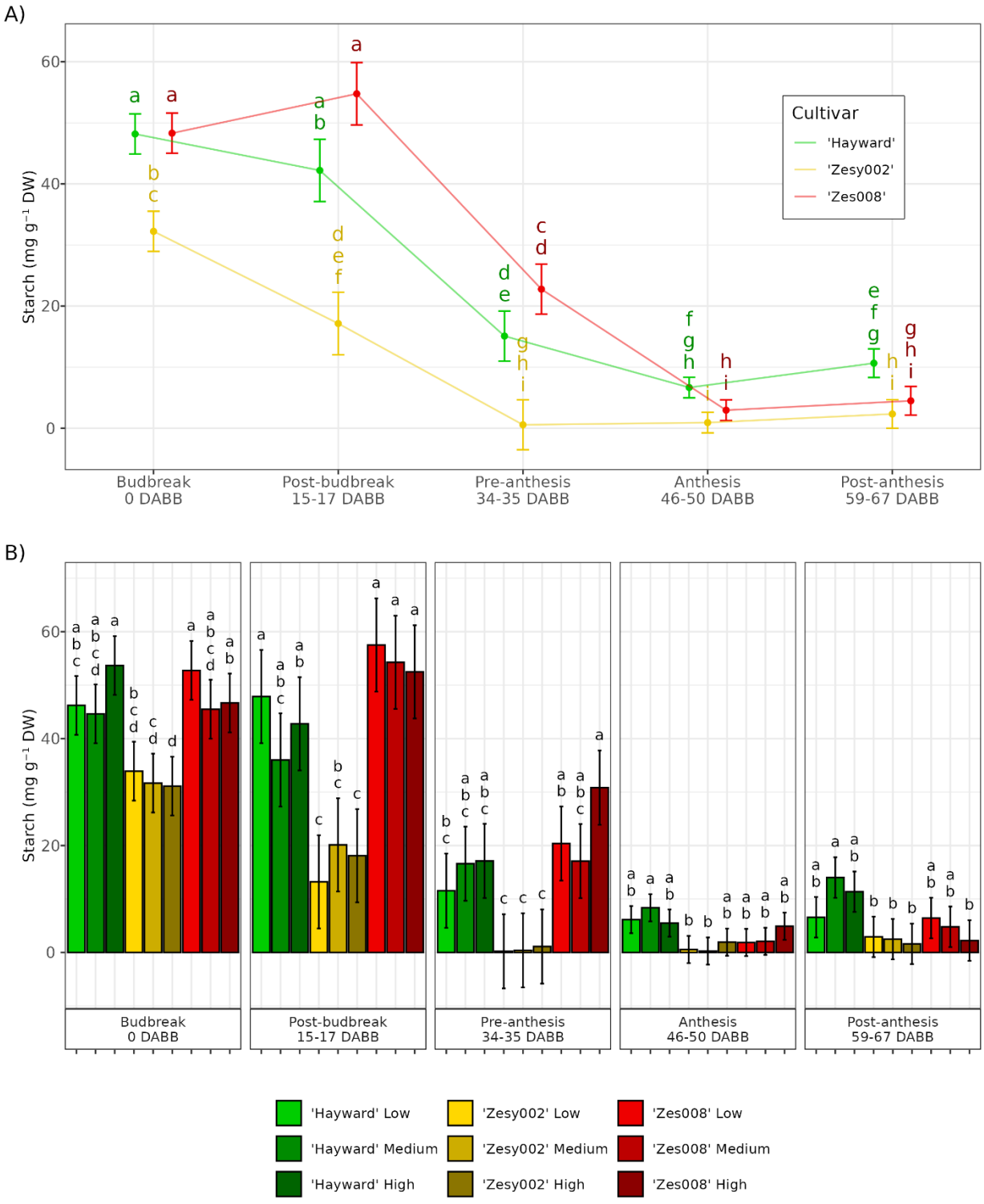


Figure 3.11. Starch concentrations of kiwifruit cane internodes across spring. Cultivars were *Actinidia chinensis var. deliciosa* 'Hayward' (green), *A. chinensis var. chinensis* 'Zesy002' (yellow), and *A. chinensis var. chinensis* 'Zes008' (red). Panel A shows the interaction effect of cultivar and time point, and significance groupings apply across all cultivar and time point combinations. Panel B shows the interaction effect of cultivar and cane vigour for each time point, and significance groupings apply only within each time point sub-panel. Points in panel A and bars in panel B show estimated marginal means from a mixed effects model; error bars are 95% confidence intervals. Groups that do not share a letter were significantly different (Šidák adjusted $\alpha = 0.05$). DABB = days after budbreak.

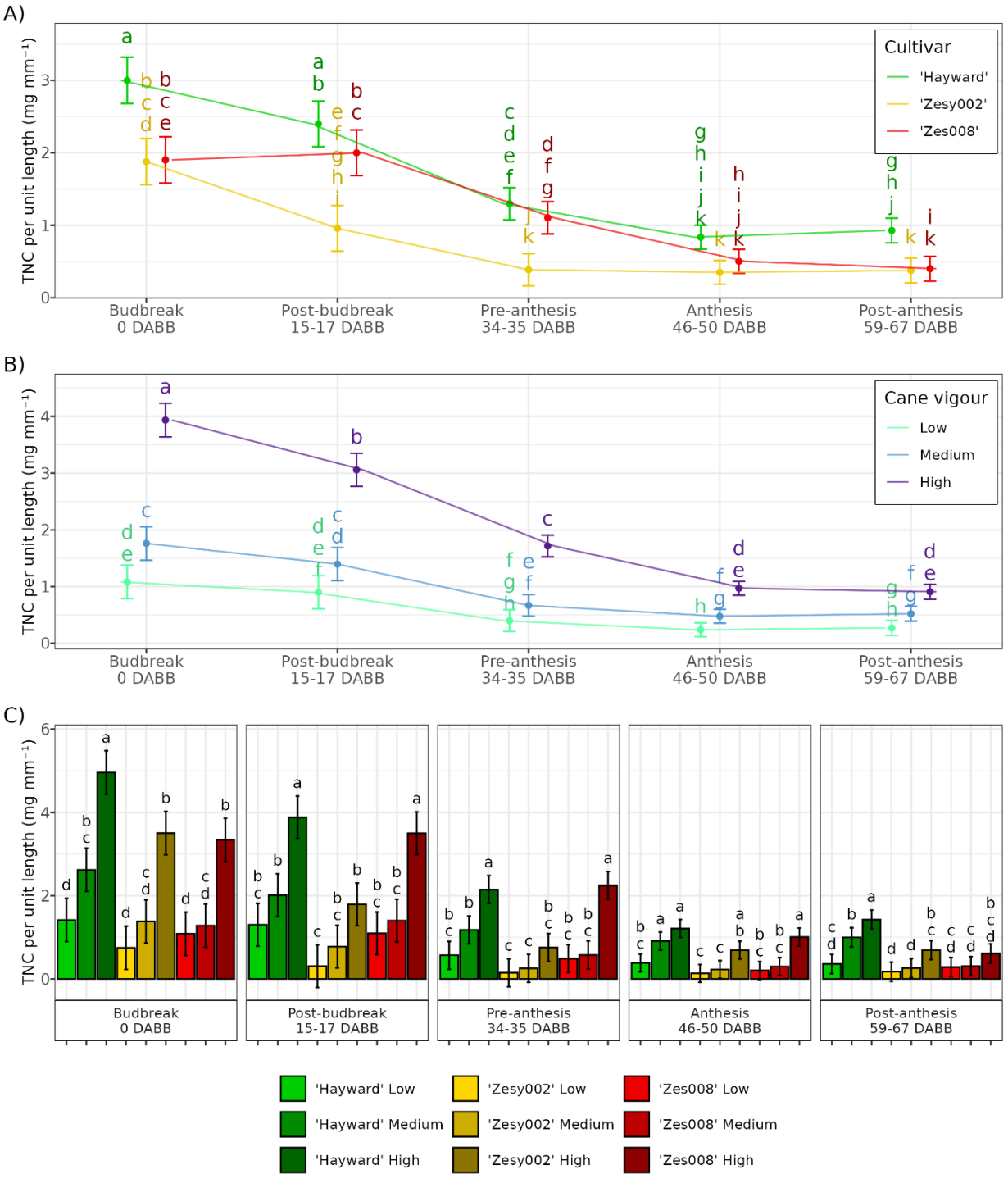


Figure 3.12. Total non-structural carbohydrates (TNC) per unit length of kiwifruit cane internodes across spring. Cultivars were *Actinidia chinensis var. deliciosa* 'Hayward' (green), *A. chinensis var. chinensis* 'Zesy002' (yellow), and *A. chinensis var. chinensis* 'Zes008' (red). Panel A shows the interaction of cultivar and time point and significance groupings apply across all combinations. Panel B shows the interaction of cane vigour and time point and significance groupings apply across all combinations. Panel C shows interaction effects of cultivar and cane vigour for each time point, and significance groupings apply only within each time point sub-panel. Points (A, B) and bars (C) show estimated marginal means from a mixed-effects model; error bars are 95% confidence intervals. Groups that do not share a letter were significantly different (Šidák adjusted $\alpha = 0.05$). DABB = days after budbreak.

## 3.4 Discussion

This study revealed substantial and structured variation in carbohydrate reserves among one-year-old kiwifruit cane internodes, arising from differences in cultivar, cane vigour, and position. These differences reflect two distinct but interacting properties of canes: the concentration of non-structural carbohydrates within tissues, and the total reserve pool available per unit length. In addition, seasonal mobilisation patterns determine how rapidly and completely these reserves are depleted during early spring growth. Interpreting these results therefore requires separating the effects of storage capacity, governed by internode anatomy and diameter, from those of reserve concentration and mobilisation dynamics. The following sections consider how these factors contribute to winter reserve status, anatomical differences among canes, and cultivar-specific patterns of reserve mobilisation in spring.

### 3.4.1 Drivers of winter NSC reserve pools

Cultivar, cane vigour, and internode position each contributed significantly to variation in winter carbohydrate reserves, but their effects differed depending on whether reserves were expressed as TNC concentration or as TNC per unit length. Cultivar differences were most evident in TNC concentration, whereas cane vigour and internode position primarily influenced reserve pool size through their effects on internode diameter.

Differences in crop load were not controlled for in the previous season, potentially contributing to variability between cultivars and cane types. Previous research into the NSC reserve dynamics of apples trees has shown that while differences in crop loading can contribute to differences in branch starch reserves while fruit are still attached, these differences can be negated by dormancy once the competing fruit sinks are removed (McQueen et al., 2004). However, research in grapevines suggest that root reserve pools may be more sensitive to timings of harvest and defoliation, with subsequent effects on fruit production (Smith & Holzapfel, 2009).

While the three cultivars in this trial differ in their typical harvest times, the similar overall TNC concentrations observed across cultivars suggest that even in ‘Hayward’, the latest harvested cultivar, there was sufficient time after fruit harvest for cane reserves to saturate. However, ‘Hayward’ also typically carries significantly lower crop loads than either ‘Zesy002’ or ‘Zes008’. The combination of high crop loads and late harvest may be more detrimental to reserve replenishment and subsequent floral productivity in ‘Hayward’ and could warrant further investigation, particularly for root reserve pools (Martínez-Lüscher & Kurtural, 2021).

Indeed, contrary to expectations based on typical floral productivity, 'Hayward' canes exhibited both higher TNC concentrations and higher TNC per unit length than canes of 'Zesy002' or 'Zes008'. This indicates that total carbohydrate availability within one-year-old cane internodes may not be the primary constraint on flowering in 'Hayward', despite the well-established responsiveness of floral productivity to carbohydrate availability treatments (Richardson et al., 2022). This suggests that differences in reproductive performance between cultivars may be more strongly influenced by the distribution and accessibility of reserves, or by other physiological factors governing floral development and budbreak, than by the total NSC concentration within individual cane internodes.

Cane vigour showed a clear trade-off between reserve concentration and reserve pool size. Low-vigour canes had higher TNC concentrations but substantially lower TNC per unit length than medium- and high-vigour canes. This pattern mirrors observations in grapevine and other woody perennials, where carbohydrate pools increase with stem cross-sectional area even though concentrations decline (Barbaroux & Bréda, 2002; Barbaroux et al., 2003; Eltom et al., 2013). Thus, although low-vigour canes store carbohydrates more densely on a dry-mass basis, their smaller diameters constrain the total amount of reserve available to support spring growth.

A similar decoupling of concentration and pool size occurred along the length of canes. TNC per unit length declined with increasing distance from the cane base, consistent with modelled effects of cane diameter tapering (Greaves et al., 1999). In contrast, TNC concentration increased distally, indicating that younger internodes allocate a greater proportion of dry matter to carbohydrate storage. Together, these patterns show that reserve pool size within canes is dominated by anatomical scaling effects, whereas reserve concentration reflects tissue composition and developmental age. Both dimensions must therefore be considered when assessing the functional significance of winter carbohydrate reserves.

### 3.4.2 Internode anatomy

Across all internodes, the proportions of wood and PMZ were the strongest anatomical predictors of TNC concentration. Wood contains ray and axial parenchyma (RAP) which are the principal starch-storing cells in most woody species (Plavcová & Jansen, 2015), and the fractions of RAP, fibres and vessels can strongly influence the carbohydrate storage capacity (Plavcová et al., 2016; Słupianek et al., 2021; Zhang et al., 2022). In kiwifruit canes, the PMZ is composed entirely of parenchyma cells and can be densely packed with starch (Ferguson, 1990). Accordingly, higher PMZ and lower wood proportions were correlated with higher TNC

concentration, supporting the interpretation that anatomical allocation among tissue layers strongly influences internode NSC storage.

Within a cane, anatomical proportions reflect internode developmental timing and degree of radial growth. The absolute PMZ area is determined by pith diameter and PMZ thickness, both of which are essentially fixed during primary growth. In contrast, wood area can progressively increase through secondary growth from the cambium. Internodes closer to the cane base form earlier in the growing season and therefore experience a longer period of radial thickening, contributing to their greater wood fractions and larger diameters relative to younger, distal internodes.

Hydraulic demands further reinforce this pattern. Basal shoot internodes must conduct water to supply the entire distal leaf area, which increases from tip to base. To meet this demand and maintain a relatively conservative Huber value (sapwood area : leaf area), stems typically increase xylem cross-sectional area via secondary growth (Tyree & Ewers, 1991). Similarly, longer, higher vigour shoots support greater leaf area during the growing season (Figure 2.15). These processes are consistent with the observed increase in wood proportion and decrease in PMZ proportion with increasing internode diameter, as well as the lower PMZ-to-wood ratios observed in high-vigour canes and in more basal internodes.

Thicker internodes had greater TNC per unit length, likely due to the formation of additional carbohydrate-storing RAP cells during secondary wood growth. Thicker internodes also had a larger absolute area of both phloem and outer bark (Appendix Figure B1), which also contribute to TNC per unit length. Although these tissues show less visible starch than wood or PMZ, studies in other deciduous species indicate they can contain substantial soluble sugar pools (Davidson et al., 2021; Keller & Loescher, 1989; Tixier et al., 2017; Yu et al., 2017).

These spatial differences in reserve pool size may have consequences for the development of individual buds along a cane. Buds associated with larger, basal internodes potentially have access to a greater local carbohydrate pool during early spring growth than those associated with smaller, distal internodes. Higher vigour shoots also typically have longer internodes (Seleznyova et al., 2002), also increasing the total volume of subsequent cane reserves proximal to each bud. This may contribute to spatial differences in shoot vigour and reproductive development, particularly during the period before developing leaves become significant sources of photoassimilates.

Together, these results indicate that internode diameter primarily governs the size of the carbohydrate reserve pool, whereas PMZ-to-wood allocation contributes to variation in reserve concentration. In addition to these anatomical factors, abiotic and biotic factors such as light interception and number and proximity to other vine sinks also likely contribute to variability in reserve accumulation during the previous growing season.

### 3.4.3 Spring mobilisation patterns

Across cultivars and cane vigour types, spring mobilisation followed a consistent pattern: starch reserves declined rapidly from budbreak to reach minimums near anthesis, while soluble sugar concentrations peaked at budbreak and were subsequently maintained within a narrow range. This pattern indicates that reserve mobilisation functions primarily to sustain a relatively stable supply of soluble carbohydrates during early shoot growth and flowering, rather than to maximise soluble sugar concentrations. Such NSC buffering is consistent with the high carbohydrate demands of expanding shoots and developing flowers during this period.

This period of rapid reserve mobilisation coincides with the development of shoots and flowers, when the photosynthetic contribution of newly developing leaves remains limited. Consequently, the capacity to mobilise stored carbohydrates during this period is likely to influence the initial growth of shoots and reproductive structures, with potential downstream consequences for flower retention and early fruit development.

Despite this shared mobilisation trajectory, cultivars showed differences in their NSC composition at budbreak and in the rate at which starch was depleted thereafter. Internodes of ‘Zesy002’ consistently exhibited higher soluble sugar concentrations and lower starch concentrations than those of both ‘Hayward’ and ‘Zes008’, a pattern already evident during winter dormancy (Appendix Figure B3). Because all vines were grown within a common orchard block and experienced near-identical winter chilling conditions, these differences most likely reflect cultivar-specific physiological responses to winter cold acclimation rather than environmental variation. Similar cultivar-dependent differences in starch–sugar partitioning during dormancy and early spring have been reported in other woody perennials, (Ouyang et al., 2020; Palonen, 1999; Sun et al., 2020; Yu et al., 2017), consistent with differences in cold-tolerance strategy and regulation of starch and raffinose-family oligosaccharide metabolism (Kaplan et al., 2006).

After the initial peak at budbreak, soluble sugar concentrations declined sharply by 15–17 DABB and were thereafter maintained at relatively constant levels across cultivars. This stability,

despite continued starch depletion, suggests that mobilisation is tightly regulated to buffer sink demand and maintain local sugar availability for respiration and growth. Early in spring, soluble sugars are likely derived mainly from starch hydrolysis and the breakdown of raffinose-family oligosaccharides, which were abundant during dormancy but declined to near-zero concentrations by approximately 35 DABB (Appendix Figure B2). As cane starch reserves approach depletion, the stable concentration of soluble sugars suggests that an increasing proportion of these sugars must be supplied via import from more distal reserve pools such as the trunk or roots, or from recently fixed photoassimilates once leaves become autotrophic.

Starch depletion proceeded most rapidly in 'Zesy002' canes. Although this cultivar initially exhibited elevated soluble sugar concentrations, starch continued to decline at a similar rate through to the pre-anthesis stage, such that by this time cane internode reserves were effectively exhausted. By anthesis, all cultivars reached minimum starch concentrations; however, 'Hayward' retained higher residual starch than 'Zesy002'. This difference appears to reflect higher initial starch concentrations rather than a slower mobilisation rate, as the absolute decline in starch concentration over spring was greater in 'Hayward'.

In contrast to starch concentration, the dynamics of TNC per unit length highlighted pronounced effects of cane vigour on reserve pool size and mobilisation capacity. High vigour canes contained substantially larger TNC pools at budbreak and mobilised several times more TNC per unit length over spring than medium or low vigour canes. Because high vigour canes also have longer internodes (Piller & Meekings, 1997; Seleznyova et al., 2002), the reserve pool available to individual buds would be even greater than indicated by TNC per unit length alone. This enhanced carbohydrate availability likely contributes to the consistently higher floral productivity and increased fruit size reported for higher vigour or larger-diameter canes in the literature (Thorp et al., 2018; Thorp et al., 2003; Volz et al., 1992). Larger reserve pools may provide a greater carbohydrate supply to support early shoot and flower development, potentially increasing the capacity of individual canes to sustain reproductive growth and maximise fruit developmental trajectories. Furthermore, because high-vigour canes typically contain longer internodes, the total reserve pool available along an individual cane may be substantially greater than indicated by comparisons of TNC per unit length alone. This highlights the importance of considering both reserve concentration and total pool size when assessing the potential contribution of individual canes to vine productivity.

## 3.5 Conclusions

Across three kiwifruit cultivars, carbohydrate reserves in dormant canes were associated with two main anatomical factors. Internode diameter was the strongest predictor of TNC per unit length, reflecting the greater volume of carbohydrate-storing tissue in thicker internodes, whereas the PMZ-to-wood area ratio was associated with differences in TNC concentration across cane vigour types and with distance along the cane. Internode length also contributes to the structural differences between canes, with longer internodes in more vigorous shoots potentially increasing the total reserve pool along an individual cane. Contrary to expectation, 'Hayward' canes combined higher winter TNC concentration with higher TNC per unit length, despite having lower PMZ-to-wood area ratios. This suggests that differences in tissue composition or carbohydrate storage within the wood may contribute to cultivar differences in reserve accumulation, warranting further investigation.

In spring, all cultivars and cane vigour types followed a broadly similar reserve mobilisation trajectory. Starch declined steeply from budbreak to minima near anthesis, while soluble sugars were initially high at budbreak before declining and being maintained within a relatively narrow range. High-vigour canes contained larger TNC pools at budbreak, retained higher residual TNC per unit length at anthesis, and mobilised more TNC per unit length throughout spring. This greater reserve pool and mobilisation capacity may contribute to the enhanced early shoot and reproductive development associated with more vigorous canes, potentially supporting greater floral productivity and fruit growth. However, the extent to which differences in cane reserve availability influence subsequent fruit FW and DM variability remains to be determined.

# Chapter 4: Exogenous sucrose uptake and effects on growth

## 4.1 Introduction

Carbohydrate reserves in kiwifruit vines are essential for supporting shoot, leaf, and flower development during the period between budbreak and the establishment of net positive carbon balance in spring (Piller et al., 1998; Richardson et al., 2017). Reductions in reserve accumulation caused by excessive shading, defoliation, or high crop load are associated with reduced budbreak, shoot vigour, and flower production (Buwalda & Smith, 1990; Cruz-Castillo et al., 2010; Grant & Ryugo, 1984a; Richardson, 2015). At finer spatial scales, heterogeneous carbohydrate availability within canes can result in differential shoot growth (Greaves et al., 1999; Piller et al., 1998; Piller & Meekings, 1997), and intense competition for carbohydrates during flower development has been proposed as a contributor to the strong effects of anthesis timing on subsequent fruit growth (Lai et al., 1990; Lawes et al., 1990; Richardson et al., 2019) (see also Chapter 2).

Techniques such as fruit thinning and girdling can improve spring floral productivity by enhancing carbohydrate availability and reserve accumulation in canopy tissues (Boyd, 2012; Burge et al., 1987; Currie, 1997). However, these techniques can require trade-offs between individual fruit growth, total yield, and root reserve replenishment (Burge et al., 1987; Gould et al., 2025; Lahav et al., 1989; Richardson & McAneney, 1990) and are ultimately limited by the plant's net carbon balance during the growing season.

Plants are capable of absorbing and metabolising exogenous sugars through roots and leaves, and of utilising these sugars to support growths or reserve accumulation. Root-applied sugars have been shown to increase carbohydrate concentrations or growth responses in a range of herbaceous and woody species (Arigita et al., 2002; Mao et al., 2017; Percival & Fraser, 2005), while exogenous sugars supplied to leaves can be absorbed and incorporated into soluble sugar and starch pools (Böhning et al., 1953; Spoehr, 1942; Wan et al., 2024). Supplementing plants with exogenous carbohydrates provides a means to experimentally increase carbohydrate availability independently of endogenous assimilation.

Sugar solutions can also be infused (slowly absorbed at low pressure) or injected (rapidly introduced under high pressure) into stem tissues. Studies in cut flowers have shown that $^{14}C$-labelled sugars can be infused via cut stem ends, are absorbed in both stem and leaf tissues, and

subsequently translocated into flower heads (Horibe et al., 2014; Sacalis & Durkin, 1972). Infusions or injections of exogenous sugars into stem tissues have been shown to support reproductive development and increase yields in maize (Mclaughlin & Boyer, 2004; Zhou et al., 1997; Zinselmeier et al., 1995), decrease fruitlet abscission and improve peel colour development in satsuma mandarins (Iglesias et al., 2001; Iglesias et al., 2003), increase twig and root starch concentrations in oak trees (Martínez-Trinidad et al., 2009), and increase flower bud dry mass and cannabinoid yield in *Cannabis sativa* (Zupančič et al., 2025). Stem infusion of glucose into tree seedlings increased leaf NSC and decreased assimilation rates and root NSC in Sycamore maple, but increased root NSC without leaf affecting assimilation in Scots pine (Zhang et al., 2025b). In, contrast trunk infusions of 5% sucrose to grapevines had no significant effects on subsequent flower production or yield (Dahal et al., 2024).

Previous experiments have shown that broadleaf species may be more sensitive to exogenous sugar infusions than needle-leaved species (Zhang et al., 2025b), potentially reflecting differences in transpiration rates as well as osmotic or feedback inhibition effects on leaf function. When creating wounds and providing energy rich sugar solutions to plants, risk of microbial growth and infection also need to be considered. For these reasons, experimental approaches that involve pulsed, high concentrations of sugars likely create shorter periods of risk of microbial growth than longer term, lower sugar concentration approaches. Because higher concentrations of exogenous sugars are more likely to detrimentally affect leaf function, the winter dormancy period of deciduous species represents a favourable time to introduce such exogenous sugars.

If cane carbohydrate reserve availability is a constraint on spring growth and floral development, then increasing NSC reserve pools via exogenous sugars would be expected to produce detectable effects on growth and reproductive outcomes. To this end, first experiment in this chapter tests whether excised dormant canes are able to absorb exogenous sucrose injected into the xylem apoplast. Experiment 2 investigates the effects of sucrose concentrations on the bark and wood reserve pools of excised canes and subsequent spring growth. Experiment 3 tests whether exogenous sucrose injections to intact vines can influence cane carbohydrate pools and subsequent spring growth, under both normal and strongly carbohydrate limited conditions.

## 4.2 Methods:

### 4.2.1 Experiment 1: Sucrose uptake in excised canes

#### *4.2.1.1 Plant material*

During late dormancy (05/09/2023, before sap flow had commenced), 20 high-vigour, one-year-old canes (at least 1.5 m long) were cut from *Actinidia chinensis* var. *deliciosa* 'Hayward' vines at the Bioeconomy Science Institute research orchard, Te Puke, Bay of Plenty, New Zealand. Canes were cut from scions that had been grafted in 1984 onto two-year-old *A. chinensis* var. *deliciosa* 'Bruno' rootstocks. Vines were trained on T-bar structures.

#### *4.2.1.2 Treatments*

Ten canes were randomly assigned to each of two injection treatments: 5% food grade sucrose (w/v) or tap water. Solutions were adjusted to pH 5.5 with phosphoric acid and dye (brilliant blue FCF) was added. Three samples of each solution were taken prior to injections and analysed as per sections 4.2.1.3 and 4.2.1.4. To inject solutions into canes, cable glands were used to couple the basal ends of excised canes to hydraulic fittings (Figure 4.1 A). Teflon tape was used to improve seals where needed. Canes were simultaneously injected via a manifold constructed from Pneufit hydraulic components (Norgren Ltd, United Kingdom). Pump pressure was maintained at approximately 700 kPa. Solutions were deemed to have permeated the full length of canes when the colour of drips from the distal end of canes was visibly similar to that of the original solution (Figure 4.1 B), which was typically 2 minutes after initial weak colouration was visible. Complete permeation of all canes across both treatments took approximately 10 minutes.

#### *4.2.1.3 Sample collection*

After injections, canes were cut into four 30 cm long sections each and kept at 20 °C. Each section was randomly assigned to a sampling time point, these being 2, 5, 24 and 48 hours after the completion of injection treatments. For each time point, sap from five randomly selected cane section replicates were individually extracted and analysed (Figure 4.1 C). Fresh transverse cuts were made to cane sections, removing approximately 1 cm from each end. Phloem and bark tissues were carefully removed from the distal 2 cm of each section using a craft knife (Ferguson, 1980). The exposed wood was wiped clean with a tissue, then attached to a piece of silicone rubber tubing (Figure 4.1 D). The tubing was connected to a specimen collection vial, which in turn was connected

to a lockable syringe. This allowed a pressure differential to be applied and maintained on multiple sections simultaneously. The ends of cane sections were progressively re-cut to improve extraction rates (Bollard, 1953).

#### *4.2.1.4 Extracted sap measurements*

Once at least 1 mL of solution was extracted per section, 1 mL of the extracted sap was pipetted into a prepared vial with 4 ml of 96% ethanol, which was then frozen in liquid nitrogen prior to analysis. Concentrations of glucose, fructose, sucrose were quantified by ion chromatography using a DIONEX ICS-5000 Reagent-Free™ IC system (Thermo Scientific, San Jose, CA, USA) equipped with an amino trap and CarboPac PA20 column. Final concentrations were calculated after accounting for dilution factors.




Figure 4.1. Methods used for exogenous sucrose uptake experiment 1. A) Cable glands were used to connect an injection manifold to ten individual canes. B) Dye was included in solutions and used to visually determine when solutions had fully permeated the length of canes. After injections were completed, canes were sub-divided into four 30 cm sections. C) At each time point, sap from five cane sections per treatment were extracted simultaneously. D) Sap was collected by first removing a section of bark, then connecting cane sections to specimen vials with silicone rubber tubing and applying a partial vacuum. To facilitate sap extraction, approximately 1 cm was periodically cut from the distal ends of canes when necessary.

#### *4.2.1.5 Statistical analysis*

For each treatment, changes in sap sugar concentrations were analysed using one-way linear models with sampling time as a fixed factor. Where pre-injection concentrations were zero, pre-injection observations were excluded from pairwise analysis due to null variance. Overall effects of timing were assessed using heteroscedasticity-robust Wald tests based on HC3 covariance

estimators (summary table included in Appendix Table C1). Estimated marginal means and 95% confidence intervals were calculated for each time point, and pairwise comparisons among time points were conducted using Tukey-adjusted contrasts.

### 4.2.2 Experiment 2: Sucrose concentration effects on excised canes

#### *4.2.2.1 Plant material*

Five canes (at least 1.5 m long) were selected from each of ten *A. chinensis* var. *deliciosa* 'Hayward' vines at the Bioeconomy Science Institute research orchard, Te Puke, New Zealand. Canes were sourced from scions that had been grafted in 2015 onto three-year-old *A. chinensis* var. *deliciosa* 'Bruno' rootstocks. Canes were excised on 14/06/2022 and had accumulated approximately 150 hours below 7 °C (winter chilling) since the first of May.

#### *4.2.2.2 Treatments*

Ten canes were randomly assigned to each of five treatments (blocked by original vine), these being control (non-injected), and injection of either 0%, 5%, 10% or 15% (w/v) solutions of food grade sucrose. All solutions were adjusted to pH 5.5 with phosphoric acid. Canes were injected with solutions three times over four weeks, using apparatus and methods as described in section 4.2.1 (Figure 4.2 A). After each injection, canes were rinsed with water to remove any external sugar. Between injections, canes were kept at a constant 10 °C in sealed plastic bags.

One week after the third injections were applied, canes were moved into a glasshouse where temperatures were maintained between 14 °C minimum at night and 29 °C maximum during the day. Following previously established methods (Snelgar et al., 1997; Snowball, 1997a), canes were connected to water bottles with silicone rubber tubing and laid horizontally on supporting wires (Figure 4.2 B). Bottles were emptied, cleaned with sodium percarbonate and refilled with water every 3–4 days. Other than during cleaning, bottles were kept covered with aluminium foil to reduce solar heating and microbial growth (Figure 4.2 C).

#### *4.2.2.3 Measurements*

Carbohydrate samples were taken from the most basal internode on each cane, once prior to any injection of solutions, and again one week after the final injections were applied. Internode samples were divided by tissue (bark and wood), then analysed as per methods in section 3.2.2. Soluble sugars concentrations were the combined sum of sucrose, glucose, fructose, raffinose, stachyose,

and planteose. Total non-structural carbohydrate (TNC) concentrations were the combined sum of soluble sugar and starch concentrations.

When flowers had reached a sufficiently advanced stage of development (approx. 1–2 weeks prior to anthesis), cane-level counts were made of the total axillary buds (i.e. both dormant axillary buds and axillary buds that had developed into a shoot), total number of shoots, number of shoots with flowers, and total number of inflorescences (Figure 4.2 D).

From these values the following metrics of spring growth and flower production were calculated:

Budbreak percentage = total shoots / total axillary buds

Floral shoot percentage = total floral shoots / total shoots

Inflorescences per axillary bud = total inflorescences / total axillary buds

#### *4.2.2.4 Statistical analysis*

Carbohydrate data were expressed as the change in concentration over the course of the experiment (i.e. final – initial). A linear model was fitted for each tissue × carbohydrate group combination, with change in concentration as the response, treatment as a fixed factor, and parent vine as a blocking factor. Similarly, linear models for budbreak percentage, floral shoot percentage, and inflorescences per axillary buds were fitted using treatment as a fixed factor and vine as a blocking factor. Estimated marginal means and 95% confidence intervals were calculated for each treatment, and significant differences between treatments were assessed via Šidák-adjusted pairwise comparisons. Type II ANOVA summary tables for carbohydrate and spring growth metrics are provided in Appendix Table C2 and Table C3, respectively.

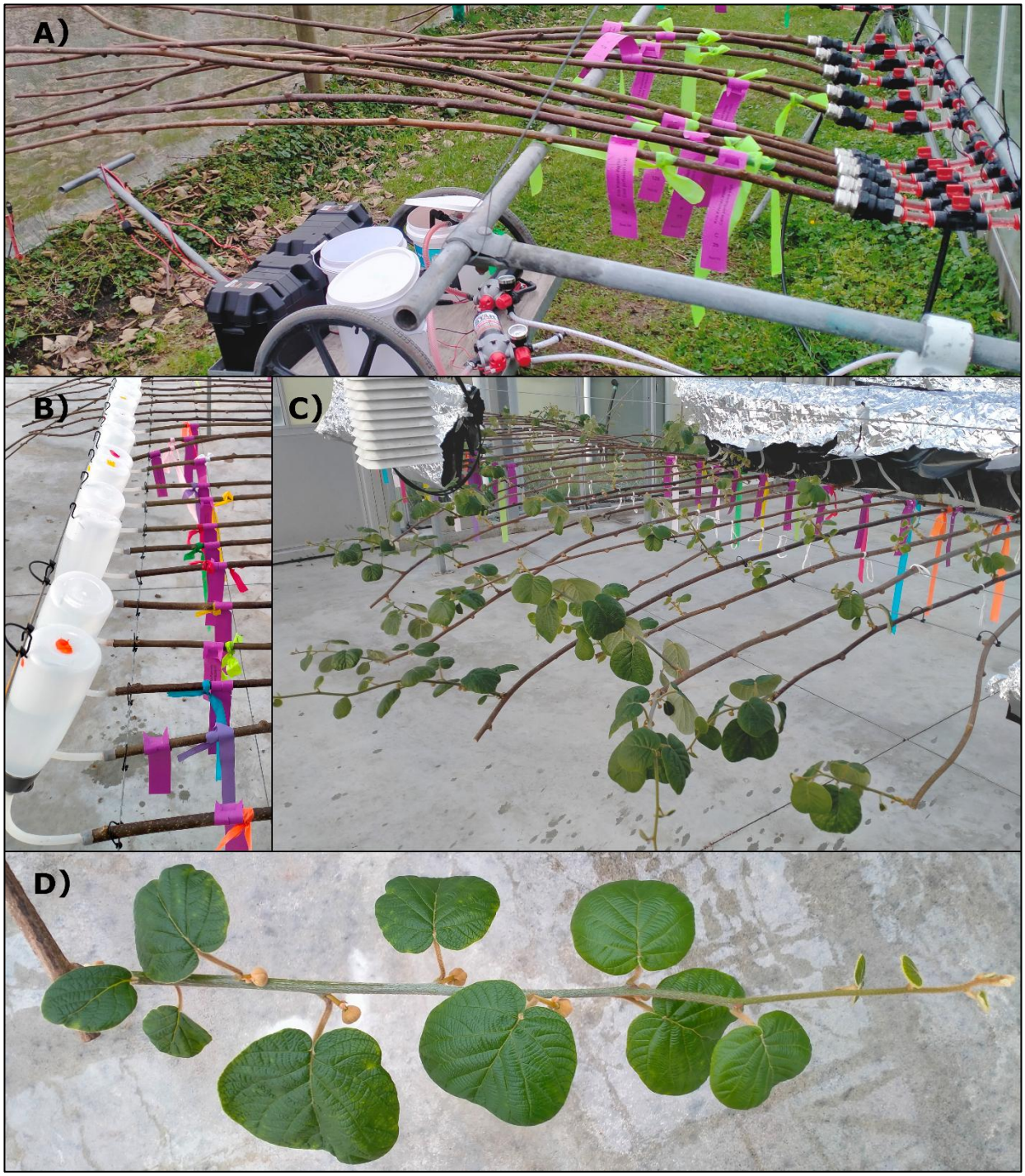


Figure 4.2. Methods used for exogenous sucrose injections on excised canes. A) *Actinidia chinensis* var. *deliciosa* 'Hayward' canes were injected three times across four weeks with differing concentrations of sucrose (0–15% w/v) at 700 kPa. B) Following injections, canes were connected to water bottles and placed into warm glasshouse conditons. C) Bottles were covered with aluminium foil to reduce sun exposure. D) Budbreak, floral shoot percentage and inflorescences per axillary bud were assessed six weeks after being placed in a glasshouse. The shoot shown in D has five inflorescences where all but the terminal flowers have aborted.

### 4.2.3 Experiment 3: Defoliation × sucrose injection of intact vines

#### *4.2.3.1 Plant material and experimental design*

Experimental vines were *A. chinensis* var. *chinensis* 'Zesy002' located at the Bioeconomy Science Institute research orchard, Te Puke, New Zealand. Vines had been grafted in 2012 onto established 'Bruno' rootstocks (planted 1972). In early autumn (01/03/2024), 12 vines were selected and divided into three statistical blocks of four. Canopy dimensions were approximately 3 m × 6 m, with separate rows for male and female vines ("strip-male" layout). Within each block, vines were randomly assigned to a canopy treatment (intact or ¾ defoliation) and an injection treatment (no injection or 10% sucrose), using a two-way factorial design. Vine management was similar to that described for conventional vines in Chapter 2, with the exception of experimental treatments detailed in section 4.2.3.2. Additionally, no trunk girdles were applied, and fruit were left attached to vines until all treatments were complete and carbohydrate samples were collected. Hydrogen cyanamide was applied at 6% on 14/08/2024.

#### *4.2.3.2 Treatments*

Defoliation treatment vines had ¾ of their leaves removed in early autumn (09/03/2024) (Figure 4.3 A). Defoliation was maintained until winter leaf fall by weekly removal of ¾ of new leaf growth.

Trunk injections were applied to vines in early winter (03/06/2024). Solutions of 10% (w/v) food grade sucrose were prepared and adjusted to pH 5.5 using phosphoric acid. For injection treatment vines, four 5 mm holes were drilled equidistantly around the trunk circumference. Drill holes were thoroughly rinsed with water, then custom-built pressure ports were screwed into the holes and connected to a pump (Figure 4.3 B, C). Solutions were injected at approximately 700 kPa, taking approximately 30–45 minutes to inject approximately 10 litres of solution into each vine, with minor losses occurring due to leakage around the injection ports. Pressurisation of the xylem network throughout the canopy was evident from widespread leaf guttation and sap dripping from cut cane ends (Figure 4.3 D).

#### *4.2.3.3 Measurements*

Three non-terminated shoots (at least 1.5 m long) were removed from each vine in early autumn (08/03/2024), prior to any treatment applications. An internode located approximately 0.3 m from the base of each shoot was divided into bark and wood tissues and analysed for carbohydrates as

per methods detailed in section 4.2.2.3. In late autumn (30/05/2024), shortly prior to injection treatments, a second round of carbohydrate samples were taken from another set of three shoots. A third round of carbohydrate samples were taken from three shoots (now fully lignified canes) per vine in winter (16/06/2024), 13 days after the injection treatments were applied.

Xylem exudate dripping from cane ends was collected at both the start and near the end of injection treatments. Exudate soluble solids content (SSC) was measured via digital refractometer (Atago PAL-1, Japan) and pH was measured via pH meter (Bluelab, New Zealand).

In spring, budbreak percentage, floral shoot percentage, and inflorescences per axillary bud were assessed on four canes per vine, as described in section 4.2.2.3.

#### *4.2.3.4 Statistical analyses*

The SSC and pH data of collected cane exudate were analysed using linear mixed-effects models with time of sample (start or end of injection) as a fixed effect and random intercepts for replicate canes within vines. For SSC data, a variance-identification structure was included to account for heteroscedasticity between start and end measurements.

For carbohydrate data, linear mixed-effects models were fitted separately for each carbohydrate pool (soluble sugars, starch, and TNC), tissue (bark and wood), and sampling period (March, May, June). Models included canopy treatment (intact vs ¾ defoliated) and injection treatment (no injection vs 10 % sucrose) as fixed effects, with vine nested within block as a random factor. Type III ANOVA tables are included in Appendix C. Where interaction effects were significant, means were compared using Holm-adjusted pairwise comparisons. Individual carbohydrate concentrations per treatment and sample combination are provided for bark in Appendix Table C10 and for wood in Appendix Table C11.

For spring growth metrics (budbreak percentage, floral shoot percentage, and inflorescences per axillary bud), results were analysed as a two-way factorial with canopy treatment (intact vs ¾ defoliated) and injection treatment (no injection vs 10 % sucrose) as fixed effects, with vine nested within block as a random factor. There were no significant interactions, so pairwise comparisons were not required. A Type III ANOVA summary table is included as Appendix Table C9.




Figure 4.3. Methods used for defoliation and sucrose injections in experiment 3 on *Actinidia chinensis var. chinensis* 'Zesy002' vines. A) Defoliation treatment vines had three of every four leaves removed, commencing in early March after initial carbohydrate samples were taken. Defoliation treatments were maintained until final carbohydrate samples were taken in June. Fruit was left attached to all vines for the duration of the experiment. B) Vines were injected with 10% (w/v) food grade sucrose adjusted to pH 5.5 with phosphoric acid. 5 mm holes were drilled into the trunk and rinsed with water before custom-built ports (inset, scale is cm) were screwed into the hole. Approximately 10 litres of solution were injected into each treated vine at approximately 700 kPa. C) Close-up of ports from B, spaced approximately equally around the trunk. Teflon tape was wrapped around port threads to reduce leakage. D) Injections rapidly pressurised the entire canopy vascular network, causing visible guttation on leaves throughout the vine (photo taken at 1630 hrs) and dripping of sap/exudate from cut ends of canes.

### 4.2.4 Statistical analyses

All analyses and data visualisations were performed in R software (R Core Team, 2025). Linear mixed-effects models were fitted with the *lme4* and *lmerTest* packages (Bates et al., 2015; Kuznetsova et al., 2017). Estimated marginal means and 95% confidence intervals were obtained using the *emmeans* package (Lenth, 2024), and significance groupings were assigned using the *multcomp* package (Graves et al., 2024). Plots were generated with *ggplot* (Wickham, 2016) and arranged with *patchwork* (Pedersen, 2025).

## 4.3 Results

### 4.3.1 Experiment 1: Sucrose uptake rate

For sucrose-injected canes, the xylem sap sucrose concentrations fell rapidly over the sampling period, reaching ~53% of the injected solution concentration (50 mg $ml^{-1}$) after five hours, 6.4% after 24 hours, and 2.8% after 48 hours (Figure 4.4 A). Glucose and fructose were detected two hours after injection and reached maximum values at 24 hours (glucose 5 mg $ml^{-1}$, Figure 4.4 B; fructose 11 mg $ml^{-1}$, Figure 4.4 C). The combined concentration of sucrose, glucose and fructose fell steadily over time, reaching 15.5 mg $ml^{-1}$ after 48 hours (Figure 4.4 D).

For canes injected with water, low concentrations of sucrose, glucose and fructose were detected in the extracted sap, with concentrations peaking at 48 hours. The mean concentrations after 48 hours were ~0.68 mg $ml^{-1}$ for sucrose, ~0.06 mg $ml^{-1}$ for glucose, and ~0.1 mg $ml^{-1}$ for fructose, for a combined total of 0.84 mg $ml^{-1}$.

### 4.3.2 Experiment 2: Sucrose concentration effects

Sucrose injections to excised canes had dose-dependent effects on their carbohydrate pools. Significant differences between treatments were detected for all carbohydrate groups in both bark and wood tissues (Appendix Table C2).

For bark tissues, relative to the control, injections of 0% sucrose significantly decreased the soluble sugar and TNC concentrations; 5% sucrose injections did not significantly affect any carbohydrate concentration; and both 10 and 15% sucrose increased concentrations of starch, soluble sugars, and TNC (Figure 4.5 A–C).

In wood tissues, injections of 0% and 5% sucrose did not significantly affect any carbohydrate concentration relative to the control. In contrast, both 10% and 15% sucrose injections significantly increased both soluble sugar and total carbohydrate concentrations, and 10% sucrose injections also significantly increased starch concentration relative to the control (Figure 4.5 D–F).

Effects of injection treatments on spring growth metrics were minor. Only 10% sucrose-injected canes had significantly higher budbreak percentage compared with control canes (Figure 4.6 A). There were no significant effects between any treatments and/or control canes for either floral shoot percentage or inflorescences per axillary bud (Appendix Table C3, Figure 4.6 B, C).

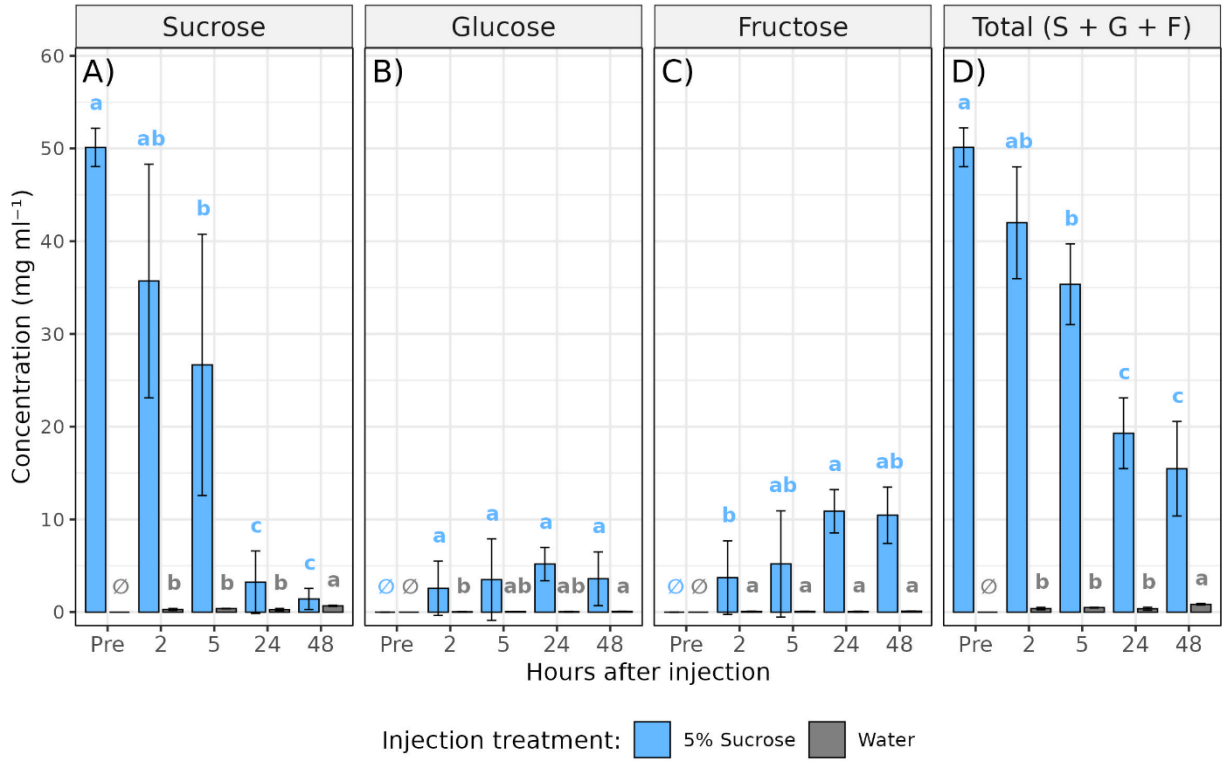


Figure 4.4. Change in xylem sap sugar concentrations over time for *Actinidia chinensis* var. *deliciosa* 'Hayward' canes injected with water or a 5% w/v (50 mg ml$^{-1}$) sucrose solution. Injected solutions were adjusted to pH 5.5 with phosphoric acid. Xylem sap was vacuum extracted from cane sections at fixed lengths of time after injections. 'Total' is the summed concentrations of sucrose, glucose and fructose. Columns are estimated marginal means and error bars are 95% confidence limits. Within each treatment (colour-coded), groups that do not share a letter were significantly different (Tukey-adjusted $\alpha = 0.05$). Ø indicates pairwise comparisons were not computable due to exact zero values pre-injection.

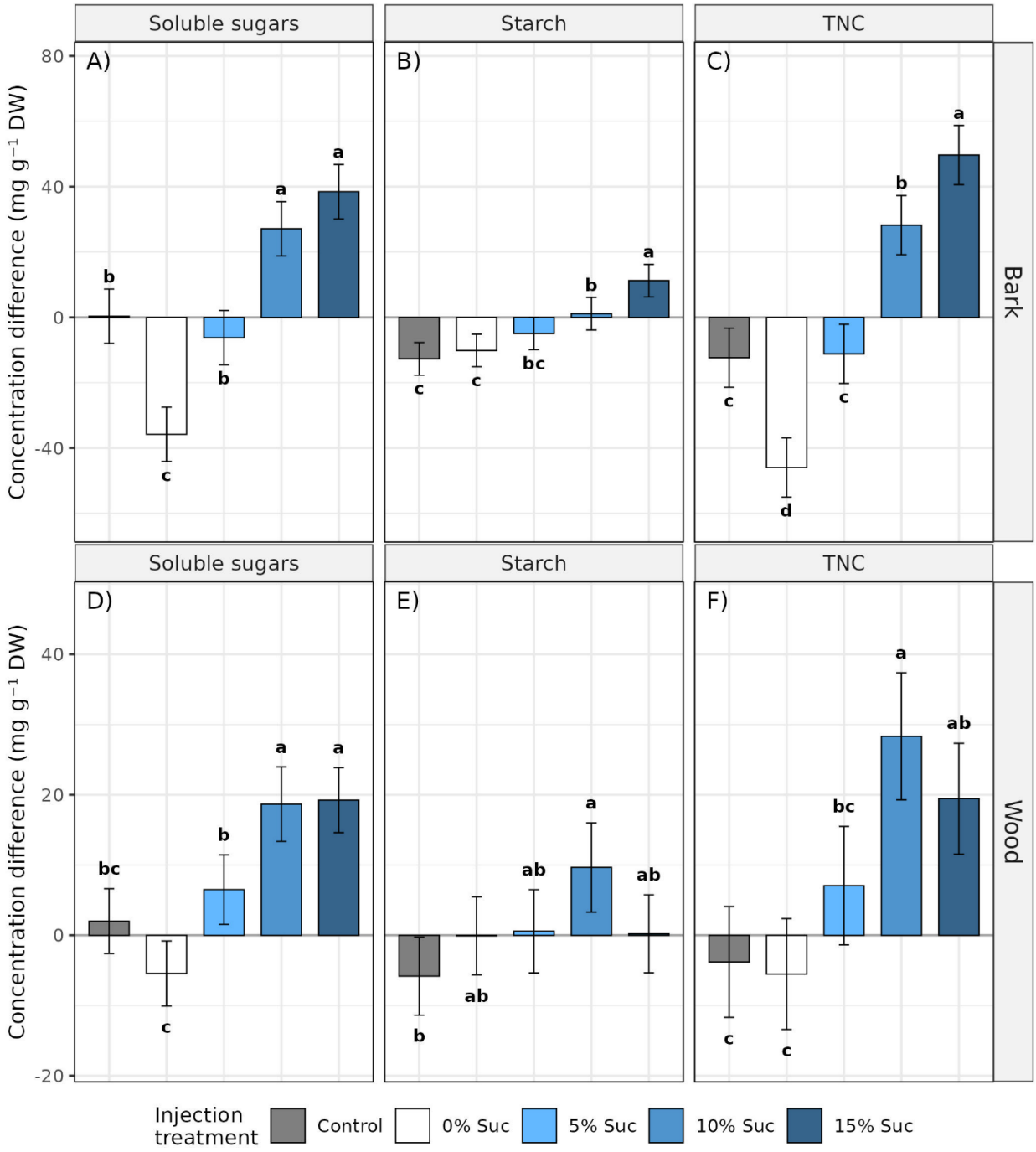


Figure 4.5. Changes in cane bark (A–C) and wood (D–F) carbohydrate concentration following injections of sucrose. Dormant *Actinidia chinensis* var. *deliciosa* 'Hayward' canes were injected three times over four weeks with solutions with 0%–15% (w/v) of food grade sucrose. All injected solutions were adjusted to pH 5.5 with phosphoric acid. Soluble sugars are the sum of sucrose, glucose, fructose, planteose, raffinose and stachyose concentrations. Total non-structural carbohydrate (TNC) is the summed concentrations of soluble sugars and starch. Concentration differences were calculated as post-treatment concentration – pre-treatment concentration. Columns show estimated marginal means ±95% confidence intervals. Within each panel, groups that do not share a letter were significantly different (Tukey-adjusted $\alpha = 0.05$).

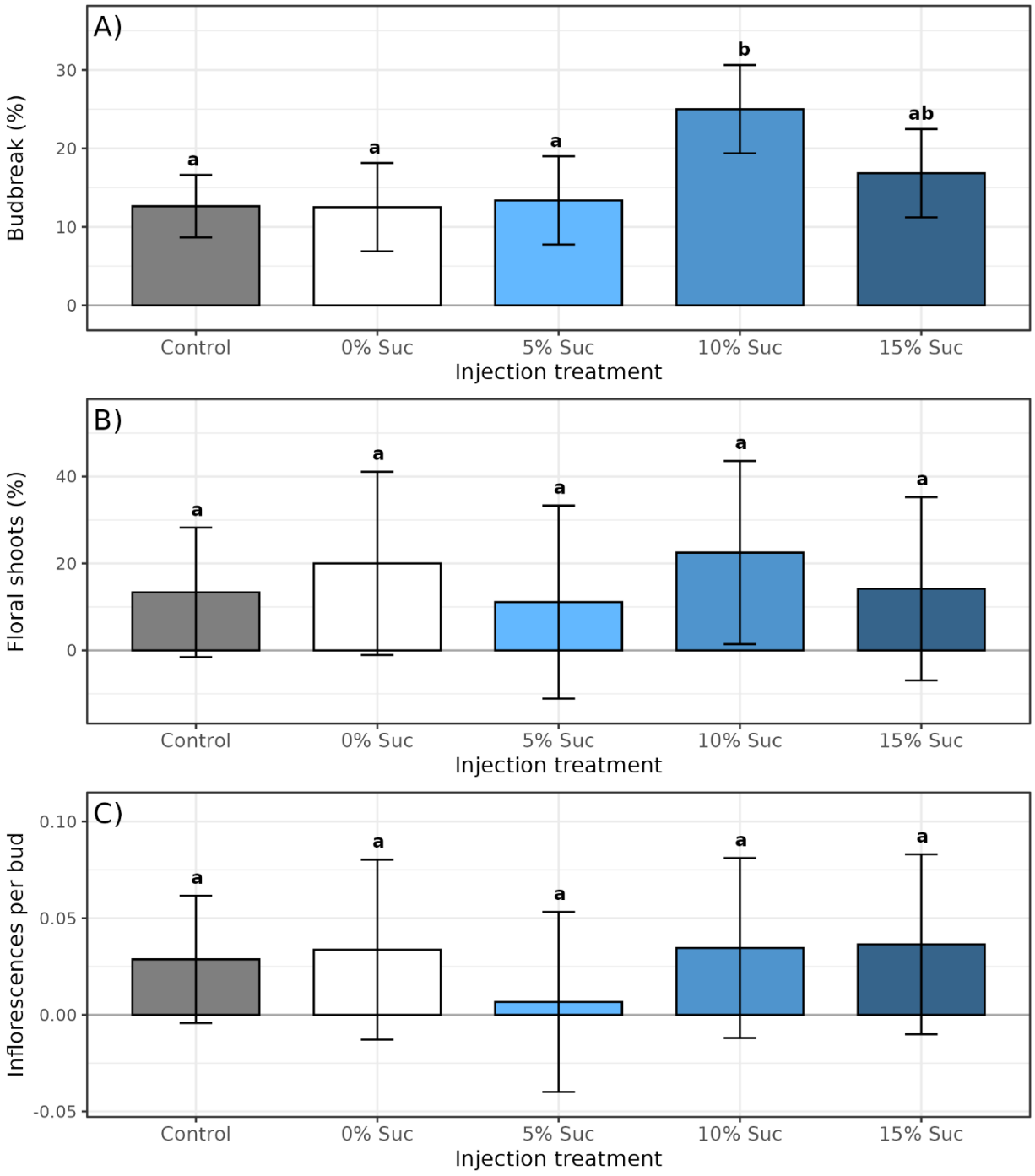


Figure 4.6. Effects of sucrose injection treatments on A) budbreak percent; B) floral shoot percent; and C) inflorescences per axillary bud. Dormant *Actinidia chinensis* var. *deliciosa* 'Hayward' canes were injected three times over four weeks with solutions with 0%–15% (w/v) of food grade sucrose. All injected solutions were adjusted to pH 5.5 with phosphoric acid. Columns show estimated marginal means ±95% confidence intervals. Within each panel, groups that do not share a letter were significantly different (Tukey-adjusted $\alpha = 0.05$).

### 4.3.3 Experiment 3: Whole vine injection × defoliation

Exudate collected from cut cane ends had significant increases in both pH and SSC between the start and end of injection treatments (Figure 4.7). The increase in pH was moderate, increasing from 5.4 to 5.9. In contrast, the change in SSC was large, increasing from approximately 0.1 °Bx to 5.7 °Bx, although there was substantial variability among samples at the end of injections. Within three days of sucrose injection treatments, widespread leaf phytotoxicity was evident in the canopies of treated vines (Figure 4.8).

Carbohydrate concentrations of samples collected in March did not significantly differ between treatment groups, as expected because samples were collected prior to any treatment application. Similarly, carbohydrate concentrations of samples collected in May did not significantly differ between injection treatment groups (Appendix Table C6–Table C8).

For samples collected in June, there was a significant interaction effect between defoliation and injection treatments for soluble sugars in both bark and wood tissues (Appendix Table C6). In both tissues, soluble sugar concentrations were significantly higher in the defoliated × sucrose-injected treatment than in the defoliated × non-injected treatment (Figure 4.9 C, F).

Defoliation treatments did not significantly affect soluble sugar concentrations in May samples but did significantly reduce starch concentrations in both bark and wood (Figure 4.10 B, E), as well as total NSC concentration in both tissues (Figure 4.11 B, E). In June, the main effect of defoliation also significantly reduced starch concentrations in both bark and wood (Figure 4.10 C, F), with no significant interaction effects detected for either tissue (Appendix Table C7).

In June samples, sucrose injection significantly increased bark TNC concentration (Figure 4.11 C), while defoliation significantly reduced TNC concentration in wood tissue (Figure 4.11 F). No significant interaction effects were detected for TNC concentration in either tissue (Appendix Table C8).

Defoliation treatments significantly reduced spring budbreak percentage (Figure 4.12 A), floral shoot percentage (Figure 4.12 B), and inflorescences per axillary bud (Figure 4.12 C). There were no significant main effects of sucrose injection, nor any significant interaction effects, for any spring growth metric (Appendix Table C9).

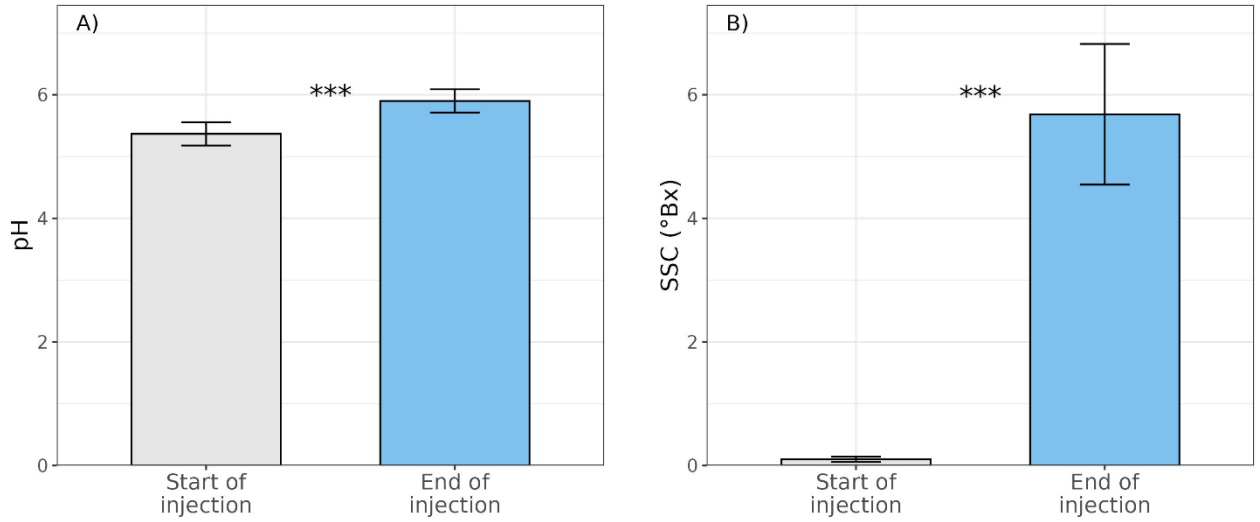


Figure 4.7. A) pH; B) soluble solids concentration of exudate dripping from cane ends at the start and finish of the injection period. *Actinidia chinensis* var. *chinensis* 'Zesy002' vines were injected with 10% sucrose solution adjusted to pH 5 with phosphoric acid, delivered via ports screwed into the trunk. Columns show estimated means ±95% confidence intervals derived from linear models. Asterisks denote significant differences between start and end concentrations (***, $p < 0.001$).

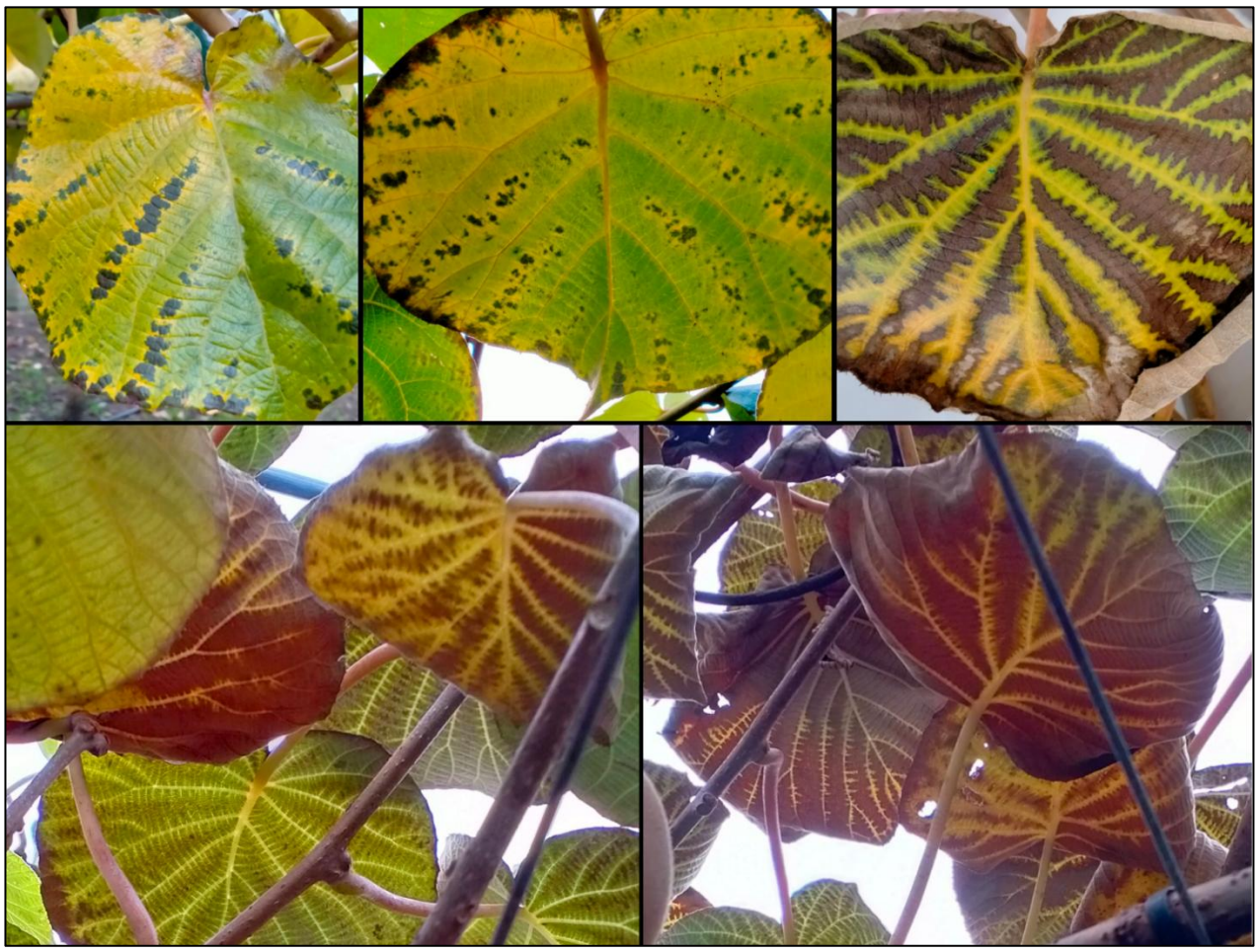

Figure 4.8. Examples of leaf phytotoxicity and damage following trunk injections of 10% (w/v) sucrose in experiment 3.

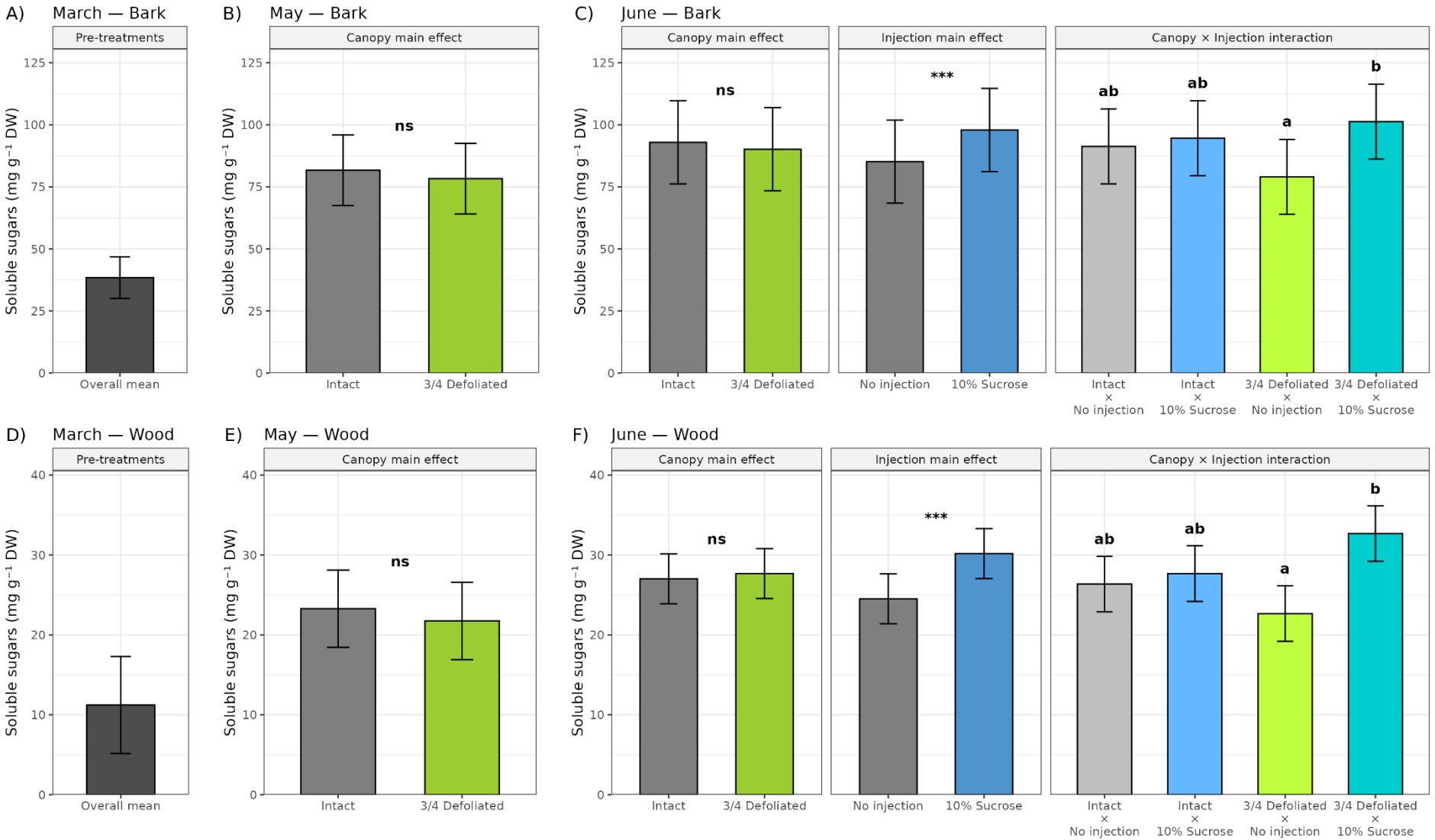


Figure 4.9. Effects of defoliation and trunk injection on soluble sugar concentrations in the bark (A–C) and wood (D–F) of *Actinidia chinensis* var. *chinensis* 'Zesy002' shoots. Defoliation treatments were applied immediately after the March sampling and maintained until June sampling. Trunk injections were of approximately 10 L of 10% (w/v) food grade sucrose adjusted to pH 5.5. with phosphoric acid, applied shortly after the May sampling. June samples were collected two weeks after injection treatments. Soluble sugars are the sum of sucrose, glucose, fructose, planteose, raffinose and stachyose concentrations. Columns show estimated marginal means ± 95% confidence intervals. March panels show the overall mean of all four treatment combinations as treatments had not yet been applied. May panels show canopy treatment main effects only as the injection treatments were applied subsequently. For May and June panels, asterisks indicate significant main effects (*** $p < 0.001$; ns = not significant). For the June interaction panels, groups sharing a letter were not significantly different (Holm-adjusted $\alpha = 0.05$).

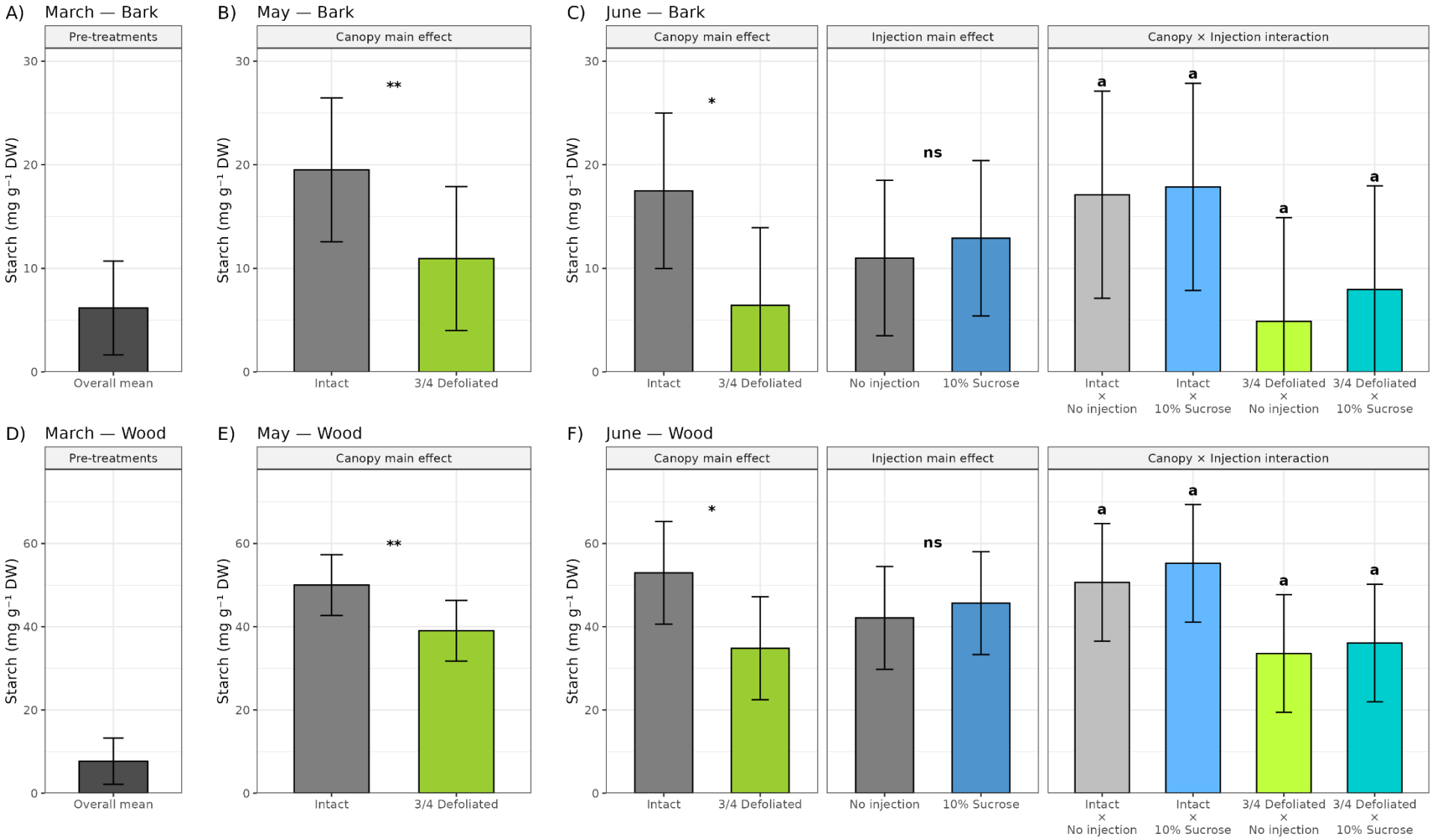


Figure 4.10. Effects of defoliation and trunk injection on starch concentrations in the bark (A–C) and wood (D–F) of *Actinidia chinensis* var. *chinensis* 'Zesy002' shoots. Defoliation treatments were applied immediately after the March sampling and maintained until June sampling. Trunk injections were of approximately 10 L of 10% (w/v) food grade sucrose adjusted to pH 5.5. with phosphoric acid, applied shortly after the May sampling. June samples were collected two weeks after injection treatments. Columns show estimated marginal means ± 95% confidence intervals. March panels show the overall mean of all four treatment combinations as treatments had not yet been applied. May panels show canopy treatment main effects only as the injection treatments were applied subsequently. For May and June panels, asterisks indicate significant main effects (* $p < 0.05$; ** $p < 0.01$; ns = not significant). For the June interaction panels, groups sharing a letter were not significantly different (Holm-adjusted $\alpha = 0.05$).

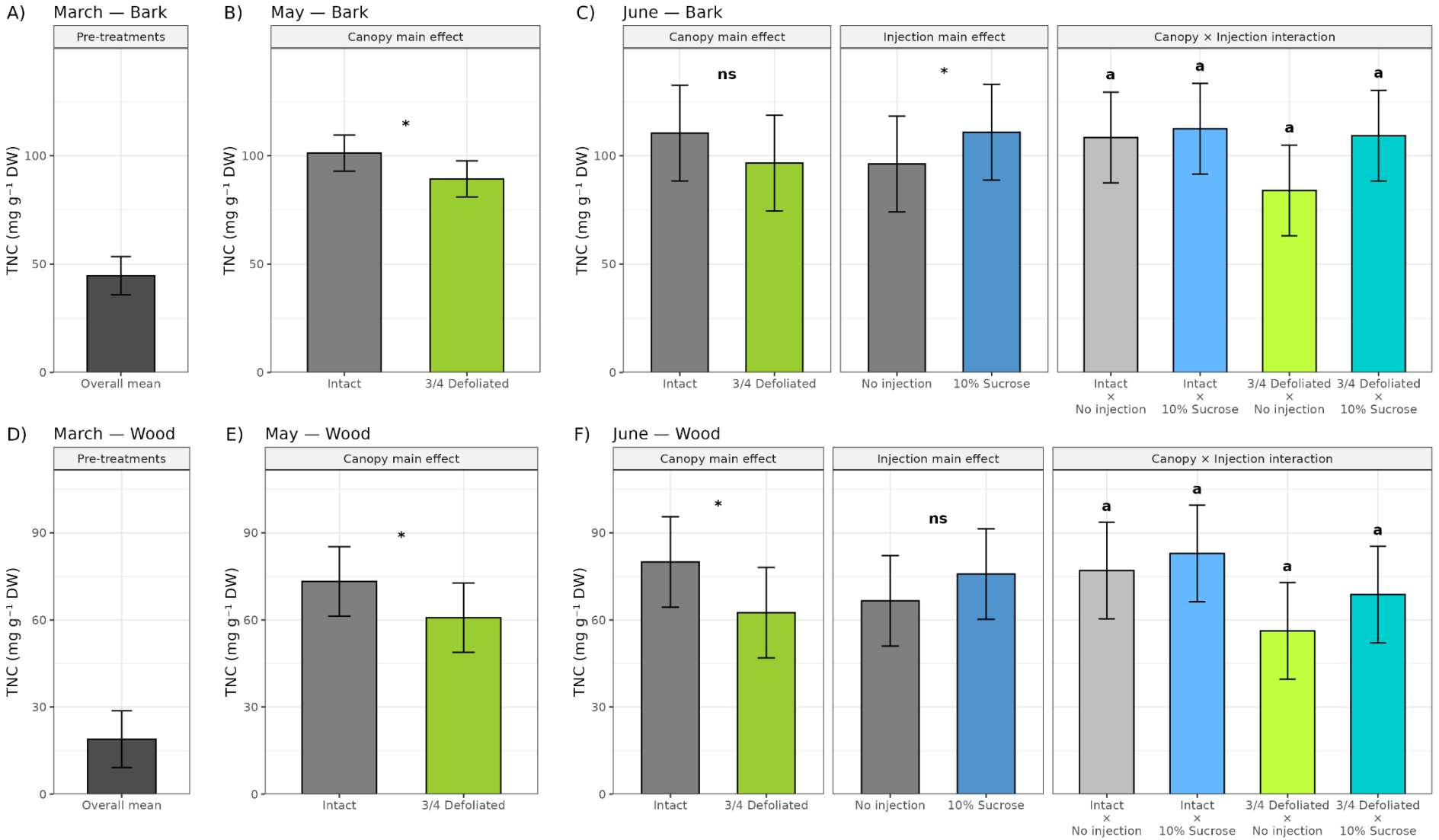


Figure 4.11. Effects of defoliation and trunk injection on total non-structural carbohydrate (TNC) concentrations in the bark (A–C) and wood (D–F) of *Actinidia chinensis* var. *chinensis* 'Zesy002' shoots. Defoliation treatments were applied immediately after the March sampling and maintained until June sampling. Trunk injections were of approximately 10 L of 10% (w/v) food grade sucrose adjusted to pH 5.5. with phosphoric acid, applied shortly after the May sampling. June samples were collected two weeks after injection treatments. TNC is the sum of sucrose, glucose, fructose, planteose, raffinose, stachyose and starch concentrations. Columns show estimated marginal means ± 95% confidence intervals. March panels show the overall mean of all four treatment combinations as treatments had not yet been applied. May panels show canopy treatment main effects only as the injection treatments were applied subsequently. For May and June panels, asterisks indicate significant main effects (* $p \leq 0.05$; ns = not significant). For the June interaction panels, groups sharing a letter were not significantly different (Holm-adjusted $\alpha = 0.05$).

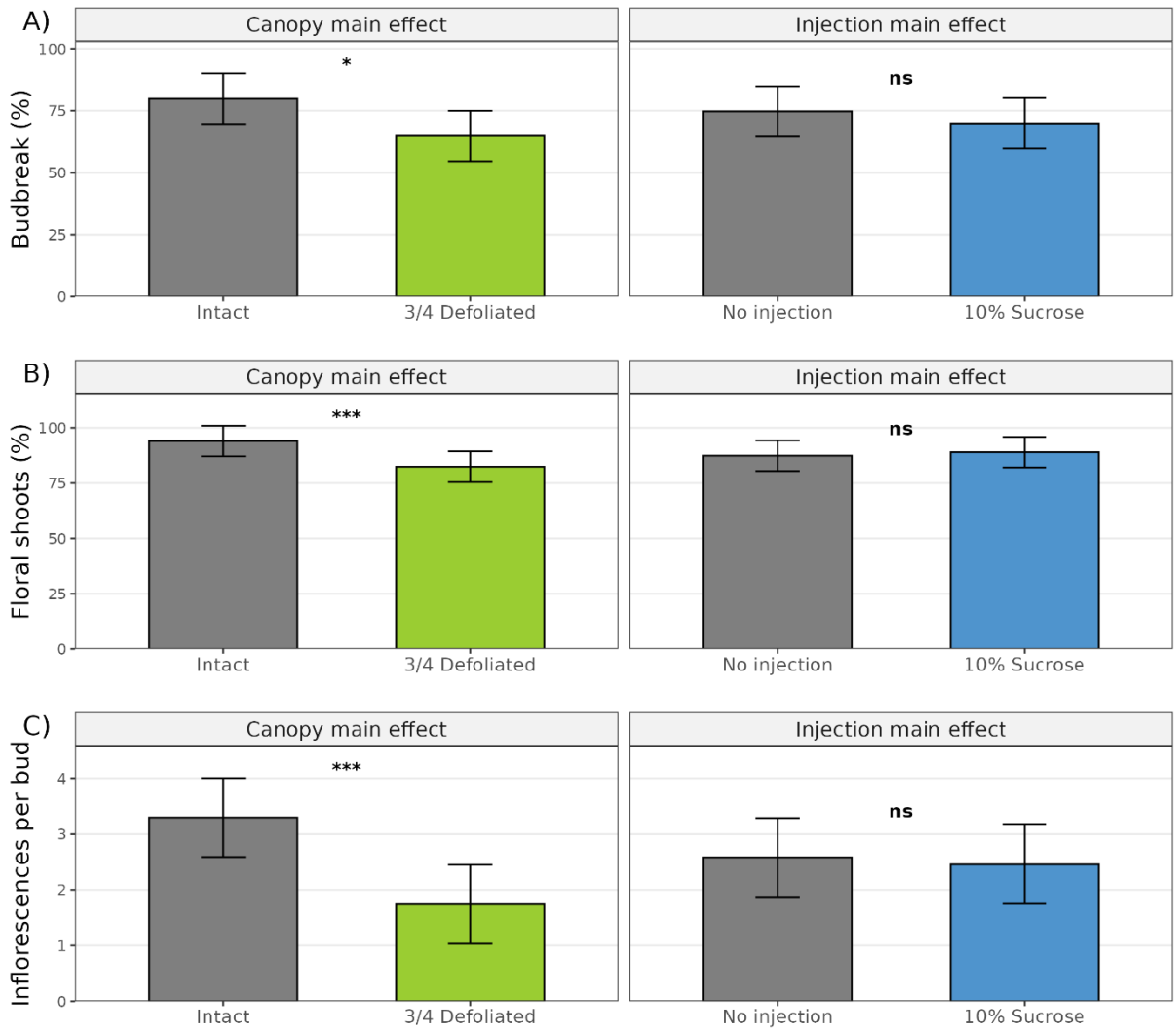


Figure 4.12. Effects of trunk injection and defoliation on budbreak percentage, floral shoot percentage and inflorescences per bud of *Actinidia chinensis* 'Zesy002' canes. Columns show estimated marginal means, error bars are ±95% confidence intervals. Trunk injections were of approximately 10 litres of 10% (w/v) food grade sucrose adjusted to pH 5.5. with phosphoric acid. Injections were applied in late May before leaf fall. Only main effects are shown as no interaction effects were significant. ns, not significant ($p > 0.05$); *, $p < 0.05$; **, $p < 0.01$; ***, $p<0.001$.

## 4.4 Discussion

### 4.4.1 Exogenous sucrose injections can increase cane NSC pools

Kiwifruit canes are readily able to absorb sucrose injected into the xylem, as indicated by the rapid decrease in the sucrose concentrations of vacuum-extracted solutions over 48 hours in experiment 1. Similar rapid rates of absorption of exogenous sucrose have been documented in xylem infusion experiments in dormant branches of both *Salix* and *Populus* (Sauter, 1981a, 1981b). The detection of both glucose and fructose in the extracted solutions after only 2 hours indicates that sucrose is being rapidly hydrolysed in the apoplast, likely catalysed by cell wall invertase (Ruan et al., 2010). The decreasing total sugar concentration over time in sucrose-injected canes indicates that sugars are being progressively absorbed from the injected

solutions, although it is not clear whether both sucrose and hexoses are being absorbed or if sucrose hydrolysis is a prerequisite for symplastic uptake. Immunolocalisation experiments have demonstrated high expression of SUT1 sucrose transporters in vessel associated cells (VAC) of *Nicotiana tabacum* (Schmitt et al., 2008), and both sucrose (SUT1) and hexose (HT1, HT2) transporters have been localised to VAC in *Juglans regia* (Decourteix et al., 2008; Decourteix et al., 2006). Immulocalisation studies complemented by sucrose transporter inhibition (M'Batchi & Delrot, 1984) could elucidate whether both sucrose and hexoses transporters are present in kiwifruit VAC.

Repeat injections of kiwifruit canes in experiment 2 strongly affected the starch and soluble sugar pools of both bark and wood tissues. While the phloem of the excised canes was exposed to sucrose solutions at the cut cane surface, bulk sucrose uptake directly into the phloem is unlikely due to the rapid occlusion of sieve elements by P-proteins (Knoblauch & van Bel, 1998; van Bel, 2006), and the relatively small area of phloem directly exposed. These results therefore suggest that sugars were absorbed from the xylem apoplast and subsequently transported into the bark, presumably via ray parenchyma (Thorpe et al., 2005; van Bel, 1990). The dose-dependent response observed in the bark suggests that canes were able to tolerate and metabolise even the highest concentrations of exogenous sucrose. While these results suggest that the exogenous sucrose was at least partially absorbed and transported within the cane tissues, it remains unclear whether in was subsequently mobilised. As the sucrose used in these experiments was derived from sugar cane, it may be possible to use mass spectrometry to detect an elevated $\delta^{13}C$ signature in spring growth (Zhang et al., 2025a), providing more conclusive evidence whether the injected sugar was indeed bioavailable and incorporated into new shoots and flowers.

In contrast, changes to starch concentrations were more variable in the wood and were only significantly increased by injections with 10% sucrose. High concentrations of injected osmolytes would create a highly atypical osmotic gradient where the apoplast has a more negative osmotic potential than the symplast. This could theoretically trigger hydrolysis of starch or RFOs in wood parenchyma cells to decrease the symplastic osmotic potential, protecting against excessive water loss and plasmolysis. However, in experiments where similar high concentrations of osmolytes are introduced into the xylem apoplast it appears that sucrose may cause specific, non-osmotically driven effects on stem starch hydrolysis (Secchi & Zwieniecki, 2011). Because of these considerations, it is possible that different concentrations of apoplastic sucrose could cause either starch accumulation or degradation in the wood.

Furthermore, in leafless excised canes, the physiological responses to by exogenous sucrose are likely to be intensified and/or prolonged by the absence of a diluting transpiration stream.

### 4.4.2 Trunk sucrose injections increased cane soluble sugar but not starch

In experiment 3, whole vines were subjected to defoliation throughout autumn, a key period when vines replenish their woody internode carbohydrate reserves (Richardson et al., 2017; Smith et al., 1992). Defoliation treatments significantly decreased the starch and TNC concentrations in both the wood and bark of shoots/canes but did not significantly affect the soluble sugar concentrations in either tissue. This is consistent with previous studies in both grapevines and kiwifruit where defoliation reduced starch concentrations in both trunk and roots more than soluble sugars (Bennett et al., 2005; Kwack et al., 2014), and is also similar to results from Chapter 3 where soluble sugar concentrations stayed relatively stable during spring while starch pools were rapidly depleted, suggesting a baseline concentration of soluble sugars is sustained to support respiration and growth, with starch synthesis and hydrolysis regulated to maintain osmotic homeostasis.

Sucrose injected via the trunk was detectable in exudate dripping from cut cane ends near the end of the experiment, indicating that the 10 L injections of sucrose per vine were sufficient to perfuse throughout the xylem network. As was observed in excised canes, this sucrose was likely absorbed via VAC and successfully crossed the cambium to increase the soluble sugar concentrations in both cane wood and bark. Interestingly, a significant interaction indicated that the effect of sucrose injection was much larger in defoliated vines than in intact vines, and this may directly relate to their reduced leaf number. After injections were complete, vines with comparatively low leaf area would lose less water to transpiration, causing the exogenous sucrose to have a longer residence time within the xylem water column, which as shown in experiments 1 and 2 is able to rapidly absorb and integrate exogenous sugars over 48 hours, consistent with previous studies (Sauter, 1981b; Sauter, 1983; Vogelmann et al., 1985). In contrast, sugars carried to leaves in the transpiration stream apparently accumulated more rapidly than they were able to be absorbed and polymerised for osmotic regulation (Charrier, 2020), with excessive symplastic water loss and cell plasmolysis the presumed cause of observed phytotoxic effects. Due to this damage, it is not clear what capacity these leaves retained to export sugars via the phloem, and over the subsequent weeks after sucrose injections many damaged leaves abscised. On defoliated vines there was similar phytotoxicity observed, however

there were also fewer leaves for this sugar to accumulate in and therefore a smaller proportion of the exogenous sucrose may have been 'lost' in this way.

In contrast, there were no significant effects of trunk sucrose injections on the starch concentrations of either cane bark or wood tissues. This contrasts with results from experiment 2, where injections of 10% sucrose increased both bark and wood starch concentrations. It is likely that in experiment 2 the repeat injections, absence of leaves and short path length from the cut cane end allowed for more sucrose to be absorbed and synthesised into starch. Temperature may also be a contributing factor, as it can affect the rates of starch synthesis and degradation both via regulation of enzyme expression or by differential effects of temperature on specific enzymes (Koussa et al., 2005; Schrader & Sauter, 2002; Zwieniecki et al., 2015). Canes in experiment 2 were kept at a constant 10 °C between injections, which may have been sufficient to favour starch synthesis over starch degradation (Pollock & Lloyd, 1987). In contrast, the vines in experiment 3 were in field conditions, and were exposed to temperatures <5 °C in the first three nights after injections. This may have favoured starch degradation and accumulation of soluble sugars for cryoprotection (Sakai & Yoshida, 1968; Sun et al., 2020).

Sucrose injections appear to have compensated for the reduction in total NSC concentration caused by defoliation in the bark not in the wood. As the wood represents a substantially larger proportion of the cane biomass by dry weight, this indicates sucrose injections were insufficient to restore overall cane NSC pools where they had been reduced by defoliation treatments. It is possible that repeat injection treatments could increase the total amount of sucrose delivered to vines, particularly after initial treatments cause leaf phytotoxicity and abscission.

### 4.4.3 Exogenous sucrose did not increase spring growth

Despite significantly increasing the total carbohydrate concentrations in both the bark and wood of sucrose-injected dormant canes in experiment 2, the effects on subsequent growth were minimal, with only 10% sucrose injections having a significant increase in budbreak relative to control. This aligns with changed to wood starch concentrations between treatments, however neither floral shoot percentage nor inflorescences per axillary bud were similarly affected. Due to high variability of spring growth between canes, it would be prudent to repeat this experiment before attributing the increase in budbreak to increased carbohydrate reserves. The canes used in this experiment had experienced only ~150 hours of winter chilling, reflected in particularly low budbreak percentages (13–25%) and very low inflorescence production across all treatments. Using canes that had experienced more winter chilling should increase the baseline

budbreak and flower production (Brundell, 1976; Lionakis & Schwabe, 1984a), thereby increasing competition for carbohydrates and emphasizing any effects of increasing cane NSC reserve pools. Similarly, cultivars with naturally higher budbreak and flower production may also be more sensitive to alterations in cane carbohydrate reserves.

Experimentally manipulating photosynthate availability and translocation by shading and girdling in autumn can also respectively decrease and increase the sucrose concentrations of kiwifruit axillary buds (Richardson et al., 2007). During the induction of endodormancy in deciduous woody plants, buds become symplastically isolated via callose deposition in plasmodesmata (Fadón et al., 2020), stopping further NSC import. Short day photoperiods have been demonstrated to induce dormancy in deciduous tree species and grapes (Fennell & Hoover, 1991; Kramer, 1936), and induce ABA-mediated plasmodesmata closure in aspen buds (Tylewicz et al., 2018). However, temperature cues appear to be more important in dormancy induction in other species including apple and pear (Heide, 2011; Heide & Prestrud, 2005). Under controlled conditions, endodormancy can be induced in shoots grown from kiwifruit cuttings by nine weeks of eight-hour day length, and is associated with an ABA-like compound accumulating in bud covers (Lionakis & Schwabe, 1984b). The role of these factors in establishing kiwifruit bud isolation in intact vines and field conditions has yet to be fully established, however it is possible that kiwifruit bud dormancy may be induced long before leaf fall.

Experiments by Kwack et al. (2013) show that axillary bud regrowth in response to defoliation declined through summer and autumn, and by mid-autumn defoliation treatments did not cause bud outgrowth, possibly indicating that buds are unresponsive to endogenous signals at this time. At the time of sucrose injections in both experiments 2 and 3, buds may already have been symplastically isolated. Although injection of sucrose into canes or vines has been demonstrated to affect bark and wood NSC pools, they are unlikely to have affected bud NSC pools. Bud NSC pools may be vitally important for sustaining increased bud respiration during late dormancy (McPherson et al., 1997a; McPherson et al., 1997b) and spring growth prior to symplastic or apoplastic reconnection, which at least in grape buds does not occur until after budbreak (Signorelli et al., 2019; Xie et al., 2018). If bud reserve pools are insufficient to maintain metabolism through the winter, buds may expire from energetic starvation prior to reconnection (Bonhomme et al., 2005).

Taken together, the results of this chapter indicate that while exogenous sucrose injections can measurably alter non-structural carbohydrate pools in kiwifruit canes, increasing cane carbohydrate availability alone was not sufficient to consistently enhance spring growth or floral development. This contrasts with the strong effects of seasonal manipulations such as defoliation or shading, which may alter carbohydrate dynamics across roots, canes, and buds simultaneously. These findings suggest that access to local reserve pools and developmental constraints associated with bud dormancy may play a more critical role in determining reproductive outcomes than bulk carbohydrate availability within woody tissues.

## 4.5 Conclusions

Consistent with findings from other species, kiwifruit canes are able to rapidly absorb exogenous sucrose injected via the xylem, although whether both sucrose and hexoses are directly absorbed remains to be determined. Repeat injections of concentrated sucrose solutions to excised canes showed a dose-dependent response on soluble sugar and starch concentrations, particularly in bark tissues. Despite significant increases or decreases to cane carbohydrate pools, effects on spring growth were minimal except for a slight increase in budbreak for canes injected with 10% sucrose. When vines were carbohydrate-limited by defoliation throughout autumn, cane starch concentrations and spring growth were reduced. Trunk injections of exogenous sucrose showed potential to increase cane soluble sugars but did not improve spring growth in either defoliated or intact vines.

Overall, these results are somewhat paradoxical, as there is a strong base of evidence demonstrating that changes to NSC availability in summer and autumn have strong effects on winter reserve pools and subsequent spring shoot growth and flower development; yet despite influencing NSC pools with exogenous sucrose in this chapter, effects on spring growth were minimal. However, techniques such as defoliation and shading applied in summer or early autumn likely affect cane and bud NSC pools simultaneously, while sucrose injections in later autumn or winter may potentially not influence bud reserves if they are already isolated. Future approaches that manipulate carbohydrate availability at different developmental stages, particularly before and after bud isolation, may help to disentangle the relative contributions of bud and cane NSC pools to spring growth.

# Chapter 5: Conclusions and future directions

## 5.1 Thesis overview

Understanding how carbohydrate availability across the growing season influences flower and fruit development is central to explaining within-vine variability in fruit qualities. This thesis examined these processes across three complementary areas: 1) within-vine predictors of fruit fresh weight (FW) and dry matter (DM); 2) the size, distribution, and mobilisation of cane non-structural carbohydrate (NSC) reserves; and 3) the potential to augment endogenous NSC pools with exogenous sucrose. Although these studies address distinct questions, they collectively characterise the constraints imposed by carbohydrate supply during the critical period spanning budbreak, anthesis, and early fruitlet growth.

## 5.2 Chapter summaries

### 5.2.1 Chapter 2: Within-vine drivers of fruit variability

This chapter investigated within-vine variability in fruit FW and DM, comparing and contrasting the influence of several drivers of across conventional, strung and spur pruning canopy management systems.

Of the factors measured in this study, FW was most strongly influenced by position within shoot (nested within fruit per shoot), timing of anthesis, and shoot diameter. These factors were consistently strong drivers across the three canopy management systems studied. In contrast, influences on fruit DM were more varied across canopy management systems. Position within shoot (nested within fruit per shoot) and shoot length were consistently strong predictors of fruit DM content across all three management systems, however in the two 'replacement cane' systems (conventional and strung) there was also a strong effect of distance east/west from the cordon.

A correlation matrix between measured factors revealed some of the biological relationships inherent within vines, and how these can be influenced by canopy management. In all three management systems there were strong positive correlations between internode diameter and shoot diameter; moderate to strong negative correlations between fruit relative height and distance from the cordon; and moderate negative correlations between fruit per shoot and timing of anthesis. In replacement cane vines, shoot length and shoot diameter were strongly positively correlated, and were both strongly negatively correlated with distance from the cordon. In contrast, in spur vines shoot length and shoot diameter were only weakly positively

correlated, reflecting the more intensive canopy management and resulting decoupling of shoot length and diameter.

### 5.2.2 Chapter 3: Cane carbohydrate reserves and mobilisation

In dormant cane internodes, total non-structural carbohydrate (TNC) concentrations were highest in low vigour canes and/or internodes further from the cane base. In contrast, internodes of high vigour canes and internodes closer to the base of canes had lower TNC concentrations but higher TNC per unit length. TNC concentrations were positively correlated with PMZ to wood area ratio, while TNC per unit length was strongly positively correlated with internode diameter. Of the three cultivars studied, 'Hayward' had both the highest average TNC concentration and the highest average TNC per unit length.

Internodes from high, medium and low vigour canes followed similar mobilisation patterns of starch and soluble sugars in spring. Soluble sugars were highest at budbreak, but by 17 days after budbreak all cultivars and cane vigour types had fallen to a relatively stable plateau. All cultivars and cane vigour types had rapid drops in starch concentrations after budbreak, and all reached minimal starch concentrations at or just prior to anthesis (46–50 days after budbreak). 'Zesy002' cane internodes had higher soluble sugar concentrations at budbreak and reached starch depletion earlier than either 'Hayward' or 'Zes008'. High vigour cane internodes had the highest TNC per unit length at budbreak and by anthesis had the largest remobilisation of TNC per unit length but still retained more TNC per unit length after anthesis.

### 5.2.3 Chapter 4: Testing carbohydrate availability using exogenous sucrose

Experiment 1 demonstrated that a relatively high concentration of exogenous sucrose (5% w/v) was able to be rapidly absorbed when injected into the xylem of excised dormant kiwifruit canes, with increases of hexoses indicating apoplastic sucrose cleavage.

Dormant excised canes injected with exogenous sucrose in experiment 2 had their carbohydrate pools affected in a dose dependent manner, particularly for bark soluble sugars and starch. Changes in bark carbohydrate concentrations indicate that exogenous sucrose was able to move across the cambium. Bark soluble sugars were reduced in canes injected with water alone. Canes injected with 10% (w/v) sucrose had a small but significant increase in budbreak percentage, however there were no other treatment effects on spring flower production.

Experiment 3 combined autumn defoliation and trunk injections of sucrose to manipulate carbohydrate availability in intact vines and examine effects on subsequent spring growth.

Sustained defoliation reduced cane bark and wood starch concentrations and significantly reduced subsequent spring growth and floral development. Trunk injection of 10% (w/v) sucrose was detectable in cane exudate chemistry and increased soluble sugar concentrations in cane tissues, particularly in defoliated vines, but did not increase starch concentrations or improve spring growth or flowering in either defoliated or intact vines.

## 5.3 Synthesis

### 5.3.1 Integration of Chapters 2 and 3

**Early-season NSC availability, fruit and shoot developmental trajectories**Chapter 3 provides empirical evidence to support modelled relationships of carbohydrate availability within canes, showing that tapering of internode diameter along the length of dormant canes is associated with significant changes to TNC concentrations, and importantly, TNC availability per unit length, with similar diameter-based effects observed between cane types (Greaves et al., 1999). Chapter 3 also demonstrates that, at least in nodes near the base of canes, the vast majority of this carbohydrate pool is mobilised by anthesis, regardless of cane vigour, and that larger internodes can be expected to mobilise a larger total amount of NSC in this period (Figure 5.1 A).

Heterogeneous spatial patterns in NSC availability and effects on early flower and shoot development are supported by the results of Chapter 2. Across all three canopy management systems, larger internodes were associated with larger shoot diameters. Both shoot and internode diameter fell with distance from the cordon (i.e. predominantly due to the tapering of canes), consistent with the expected spatial distribution of cane NSC reserves shown in Chapter 3 and shoot growth modelled by Greaves et al. (1999). Shoot diameter was itself a strong predictor of fruit FW at harvest and was also associated with higher fruit per shoot (Figure 5.1 B), providing evidence that, even at the whole-vine level, the high availability of NSC that facilitates vigorous shoot growth also supports early floral development and reduces rates of floral abortion.

Proximity to cane reserves alone is insufficient to explain other strong drivers of fruit FW identified in Chapter 2. Timing of anthesis was also a strong driver of FW and yet did not correlate strongly with shoot diameter, internode diameter or distance from the cordon, although the highly condensed flowering window in the studied season may have obscured some of these relationships. Similarly, based solely on proximity to internode reserves it might be expected that all floral meristems within a bud/shoot should have similar access to carbohydrate

reserves, however the strong effect of position within shoot suggests that other within-shoot factors such as floral meristem size or early carbon balance from subtending leaves are also highly influential on flower development. Timing of anthesis and position within shoot may represent an axis of sink strength that is somewhat independent of the proximity to reserves (Figure 5.1 B). These differences may partly reflect variation in initial floral meristem development and subsequent ovary size and cell number, which can establish differences in the potential sink capacity of developing fruit. In kiwifruit, early differences in flower and ovary development have been associated with subsequent fruit size, while cell number and sink activity are recognised determinants of fruit sink strength (Marcelis, 1996; McPherson et al., 2001a; Walton et al., 1997). Consequently, early developmental advantages may be maintained or amplified through subsequent differences in the ability of individual fruit to attract and accumulate assimilates.

In addition to accessibility to carbohydrate reserves, factors such as pollination efficacy and fruit water balance likely also contribute to differences in fruit growth. While pollination efficacy was not directly quantified in this study, the strong negative correlation observed between timing of anthesis and seed counts (Figure A14) suggests that later opening flowers have reduced potential to set seeds, potentially a consequence of their smaller ovaries (Cruz-Castillo et al., 2002). This is supported by a study in 'Hayward' where individual flowers were hand-pollinated on their day of anthesis, practically minimising pollination efficacy as a factor, yet timing of anthesis was still a strong driver of FW at harvest (Smith et al., 1994). As only open pollination was used in the present study, it is possible that differential pollination efficacy within and between dates of anthesis also contributed to variability, particularly in FW.

The water balance of individual fruit can strongly affect fruit growth, particularly during early growth where skin properties contribute to relatively high fruit surface conductance (Celano et al., 2009; Morandi et al., 2010). The increased hydraulic gradient caused by greater diurnal water loss may also facilitate phloem unloading (Morandi et al., 2016). Fruit water balance is strongly influenced by surface area, therefore there may be positive feedback relationship between early fruit growth, as driven by earlier flowering and/or greater accessibility to carbohydrate reserves, and subsequent increased rates of fruit growth driven by higher amounts of diurnal water loss and associated vascular inflows. Additionally, the microclimate around individual fruit can affect vapour pressure difference and water balance (Clearwater et al., 2011), such that differences in exposure to solar radiation and wind may contribute to variation in fruit

transpiration. Further study would be required to quantify how strongly these eco-physiological factors influence within-vine differences in fruit water balance, and net effects on fruit growth.

Differences in early resource availability contributes to variability in shoot growth and the resulting local leaf-to-fruit ratio during the DM accumulation stage of fruit development. Vigorous early shoot growth results in high leaf area and corresponding local photoassimilate availability, while leaf area on terminated shoots plateaus early in the season (Figure 5.1 C). Management systems can influence the number and distribution of shoot types across the canopy, with strong spatial effects on DM. For both conventional and strung canopy management treatments, the presence of multiple long shoots near the cordon likely increases the local photoassimilate availability to neighbouring shoots/fruit in this canopy zone. These long shoots may also cause shading of more distal shoots, contributing to a spatial gradient of decreasing fruit DM further from the cordon. Notably, this spatial gradient was absent in spur-pruned vines where long replacement canes are also absent. This interpretation is supported by previous studies that have shown that while photoassimilates can translocate from areas of high to low L:F in the canopy (Lai et al., 1989b; Snelgar et al., 1986), under conditions of high competition proximity to sources becomes more important to individual fruit growth (Buwalda & Smith, 1990; Tombesi et al., 1993).

The links between position within shoot and physiological drivers of fruit DM are less clear. The strong effects of position within shoot on fresh weight may reflect early differences in fruit developmental potential, which subsequently contribute to size-based differences in sink strength and the ability to compete for photoassimilates during later fruit development and starch accumulation. It may also reflect orthostichy-based restriction of photoassimilate distribution within shoots (Lai et al., 1988), although the seasonal dynamics of these vascular constraints and their responses to management interventions are currently poorly understood.

### 5.3.2 Integration of Chapter 4

#### Sucrose supplementation and reserve compartmentalisation

When considered alongside the spatial patterns and mobilisation dynamics of cane NSC reserves described in Chapter 3, the results of Chapter 4 suggest that increasing cane internode NSC reserves alone may be insufficient to alter subsequent spring shoot and flower developmental trajectories. Kiwifruit canes were capable of rapidly absorbing exogenous sucrose via the xylem and seemingly transporting it across the cambium, resulting in dose-

dependent increases in NSC pools in bark and wood tissues. However, these substantial changes to cane NSC pools had minimal effects on spring budbreak and flower production.

Importantly, the size of a reserve pool does not necessarily reflect its availability to developing sinks, as measured NSC concentrations provide only an indirect indication of the processes governing carbohydrate storage, mobilisation and utilisation (Hartmann & Trumbore, 2016). Although sucrose supplementation substantially increased NSC concentrations in cane internodes, this does not necessarily indicate a corresponding increase in carbohydrate flux into developing buds. Such flux depends on the accessibility of reserves, the capacity for their mobilisation, and the connectivity of vascular and symplastic transport pathways between storage tissues and developing sinks (Tixier et al., 2019). Consequently, additional carbohydrate accumulated within cane internodes may not have been readily accessible to buds during early spring development. Furthermore, budbreak is not determined solely by carbohydrate availability, but is regulated by the developmental and physiological status of the bud. The transition from dormancy to active growth involves interactions between chilling and temperature cues, hormonal regulation and the activation of growth-related metabolic processes (Liu & Sherif, 2019; Voogd et al., 2021; Zhao et al., 2025). Consequently, even where carbohydrate reserves are sufficient to support subsequent growth, budbreak may remain constrained by developmental or physiological processes that regulate dormancy release and the initiation of growth.

The contrast between the results of Chapter 4 and previous studies that manipulated whole-vine carbohydrate status using defoliation, shading, or girdling further reinforces this conclusion. Such treatments, when applied during summer or early autumn, have consistently produced strong effects on subsequent spring growth and floral productivity (Brundell, 1975a; Cruz-Castillo et al., 2010; Lionakis et al., 1994; Richardson, 2015), likely because they influence multiple symplastically continuous compartments simultaneously. In contrast, the sucrose injections applied in Chapter 4 altered carbohydrate availability at a later phenological stage. While these treatments clearly affected NSC pools within cane internodes, it seems likely that they did not influence bud NSC pools or other regulatory processes that also constrain spring development, although this remains to be experimentally verified.

Overall, the results of Chapter 4 demonstrate that increasing carbohydrate availability within cane internodes alone is insufficient to overcome the constraints governing early shoot and flower development. These findings indicate that additional factors, whether related to the

spatial distribution of reserves, their accessibility to developing tissues, or the timing of carbohydrate accumulation, play a critical role in determining spring growth potential. Identifying the nature of these constraints and the relative contributions of different reserve compartments will require further experimental investigation, which will be discussed in section 5.4.3.

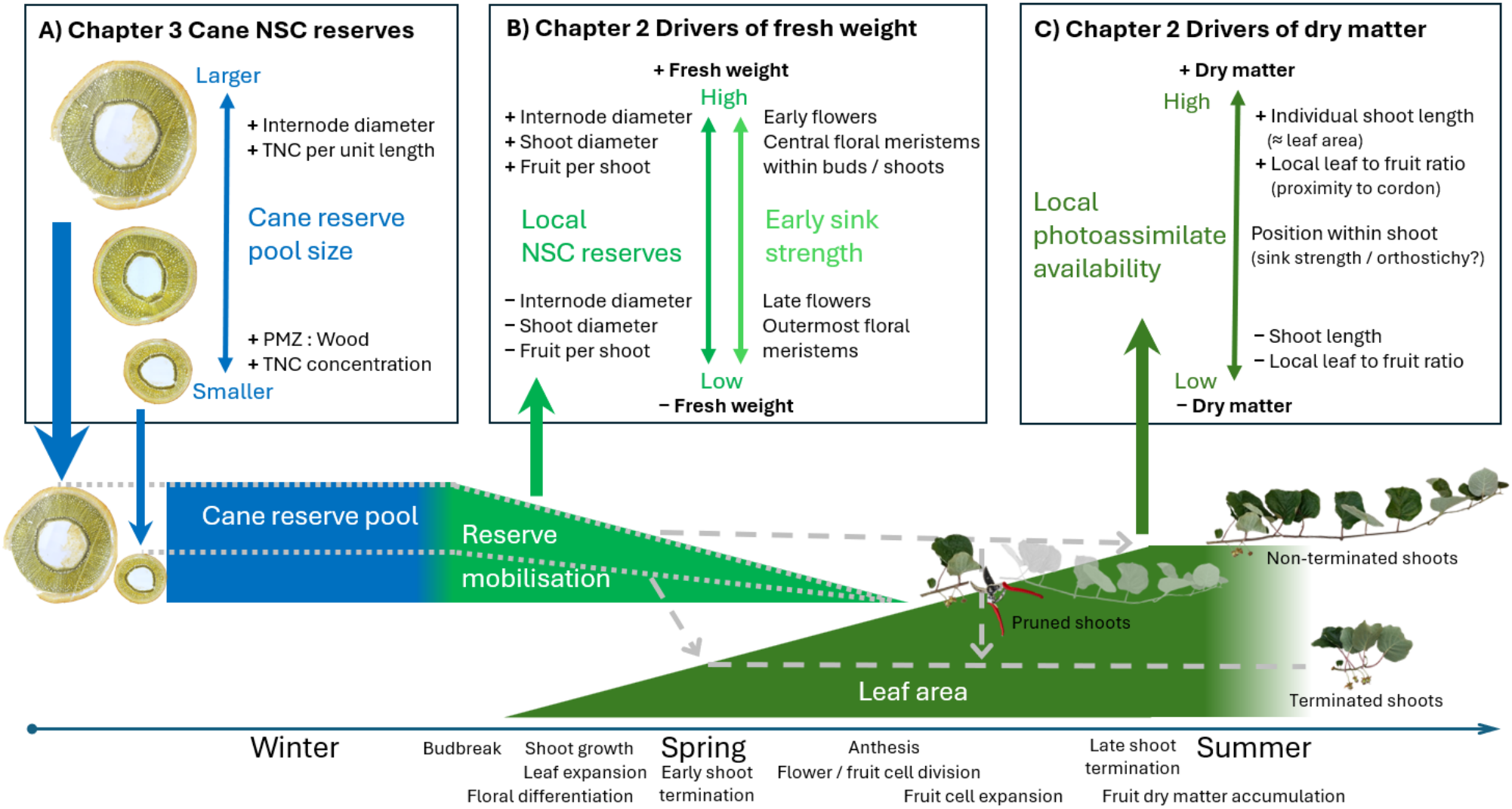


Figure 5.1. Conceptual model of seasonal carbohydrate availability and effects on fruit fresh weight and dry matter content. Solid black boxes show experimental results from Chapters 2 and 3. Timeline at the bottom shows key phenological events. Dotted lines in cane reserve pool and reserve mobilisation periods show the difference in NSC pool size depending on cane internode size. Larger internodes (A) contain larger total carbohydrate reserves, which can facilitate increased early fruit and shoot growth, increasing fruit fresh weight at harvest (B). Reserve mobilisation can influence subsequent shoot growth and leaf area. Dashed lines show a plateau in terminated shoot leaf area earlier in the season, a reduction in pruned shoots, and a longer period of increasing leaf area in non-terminated shoots. Local leaf area strongly influences fruit dry matter accumulation later in the season (C) and sink strength and within-shoots vascular connections are also influential.

## 5.4 Practical industry applications and future research priorities

### 5.4.1 Targeted fruit thinning

Flower and fruit thinning are already standard management practices in kiwifruit to regulate crop load and achieve marketable fruit size; the findings of this thesis suggest opportunities to optimise the timing and targeting of these practices to further reduce within-vine variability. On shoots with up to 5 flowers the most distal flower should be removed; additionally on shoots with at least 6 flowers the one or two most basal flowers should also be removed. Flower buds that appear visibly behind in their development (i.e. smaller) should also be targeted, as well as those from very thin and low vigour shoots. These guidelines would allow much of this thinning to be done with confidence prior to anthesis, before scarce resources are wasted on further development.

The heterogeneous distribution of leaf area inherent to replacement cane systems contributes to a strong spatial gradient in fruit dry matter content. Removing all fruit from vigorous shoots would remove a source of higher-than-average dry matter fruit, which while of higher economic value (refer to section 1.1.2) may also mature earlier, potentially increasing variability in ripening rates post-harvest. Removing these fruit may also encourage a more even distribution of photoassimilates (i.e. less constrained to orthostichies) to neighbouring shoots and fruit. Similarly, retaining more fruit near the cordon and fewer towards the ends of canes may help to equalise the leaf to fruit ratio across the canopy, leading to more uniform photoassimilate distribution to individual fruit.

The strong pattern of within-vine variability in DM could also be exploited by selective picking. Fruit near to the cordon could either be picked slightly earlier in the season than fruit in the remainder of the canopy or harvested simultaneously but segregated into different bin lines for subsequent grading and packing. While previous authors have concluded that such selective picking was unnecessary (Boyd et al., 2008a), the results of this thesis suggest the idea may be worth revisiting for replacement cane managed 'Zesy002' orchards.

These proposed management interventions will require field-testing to verify beneficial effects on within-vine fruit variability. The intensity of flower removal that can be applied without negatively impacting yield and profitability will also depend on cultivar, management factors and seasonal differences. The costs and benefits of these interventions or management of DM variability via selective picking would also require economic analysis.

### 5.4.2 Cane selection

High vigour canes have a larger pool of NSC reserves per unit length than lower vigour canes, suggesting they would be favourable to maximise NSC availability during early flower and shoot development. However, one-year-old canes are not the only source of spring NSC reserves in kiwifruit canopies. Filling canopies with low vigour canes also requires a considerable volume of older structural wood, and the NSC dynamics of structural wood reserve pools are currently largely unstudied in kiwifruit. While older structural branches might be expected to have larger NSC pools based on their larger diameters, the accessibility of these reserves may be more limited. Studies in walnut and other tree species shows that carbohydrate reserves from older stems are less labile than those of younger branches and twigs (Barbaroux & Bréda, 2002; Carbone et al., 2013; Keller & Loescher, 1989; Lacointe et al., 1993). However, this is not necessarily a universal characteristic, with evidence from peach showing similar mobilisation rates in xylem rings up to five years old compared with one-year-old rings (Da Silva et al., 2014). Consequently, the extent to which kiwifruit structural wood contributes to spring NSC availability remains uncertain.

To improve our understanding of kiwifruit canopy carbohydrate dynamics the timing and degree of mobilisation of NSC pools from structural wood of various ages should be studied. Investigations should also estimate and account for the structural carbohydrate costs of growing high or low vigour canes, the radial growth of structural wood, and how these competing sinks affect fruit growth throughout the season.

### 5.4.3 Bud isolation and carbohydrate mobility

The limited response to increased cane NSC availability suggests that constraints on spring development may relate not only to reserve size, but also to the ability of buds to attract and store carbohydrates in the season on their formation, in order to ensure they have sufficient reserves to survive the winter and eventually regain connection to more remote reserve pools.

To maximise bud NSC reserves, we first need to establish when bud symplastic isolation occurs and how this is influenced by environmental conditions. Fluorescent tracers such as carboxyfluorescein diacetate could be used to determine when in autumn symplastic transport into buds is disrupted. Apoplastic bud connectivity could be assessed with acid fuchsin, as well as anatomical studies of suberisation and lignification at the bud-cane interface. Controlled

environment studies with potted plants could be used to determine the relative influences of photoperiod and temperature on the development of bud isolation and dormancy.

Once the timing of bud isolation is established, management interventions such as shoot girdling could be employed to maximise photoassimilate availability to buds, prior to isolation. Similarly, timing of fruit harvest could affect bud reserve accumulation, with early harvests removing competing fruit sinks and potentially increasing NSC availability before buds isolate, while later harvests may relieve competition too late to affect bud NSC pools. These potential effects could be studied by tracking bud and cane NSC concentrations before and after girdling interventions of harvests at different points in the season.

We also need to establish when buds reconnect to the cane in spring, as this will determine their ability to import NSC from other reserve pools. Chill accumulation can promote the accumulation of callose degrading enzymes at plasmodesmata (Rinne et al., 2011; Rinne et al., 2001), while more variable temperatures may suppress callose degradation (Pandey et al., 2026). It may be that with sufficient chilling some degree of connectivity is restored prior to budbreak, at least for small molecules including sugars (Signorelli et al., 2019). This could provide a mechanism through which winter chilling promotes subsequent bud growth. Under this hypothesis, buds receiving sufficient chilling would regain access to NSC reserves in adjacent cane tissues before budbreak, whereas buds experiencing insufficient chilling may remain symplastically isolated for longer, potentially limiting carbohydrate availability during early flower and shoot development. Placing excised canes into controlled environments for fixed periods of chill accumulation could be used to study the progressive removal of callose. Aniline blue could be used to visualise callose distribution within buds (Mancera, 2018; Zavaliev & Epel, 2015), while acid fuchsin could again be used to study apoplastic connectivity (Xie et al., 2018).

### 5.4.4 Theoretical effects of increased carbohydrate availability

Increasing early carbohydrate availability to buds via maximising endogenous NSC pool size and accessibility during their development may be insufficient to prevent the underlying physiological causes of fruit variability. Increased NSC availability would likely have several simultaneous effects on early development, including increased shoot vigour and ovary growth rates, and reduced abortion of both lateral and terminal flowers (Piller et al., 1998). These responses would increase the potential fruit population size (Figure 5.2 A). However, individual fruit differ in developmental potential and sink strength, meaning that additional

assimilates may not be distributed equally across the fruit population. Unless the increased availability of carbohydrates is sustained, the resulting increase in sink number and activity could accelerate depletion of finite reserve pools. Consequently, greater initial resource availability may ultimately intensify competition between developing sinks.

It may be that only under conditions that approach saturating resource availability that competition between sinks and associated losses of growth potential be substantially reduced, allowing the distribution of fruit growth to be meaningfully shifted towards a genetic maximum (Figure 5.2 B). While such saturation is unlikely to be achieved in reality, targeted fruit removal as outlined in section 5.4.1 remains a pragmatic approach to reducing within-vine variability (Figure 5.2 C).

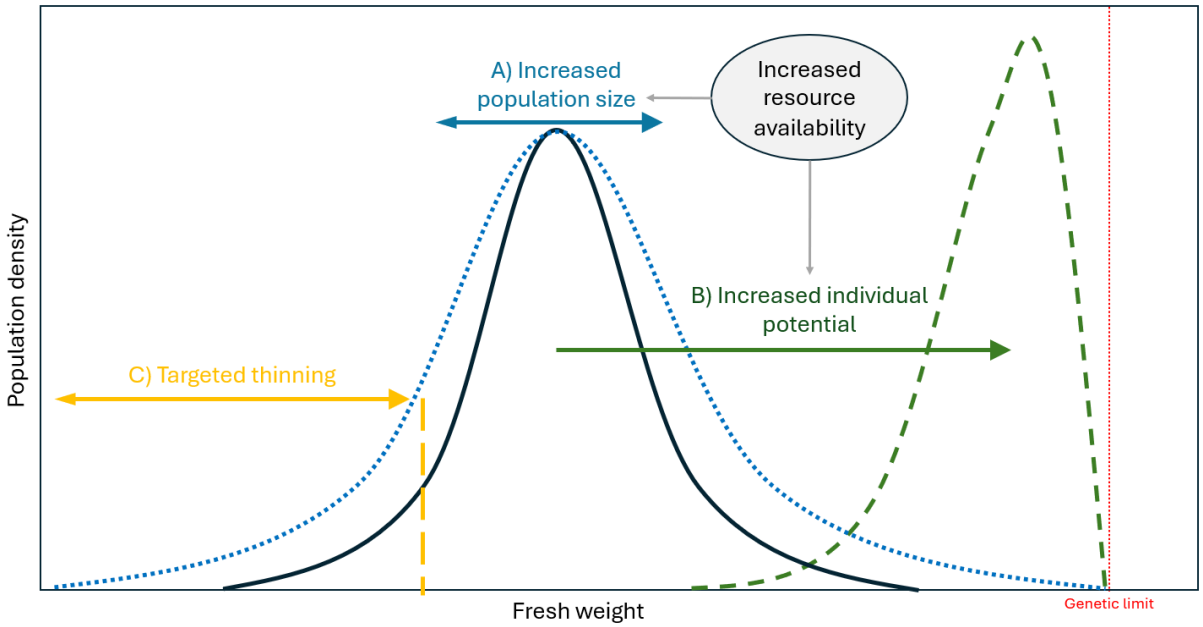


Figure 5.2. Hypothetical effects of increasing resource availability on within-vine fruit populations. The 'natural' population structure is indicated by the solid black line. Increasing resource availability may affect fruit development in several ways: A) reduced floral abortion could increase the potential population size, although competition for resources between sinks may persist (blue line); B) alleviating competition between individuals could increase individual growth potential (green line). In both cases, the upper limit of growth will be determined by genetic limits (red line). Previous studies suggest that early competition for resources can progressively reduce both the potential size of the fruit population and the individual growth potential of surviving fruit. Consequently, increasing resource availability may not necessarily restore the growth potential of individual fruit if competition between sinks remains. In theory, this would require resource availability to be sufficiently high to support both maximum fruit retention and individual fruit growth, effectively eliminating resource competition. While such resource availability may be nigh-impossible to achieve in reality, C) targeted removal of smaller, low-quality fruit (yellow line) can also effectively reduce within-vine variability at the cost of reduced yield.

## 5.5 Concluding remarks

This thesis has identified several strong drivers of within-vine variability in fruit FW and DM. While the influence of some of these drivers had been identified in previous research, this thesis advanced our understanding by comparing and ranking their respective influence on fruit FW and DM at harvest. Understanding of kiwifruit physiology at the whole-vine level has also been improved by demonstrating how predictor variables can correlate within vines and how canopy management systems can influence these relationships. Several of the strongest drivers have been previously linked to spatial and temporal differences in NSC availability within vines, the effects of which can set individual fruit and shoots on diverging developmental trajectories. In light of these findings, targeted management techniques are suggested that could reduce sources of within-vine variability via early interventions or post-harvest segregation.

This thesis also demonstrated that NSC availability in spring can be influenced via cane selection, with larger diameter cane internodes containing larger total NSC pools and mobilising these reserves to a similar degree as thinner internodes. While these patterns are consistent with previous modelling studies and observed correlations between internode and shoot diameter within vines, they do not, on their own, resolve how reserve pool size translates to developmental outcomes. Moreover, the storage and mobilisation of NSC reserves from older structural branches remain poorly quantified in kiwifruit and may represent an important, but currently unresolved, component of whole-canopy reserve dynamics and contributions to spring growth.

Finally, this thesis novelly demonstrated that it is possible to increase kiwifruit cane NSC pools via injection of exogenous sucrose. However, limited effects on spring growth prompt questions regarding the timing and regulatory roles of cane vs bud reserve pools. Further study is required to understand when bud and cane internode reserve pools can be jointly and individually manipulated, and how their respective contributions affect shoot growth and floral developmental trajectories.

# Chapter 6: References


Abbate, A., Campbell, J., & Williams, G. (2023). Artificial pollination of kiwifruit (*Actinidia chinensis* Planch. var. *chinensis*) (Ericales: Actinidiaceae) results in greater fruit set compared to flowers pollinated by managed bees (*Apis mellifera* L. (Hymenoptera: Apidae) and *Bombus impatiens* Cresson (Hymenoptera: Apidae)). *Journal of Economic Entomology*, *116*. https://doi.org/10.1093/jee/toad044

Aloni, R., & Barnett, J. R. (1996). The development of phloem anastomoses between vascular bundles and their role in xylem regeneration after wounding in *Cucurbita* and *Dahlia*. *Planta*, *198*(4), 595-603. https://doi.org/10.1007/BF00262647

Aloni, R., & Peterson, C. A. (1990). The functional significance of phloem anastomoses in stems of *Dahlia pinnata* Cav. *Planta*, *182*(4), 583-590. https://doi.org/10.1007/BF02341035

Antognozzi, E., Tombesi, A., & Palliotti, A. (1992). Relationship between leaf area, leaf area index and fruiting in kiwifruit (*Actinidia deliciosa*). *Acta Horticulturae*, *297*, 435-442. https://doi.org/10.17660/ActaHortic.1997.444.29

Arigita, L., González, A., & Tamés, R. S. (2002). Influence of CO2 and sucrose on photosynthesis and transpiration of *Actinidia deliciosa* explants cultured in vitro. *Physiologia Plantarum*, *115*(1), 166-173. https://doi.org/10.1034/j.1399-3054.2002.1150119.x

Austin, P. T., Hall, A. J., Snelgar, W. P., & Currie, M. J. (2002). Modelling kiwifruit budbreak as a function of temperature and bud interactions. *Annals of Botany*, *89*(6), 695-706. https://doi.org/10.1093/aob/mcf113

Ayala, M., & Lang, G. (2018). Current season photoassimilate distribution in sweet cherry. *Journal of the American Society for Horticultural Science*, *143*(2), 110-117. https://doi.org/10.21273/jashs04200-17

Barbaroux, C., & Bréda, N. (2002). Contrasting distribution and seasonal dynamics of carbohydrate reserves in stem wood of adult ring-porous sessile oak and diffuse-porous beech trees. *Tree Physiology*, *22*(17), 1201-1210. https://doi.org/10.1093/treephys/22.17.1201

Barbaroux, C., Bréda, N., & Dufrêne, E. (2003). Distribution of above-ground and below-ground carbohydrate reserves in adult trees of two contrasting broad-leaved species (*Quercus petraea* and *Fagus sylvatica*). *New Phytologist*, *157*(3), 605-615. https://doi.org/10.1046/j.1469-8137.2003.00681.x

Barbier, F. F., Dun, E. A., Kerr, S. C., Chabikwa, T. G., & Beveridge, C. A. (2019). An update on the signals controlling shoot branching. *Trends in Plant Science*, *24*(3), 220-236. https://doi.org/10.1016/j.tplants.2018.12.001

Bates, D., Mächler, M., Bolker, B., & Walker, S. (2015). Fitting linear mixed-effects models using lme4. *Journal of Statistical Software*, *67*(1), 1 - 48. https://doi.org/10.18637/jss.v067.i01

Bebbington, M., Hall, A. J., Lai, C. D., & Zitikis, R. (2009). Dynamics and phases of kiwifruit (*Actinidia deliciosa*) growth curves. *New Zealand Journal of Crop and Horticultural Science*, *37*(3), 179-188. https://doi.org/10.1080/01140670909510263

Bennett, J., Jarvis, P., Creasy, G. L., & Trought, M. C. (2005). Influence of defoliation on overwintering carbohydrate reserves, return bloom, and yield of mature Chardonnay grapevines. *American Journal of Enology and Viticulture*, *56*(4), 386-393. https://doi.org/10.5344/ajev.2005.56.4.386

Bertheloot, J., Barbier, F., Boudon, F., Perez-Garcia, M. D., Péron, T., Citerne, S., . . . Sakr, S. (2020). Sugar availability suppresses the auxin-induced strigolactone pathway to promote bud outgrowth. *New Phytologist*, *225*(2), 866-879. https://doi.org/10.1111/nph.16201

Black, M. Z. (2012). *The kiwifruit (Actinidia sp.) vine root system: Responses to vine manipulations* [Doctoral dissertation, University of Waikato]. Hamilton, New Zealand. https://researchcommons.waikato.ac.nz/entities/publication/ad3556a1-1444-467e-b634-a1eba6a308d7

Bohner, J., & Bangerth, F. (1988). Effects of fruit set sequence and defoliation on cell number, cell size and hormone levels of tomato fruits (*Lycopersicon esculentum* Mill.) within a truss. *Plant Growth Regulation*, *7*(3), 141-155. https://doi.org/10.1007/BF00028237

Böhning, R. H., Kendall, W. A., & Linck, A. J. (1953). Effect of temperature and sucrose on growth and translocation in tomato. *American Journal of Botany*, *40*(3), 150-153. https://doi.org/10.2307/2438772

Boini, A., Bortolotti, G., Perulli, G. D., Grappadelli, L. C., & Manfrini, L. (2025). Fruit vascular flows in yellow-fleshed kiwi reveal tight relations between water availability and fruit growth potential, until harvest. *Scientia Horticulturae*, *350*, 114337. https://doi.org/10.1016/j.scienta.2025.114337

Boldingh, H., Smith, G. S., & Klages, K. (2000). Seasonal concentrations of non-structural carbohydrates of five *Actinidia* species in fruit, leaf and fine root tissue. *Annals of Botany*, *85*(4), 469-476. https://doi.org/10.1006/anbo.1999.1094

Bollard, E. (1953). The use of tracheal sap in the study of apple-tree nutrition. *Journal of Experimental Botany*, *4*(3), 363-368. https://doi.org/10.1093/jxb/4.3.363

Bonhomme, M., Rageau, R., Lacointe, A., & Gendraud, M. (2005). Influences of cold deprivation during dormancy on carbohydrate contents of vegetative and floral primordia and nearby structures of peach buds (*Prunus persica* L. Batch). *Scientia Horticulturae*, *105*(2), 223-240. https://doi.org/10.1016/j.scienta.2005.01.015

Boyd, L. (2012). *Resource allocation in kiwifruit (Actinidia chinensis)* [Doctoral dissertation, Massey University]. Albany, New Zealand. http://hdl.handle.net/10179/5109

Boyd, L. M., & Barnett, A. M. (2011). Manipulation of whole-vine carbon allocation using girdling, pruning, and fruit thinning affects fruit numbers and quality in kiwifruit. *HortScience*, *46*(4), 590-595. https://doi.org/10.21273/HortSci.46.4.590

Boyd, L. M., Ramankutty, P., Barnett, A. M., Dawson, T., Wegrzyn, T., Le Guevel, A., & Mowat, A. D. (2008a). Effect of canopy position on fruit quality in 'Hort16A' kiwifruit in New Zealand. *Journal of Horticultural Science & Biotechnology*, *83*(6), 791-797. https://doi.org/10.1080/14620316.2008.11512462

Boyd, L. M., Ramankutty, P., Mowat, A. D., & Ferguson, I. B. (2008b). Variation in fruit quality among 'Hort16A' kiwifruit vines in New Zealand. *Journal of Horticultural Science & Biotechnology*, *83*(6), 798-803. https://doi.org/10.1080/14620316.2008.11512463

Brantley, A. K., Spiers, J. D., Thompson, A. B., Pitts, J. A., Kessler, J. R., Wright, A. N., & Coneva, E. D. (2019). Effective pollination period of *Actinidia chinensis* 'AU Golden Sunshine' and *A. deliciosa* 'AU Fitzgerald' kiwifruit. *HortScience*, *54*(4), 656-660. https://doi.org/10.21273/HortSci13617-18

Broussard, M. A., Goodwin, M., McBrydie, H. M., Evans, L. J., & Pattemore, D. E. (2021). Pollination requirements of kiwifruit (*Actinidia chinensis* Planch.) differ between cultivars 'Hayward'and 'Zesy002'. *New Zealand Journal of Crop and Horticultural Science*, *49*(1), 30-40. https://doi.org/10.1080/01140671.2020.1861032

Broussard, M. A., & Pattemore, D. E. (2023). Kiwifruit Pollination. In A. Richardson, J. Burdon, & A. R. Ferguson (Eds.), *Kiwifruit: Botany, Production and Uses* (pp. 207–227). CABI GB. https://doi.org/10.1079/9781800620933.0013

Brundell, D. J. (1975a). Effect of defoliation, shading and tipping of shoots on flower bud development and vegetative growth of Chinese gooseberry (*Actinidia chinensis* Planch.). *New Zealand Journal of Experimental Agriculture*, *18*, 365-370. https://doi.org/10.1080/00288233.1975.10421060

Brundell, D. J. (1975b). Flower development of the chinese gooseberry (*Actinidia chinensis* Planch) I. Development of the flowering shoot. *New Zealand Journal of Botany*, *13*(3), 473-483. https://doi.org/10.1080/0028825X.1975.10430338

Brundell, D. J. (1975c). Flower development of the Chinese gooseberry (*Actinidia chinensis* Planch.) II. Development of the flower bud. *New Zealand Journal of Botany*, *13*(3), 485-496. https://doi.org/10.1080/0028825X.1975.10430339

Brundell, D. J. (1975d). Quantitative aspects of flowering in the Chinese gooseberry (*Actinidia chinensis* Planch.). *New Zealand Journal of Agricultural Research*, *18*(4), 371-374. https://doi.org/10.1080/00288233.1975.10421061

Brundell, D. J. (1976). The effect of chilling on the termination of rest and flower bud development of the Chinese gooseberry. *Scientia Horticulturae*, *4*, 175-182. https://doi.org/10.1016/S0304-4238(76)80010-6

Burdon, J. (2022). Understanding kiwifruit physiology: why we can predict aspects of postharvest performance. *Acta Horticulturae*, 253-260. https://doi.org/10.17660/ActaHortic.2022.1332.34

Burdon, J., Lallu, N., Francis, K., & Boldingh, H. (2007). The susceptibility of kiwifruit to low temperature breakdown is associated with pre-harvest temperatures and at-harvest soluble solids content. *Postharvest Biology and Technology*, *43*(3), 283-290. https://doi.org/10.1016/j.postharvbio.2006.09.011

Burdon, J., Lallu, N., Pidakala, P., & Barnett, A. (2013). Soluble solids accumulation and postharvest performance of 'Hayward'kiwifruit. *Postharvest Biology and Technology*, *80*, 1-8. https://doi.org/10.1016/j.postharvbio.2013.01.009

Burdon, J., Martin, P., Ireland, H., Schaffer, R., McAtee, P., Boldingh, H., & Nardozza, S. (2021). Transcriptomic analysis reveals differences in fruit maturation between two kiwifruit cultivars. *Scientia Horticulturae*, *286*, 110207. https://doi.org/10.1016/j.scienta.2021.110207

Burdon, J., McLeod, D., Lallu, N., Gamble, J., Petley, M., & Gunson, A. (2004). Consumer evaluation of "Hayward" kiwifruit of different at-harvest dry matter contents. *Postharvest Biology and Technology*, *34*(3), 245-255. https://doi.org/10.1016/j.postharvbio.2004.04.009

Burdon, J., Pidakala, P., Martin, P., & Billing, D. (2017). Softening of 'Hayward' kiwifruit on the vine and in storage: The effects of temperature. *Scientia Horticulturae*, *220*, 176-182. https://doi.org/https://doi.org/10.1016/j.scienta.2017.04.004

Burdon, J., Pidakala, P., Martin, P., Billing, D., & Boldingh, H. (2016). Fruit maturation and the soluble solids harvest index for 'Hayward' kiwifruit. *Scientia Horticulturae*, *213*, 193-198. https://doi.org/10.1016/j.scienta.2016.10.027

Burdon, J., Pidakala, P., Martin, P., McAtee, P. A., Boldingh, H. L., Hall, A., & Schaffer, R. J. (2014). Postharvest performance of the yellow-fleshed 'Hort16A' kiwifruit in relation to fruit maturation. *Postharvest Biology and Technology*, *92*, 98-106. https://doi.org/10.1016/j.postharvbio.2014.01.004

Burge, G. K., Spence, C. B., & Marshall, R. R. (1987). Kiwifruit: effects of thinning on fruit size, vegetative growth, and return bloom. *New Zealand Journal of Experimental Agriculture*, *15*, 317-324. https://doi.org/10.1080/03015521.1987.10425577

Buwalda, J. G. (1991a). A mathematical model of carbon acquisition and utilisation by kiwifruit vines. *Ecological Modelling*, *57*(1-2), 43-64. https://doi.org/10.1016/0304-3800(91)90054-5

Buwalda, J. G. (1991b). Root growth of kiwifruit vines and the impact of canopy manipulations. https://doi.org/10.1016/B978-0-444-89104-4.50059-1

Buwalda, J. G. (1994). The impact of canopy growth and temporal changes in radiation on the dynamics of canopy carbon assimilation for kiwifruit (*Actinidia deliciosa*) vines during spring. *Environmental and Experimental Botany*, *34*(2), 141-151. https://doi.org/10.1016/0098-8472(94)90033-7

Buwalda, J. G., Green, T. G. A., & Curtis, J. P. (1992). Canopy photosynthesis and respiration of kiwifruit (*Actinidia deliciosa* var. *deliciosa*) vines growing in the field. *Tree Physiology*, *10*(4), 327-341. https://doi.org/10.1093/treephys/10.4.327

Buwalda, J. G., Meekings, J. S., & Smith, G. S. (1991). Seasonal changes in photosynthetic capacity of leaves of kiwifruit (*Actinidia deliciosa*) vines. *Physiologia Plantarum*, *83*(1), 93-98. https://doi.org/10.1111/j.1399-3054.1991.tb01286.x

Buwalda, J. G., & Smith, G. S. (1990). Effects of partial defoliation at various stages of the growing season on fruit yields, root growth and return bloom of kiwifruit vines. *Scientia Horticulturae*, *42*(1-2), 29-44. https://doi.org/10.1016/0304-4238(90)90145-5

Buxton, K. N. (2005). *Preharvest practices affecting postharvest quality of 'Hayward' kiwifruit* [Doctoral dissertation, Massey University]. Palmerston North, New Zealand. http://hdl.handle.net/10179/1630

Cao, D., Chabikwa, T., Barbier, F., Dun, E. A., Fichtner, F., Dong, L., . . . Beveridge, C. A. (2023). Auxin-independent effects of apical dominance induce changes in phytohormones correlated with bud outgrowth. *Plant Physiology*, *192*(2), 1420-1434. https://doi.org/10.1093/plphys/kiad034

Caporali, E., Testolin, R., Pierce, S., & Spada, A. (2019). Sex change in kiwifruit (*Actinidia chinensis* Planch.): a developmental framework for the bisexual to unisexual floral transition. *Plant Reproduction*, *32*(3), 323-330. https://doi.org/10.1007/s00497-019-00373-w

Carbone, M. S., Czimczik, C. I., Keenan, T. F., Murakami, P. F., Pederson, N., Schaberg, P. G., . . . Richardson, A. D. (2013). Age, allocation and availability of nonstructural carbon in mature red maple trees. *New Phytologist*, *200*(4), 1145-1155. https://doi.org/10.1111/nph.12448

Celano, G., Minnocci, A., Sebastiani, L., D'Auria, M., & Xiloyannis, C. (2009). Changes in the structure of the skin of kiwifruit in relation to water loss. *Journal of Horticultural Science & Biotechnology*, *84*(1), 41-46. https://doi.org/10.1080/14620316.2009.11512477

Charrier, G. (2020). Gaining sugars while sweating: How do leaves regulate their osmolarity? *Plant Physiology*, *183*(4), 1412-1413. https://doi.org/10.1104/pp.20.00813

Chen, C., Yuan, Y., Zhang, C., Li, H., Ma, F., & Li, M. (2017). Sucrose phloem unloading follows an apoplastic pathway with high sucrose synthase in *Actinidia* fruit. *Plant Science*, *255*, 40-50. https://doi.org/10.1016/j.plantsci.2016.11.011

Chen, L., Wang, S.-Y., Zhong, M., Huang, C.-H., Liao, G.-L., & Xu, X.-B. (2019). Effects of pollens from the 10 selected *Actinidia* male genotypes on 4 commercial planting kiwifruit female cultivars in Southern China. *New Zealand Journal of Crop and Horticultural Science*, *47*(3), 155-169. https://doi.org/10.1080/01140671.2019.1616569

Chen, Q.-Q., Man, Y.-P., Lu, X.-M., Wang, J., Zhang, Y.-Q., Liu, Y., . . . Wang, Y.-C. (2026). High temperature affects synthesis and degradation of anthocyanin in red-fleshed kiwifruit (*Actinidia chinensis*): pathway and kinetics analysis. *Plant Physiology and Biochemistry*, *230*, 110936. https://doi.org/https://doi.org/10.1016/j.plaphy.2025.110936

Cieslak, M., Seleznyova, A. N., & Hanan, J. (2011). A functional-structural kiwifruit vine model integrating architecture, carbon dynamics and effects of the environment. *Annals of Botany*, *107*(5), 747-764. https://doi.org/10.1093/aob/mcq180

Clark, C. J., McGlone, V. A., De Silva, H. N., Manning, M. A., Burdon, J., & Mowat, A. D. (2004). Prediction of storage disorders of kiwifruit (*Actinidia chinensis*) based on visible-NIR spectral characteristics at harvest. *Postharvest Biology and Technology*, *32*(2), 147-158. https://doi.org/10.1016/j.postharvbio.2003.11.004

Clearwater, M. J., Luo, Z., Ong, S. E. C., Blattmann, P., & Thorp, T. G. (2011). Vascular functioning and the water balance of ripening kiwifruit (*Actinidia chinensis*) berries. *Journal of Experimental Botany*, *63*(5), 1835-1847. https://doi.org/10.1093/jxb/err352

Clearwater, M. J., Mezzana, S., Richardson, A. C., Boldingh, H. L., Marsh, H., Clarke, J., . . . MacRae, E. A. (2007). Physiological processes contributing to genotypic variation in fruit composition of *Actinidia deliciosa*. *Acta Horticulturae*, *753*(1), 375-381. https://doi.org/10.17660/ActaHortic.2007.753.47

Clearwater, M. J., Seleznyova, A. N., Thorp, T. G., Blattmann, P., Barnett, A. M., Lowe, R. G., & Austin, P. T. (2006). Vigor-controlling rootstocks affect early shoot growth and leaf area development of kiwifruit. *Tree Physiology*, *26*(4), 505-515. https://doi.org/10.1093/treephys/26.4.505

Cooper, K., & Marshall, R. (1992). Croploading and canopy management. *Acta Horticulturae*, *297*, 501-508. https://doi.org/10.17660/ActaHortic.1992.297.65

Costa, G., Testolin, R., & Vizzotto, G. (1993). Kiwifruit pollination: an unbiased estimate of wind and bee contribution. *New Zealand Journal of Crop and Horticultural Science*, *21*(2), 189-195. https://doi.org/10.1080/01140671.1993.9513767

Costa, G., Vizzotto, G., & Testolin, R. (1991). Kiwifruit: variations in vegetative gradient and cropping performance as related to cane orientation. *Advances in Horticultural Science*, *5*(1), 15-18. https://doi.org/10.17660/ActaHortic.1990.282.13

Cotter, R. L., MacRae, E. A., Ferguson, A. R., McMath, K. L., & Brennan, C. J. (1991). A comparison of the ripening, storage and sensory qualities of seven cultivars of kiwifruit. *Journal of Horticultural Science*, *66*(3), 291-300. https://doi.org/10.1080/00221589.1991.11516156

Cruz-Castillo, J., Woolley, D., & Famiani, F. (2010). Effects of defoliation on fruit growth, carbohydrate reserves and subsequent flowering of 'Hayward' kiwifruit vines. *Scientia Horticulturae*, *125*(4), 579-583. https://doi.org/10.1016/j.scienta.2010.05.004

Cruz-Castillo, J. G., Lawes, G. S., & Woolley, D. J. (1991). The influence of the time of anthesis, seed factor(s), and the application of a growth regulator mixture on the growth of kiwifruit. *Acta Horticulturae*, *297*, 475-480. https://doi.org/10.17660/ActaHortic.1992.297.62

Cruz-Castillo, J. G., Woolley, D. J., & Lawes, G. S. (2002). Kiwifruit size and CPPU response are influenced by the time of anthesis. *Scientia Horticulturae*, *95*(1-2), 23-30. https://doi.org/10.1016/S0304-4238(01)00384-3

Currie, M., Patterson, K., Snelgar, W., & Blattmann, P. (2018). Girdling kiwifruit vines for commercial advantage: opportunities and risks. *Acta Horticulturae*(1218), 405-412. https://doi.org/10.17660/ActaHortic.2011.913.43

Currie, M. B. (1997). *Source-sink relations in kiwifruit: carbohydrate and hormone effects on fruit growth at the cell, organ and whole plant level* [Doctoral dissertation, Massey University]. Palmerston North, New Zealand. http://hdl.handle.net/10179/2737

Currie, M. B., Patterson, K. J., Dawson, T., Ramankutty, P., & Blattmann, P. (2011). Careful use of NAA pruning gels is needed to avoid compromising 'Hort16A' fruit quality. *Acta Horticulturae*, *913*, 327-335. https://doi.org/10.17660/ActaHortic.2011.913.43

Cutting, B., Evans, L., Paugam, L., McBrydie, H., Jesson, L., Pomeroy, N., . . . Pattemore, D. (2018). Managed bumble bees are viable as pollinators in netted kiwifruit orchards. *New Zealand Plant Protection*, *71*, 214-220. https://doi.org/10.30843/nzpp.2018.71.178

Da Silva, D., Qin, L., DeBuse, C., & DeJong, T. M. (2014). Measuring and modelling seasonal patterns of carbohydrate storage and mobilization in the trunks and root crowns of peach trees. *Annals of Botany*, *114*(4), 643-652. https://doi.org/10.1093/aob/mcu033

Dahal, K. C., Bhattarai, S. P., Midmore, D. J., Oag, D., Sapkota, R., & Walsh, K. B. (2024). In situ sucrose injection for alteration of carbohydrate reserve dynamics in grapevine. *Agronomy*, *14*(3), 425. https://doi.org/doi.org/10.3390/agronomy14030425

Dattola, A., Accardo, A., Zappia, R., & Gullo, G. A. M. (2024). Fruit variation in yellow-fleshed Actinidia (*Actinidia chinensis* Planch) plants grown in southern italy as a function of shoot type. *Agriculture*, *14*(8), 1335. https://doi.org/10.3390/agriculture14081335

Davidson, A. M., Le, S. T., Cooper, K. B., Lange, E., & Zwieniecki, M. A. (2021). No time to rest: seasonal dynamics of non-structural carbohydrates in twigs of three Mediterranean tree species suggest year-round activity. *Scientific Reports*, *11*(1), 5181. https://doi.org/10.1038/s41598-021-83935-1

De Schepper, V., Bühler, J., Thorpe, M., Roeb, G., Huber, G., van Dusschoten, D., . . . Steppe, K. (2013). $^{11}$C-PET imaging reveals transport dynamics and sectorial plasticity of oak phloem after girdling. *Frontiers in Plant Science*, *4*(200), 1-9. https://doi.org/10.3389/fpls.2013.00200

De Silva, H. N., & Ball, R. D. (1997). Mixed model analysis of within-plant variation of fruit weight with implications for sampling of kiwifruit vines. *Annals of Botany*, *79*, 411-418. https://doi.org/10.1006/anbo.1996.0362

Decourteix, M., Alves, G., Bonhomme, M., Peuch, M., Baaziz, K. B., Brunel, N., . . . Petel, G. (2008). Sucrose (JrSUT1) and hexose (JrHT1 and JrHT2) transporters in walnut xylem parenchyma cells: their potential role in early events of growth resumption. *Tree Physiology*, *28*(2), 215-224. https://doi.org/10.1093/treephys/28.2.215

Decourteix, M., Alves, G., Brunel, N., Ameglio, T., Guilliot, A., Lemoine, R., . . . Sakr, S. (2006). JrSUT1, a putative xylem sucrose transporter, could mediate sucrose influx into xylem parenchyma cells and be up-regulated by freeze–thaw cycles over the autumn–winter period in walnut tree (*Juglans regia* L.). *Plant, Cell & Environment*, *29*(1), 36-47. https://doi.org/10.1111/j.1365-3040.2005.01398.x

Dietze, M. C., Sala, A., Carbone, M. S., Czimczik, C. I., Mantooth, J. A., Richardson, A. D., & Vargas, R. (2014). Nonstructural carbon in woody plants. *Annual Review of Plant Biology*, *65*(1), 667-687. https://doi.org/10.1146/annurev-arplant-050213-040054

Eltom, M., Trought, M., & Winefield, C. (2013). The effects of cane girdling before budbreak on shoot growth, leaf area and carbohydrate content of *Vitis vinifera* L. Sauvignon Blanc grapevines. *Functional Plant Biology*, *40*(7), 749-757. https://doi.org/10.1071/FP12278

Engin, H., Gokbayrak, Z., & Dardeniz, A. (2011). Flower aberrations in kiwifruit (*Actinidia deliciosa*). *European Journal of Horticultural Science*, *76*(3), 91-94. https://doi.org/10.17660/eJHS.2011/2593888

Fadón, E., Fernandez, E., Behn, H., & Luedeling, E. (2020). A conceptual framework for winter dormancy in deciduous trees. *Agronomy*, *10*(2), 241. https://doi.org/10.3390/agronomy10020241

Famiani, F., Antognozzi, E., Boco, M., Tombesi, A., Battistelli, A., Moscatello, S., & Spaccino, L. (1995). Effects of altered source-sink relationships on fruit development and quality in *Actinidia deliciosa*. *Acta Horticulturae*, *444*, 355-360. https://doi.org/10.17660/ActaHortic.1997.444.55

Famiani, F., Baldicchi, A., Farinelli, D., Cruz-Castillo, J. G., Marocchi, F., Mastroleo, M., . . . Battistelli, A. (2012). Yield affects qualitative kiwifruit characteristics and dry matter content may be an indicator of both quality and storability. *Scientia Horticulturae*, *146*, 124-130. https://doi.org/10.1016/j.scienta.2012.08.009

Faust, M., Erez, A., Rowland, L. J., Wang, S. Y., & Norman, H. A. (1997). Bud dormancy in perennial fruit trees: physiological basis for dormancy induction, maintenance, and release. *HortScience*, *32*(4), 623-629. https://doi.org/10.21273/HortSci.32.4.623

Fennell, A., & Hoover, E. (1991). Photoperiod influences growth, bud dormancy, and cold acclimation in *Vitis labruscana* and *V. riparia*. *Journal of the American Society for Horticultural Science*, *116*(2), 270-273. https://doi.org/10.21273/JASHS.116.2.270

Ferguson, A. (1990). Stem, branches, leaves and roots of the kiwifruit vine. In I. J. Warrington & G. C. Weston (Eds.), *Kiwifruit: Science and management* (pp. 58-70). Ray Richards

Ferguson, A. (2004). 1904—the year that kiwifruit (*Actinidia deliciosa*) came to New Zealand. *New Zealand Journal of Crop and Horticultural Science*, *32*(1), 3-27. https://doi.org/10.1080/01140671.2004.9514276

Ferguson, A. R. (1980). Xylem sap from *Actinidia chinensis*: apparent differences in sap composition arising from the method of collection. *Annals of Botany*, *46*(6), 791-801. https://doi.org/10.1093/oxfordjournals.aob.a085977

Ferguson, A. R. (1984). Kiwifruit: A botanical review. *Horticultural Reviews*, *6*, 1-64. https://doi.org/10.1002/9781118060797.ch1

Ferguson, A. R. (1999). Kiwifruit cultivars: Breeding and selection. *Acta Horticulturae*, *498*, 43–52. https://doi.org/10.17660/ActaHortic.1999.498.4

Ferguson, A. R., Fang, J., & Costa, G. (2023a). Fruiting cultivars. In A. Richardson, J. Burdon, & A. R. Ferguson (Eds.), *Kiwifruit: Botany, Production and Uses* (pp. 52–71). CABI GB. https://doi.org/10.1079/9781800620933.0004

Ferguson, A. R., Huang, H., & Costa, G. (2023b). History of kiwifruit: evolution of a global crop. In *Kiwifruit: Botany, Production and Uses* (pp. 1-15). CABI GB. https://doi.org/10.1079/9781800620933.0001

Foster, T. M., Seleznyova, A. N., & Barnett, A. M. (2007). Independent control of organogenesis and shoot tip abortion are key factors to developmental plasticity in kiwifruit (*Actinidia*). *Annals of Botany*, *100*(3), 471-481. https://doi.org/10.1093/aob/mcm140

Friend, A., Alspach, P., Diack, R., Seymour, S., Shirtliff, A., van Hooijdonk, B., . . . Richardson, A. (2014). Bud orientation on horizontally trained canes modifies budbreak and shoot fruitfulness of *Actinidia deliciosa* 'Hayward' vines. *Acta Horticulturae*, *1096*, 87-92. https://doi.org/10.17660/ActaHortic.2015.1096.6

Gallego, P. P., Martinez, A., & Zarra, I. (1997). Analysis of the growth kinetic of fruits of *Actinidia deliciosa*. *Biologia Plantarum*, *39*(4), 615-622. https://doi.org/10.1023/a:1000991101418

Gökbayrak, Z., Engin, H., & Dardeniz, A. (2010). Examination of flower bud differentiation and development in kiwifruit. *Journal of Biology & Life Sciences*, *1*, 1-4. https://www.researchgate.net/publication/250002498_Examination_of_Flower_Bud_Differentiation_and_Development_in_Kiwifruit

Gonzalez, M. V., Coque, M., & Herrero, M. (1994). Pollinator selection in kiwifruit (*Actinidia deliciosa*). *Journal of Horticultural Science*, *69*(4), 697-702. https://doi.org/10.1080/14620316.1994.11516502

Goodwin, R. M., McBrydie, H. M., & Taylor, M. A. (2013). Wind and honey bee pollination of kiwifruit (*Actinidia chinensis* 'Hort16A'). *New Zealand Journal of Botany*, *51*(3), 229-240. https://doi.org/10.1080/0028825X.2013.806934

Gould, N., Morrison, D., Clearwater, M. J., Ong, S., Boldingh, H., & Minchin, P. E. (2013). Elucidating the sugar import pathway into developing kiwifruit berries (Actinidia deliciosa). *New Zealand Journal of Crop and Horticultural Science*, *41*(4), 189-206. https://doi.org/10.1080/01140671.2013.801356

Gould, N., Snelgar, P., Kramer-Walter, K., McKenzie, C., Haisman, N., Anderson, R., . . . Martin, P. (2025). Effects of trunk girdling over three years on vine reserves, productivity and yield in *Actinidia chinensis* var. *chinensis* and *A*. *chinensis* var. *deliciosa*. *Acta Horticulturae*, *1431*, 329-338. https://doi.org/10.17660/ActaHortic.2025.1431.43

Grant, J. A., & Ryugo, K. (1984a). Influence of within-canopy shading on fruit size, shoot growth, and return bloom in kiwifruit. *Journal of the American Society for Horticultural Science*, *109*(6), 799-802. https://doi.org/10.21273/JASHS.109.6.799

Grant, J. A., & Ryugo, K. (1984b). Influence of within-canopy shading on net photosynthetic rate, stomatal conductance, and chlorophyll content of kiwifruit leaves. *HortScience*, *19*(6), 834-836. https://doi.org/10.21273/HortSci.19.6.832

Graves, S., Piepho, H., Selzer, L., & Dorai-Raj, S. (2024). *multcompView: Visualizations of paired comparisons*. (Version 0.1-10.) https://cran.r-project.org/package=multcompView

Greaves, A. J., Henton, S. M., Piller, G. J., Meekings, J. S., & Walton, E. F. (1999). Carbon supply from starch reserves to spring growth: modelling spatial patterns in kiwifruit canes. *Annals of Botany*, *83*(4), 431-439. https://doi.org/10.1006/anbo.1998.0839

Greer, D. H. (1996). Photosynthetic development in relation to leaf expansion in kiwifruit (*Actinidia deliciosa*) vines during growth in a controlled environment. *Australian Journal of Plant Physiology*, *23*(5), 541-549. https://doi.org/10.1071/PP9960541

Greer, D. H., Cirillo, C., & Norling, C. L. (2003). Temperature-dependence of carbon acquisition and demand in relation to shoot and fruit growth of fruiting kiwifruit (*Actinidia deliciosa*) vines grown in controlled environments. *Functional Plant Biology*, *30*(9), 927-937. https://doi.org/10.1071/FP03111

Greer, D. H., & Halligan, E. A. (2001). Photosynthetic and fluorescence light responses for kiwifruit (*Actinidia deliciosa*) leaves at different stages of development on vines grown at two different photon flux densities. *Functional Plant Biology*, *28*(5), 373-382. https://doi.org/10.1071/PP00146

Greer, D. H., & Jeffares, D. (1998). Temperature-dependence of carbon acquisition and demand in relation to shoot growth of kiwifruit (*Actinidia deliciosa*) vines grown in controlled environments. *Australian Journal of Plant Physiology*, *25*(7), 843-850. https://doi.org/10.1071/PP98055

Greer, D. H., Seleznyova, A. N., & Green, S. R. (2004). From controlled environments to field simulations: leaf area dynamics and photosynthesis of kiwifruit vines (*Actinidia deliciosa*). *Functional Plant Biology*, *31*(2), 169-179. https://doi.org/10.1071/FP03151

Guerriero, P., Scalabrelli, G., & Grazzini, G. (1990). Chilling effect on inhibition removal in kiwifruit dormant lateral buds. *Acta Horticulturae*, *282*, 79-86. https://doi.org/10.17660/ActaHortic.1990.282.7

Guerriero, R., Scalabrelli, G., & Vitagliano, C. (1992). Effect of natural and artificial chilling on bud opening and fruitfulness of *Actinidia deliciosa* Chev. (Liang & Ferguson) single node cuttings (cv. Hayward and Tomuri). *Acta Horticulturae*, *292*, 223-229. https://doi.org/10.17660/ActaHortic.1992.297.29

Gullo, G., Barbera, S., Cannizzaro, A., Scarano, M., Larocca, F., Branca, V., & Dattola, A. (2025). Differences in vegetative, productive, and physiological behaviors in *Actinidia chinensis* plants, cv. Gold 3, as a function of cane type. *Plants (Basel)*, *14*(14). https://doi.org/10.3390/plants14142199

Hall, A. J., McPherson, H. G., Crawford, R. A., & Seager, N. G. (1996). Using early-season measurements to estimate fruit volume at harvest in kiwifruit. *New Zealand Journal of Crop and Horticultural Science*, *24*(4), 379-391. https://doi.org/10.1080/01140671.1996.9513975

Hall, A. J., Minchin, P. E., Clearwater, M. J., & Génard, M. (2013). A biophysical model of kiwifruit (*Actinidia deliciosa*) berry development. *Journal of Experimental Botany*, *64*(18), 5473-5483. https://doi.org/10.1093/jxb/ert317

Hallett, I. C., & Sutherland, P. W. (2005). Structure and development of kiwifruit skins. *International Journal of Plant Sciences*, *166*(5), 693-704. https://doi.org/10.1086/431232

Hansen, P. (1969). 14C-studies on apple trees. IV. Photosynthate consumption in fruits in relation to the leaf-fruit ratio and to the leaf-fruit position. *Physiologia Plantarum*, *22*(1), 186-198. https://doi.org/10.1111/j.1399-3054.1969.tb07855.x

Harman, J. (1981). Kiwifruit maturity. *Orchardist of New Zealand*, *54*, 126-128

Hartmann, H., & Trumbore, S. (2016). Understanding the roles of nonstructural carbohydrates in forest trees – from what we can measure to what we want to know. *New Phytologist*, *211*(2), 386-403. https://doi.org/10.1111/nph.13955

Hasegawa, K., & Nakajima, Y. (1990). Effects of bloom date, seediness, GA treatment and location of fruits in the foliar canopy on the fruit quality of persimmon *Diospyros kaki* Thunb. *Journal of the Japanese Society for Horticultural Science*, *59*(2), 263-270. https://doi.org/10.2503/jjshs.59.263

Heide, O. M. (2011). Temperature rather than photoperiod controls growth cessation and dormancy in *Sorbus* species. *Journal of Experimental Botany*, *62*(15), 5397-5404. https://doi.org/10.1093/jxb/err213

Heide, O. M., & Prestrud, A. K. (2005). Low temperature, but not photoperiod, controls growth cessation and dormancy induction and release in apple and pear. *Tree Physiology*, *25*(1), 109-114. https://doi.org/10.1093/treephys/25.1.109

Hernández, G., Craig, R., & Tanner, D. (2015). Assessment of alternative bud break enhancers for commercial kiwifruit production of 'Zesy002' (Gold3). In *Advances in Plant Dormancy* (pp. 289-300). Springer. https://doi.org/10.1007/978-3-319-14451-1_18

Ho, L. C. (1988). Metabolism and compartmentation of imported sugars in sink organs in relation to sink strength. *Annual Review of Plant Physiology and Plant Molecular Biology*, *39*(1), 355-378. https://doi.org/10.1146/annurev.pp.39.060188.002035

Hoch, G., Richter, A., & Körner, C. (2003). Non-structural carbon compounds in temperate forest trees. *Plant, Cell & Environment*, *26*(7), 1067-1081. https://doi.org/10.1046/j.0016-8025.2003.01032.x

Hopkirk, G., Snelgar, W. P., Horne, S. F., & Manson, P. J. (1989). Effect of increased preharvest temperature on fruit quality of kiwifruit (*Actinidia deliciosa*). *Journal of Horticultural Science*, *64*(2), 227-237. https://doi.org/10.1080/14620316.1989.11515949

Hopping, M., Martyn, J., & Hacking, N. (1993). Comparison of growth and yield of kiwifruit on different vine support structures. *New Zealand Journal of Crop and Horticultural Science*, *21*(4), 295-301. https://doi.org/10.1080/01140671.1993.9513785

Hopping, M. E. (1976). Structure and development of fruit and seeds in Chinese gooseberry (*Actinidia chinensis* Planch.). *New Zealand Journal of Botany*, *14*(1), 63-68. https://doi.org/10.1080/0028825X.1976.10428651

Hopping, M. E. (1990). Floral biology, pollination, and fruit set. In I. J. Warrington & G. C. Weston (Eds.), *Kiwifruit: Science and Management* (pp. 71-96). Ray Richards

Horibe, T., Yamaki, S., & Yamada, K. (2014). Leaves of cut rose flower convert exogenously applied glucose to sucrose and translocate it to petals. *Journal of Horticultural Research*, *22*. https://doi.org/10.2478/johr-2014-0020

Horner, I., & Manning, M. (2012). *Psa progression within orchards*. https://kvh.org.nz/assets/projects/91145_2021-10-26-225047_gwmf.pdf

Hothorn, T., Bretz, F., & Westfall, P. (2008). Simultaneous inference in general parametric models. *Biometrical Journal*, *50*(3), 346-363. https://doi.org/10.1002/bimj.200810425

Iglesias, D. J., Tadeo, F. R., Legaz, F., Primo Millo, E., & Talon, M. (2001). In vivo sucrose stimulation of colour change in citrus fruit epicarps: interactions between nutritional and hormonal signals. *Physiologia Plantarum*, *112*(2), 244-250. https://doi.org/10.1034/j.1399-3054.2001.1120213.x

Iglesias, D. J., Tadeo, F. R., Primo-Millo, E., & Talon, M. (2003). Fruit set dependence on carbohydrate availability in citrus trees. *Tree Physiology*, *23*(3), 199-204. https://doi.org/10.1093/treephys/23.3.199

Jaeger, S. R., Harker, R., Triggs, C. M., Gunson, A., Campbell, R. L., Jackman, R., & Requejo-Jackman, C. (2011). Determining consumer purchase intentions: The importance of dry matter, size, and price of kiwifruit. *Journal of Food Science*, *76*(3), S177-S184. https://doi.org/10.1111/j.1750-3841.2011.02084.x

Jaeger, S. R., Rossiter, K. L., Wismer, W. V., & Harker, F. R. (2003). Consumer-driven product development in the kiwifruit industry. *Food Quality and Preference*, *14*(3), 187-198. https://doi.org/10.1016/S0950-3293(02)00053-8

Jean, D., & Lapointe, L. (2001). Limited carbohydrate availability as a potential cause of fruit abortion in *Rubus chamaemorus*. *Physiologia Plantarum*, *112*(3), 379-387. https://doi.org/10.1034/j.1399-3054.2001.1120311.x

Jordan, R. B., Walton, E. F., Klages, K. U., & Seelye, R. J. (2000). Postharvest fruit density as an indicator of dry matter and ripened soluble solids of kiwifruit. *Postharvest Biology and Technology*, *20*(2), 163-173. https://doi.org/10.1016/S0925-5214(00)00125-3

Joy, K. W. (1964). Translocation in sugar-beet: I. Assimilation of $^{14}CO2$ and distribution of materials from leaves. *Journal of Experimental Botany*, *15*(3), 485-494. https://doi.org/10.1093/jxb/15.3.485

Jupa, R., Mészáros, M., & Plavcová, L. (2021). Linking wood anatomy with growth vigour and susceptibility to alternate bearing in composite apple and pear trees. *Plant Biology*, *23*(1), 172-183. https://doi.org/10.1111/plb.13182

Kabir, M. S., Parry, B. E., Tyson, J. L., & Beresford, R. M. (2019). Understanding flower-bud rot development caused by *Pseudomonas syringae* pv. *actinidiae* in green-fleshed kiwifruit. *New Zealand Plant Protection*, *72*, 83-88. https://doi.org/10.30843/nzpp.2019.72.252

Kaplan, F., Sung, D. Y., & Guy, C. L. (2006). Roles of β-amylase and starch breakdown during temperatures stress. *Physiologia Plantarum*, *126*(1), 120-128. https://doi.org/10.1111/j.1399-3054.2006.00604.x

Keller, J. D., & Loescher, W. H. (1989). Nonstructural carbohydrate partitioning in perennial parts of sweet cherry. *Journal of the American Society for Horticultural Science*, *114*(6), 969-975. https://doi.org/10.21273/jashs.114.6.969

Keller, M., & Koblet, W. (1994). Is carbon starvation rather than excessive nitrogen supply the cause of inflorescence necrosis in *Vitis vinifera* L.? *Vitis*, *33*, 81-86. https://doi.org/10.5073/vitis.1994.33.81-86

Keller, M., Scheele-Baldinger, R., Ferguson, J. C., Tarara, J. M., & Mills, L. J. (2022). Inflorescence temperature influences fruit set, phenology, and sink strength of Cabernet Sauvignon grape berries. *Front Plant Sci*, *13*, 864892. https://doi.org/10.3389/fpls.2022.864892

Khan, A. A., & Sagar, G. R. (1966). Distribution of $^{14}C$-labelled products of photosynthesis during the commercial life of the tomato crop. *Annals of Botany*, *30*(4), 727-743. https://doi.org/10.1093/oxfordjournals.aob.a084109

Kirchoff, B. K. (2008). On the relationship between phyllotaxy and vasculature: a synthesis. *Botanical Journal of the Linnean Society*, *89*(1), 37-51. https://doi.org/10.1111/j.1095-8339.1984.tb00999.x

Knoblauch, M., Knoblauch, J., Mullendore, D. L., Savage, J. A., Babst, B. A., Beecher, S. D., . . . Holbrook, N. M. (2016). Testing the Münch hypothesis of long distance phloem transport in plants. *eLife*, *5*, e15341. https://doi.org/10.7554/eLife.15341

Knoblauch, M., & van Bel, A. J. (1998). Sieve tubes in action. *The Plant Cell*, *10*(1), 35-50. https://doi.org/10.1105/tpc.10.1.35

Koussa, T., Rifai, L. A., & Cherrad, M. (2005). Annual variations of alpha-amylase and invertases activities in buds and internodes of grapevines and their relation with carbohydrates and abscisic acid contents. *OENO One*, *39*(3), 129-136. https://doi.org/10.20870/oeno-one.2005.39.3.894

Kramer, P. J. (1936). Effect of variation in length of day on growth and dormancy of trees. *Plant Physiology*, *11*(1), 127-137. https://doi.org/10.1104/pp.11.1.127

Kuhlemeier, C. (2007). Phyllotaxis. *Trends in Plant Science*, *12*(4), 143-150. https://doi.org/10.1016/j.tplants.2007.03.004

Kuznetsova, A., Brockhoff, P. B., & Christensen, R. H. B. (2017). LmerTest package: Tests in linear mixed effects models. *Journal of Statistical Software*, *82*(13), 1 - 26. https://doi.org/10.18637/jss.v082.i13

Kwack, Y.-B., Kim, H. L., Chae, W.-B., Kim, S. H., Lee, Y.-B., & Kim, J. G. (2014). Carbohydrate reserves of non-fruiting young kiwifruit vines as affected by early artificial defoliation. *Horticulture, Environment, and Biotechnology*, *55*(6), 462-470. https://doi.org/10.1007/s13580-014-0042-5

Kwack, Y.-B., Kim, H. L., Chae, W.-B., Lee, J. H., Lee, E. H., Kim, J. G., & Lee, Y. B. (2013). Regrowth of buds and flower bud formation in kiwifruit as affected by early defoliation. *Korean Journal of Environmental Agriculture*, *32*(3), 201-206. https://doi.org/10.5338/KJEA.2013.32.3.201

Lacointe, A., Kajji, A., Daudet, F.-A., Archer, P., Frossard, J.-S., Saint-Joanis, B., & Vandame, M. (1993). Mobilization of carbon reserves in young walnut trees. *Acta Botanica Gallica*, *140*(4), 435-441. https://doi.org/10.1080/12538078.1993.10515618

Lahav, E., Korkin, A., & Adar, G. (1989). Thinning stage influences fruit size and yield of kiwifruit. *HortScience*, *24*(3), 438-440. https://doi.org/10.21273/HortSci.24.3.438

Lai, R., Woolley, D. J., & Lawes, G. S. (1988). Patterns of assimilate transport from leaves to fruit within a kiwifruit (*Actinidia deliciosa*) lateral. *Journal of Horticultural Science*, *63*(4), 725-730. https://doi.org/10.1080/14620316.1988.11515917

Lai, R., Woolley, D. J., & Lawes, G. S. (1989a). Effect of leaf to fruit ratio on fruit growth of kiwifruit (*Actinidia deliciosa*). *Scientia Horticulturae*, *39*(3), 247-255. https://doi.org/10.1016/0304-4238(89)90137-4

Lai, R., Woolley, D. J., & Lawes, G. S. (1989b). Fruit growth in kiwifruit (*Actinidia deliciosa*): Patterns of assimilate distribution between laterals. *Scientia Horticulturae*, *40*(1), 43-52. https://doi.org/10.1016/0304-4238(89)90006-X

Lai, R., Woolley, D. J., & Lawes, G. S. (1989c). Retardation of fruit growth of kiwifruit (*Actinidia deliciosa*) by leaves: interactions with vine performance and seed number. *Scientia Horticulturae*, *39*(4), 319-329. https://doi.org/10.1016/0304-4238(89)90125-8

Lai, R., Woolley, D. J., & Lawes, G. S. (1990). The effect of inter-fruit competition, type of fruiting lateral and time of anthesis on the fruit-growth of kiwifruit (*Actinidia deliciosa*). *Journal of Horticultural Science*, *65*(1), 87-96. https://doi.org/10.1080/00221589.1990.11516034

Lang, G. A. (1987). Dormancy: A new universal terminology. *HortScience*, *22*, 817-920. https://doi.org/10.21273/HortSci.22.5.817

Lawes, G. S. (1979). *Aspects of growth control in kiwifruit and blackcurrant* [Doctoral dissertation, Massey University]. http://hdl.handle.net/10179/3521

Lawes, G. S., Woolley, D. J., & Lai, R. (1990). Seeds and other factors affecting fruit size in kiwifruit. *Acta Horticulturae*, *282*, 257-264. https://doi.org/10.17660/ActaHortic.1990.282.33

Le Lievre, D., Anderson, R., Boldingh, H., Cooney, J., Seelye, R., Gould, N., . . . Richardson, A. (2021). Modifying carbohydrate supply to fruit during development changes the composition and flavour of *Actinidia chinensis* var. *chinensis* 'Zesy002' kiwifruit. *Plants*, *10*(7), 1328. https://doi.org/10.3390/plants10071328

Legendre, P., & Oksanen, J. (2025). *lmodel2: Model II regression*. (Version 1.7-4) https://CRAN.R-project.org/package=lmodel2

Lenth, R. V. (2024). *emmeans: Estimated marginal means, aka least-squares means*. (Version 1.10.2) https://doi.org/10.32614/CRAN.package.emmeans

Li, Q., Chai, L., Tong, N., Yu, H., & Jiang, W. (2022). Potential carbohydrate regulation mechanism underlying starvation-induced abscission of tomato flower. *International Journal of Molecular Sciences*, *23*(4). https://doi.org/10.3390/ijms23041952

Li, Y. F., Jiang, W., Liu, C., Fu, Y., Wang, Z., Wang, M., . . . Liu, Z. B. (2021). Comparison of fruit morphology and nutrition metabolism in different cultivars of kiwifruit across developmental stages. *PeerJ*, *9*, e11538. https://doi.org/10.7717/peerj.11538

Linsley-Noakes, G. C., & Allan, P. (1987). Effects of winter temperatures on flower development in two clones of kiwifruit (*Actinidia deliciosa* (A. Chev.) C.F. Liang et A.R. Ferguson). *Scientia Horticulturae*, *33*(3/4), 249-260. https://doi.org/10.1016/0304-4238(87)90072-0

Lionakis, S., Chouliaras, V., & Gerasopoulos, D. (1994). Effects of shading on vegetative, reproductive and fruit maturity aspects of `*Hayward*' kiwifruit. *Advances in Horticultural Science*, *8*, 221-224. https://www.jstor.org/stable/42883144

Lionakis, S. M., & Schwabe, W. W. (1984a). Bud dormancy in the kiwifruit, *Actinidia chinensis* Planch. *Annals of Botany*, *54*(4), 467-484. https://doi.org/10.1093/oxfordjournals.aob.a086818

Lionakis, S. M., & Schwabe, W. W. (1984b). Some effects of daylength, temperature and exogenous growth regulator application on the growth of *Actinidia chinensis* Planch. *Annals of Botany*, *54*, 485-501. https://doi.org/10.1093/oxfordjournals.aob.a086819

Liu, J., & Sherif, S. M. (2019). Hormonal orchestration of bud dormancy cycle in deciduous woody perennials. *Frontiers in Plant Science*, *10*, 1136. https://doi.org/10.3389/fpls.2019.01136

Lüdecke, D. (2018). Ggeffects: Tidy data frames of marginal effects from regression models. *Journal of Open Source Software*, *3*(26), 772. https://doi.org/10.21105/joss.00772

M'Batchi, B., & Delrot, S. (1984). Parachloromercuribenzenesulfonic acid: a potential tool for differential labeling of the sucrose transporter. *Plant Physiology*, *75*(1), 154-160. https://doi.org/10.1104/pp.75.1.154

Mancera, H. A. Z. (2018). Fluorescent staining for callose with aniline blue. https://doi.org/10.17504/protocols.io.q83dzyn

Mao, J., Li, W., Mi, B., Dawuda, M. M., Calderón-Urrea, A., Ma, Z., . . . Chen, B. (2017). Different exogenous sugars affect the hormone signal pathway and sugar metabolism in "Red Globe" (*Vitis vinifera* L.) plantlets grown in vitro as shown by transcriptomic analysis. *Planta*, *246*(3), 537-552. https://doi.org/10.1007/s00425-017-2712-x

Marcelis, L. F. (1996). Sink strength as a determinant of dry matter partitioning in the whole plant. *Journal of Experimental Botany*, *47*(Special Issue), 1281-1291. https://doi.org/10.1093/jxb/47.Special_Issue.1281

Marsh, K., Attanayake, S., Walker, S., Gunson, A., Boldingh, H., & MacRae, E. (2004). Acidity and taste in kiwifruit. *Postharvest Biology and Technology*, *32*(2), 159-168. https://doi.org/10.1016/j.postharvbio.2003.11.001

Marsh, K. B., Friel, E. N., Gunson, A., Lund, C., & MacRae, E. (2006). Perception of flavour in standardised fruit pulps with additions of acids or sugars. *Food Quality and Preference*, *17*(5), 376-386. https://doi.org/https://doi.org/10.1016/j.foodqual.2005.04.011

Martínez-Lüscher, J., & Kurtural, S. K. (2021). Same season and carry-over effects of source-sink adjustments on grapevine yields and non-structural carbohydrates. *Frontiers in Plant Science*, *12*. https://doi.org/10.3389/fpls.2021.695319

Martínez-Trinidad, T., Watson, W. T., Arnold, M. A., Lombardini, L., & Appel, D. N. (2009). Carbohydrate injections as a potential option to improve growth and vitality of live oaks. *Journal of Arboriculture*, *35*(3), 142. https://doi.org/10.48044/jauf.2009.025

Martínez-Vilalta, J., Sala, A., Asensio, D., Galiano, L., Hoch, G., Palacio, S., . . . Lloret, F. (2016). Dynamics of non-structural carbohydrates in terrestrial plants: a global synthesis. *Ecological Monographs*, *86*(4), 495-516. https://doi.org/10.1002/ecm.1231

Mason, M. G., Ross, J. J., Babst, B. A., Wienclaw, B. N., & Beveridge, C. A. (2014). Sugar demand, not auxin, is the initial regulator of apical dominance. *Proceedings of the National Academy of Sciences*, *111*(16), 6092-6097. https://doi.org/10.1073/pnas.1322045111

McGhie, T. K., & Ainge, G. D. (2002). Color in fruit of the genus *Actinidia*: carotenoid and chlorophyll compositions. *Journal of Agricultural and Food Chemistry*, *50*(1), 117-121. https://doi.org/10.1021/jf0106771

Mclaughlin, J. E., & Boyer, J. S. (2004). Glucose localization in maize ovaries when kernel number decreases at low water potential and sucrose is fed to the stems. *Annals of Botany*, *94*(1), 75-86. https://doi.org/10.1093/aob/mch123

McPherson, H., Manson, P., & Snelgar, W. (1997a). Non-destructive measurement of dormant bud respiration rates. *Photosynthetica*, *33*(1), 125-138. https://doi.org/10.1023/A:1022187524539

McPherson, H., Richardson, A., Snelgar, W., Patterson, K., & Currie, M. (2001a). Flower quality and fruit size in kiwifruit (*Actinidia deliciosa*). *New Zealand Journal of Crop and Horticultural Science*, *29*(2), 93-101. https://doi.org/10.1080/01140671.2001.9514167

McPherson, H., Snelgar, W., Manson, P., & Snowball, A. (1997b). Bud respiration and dormancy of kiwifruit (*Actinidia deliciosa*). *Annals of Botany*, *80*(4), 411-418. https://doi.org/10.1006/anbo.1997.0455

McPherson, H. G., Hall, A. J., & Stanley, C. J. (1992). The influence of current temperature on the time from bud break to flowering in kiwifruit (*Actinidia deliciosa*). *Journal of Horticultural Science*, *67*(4), 509-519. https://doi.org/10.1080/00221589.1992.11516277

McPherson, H. G., Hall, A. J., & Stanley, C. J. (1994). Seasonal and regional variation in budbreak and flowering of kiwifruit vines in New Zealand. *New Zealand Journal of Crop and Horticultural Science*, *22*(3), 263-276. https://doi.org/10.1080/01140671.1994.9513835

McPherson, H. G., Richardson, A. C., Snelgar, W. P., & Currie, M. B. (2001b). Effects of hydrogen cyanamide on budbreak and flowering in kiwifruit (*Actinidia deliciosa* 'Hayward'). *New Zealand Journal of Crop and Horticultural Science*, *29*(4), 277-285. https://doi.org/10.1080/01140671.2001.9514189

McQueen, J. C., Minchin, P. E. H., Silvester, W. B., & Green, T. G. A. (2004). Carbohydrate allocation in apple stems can be altered by fruit load. *Acta Horticulturae*, *636*, 267-273. https://doi.org/10.17660/ActaHortic.2004.636.32

Miles, D. B., Smith, G. S., & Miller, S. A. (1996). Within plant sampling procedures - fruit variation in kiwifruit vines. *Annals of Botany*, *78*(3), 289-294. https://doi.org/10.1006/anbo.1996.0123

Miller, S. A., Broom, F. D., Thorp, T. G., & Barnett, A. M. (2001). Effects of leader pruning on vine architecture, productivity and fruit quality in kiwifruit (*Actinidia deliciosa* cv. Hayward). *Scientia Horticulturae*, *91*(3-4), 189-199. https://doi.org/10.1016/s0304-4238(01)00259-x

Mills, T., Boldingh, H., Blattmann, P., Green, S., & Meekings, J. (2009). Nitrogen application rate and the change in carbohydrate concentration in leaves, fruit, and canes of gold kiwifruit. *Journal of Plant Nutrition*, *32*(12), 2140-2157. https://doi.org/10.1080/01904160903351606

Minchin, P. E. H., Snelgar, W. P., Blattmann, P., & Hall, A. J. (2010). Competition between fruit and vegetative growth in Hayward kiwifruit. *New Zealand Journal of Crop and Horticultural Science*, *38*(2), 101-112. https://doi.org/10.1140671003781728

Minchin, P. E. H., & Thorpe, M. R. (1996). What determines carbon partitioning between competing sinks? *Journal of Experimental Botany*, *47*(Special Issue), 1293-1296. https://doi.org/10.1093/jxb/47.Special_Issue.129

Minchin, P. E. H., Thorpe, M. R., & Farrar, J. F. (1993). A simple mechanistic model of phloem transport which explains sink priority. *Journal of Experimental Botany*, *44*(5), 947-955. https://doi.org/10.1093/jxb/44.5.947

Minchin, P. E. H., Thorpe, M. R., Wünsche, J. N., Palmer, J. W., & Picton, R. F. (1997). Carbon partitioning between apple fruits: short- and long-term response to availability of photosynthate. *Journal of Experimental Botany*, *48*(312), 1401-1406. https://doi.org/10.1093/jxb/48.7.1401

Ministry for Primary Industries. (2012). *Horticulture Monitoring 2012: Bay of Plenty Kiwifruit*. https://www.mpi.govt.nz/dmsdocument/4208/direct

Ministry for Primary Industries. (2025). *Situation and Outlook for Primary Industries* https://www.mpi.govt.nz/dmsdocument/69612-Situation-and-Outlook-for-Primary-Industries-SOPI-June-2025

Mitchell, F. G., Mayer, G., & Biasi, W. (1992). Effect of harvest maturity on storage performance of 'Hayward' kiwifruit. *Acta Horticulturae*, *297*, 617-625. https://doi.org/10.17660/ActaHortic.1992.297.82

Montanaro, G., Dichio, B., Xiloyannis, C., & Lang, A. (2012). Fruit transpiration in kiwifruit: environmental drivers and predictive model. *Aob Plants*, *2012*, pls036. https://doi.org/10.1093/aobpla/pls036

Montefiori, M., McGhie, T. K., Hallett, I. C., & Costa, G. (2009). Changes in pigments and plastid ultrastructure during ripening of green-fleshed and yellow-fleshed kiwifruit. *Scientia Horticulturae*, *119*(4), 377-387. https://doi.org/10.1016/j.scienta.2008.08.022

Morandi, B., Manfrini, L., Losciale, P., Zibordi, M., & Grappadelli, L. (2010). Changes in vascular and transpiration flows affect the seasonal and daily growth of kiwifruit (*Actinidia deliciosa*) berry. *Annals of Botany*, *105*(6), 913-923. https://doi.org/10.1093/aob/mcq070

Morandi, B., Manfrini, L., Zibordi, M., Corelli-Grappadelli, L., & Losciale, P. (2016). From fruit anatomical features to fruit growth strategy: is there a relationship? *Acta Horticulturae*, *1130*, 185-192. https://doi.org/10.17660/ActaHortic.2016.1130.27

Morgan, D. C., Stanley, C. J., & Warrington, I. J. (1985a). The effects of simulated daylight and shade-light on vegetative and reproductive growth in kiwifruit and grapevine. *Journal of Horticultural Science*, *60*(4), 473-484. https://doi.org/10.1080/14620316.1985.11515654

Morgan, D. C., Warrington, I. J., & Halligan, E. A. (1985b). Effect of temperature and photosynthetic photon flux density on vegetative growth of kiwifruit (*Actinidia chinensis*). *New Zealand Journal of Agricultural Research*, *28*(1), 109-116. https://doi.org/10.1080/00288233.1985.10427003

Morrison, D. (2012). *Vascular functioning and development of the kiwifruit berry (Actinidia deliciosa)* [Master's thesis, University of Waikato]. Hamilton, New Zealand. https://hdl.handle.net/10289/6498

Mowat, A., & Collins, R. (2000). Consumer behaviour and fruit quality: supply chain management in an emerging industry. *Supply Chain Management: An International Journal*, *5*(1), 45–54. https://doi.org/10.1108/13598540010312963

Mowat, A. D., & Kay, C. (2007). Geographic patterns in fruit attributes for New Zealand grown kiwifruit. *Acta Horticulturae*, *753*, 325-332. https://doi.org/10.17660/ActaHortic.2007.753.40

Mullins, M. (1966). Test-plants for investigations of the physiology of fruiting in *Vitis vinifera* L. *Nature*, *209*(5021), 419-420. https://doi.org/10.1038/209419a0

Mullins, M. G., & Rajasekaran, K. (1981). Fruiting cuttings: revised method for producing test plants of grapevine cultivars. *American Journal of Enology and Viticulture*, *32*(1), 35-40. https://doi.org/10.5344/ajev.1981.32.1.35

Nardozza, S., Boldingh, H. L., Kashuba, M. P., Feil, R., Jones, D., Thrimawithana, A. H., . . . McGhie, T. K. (2019). Carbon starvation reduces carbohydrate and anthocyanin accumulation in red-fleshed fruit via trehalose 6-phosphate and MYB27. *Plant, Cell & Environment*. https://doi.org/10.1111/pce.13699

Nardozza, S., Boldingh, H. L., Osorio, S., Höhne, M., Wohlers, M., Gleave, A. P., . . . Sulpice, R. (2013). Metabolic analysis of kiwifruit (*Actinidia deliciosa*) berries from extreme genotypes reveals hallmarks for fruit starch metabolism. *Journal of Experimental Botany*, *64*(16), 5049-5063. https://doi.org/10.1093/jxb/ert293

Nardozza, S., Boldingh, H. L., Richardson, A. C., Costa, G., Marsh, H., MacRae, E. A., & Clearwater, M. J. (2010). Variation in carbon content and size in developing fruit of *Actinidia deliciosa* genotypes. *Functional Plant Biology*, *37*(6), 545-554. https://doi.org/10.1071/fp09301

Nardozza, S., Kashuba, P., McCaughan, L., Philippe, M., Wohlers, M., Montefiori, M., . . . Richardson, A. (2015). Leaves are important to obtain consistent red flesh pigmentation in *Actinidia chinensis* fruit. *Scientia Horticulturae*, *197*, 496-503. https://doi.org/10.1016/j.scienta.2015.10.008

New Zealand Kiwifruit Growers Incorporated. (2024). *The Kiwifruit Book* https://www.nzkgi.org.nz/wp-content/uploads/2024/12/J003459_NZKGI_KF_Book_24_R2C_FINAL_COMPLETE_DIGITAL-1.pdf

New Zealand Kiwifruit Growers Incorporated. (2025). *Kiwifruit Industry Performance Report 2025*. https://www.nzkgi.org.nz/wp-content/uploads/2025/07/NZKGI_KPI-Document-2025.pdf

Okuse, I., & Ryugo, K. (1981). Compositional changes in the developing 'Hayward' kiwi fruit in California. *Journal of the American Society for Horticultural Science*, *106*, 73-76. https://doi.org/10.21273/JASHS.106.1.73

Ouyang, L., Leus, L., De Keyser, E., & Van Labeke, M. C. (2020). Cold acclimation and deacclimation of two garden rose cultivars under controlled daylength and temperature. *Frontiers in Plant Science*, *11*, 327. https://doi.org/10.3389/fpls.2020.00327

Pailly, O., Habib, R., & Delecolle, R. (1995). Effect of soil and climate conditions on soluble solids evolution during maturation of kiwifruit. *New Zealand Journal of Crop and Horticultural Science*, *23*(2), 145-153. https://doi.org/10.1080/01140671.1995.9513881

Pailly, O., Habib, R., & Delecolle, R. (1997). Relationship between mean air temperature and soluble solids evolution during maturing of kiwifruit in orchard. *Acta Horticulturae*, *444*, 493-499. https://doi.org/10.17660/ActaHortic.1997.444.75

Palonen, P. (1999). Relationship of seasonal changes in carbohydrates and cold hardiness in canes and buds of three red raspberry cultivars. *Journal of the American Society for Horticultural Science*, *124*(5), 507-513. https://doi.org/10.21273/JASHS.124.5.507

Pandey, S. K., Moraes, T. S., Nair, A., Aryal, B., Azeez, A., Miskolczi, P., . . . Bhalerao, R. P. (2026). Variable temperature processing by plasmodesmata regulates robust bud dormancy release. *Nature Communications*, *17*(1), 348. https://doi.org/10.1038/s41467-025-67260-z

Park, Y., Jung, S., & Gorinstein, S. (2006). Ethylene treatment of 'Hayward'kiwifruits (*Actinidia deliciosa*) during ripening and its influence on ethylene biosynthesis and antioxidant activity. *Scientia Horticulturae*, *108*(1), 22-28. https://doi.org/10.1016/j.scienta.2006.01.001

Patten, K., Patterson, M. E., & Proebsting, E. L. (1986). Factors accounting for the within-tree variation of fruit quality in sweet cherries. *Journal of the American Society for Horticultural Science*, *111*, 356-360. https://doi.org/10.21273/JASHS.111.3.356

Patterson, K., Burdon, J., & Lallu, N. (2003). 'Hort16A' kiwifruit: progress and issues with commercialisation. *Acta Horticulturae*(610), 267-273. https://doi.org/10.17660/ActaHortic.2003.610.35

Patterson, K. J., & Currie, M. B. (2011). Optimising kiwifruit vine performance for high productivity and superior fruit taste. *Acta Horticulturae*(913), 257-268. https://doi.org/10.17660/ActaHortic.2011.913.33

Patterson, K. J., Snelgar, W. P., Richardson, A. C., & McPherson, H. G. (1999). Flower quality and fruit size of Hayward kiwifruit. *Acta Horticulturae*, 143-150. https://doi.org/10.17660/ActaHortic.1999.498.16

Patterson, K. J., & Thorp, G. (2023). Vine management systems. In A. Richardson, J. Burdon, & A. R. Ferguson (Eds.), *Kiwifruit: botany, production and uses* (pp. 184–206). CABI GB. https://doi.org/10.1079/9781800620933.0012

Pedersen, T. L. (2025). *patchwork: the composer of plots*. (Version 1.3.2) https://cran.r-project.org/web/packages/patchwork/index.html

Percival, G. C., & Fraser, G. A. (2005). Use of sugars to improve root growth and increase transplant success of Birch (*Betula pendula* Roth.). *Arboriculture & Urban Forestry*, *31*(2), 66. https://doi.org/10.48044/jauf.2005.008

Pilkington, S. M., Montefiori, M., Jameson, P. E., & Allan, A. C. (2012). The control of chlorophyll levels in maturing kiwifruit. *Planta*, *236*(5), 1615-1628. https://doi.org/10.1007/s00425-012-1723-x

Piller, G., Greaves, A., & Meekings, J. (1998). Sensitivity of floral shoot growth, fruit set and early fruit size in *Actinidia deliciosa* to local carbon supply. *Annals of Botany*, *81*(6), 723-728. https://doi.org/10.1006/anbo.1998.0624

Piller, G., & Meekings, J. (1997). The acquisition and utilization of carbon in early spring by kiwifruit shoots. *Annals of Botany*, *79*(5), 573-581. https://doi.org/10.1006/anbo.1996.0382

Pinheiro, J., Bates D, & R Core Team. (2023). *nlme: linear and nonlinear mixed effects models*. (Version 3.1-164) https://CRAN.R-project.org/package=nlme

Plavcová, L., Hoch, G., Morris, H., Ghiasi, S., & Jansen, S. (2016). The amount of parenchyma and living fibers affects storage of nonstructural carbohydrates in young stems and roots of temperate trees. *American Journal of Botany*, *103*(4), 603-612. https://doi.org/10.3732/ajb.1500489

Plavcová, L., & Jansen, S. (2015). The role of xylem parenchyma in the storage and utilization of nonstructural carbohydrates. In *Functional and ecological xylem anatomy* (pp. 209-234). Springer. https://doi.org/10.1007/978-3-319-15783-2_8

Polito, V. S., & Grant, J. A. (1984). Initiation and development of pistillate flowers in *Actinidia chinensis*. *Scientia Horticulturae*, *22*(4), 365-371. https://doi.org/10.1016/S0304-4238(84)80008-4

Pollock, C., & Lloyd, E. (1987). The effect of low temperature upon starch, sucrose and fructan synthesis in leaves. *Annals of Botany*, *60*(2), 231-235. https://doi.org/10.1093/oxfordjournals.aob.a087441

Praat, J.-P., Bollen, A., & Mowat, A. (2006). Characterising spatial variation in quality. *Acta Horticulturae*, *753*, 305-316. https://doi.org/10.17660/ActaHortic.2007.753.38

Pratt, H. K., & Reid, M. S. (1974). Chinese gooseberry: Seasonal patterns in fruit growth and maturation, ripening, respiration and the role of ethylene. *Journal of the Science of Food and Agriculture*, *25*(7), 747-757. https://doi.org/10.1002/jsfa.2740250702

Preston, K. A. (1998). The effects of developmental stage and source leaf position on integration and sectorial patterns of carbohydrate movement in an annual plant, *Perilla frutescens* (Lamiaceae). *American Journal of Botany*, *85*(12), 1695-1703. https://doi.org/10.2307/2446503

Proietti, P., Nasini, L., & Famiani, F. (2006). Effect of different leaf-to-fruit ratios on photosynthesis and fruit growth in olive (*Olea europaea* L.). *Photosynthetica*, *44*(2), 275-285. https://doi.org/10.1007/s11099-006-0019-4

Puławska, Z. (1965). Correlations in the development of the leaves and leaf traces in the shoot of *Actinidia arguta* Planch. *Acta Societatis Botanicorum Poloniae*, *34*, 697-712. https://doi.org/10.5586/asbp.1965.048

R Core Team. (2025). R: A language and environment for statistical computing. https://www.R-project.org

Reid, M. S., Heatherbell, D. A., & Pratt, H. K. (1982). Seasonal patterns in chemical composition of the fruit of *Actinidia chinensis*. *Journal of the American Society for Horticultural Science*, *107*(2), 316-319. https://doi.org/10.21273/jashs.107.2.316

Richardson, A., Boldingh, H., Kashuba, M., Nardozza, S., & Greer, D. (2017). Kiwifruit reserves: balancing vine growth and fruit productivity. *Acta Horticulturae*, *1218*, 163-170. https://doi.org/10.17660/ActaHortic.2018.1218.22

Richardson, A., Boldingh, H., Kashuba, P., Knight, G., & Ellingham, D. (2019). Flowering time determines the weight and composition of *Actinidia chinensis* var. *chinensis* 'Zesy002' kiwifruit. *Scientia Horticulturae*, *246*, 741-748. https://doi.org/10.1016/j.scienta.2018.11.043

Richardson, A., Eyre, V., Kashuba, P., Ellingham, D., Jenkins, H., & Nardozza, S. (2021). Early shoot development affects carbohydrate supply and fruit quality of red-fleshed *Actinidia chinensis* var. *chinensis* 'Zes008'. *Agronomy*, *11*(1), 66. https://doi.org/10.3390/agronomy11010066

Richardson, A., Eyre, V., Rebstock, R., Popowski, E., & Nardozza, S. (2022). Factors influencing flower development in kiwifruit vines. *Acta Horticulturae*, *1332*, 141-154. https://doi.org/10.17660/ActaHortic.2022.1332.20

Richardson, A., Kramer-Walter, K., Eyre, V. A., Brecko, K., Mohajer, M., Gould, N., & Nardozza, S. (2025). The fate of inflorescence meristems during their transition to inflorescences at anthesis. *Acta Horticulturae*, 301-308. https://doi.org/10.17660/ActaHortic.2025.1431.39

Richardson, A. C. (2015). *How does carbohydrate supply limit flower development in grape and kiwifruit vines?* [Doctoral dissertation, Charles Sturt University]. Wagga Wagga, Australia. https://researchoutput.csu.edu.au/files/9314073/74794

Richardson, A. C., Boldingh, H. L., McAtee, P. A., Gunaseelan, K., Luo, Z. W., Atkinson, R. G., . . . Schaffer, R. J. (2011). Fruit development of the diploid kiwifruit, *Actinidia chinensis* 'Hort16A'. *BMC Plant Biology*, *11*, 182-182. https://doi.org/10.1186/1471-2229-11-182

Richardson, A. C., & McAneney, K. J. (1990). Influence of fruit number on fruit weight and yield of kiwifruit. *Scientia Horticulturae*, *42*(3), 233-241. https://doi.org/10.1016/0304-4238(90)90085-S

Richardson, A. C., McAneney, K. J., & Dawson, T. E. (1997). Carbohydrate dynamics in kiwifruit. *Journal of Horticultural Science*, *72*(6), 907-917. https://doi.org/10.1080/14620316.1997.11515583

Richardson, A. C., Snelgar, W. P., DeSilva, H. N., & Paul, H. R. (2001). Variation in flowering within *Actinidia chinensis* vines. *New Zealand Journal of Crop and Horticultural Science*, *29*(2), 103-110. https://doi.org/10.1080/01140671.2001.9514168

Richardson, A. C., Walton, E. F., Boldingh, H. L., & Meekings, J. S. (2007). Seasonal carbohydrate changes in dormant kiwifruit buds. *Acta Horticulturae*, *753*, 567-572. https://doi.org/10.17660/ActaHortic.2007.753.75

Richardson, A. C., Walton, E. F., Meekings, J. S., & Boldingh, H. L. (2010). Carbohydrate changes in kiwifruit buds during the onset and release from dormancy. *Scientia Horticulturae*, *124*(4), 463-468. https://doi.org/10.1016/j.scienta.2010.02.010

Rinne, P., Welling, A., Vahala, J., Ripel, L., Ruonala, R., Kangasjärvi, J., & van der Schoot, C. (2011). Chilling of dormant buds hyperinduces FLOWERING LOCUS T and recruits GA-inducible 1,3-β-Glucanases to reopen signal conduits and release dormancy in *Populus*. *The Plant Cell*, *23*(1), 130-146. https://doi.org/10.1105/tpc.110.081307

Rinne, P. L., Kaikuranta, P. M., & Van Der Schoot, C. (2001). The shoot apical meristem restores its symplasmic organization during chilling-induced release from dormancy. *The Plant Journal*, *26*(3), 249-264. https://doi.org/10.1046/j.1365-313x.2001.01022.x

Rossiter, K. L., Young, H., Walker, S. B., Miller, M., & Dawson, D. M. (2000). The effects of sugars and acids on consumer acceptability of kiwifruit. *Journal of Sensory Studies*, *15*(3), 241-250. https://doi.org/10.1111/j.1745-459X.2000.tb00269.x

Ruan, Y.-L., Jin, Y., Yang, Y.-J., Li, G.-J., & Boyer, J. S. (2010). Sugar input, metabolism, and signaling mediated by invertase: roles in development, yield potential, and response to drought and heat. *Molecular Plant*, *3*(6), 942-955. https://doi.org/10.1093/mp/ssq044

Sacalis, J., & Durkin, D. (1972). Movement of 14C in cut roses and carnations after uptake of 14C-sucrose. *Journal of the American Society for Horticultural Science*, *97*(1), 481-484. https://doi.org/10.21273/JASHS.99.1.96

Sakai, A., & Yoshida, S. (1968). The role of sugar and related compounds in variations of freezing resistance. *Cryobiology*, *5*(3), 160-174. https://doi.org/10.1016/S0011-2240(68)80161-0

Salinger, M. J., Kenny, G. J., & Morley-Bunker, M. J. (1993). Climate and kiwifruit cv. 'Hayward'. 1. Influences on development and growth. *New Zealand Journal of Crop and Horticultural Science*, *21*(3), 235-245. https://doi.org/10.1080/01140671.1993.9513775

Sauter, J. J. (1981a). Evidence for sucrose efflux and hexose uptake in the xylem of *Salix*. *Zeitschrift für Pflanzenphysiologie*, *103*(2), 183-187. https://doi.org/10.1016/S0044-328X(81)80150-X

Sauter, J. J. (1981b). Sucrose uptake in the xylem of *Populus*. *Zeitschrift für Pflanzenphysiologie*, *103*(2), 165-168. https://doi.org/10.1016/S0044-328X(81)80146-8

Sauter, J. J. (1983). Efflux and reabsorption of sugars in the xylem II. Seasonal changes in sucrose uptake in *Salix*. *Zeitschrift für Pflanzenphysiologie*, *111*(5), 429-440. https://doi.org/10.1016/S0044-328X(83)80007-5

Schindelin, J., Arganda-Carreras, I., Frise, E., Kaynig, V., Longair, M., Pietzsch, T., . . . Cardona, A. (2012). Fiji: an open-source platform for biological-image analysis. *Nature Methods*, *9*(7), 676-682. https://doi.org/10.1038/nmeth.2019

Schloerke, B., Cook, D., Larmarange, J., Briatte, F., Marbach, M., Thoen, E., . . . Crowley, C. (2024). *GGally: Extension to 'ggplot2'*. (Version 2.2.0) https://CRAN.R-project.org/package=GGally

Schmitt, B., Stadler, R., & Sauer, N. (2008). Immunolocalization of solanaceous SUT1 proteins in companion cells and xylem parenchyma: new perspectives for phloem loading and transport. *Plant Physiol*, *148*(1), 187-199. https://doi.org/10.1104/pp.108.120410

Schrader, S., & Sauter, J. J. (2002). Seasonal changes of sucrose-phosphate synthase and sucrose synthase activities in poplar wood (*Populus* × *canadensis* Moench <*robusta*>) and their possible role in carbohydrate metabolism. *Journal of Plant Physiology*, *159*(8), 833-843. https://doi.org/10.1078/0176-1617-00730

Seager, N. G., Hewett, E. W., & Warrington, I. J. (1995). Manipulation of carbohydrate concentrations in kiwifruit. *New Zealand Journal of Crop and Horticultural Science*, *23*(2), 213-218. https://doi.org/10.1080/01140671.1995.9513889

Seager, N. G., Warrington, I. J., & Hewett, E. W. (1996). Maturation of kiwifruit grown at different temperatures in controlled environments. *Journal of Horticultural Science*, *71*(4), 639-652. https://doi.org/10.1080/14620316.1996.11515444

Seal, A. G., & McKenzie, C. M. (2025). The effects of interploid pollination on seed development and fruit weight in *Actinidia chinensis* (kiwifruit). *The Journal of Horticultural Science and Biotechnology*, *100*(4), 437-457. https://doi.org/10.1080/14620316.2025.2464703

Secchi, F., & Zwieniecki, M. A. (2011). Sensing embolism in xylem vessels: the role of sucrose as a trigger for refilling. *Plant, Cell & Environment*, *34*(3), 514-524. https://doi.org/10.1111/j.1365-3040.2010.02259.x

Seleznyova, A. N., & Greer, D. H. (2001). Effects of temperature and leaf position on leaf area expansion of kiwifruit (*Actinidia deliciosa*) shoots: Development of a modelling framework. *Annals of Botany*, *88*(4), 605-615. https://doi.org/10.1006/anbo.2001.1513

Seleznyova, A. N., Thorp, T. G., Barnett, A. M., & Costes, E. (2002). Quantitative analysis of shoot development and branching patterns in *Actinidia*. *Annals of Botany*, *89*(4), 471-482. https://doi.org/10.1093/aob/mcf069

Signorelli, S., Shaw, J., Hermawaty, D., Wang, Z., Verboven, P., Considine, J., & Considine, M. (2019). The initiation of bud burst in grapevine features dynamic regulation of the apoplastic pore size. *Journal of Experimental Botany*, *71*. https://doi.org/10.1093/jxb/erz200

Słupianek, A., Dolzblasz, A., & Sokołowska, K. (2021). Xylem parenchyma—role and relevance in wood functioning in trees. *Plants*, *10*(6). https://doi.org/10.3390/plants10061247

Smith, G. S., Clark, C. J., & Boldingh, H. L. (1992). Seasonal accumulation of starch by components of the kiwifruit vine. *Annals of Botany*, *70*(1), 19-25. https://doi.org/10.1093/oxfordjournals.aob.a088434

Smith, G. S., Gravett, I. M., Edwards, C. M., Curtis, J. P., & Buwalda, J. G. (1994). Spatial analysis of the canopy of kiwifruit vines as it relates to the physical, chemical, and postharvest attributes of fruit. *Annals of Botany*, *73*, 99-111. https://doi.org/10.1006/anbo.1994.1012

Smith, J. P., & Holzapfel, B. P. (2009). Cumulative responses of Semillon grapevines to late season perturbation of carbohydrate reserve status. *American Journal of Enology and Viticulture*, *60*(4), 461-470. https://doi.org/10.5344/ajev.2009.60.4.461

Snelgar, W. P., Davy, M., Richardson, A. C., & R., P. H. (2002). An efficient sampling scheme for monitoring flowering of *Actinidia chinensis*. *New Zealand Journal of Crop and Horticultural Science*, *30*, 187-195. https://doi.org/10.1080/01140671.2002.9514214

Snelgar, W. P., Hopkirk, G., Seelye, R. J., Martin, P. J., & Manson, P. J. (1998). Relationship between canopy density and fruit quality of kiwifruit. *New Zealand Journal of Crop and Horticultural Science*, *26*(3), 223-232. https://doi.org/10.1080/01140671.1998.9514058

Snelgar, W. P., & Manson, P. J. (1992). Determination of the time of flower evocation in kiwifruit vines. *New Zealand Journal of Crop and Horticultural Science*, *20*(4), 439-447. https://doi.org/10.1080/01140671.1992.10418062

Snelgar, W. P., Manson, P. J., & Hopkirk, G. (1991). Effect of overhead shading on fruit size and yield potential of kiwifruit (*Actinidia deliciosa*). *Journal of Horticultural Science*, *66*(3), 261-273. https://doi.org/10.1080/00221589.1991.11516153

Snelgar, W. P., Manson, P. J., & Martin, P. J. (1992a). Influence of time of shading on flowering and yield of kiwifruit vines. *Journal of Horticultural Science*, *67*(4), 481-487. https://doi.org/10.1080/00221589.1992.11516273

Snelgar, W. P., Manson, P. J., & McPherson, H. G. (1997). Evaluating winter chilling of kiwifruit using excised canes. *Journal of Horticultural Science*, *72*(2), 305-315. https://doi.org/10.1080/14620316.1997.11515517

Snelgar, W. P., Martin, P. J., & Manson, P. J. (1992b). Influence of shelterbelts on pollination of kiwifruit. *Acta Horticulturae*, *297*, 263-268. https://doi.org/10.17660/ActaHortic.1992.297.34

Snelgar, W. P., Minchin, P. E. H., & Blattmann, P. (2005). Altering growth and maturation of *Actinidia chinensis* 'Hort16A' fruit by heating individual berries. *Journal of Horticultural Science and Biotechnology*, *80*(6), 779-785. https://doi.org/10.1080/14620316.2005.11512014

Snelgar, W. P., Minchin, P. E. H., Blattmann, P., & Hall, A. J. (2012). Sink priority on 'Hayward' kiwifruit vines. *New Zealand Journal of Crop and Horticultural Science*, *40*(4), 253-263. https://doi.org/10.1080/01140671.2012.681386

Snelgar, W. P., & Thorp, T. G. (1988). Leaf area, final fruit weight and productivity in kiwifruit. *Scientia Horticulturae*, *36*(3-4), 241-249. https://doi.org/10.1016/0304-4238(88)90058-1

Snelgar, W. P., Thorp, T. G., & Patterson, K. J. (1986). Optimal leaf:fruit ratios for fruit growth in kiwifruit. *Acta Horticulturae*, *175*, 115-120. https://doi.org/10.17660/ActaHortic.1986.175.17

Snowball, A. (1997a). Excised canes are a suitable test system for the study of budbreak and flowering of kiwifruit canes. *New Zealand Journal of Crop and Horticultural Science*, *25*(2), 141-148. https://doi.org/10.1080/01140671.1997.9514000

Snowball, A. (1997b). Seasonal cycle of shoot development in selected *Actinidia* species. *New Zealand Journal of Crop and Horticultural Science*, *25*(3), 221-231. https://doi.org/10.1080/01140671.1997.9514011

Snowball, A. M. (1995). The seasonal cycle of leaf, shoot and bud development in kiwifruit. *Journal of Horticultural Science*, *70*(5), 787-797. https://doi.org/10.1080/14620316.1995.11515353

Snowball, A. M. (1996). The timing of flower evocation in kiwifruit. *Journal of Horticultural Science*, *71*(2), 335-347. https://doi.org/10.1080/14620316.1996.11515413

Snowball, A. M., & Considine, J. A. (1986). Flowering in kiwifruit (*Actinidia deliciosa* Liang et Ferguson): positional effects and development. *Acta Horticulturae*, *175*, 85-89. https://doi.org/10.17660/ActaHortic.1986.175.12

Snowball, A. M., Smith, R. C., & Considine, J. A. (1996). Flowering and fruiting rootless cuttings of kiwifruit. *New Zealand Journal of Crop and Horticultural Science*, *24*(4), 355-360. https://doi.org/10.1080/01140671.1996.9513972

Spadaro, D., Galliano, A., Pellegrino, C., Gilardi, G., Garibaldi, A., & Gullino, M. L. (2010). Dry matter, mineral composition, and commercial storage practices influence the development of skin pitting caused by *Cadophora luteo-olivacea* on kiwifruit 'Hayward'. *Journal of Plant Pathology*, *92*(2), 349-356. https://www.jstor.org/stable/41998808

Spencer, S., & Couvillon, G. A. (1975). The relationship of node position to bloom date, fruit size, and endosperm development of the peach, *Prunus persica* (L.) Batsch cv. Sullivan's Elberta. *Journal of the American Society for Horticultural Science*, *100*(3), 242-244. https://doi.org/10.21273/jashs.100.3.242

Spoehr, H. A. (1942). The culture of albino maize. *Plant Physiology*, *17*(3), 397-410. https://doi.org/10.1104/pp.17.3.397

Stats NZ. (2025). *Overseas merchandise trade: September 2025*. Stats NZ. https://www.stats.govt.nz/information-releases/overseas-merchandise-trade-september-2025/

Stephenson, A. G. (1981). Flower and fruit abortion: proximate causes and ultimate functions. *Annual Review of Ecology and Systematics*, *12*, 253-279. https://doi.org/10.1146/annurev.es.12.110181.001345

Sullivan, D. (1965). The effect of time of bloom of individual flowers on the size, shape and maturity of apple fruits. *Proceedings of the American Society for Horticultural Science*, *87*, 41–46

Sun, S., Fang, J., Lin, M., Qi, X., Chen, J., Wang, R., . . . Muhammad, A. (2020). Freezing tolerance and expression of β-amylase gene in two *Actinidia arguta* cultivars with seasonal changes. *Plants*, *9*(4), 515. https://doi.org/10.3390/plants9040515

Swanson, C., & El-Shishiny, E. (1958). Translocation of sugars in the concord grape. *Plant Physiology*, *33*(1), 33. https://doi.org/10.1104/pp.33.1.33

Testolin, R. (1991). Male density and arrangement in kiwifruit orchards. *Scientia Horticulturae*, *48*(1), 41-50. https://doi.org/10.1016/0304-4238(91)90151-N

Thorp, G., Barnett, A. M., Blattmann, M., Hedderley, D., & Mayston, R. (2018). Optimising vine management to increase yields and improve quality of Zespri ® SunGold kiwifruit (*Actinidia chinensis* var. *chinensis* 'Zesy002'). *Acta Horticulturae*, 397-404. https://doi.org/10.17660/ActaHortic.2018.1218.55

Thorp, T. G., Barnett, A. M., & Miller, S. A. (2003). Effects of cane size and pruning system on shoot growth, flowering and productivity of 'Hayward' kiwifruit vines. *The Journal of Horticultural Science and Biotechnology*, *78*(2), 219-224. https://doi.org/10.1080/14620316.2003.11511609

Thorpe, M., Minchin, P., Gould, N., & McQueen, J. (2005). The stem apoplast: a potential communication channel in plant growth regulation. In N. M. Holbrook & M. A. Zwieniecki (Eds.), *Vascular transport in plants* (pp. 201-220). Elsevier. https://doi.org/10.1016/B978-012088457-5/50012-5

Tixier, A., Gambetta, G. A., Godfrey, J., Orozco, J., & Zwieniecki, M. A. (2019). Non-structural carbohydrates in dormant woody perennials; the tale of winter survival and spring arrival. *Frontiers in Forests and Global Change*, *2*, 18. https://doi.org/10.3389/ffgc.2019.00018

Tixier, A., Roxas, A. A., Godfrey, J., Saa, S., Lightle, D., Maillard, P., . . . Zwieniecki, M. A. (2017). Role of bark color on stem temperature and carbohydrate management during dormancy break in persian walnut. *Journal of the American Society for Horticultural Science*, *142*(6), 454-463. https://doi.org/10.21273/JASHS04216-17

Tombesi, A., Antognozzi, E., & Palliotti, A. (1993). Influence of assimilate availability on translocation and sink strength in kiwifruit. *New Zealand Journal of Crop and Horticultural Science*, *21*(2), 177-182. https://doi.org/10.1080/01140671.1993.9513765

Tylewicz, S., Petterle, A., Marttila, S., Miskolczi, P., Azeez, A., Singh, R. K., . . . Eklund, D. M. (2018). Photoperiodic control of seasonal growth is mediated by ABA acting on cell-cell communication. *Science*, *360*(6385), 212-215. https://doi.org/10.1126/science.aan8576

van Bel, A. J. E. (1990). Xylem–phloem exchange via the rays: the undervalued route of transport. *Journal of Experimental Botany*, *41*(6), 631-644. https://doi.org/10.1093/jxb/41.6.631

van Bel, A. J. E. (2006). Sieve-pore plugging mechanisms. In *Cell-Cell Channels* (pp. 113-118). Springer New York. https://doi.org/10.1007/978-0-387-46957-7_7

Vanneste, J. L. (2012). Pseudomonas syringae pv. actinidiae (Psa): a threat to the New Zealand and global kiwifruit industry. *New Zealand Journal of Crop & Horticultural Science*, *40*(4), 265-267. https://doi.org/10.1080/01140671.2012.736084

Varkonyi-Gasic, E. (2018). Regulation of flowering in kiwifruit. *Acta Horticulturae*, *1218*, 129-134. https://doi.org/10.17660/ActaHortic.2018.1218.16

Varkonyi-Gasic, E., Moss, S. M. A., Voogd, C., Wang, T., Putterill, J., & Hellens, R. P. (2013). Homologs of FT, CEN and FD respond to developmental and environmental signals affecting growth and flowering in the perennial vine kiwifruit. *New Phytologist*, *198*(3), 732-746. https://doi.org/https://doi.org/10.1111/nph.12162

Vattiprolu, N. M. R., Woolley, D. J., & van Hooijdonk, B. M. (2011). Hormonal control of vegetative vigour in kiwifruit vines. *Acta Horticulturae*, *913*, 425-431. https://doi.org/10.17660/ActaHortic.2011.913.57

Velemis, D., Vasilakakis, M., & Manolakis, E. (1997). Effect of dry matter content of the kiwifruit at harvest on storage performance and quality. *Acta Horticulturae*, *444*, 637-642. https://doi.org/10.17660/ActaHortic.1997.444.98

Vogelmann, T. C., Dickson, R. E., & Larson, P. R. (1985). Comparative distribution and metabolism of xylem-borne amino compounds and sucrose in shoots of *Populus deltoides*. *Plant Physiology*, *77*(2), 418-428. https://doi.org/10.1104/pp.77.2.418

Volz, R. K., Gibbs, H. M., & Lupton, G. B. (1992). Variation in fruitfulness among kiwifruit replacement canes. *Acta Horticulturae*, *297*, 443-450. https://doi.org/10.17660/ActaHortic.1992.297.58

von Bennewitz, E., Suazo, S., Keutgen, A. J., Lošák, T., & Carrasco-Benavides, M. (2019). Seasonal root, shoot, and fruit growth patterns in kiwifruit (*Actinidia deliciosa* A. Chev.) in central Chile. *Erwerbs-Obstbau*, *61*(3), 283-292. https://doi.org/10.1007/s10341-019-00429-1

Voogd, C., Brian, L. A., Wu, R., Wang, T., Allan, A. C., & Varkonyi-Gasic, E. (2021). A MADS-box gene with similarity to FLC is induced by cold and correlated with epigenetic changes to control budbreak in kiwifruit. *New Phytologist*. https://doi.org/10.1111/nph.17916

Walton, E. F., & Fowke, P. J. (1993). Effect of hydrogen cyanamide on kiwifruit shoot flower number and position. *Journal of Horticultural Science*, *68*(4), 529-534. https://doi.org/10.1080/00221589.1993.11516381

Walton, E. F., Fowke, P. J., Weis, K., & McLeay, P. L. (1997). Shoot axillary bud morphogenesis in kiwifruit (*Actinidia deliciosa*). *Annals of Botany*, *80*(1), 13-21. https://doi.org/10.1006/anbo.1996.0381

Walton, E. F., Podivinsky, E., & Wu, R. M. (2001). Bimodal patterns of floral gene expression over the two seasons that kiwifruit flowers develop. *Physiologia Plantarum*, *111*(3), 396-404. https://doi.org/10.1034/j.1399-3054.2001.1110318.x

Wan, X., Zou, L.-H., Pan, X., Ge, Y., Jin, L., Cao, Q., . . . Tian, D. (2024). Auxin and carbohydrate control flower bud development in *Anthurium andraeanum* during early stage of sexual reproduction. *BMC Plant Biology*, *24*(1), 159. https://doi.org/10.1186/s12870-024-04869-0

Wardlaw, I. F. (1968). The control and pattern of movement of carbohydrates in plants. *The Botanical Review*, *34*(1), 79-105. https://doi.org/10.1007/BF02858622

Wardlaw, I. F. (1990). The control of carbon partitioning in plants. *New Phytologist*, *116*(3), 341-381. https://doi.org/10.1111/j.1469-8137.1990.tb00524.x

Watson, M., & Gould, K. S. (1994). Development of flat and fan-shaped fruit in *Actinidia chinensis* var *chinensis* and *Actinidia deliciosa*. *Annals of Botany*, *74*(1), 59-68. https://doi.org/10.1093/aob/74.1.59

Watson, M. A., & Casper, B. B. (1984). Morphogenetic constraints on patterns of carbon distribution in plants. *Annual Review of Ecology and Systematics*, *15*(1), 233-258. https://doi.org/10.1146/annurev.es.15.110184.001313

Wei, T., & Simko, V. (2017). *R package "corrplot": Visualization of a correlation matrix*. (Version 0.95) https://github.com/taiyun/corrplot

White, A. C., Rogers, A., Rees, M., & Osborne, C. P. (2016). How can we make plants grow faster? A source–sink perspective on growth rate. *Journal of Experimental Botany*, *67*(1), 31-45. https://doi.org/10.1093/jxb/erv447

Wickham, H. (2016). *ggplot2: Elegant graphics for data analysis* (2nd ed.). Springer-Verlag New York. https://doi.org/10.1007/978-3-319-24277-4

Wickham, H., François, R., Henry, L., & Müller, K. (2024). *dplyr: A grammar of data manipulation*. (Version 1.1.4) R Foundation for Statistical Computing. https://CRAN.R-project.org/package=dplyr

Wilson, G. (1989). Self-terminating canes are inferior. *New Zealand Kiwifruit*, 6

Woodward, T., J. (2006). *Variation in 'Hayward' kiwifruit quality characteristics* [Doctoral dissertation, University of Waikato]. Hamilton, New Zealand. https://researchcommons.waikato.ac.nz/server/api/core/bitstreams/0a2eb1e0-d872-4f7d-af70-dc9289c3911c/content

Woodward, T. J., & Clearwater, M. J. (2008). Relationships between 'Hayward' kiwifruit weight and dry matter content. *Postharvest Biology and Technology*, *48*(3), 378-382. https://doi.org/10.1016/j.postharvbio.2007.09.003

Wu, B. H., Mimoun, M. B., Génard, M., Lescourret, F., Besset, J., & Bussi, C. (2005). Peach fruit growth in relation to the leaf-to-fruit ratio, early fruit size and fruit position. *The Journal of Horticultural Science and Biotechnology*, *80*(3), 340-345. https://doi.org/10.1080/14620316.2005.11511941

Xie, Z., Forney, C. F., & Bondada, B. (2018). Renewal of vascular connections between grapevine buds and canes during bud break. *Scientia Horticulturae*, *233*, 331-338. https://doi.org/10.1016/j.scienta.2018.02.019

Xiloyannis, C., Massai, R., Piccotino, D., Raffaelli, M., & Bovo, M. (1997). Effects of cropload on annual growth and dry matter partitioning in young kiwi vines. *Acta Horticulturae*, *444*, 213-218. https://doi.org/10.17660/ActaHortic.1997.444.31

Yoshioka, H. (1986). Translocation and distribution of photosynthates in tomato plants. *Japan Agricultural Research Quarterly*, *19*(4), 266-270. https://www.jircas.go.jp/en/publication/jarq/19/4/266

Yu-Ping, M., Yan-Chang, W., Zuo-Zhou, L., Zheng-Wang, J., Hong-Li, Y., Jun-Jie, G., . . . Zhong-Yan, W. (2015). High-temperature inhibition of biosynthesis and transportation of anthocyanins results in the poor red coloration in red-fleshed *Actinidia chinensis*. *Physiologia Plantarum*, *153*(4), 565-583. https://doi.org/10.1111/ppl.12263

Yu, D. J., Hwang, J. Y., Chung, S. W., Oh, H. D., Yun, S. K., & Lee, H. J. (2017). Changes in cold hardiness and carbohydrate content in peach (*Prunus persica*) trunk bark and wood tissues during cold acclimation and deacclimation. *Scientia Horticulturae*, *219*, 45-52. https://doi.org/10.1016/j.scienta.2017.02.038

Zavaliev, R., & Epel, B. L. (2015). Imaging callose at plasmodesmata using aniline blue: quantitative confocal microscopy. *Plasmodesmata: methods and protocols*, *1217*, 105-119. https://doi.org/10.1007/978-1-4939-1523-1_7

Zespri Group, L. (2025). *2025 Gold3 Variety Information Guide*. https://canopy.zespri.com/content/dam/new-canopy/nz/en/documents/basic/business/licenses/buying-licence/2025/Zespri-2025-GVIG.pdf

Zespri Group Limited. (2025). *Zespri Annual Report 2024/25*. https://canopy.zespri.com/content/dam/new-canopy/nz/en/documents/public/about/annual-report/Annual-Report-2024-25.pdf

Zhang, G., Mao, Z., Fortunel, C., Martínez-Vilalta, J., Viennois, G., Maillard, P., & Stokes, A. (2022). Parenchyma fractions drive the storage capacity of nonstructural carbohydrates across a broad range of tree species. *Am J Bot*, *109*(4), 535-549. https://doi.org/10.1002/ajb2.1838

Zhang, Y.-L., Gessler, A., Lehmann, M. M., Saurer, M., Diao, H., Lambers, J. H. R., . . . Li, M.-H. (2025a). Trees use exogenous sugars for growth, but excess triggers negative feedback reducing photosynthetic carbon gain. *Tree Physiology*, *45*(9). https://doi.org/10.1093/treephys/tpaf092

Zhang, Y.-L., Gessler, A., Lehmann, M. M., Schaub, M., Saurer, M., Rigling, A., & Li, M.-H. (2025b). Exogenous sugar addition can exacerbate root carbon limitation in trees. *New Phytologist*, *247*(2), 577-594. https://doi.org/https://doi.org/10.1111/nph.70231

Zhao, Y., Ma, Y., Qiu, H., Zhou, L., He, K., & Ye, Y. (2025). Wake up: the regulation of dormancy release and bud break in perennial plants. *Frontiers in Plant Science*, *Volume 16 - 2025*. https://doi.org/10.3389/fpls.2025.1553953

Zhou, X., Dutilleul, P., MacKenzie, A., Madramootoo, C., & Smith, D. (1997). Effects of stem-injected sucrose on grain production, dry matter distribution, and chlorophyll fluorescence of field-grown corn plants. *Journal of Agronomy and Crop Science*, *178*(2), 65-71. https://doi.org/10.1111/j.1439-037X.1997.tb00352.x

Zinselmeier, C., Lauer, M. J., & Boyer, J. S. (1995). Reversing drought-induced losses in grain yield: Sucrose maintains embryo growth in maize. *Crop Science*, *35*(5), 1390-1400. https://doi.org/10.2135/cropsci1995.0011183X003500050022x

Zupančič, K., Zupančič, L., Bitežnik, L., Malík, M., Lenarčič, D., & Flajšman, M. (2025). Enhancing yield of cannabis inflorescences and cannabinoids through plant stem infusion of sucrose: a novel cannabis cultivation approach. *Industrial Crops and Products*, *228*, 120880. https://doi.org/10.1016/j.indcrop.2025.120880

Zwieniecki, M. A., Tixier, A., & Sperling, O. (2015). Temperature-assisted redistribution of carbohydrates in trees. *American Journal of Botany*, *102*(8), 1216-1218. https://doi.org/10.3732/ajb.1500218

# Appendix A

| ♂ | ♀ | ♂ | ♀ | ♂ |
|---|---|---|---|---|
| | 26 | | 25 | |
| | 27 | | 24 | |
| | X | | X | |
| | 28 | | 23 | |
| | 29 | | 22 | |
| | X | | 21 | |
| | 30 | | 20 | |
| | 31 | | 19 | |
| | 32 | | X | |
| | X | | 18 | |
| | 33 | | 17 | |
| | 34 | | 16 | |
| | 35 | | X | |
| | X | | 15 | |
| | 36 | | 14 | |
| | 37 | | X | |
| | 38 | | 13 | |
| | X | | 12 | |
| | 39 | | X | |
| | X | | 11 | |
| | 40 | | 10 | |
| | X | | 9 | |
| | 41 | | X | |
| | X | | 8 | |
| | X | | 7 | |
| | X | | 6 | |
| | 42 | | 5 | |
| | X | | X | |
| | 43 | | 4 | |
| | X | | 3 | |
| | 44 | | 2 | |
| | 45 | | 1 | |

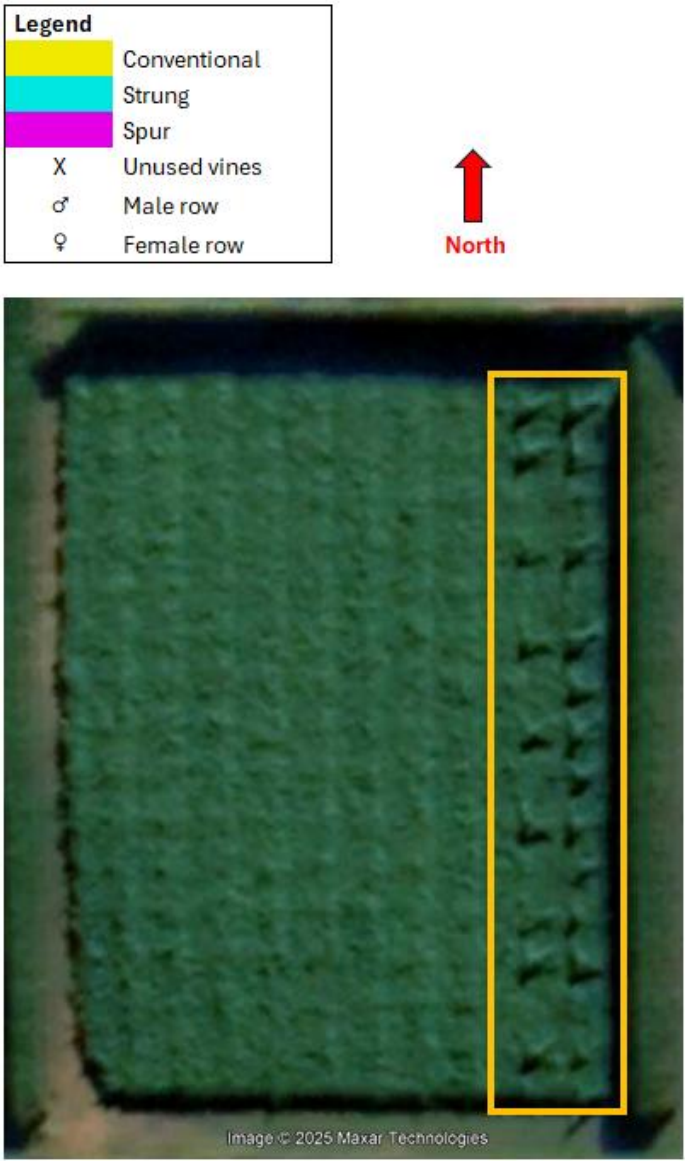


Figure A1: Orchard plan for *Actinidia chinensis* 'Zesy002' vines used in Chapter 2. Left, the entire fruit and shoot populations of vines 37-45 (bolded) were studied to determine the contribution of measured predictors on fruit fresh weight and dry matter content and how this differs in relation to three canopy management treatments (conventional replacement canes, strung replacement canes, and spur pruning). Treatments were randomly assigned within statistical blocks of three vines, and all vines were in their third consecutive season of these specific canopy management treatments. Female vines footprints were approximately 19.2 m² (3 m x 6.4 m). Female rows were alternated with rows of compactly pruned *A. chinensis* var. *chinensis* 'M33' and *A. chinensis* var. *chinensis* 'M91' male vines. Unused vines were excluded from the trial to avoid shading from stringing replacement canes, or because of visible vine health or structural issues. Right, the treatment rows (highlighted in orange) were part of an orchard block located near Paengaroa, Bay of Plenty, New Zealand. Distinct shadows are from long shoots trained up strings in strung treatment vines. Image sourced from Google Earth © 2025 Maxar Technologies.

Table A1. Harvest dates and summary statistics for nine whole-vine fruit populations of 'Zesy002' kiwifruit from three canopy management treatments. SD = standard deviation, CV = co-efficient of variation. Vine numbers refer to the block plan in Appendix Figure A1.

| Vine # | Treatment | Harvest date | Fruit count | Fresh weight (g) | | | | | Dry matter content (%) | | | | |
|---|---|---|---|---|---|---|---|---|---|---|---|---|---|
| | | | | Mean | SD | CV | Skew | Kurtosis | Mean | SD | CV | Skew | Kurtosis |
| 45 | Conventional | 24/03/2020 | 769 | 126.9 | 19.4 | 15.3 | -0.13 | -0.05 | 18.92 | 0.92 | 4.85 | -0.11 | 0.10 |
| 42 | Conventional | 29/04/2020 | 1098 | 122.3 | 20.3 | 16.7 | 0.13 | 0.61 | 18.33 | 1.02 | 5.57 | -0.41 | 0.69 |
| 37 | Conventional | 08/05/2020 | 1013 | 117.0 | 17.0 | 14.6 | 0.07 | 0.39 | 18.57 | 0.86 | 4.65 | 0.06 | 0.06 |
| | | | Mean | **122.1** | **18.9** | **15.5** | **0.02** | **0.32** | **18.61** | **0.93** | **5.02** | **-0.15** | **0.28** |
| | | | | | | | | | | | | | |
| 44 | Strung | 24/03/2020 | 1038 | 118.4 | 16.8 | 14.2 | -0.08 | 0.12 | 18.46 | 0.99 | 5.37 | -0.36 | 0.92 |
| 40 | Strung | 01/05/2020 | 1125 | 113.2 | 17.6 | 15.5 | 0.25 | 0.55 | 18.37 | 1.10 | 5.99 | 0.16 | 0.04 |
| 38 | Strung | 06/05/2020 | 1260 | 111.2 | 20.3 | 18.2 | 0.41 | 1.20 | 18.45 | 1.12 | 6.08 | -0.28 | 0.53 |
| | | | Mean | **114.3** | **18.2** | **16.0** | **0.19** | **0.62** | **18.43** | **1.07** | **5.81** | **-0.16** | **0.50** |
| | | | | | | | | | | | | | |
| 43 | Spur | 24/03/2020 | 1015 | 121.8 | 20.2 | 16.6 | -0.08 | -0.06 | 16.97 | 0.97 | 5.74 | -0.16 | 1.70 |
| 41 | Spur | 30/04/2020 | 1310 | 114.8 | 20.2 | 17.6 | 0.30 | 0.20 | 18.75 | 1.19 | 6.36 | 0.28 | 0.26 |
| 39 | Spur | 07/05/2020 | 1223 | 116.6 | 18.2 | 15.6 | 0.01 | -0.30 | 18.60 | 0.89 | 4.79 | -0.22 | 0.67 |
| | | | **Mean** | **117.7** | **19.5** | **16.6** | **0.08** | **-0.05** | **18.11** | **1.02** | **5.63** | **-0.03** | **0.88** |
| | | | | | | | | | | | | | |
| | | | **Grand Mean** | **118.0** | **18.9** | **16.0** | **0.10** | **0.30** | **18.38** | **1.01** | **5.49** | **-0.12** | **0.55** |

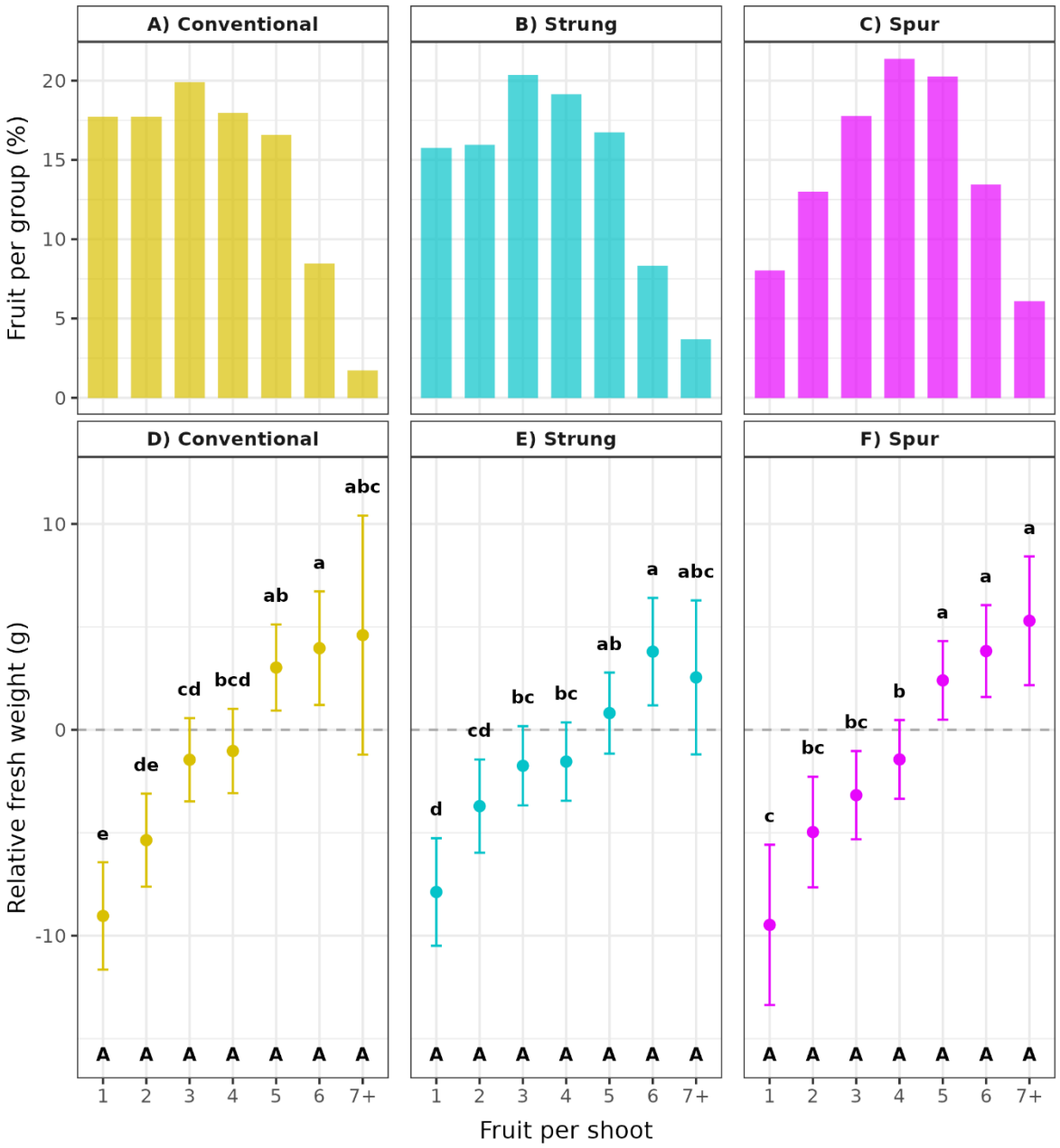


Figure A2. Distribution of fruit per shoot and model-estimated effects on fruit fresh weight in *Actinidia chinensis* 'Zesy002'. Panels A–C show the distribution of shoots bearing each number of fruit, expressed as the percentage of total shoots within each treatment. Panels D–F display estimated marginal means for fruit fresh weight (centred on the vine mean) at harvest, derived from a linear mixed-effects model. Fruit per shoot ≥7 have been pooled due to limited replication. Lowercase letters above points denote statistically significant differences between fruit per shoot categories within treatment panel, while uppercase letters along the x-axis indicate significant differences between treatments for a given fruit per shoot category. Means that do not share a letter were significantly different (Šidák adjusted $\alpha = 0.05$). Error bars represent 95% confidence intervals.

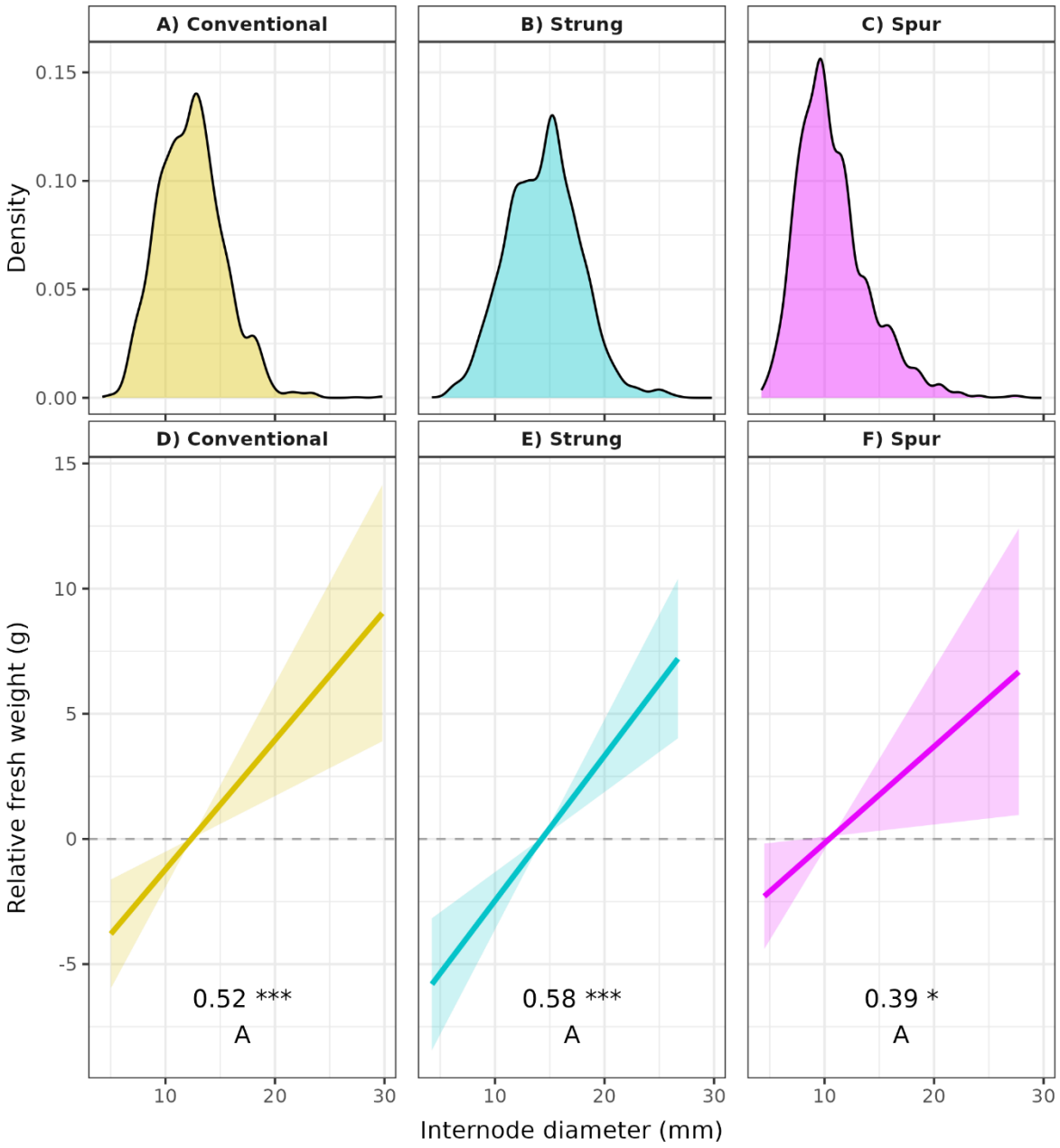


Figure A3. Distribution and model-estimated effect of internode diameter on fruit fresh weight in *Actinidia chinensis* 'Zesy002'. Internode diameter was measured at the proximal internode of each shoot (i.e., the internode closest to the trunk). Panels A–C show the distribution of internode basal diameters for each canopy management treatment, expressed as kernel density plots of all measured fruit. Panels D–F display fitted relationships between shoot diameter (mm) and fruit fresh weight (centred on the vine mean) at harvest, based on estimated marginal trends from a linear mixed-effects model. Slopes represent the expected increase in relative fruit fresh weight per millimetre increase in shoot diameter, after adjusting for other covariates in the model. Shaded ribbons indicate 95% confidence intervals. Numeric values within each panel indicate the estimated slope and its significance level (* $p<0.05$; *** $p < 0.001$), while uppercase letters below the slope denote differences in the slope between treatments. Slopes that do not share a letter were significantly different (Šidák corrected $\alpha = 0.05$).

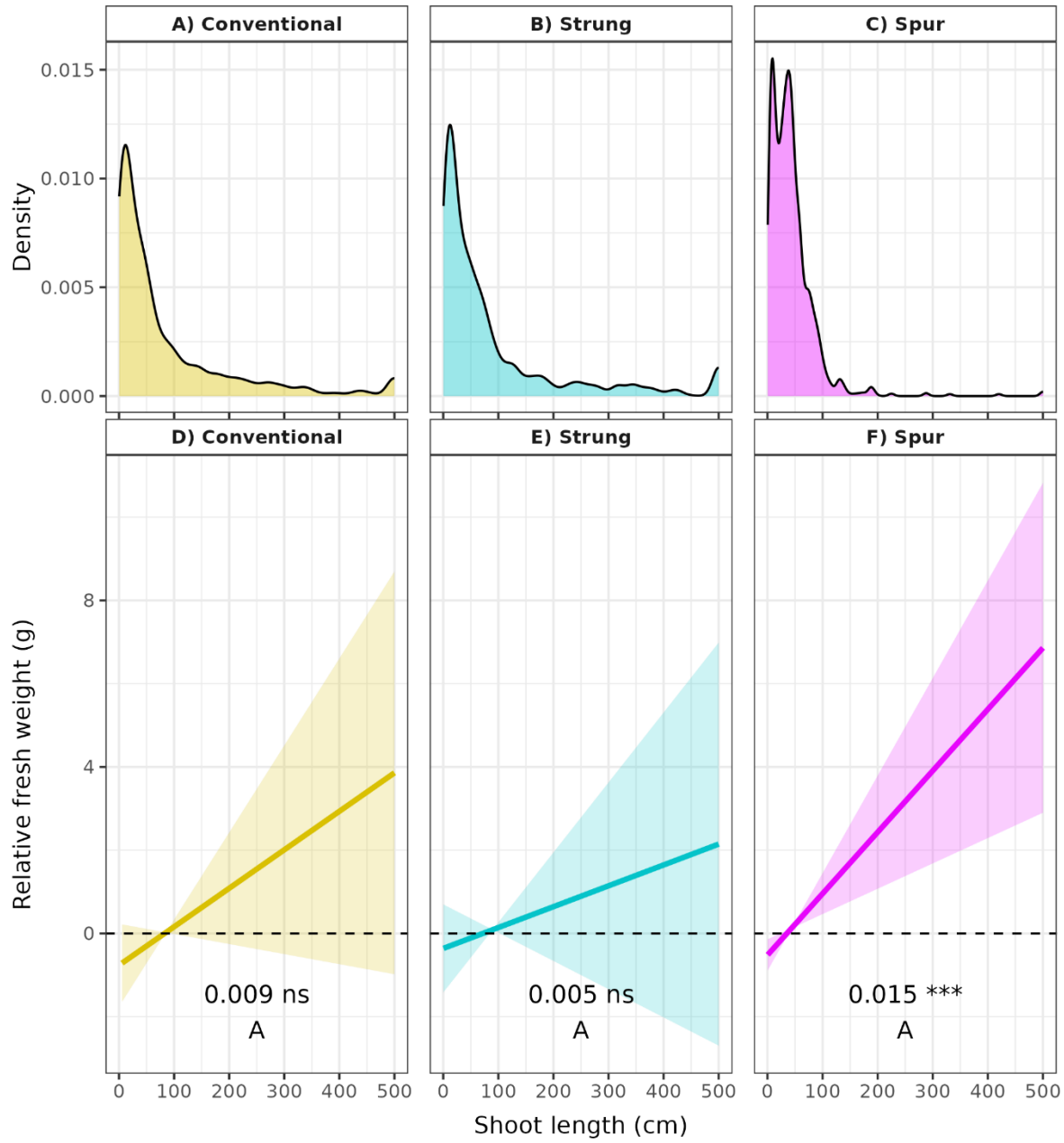


Figure A4. Distribution and model-estimated effect of shoot length on fruit fresh weight in *Actinidia chinensis* 'Zesy002'. Shoot length was measured after harvest and only includes the primary shoot axis (i.e. excludes secondary growth). Shoots longer than 500 cm were not measured in full. Panels A–C show the distribution of shoot lengths for each canopy management treatment (A: Conventional, B: Strung, C: Spur), expressed as kernel density plots of all measured fruit. Panels D–F display fitted relationships between shoot diameter (mm) and fruit fresh weight (centred on the vine mean) at harvest, based on estimated marginal trends from a linear mixed-effects model. Slopes represent the expected increase in relative fruit fresh weight per centimetre increase in shoot length, after adjusting for other covariates in the model. Shaded ribbons indicate 95% confidence intervals. Numeric values within each panel indicate the estimated slope and its significance level (ns = non-significant, *** $p < 0.001$), while uppercase letters below the slope denote differences in the slope between treatments. Slopes that do not share a letter were significantly different (Šidák adjusted $\alpha = 0.05$).

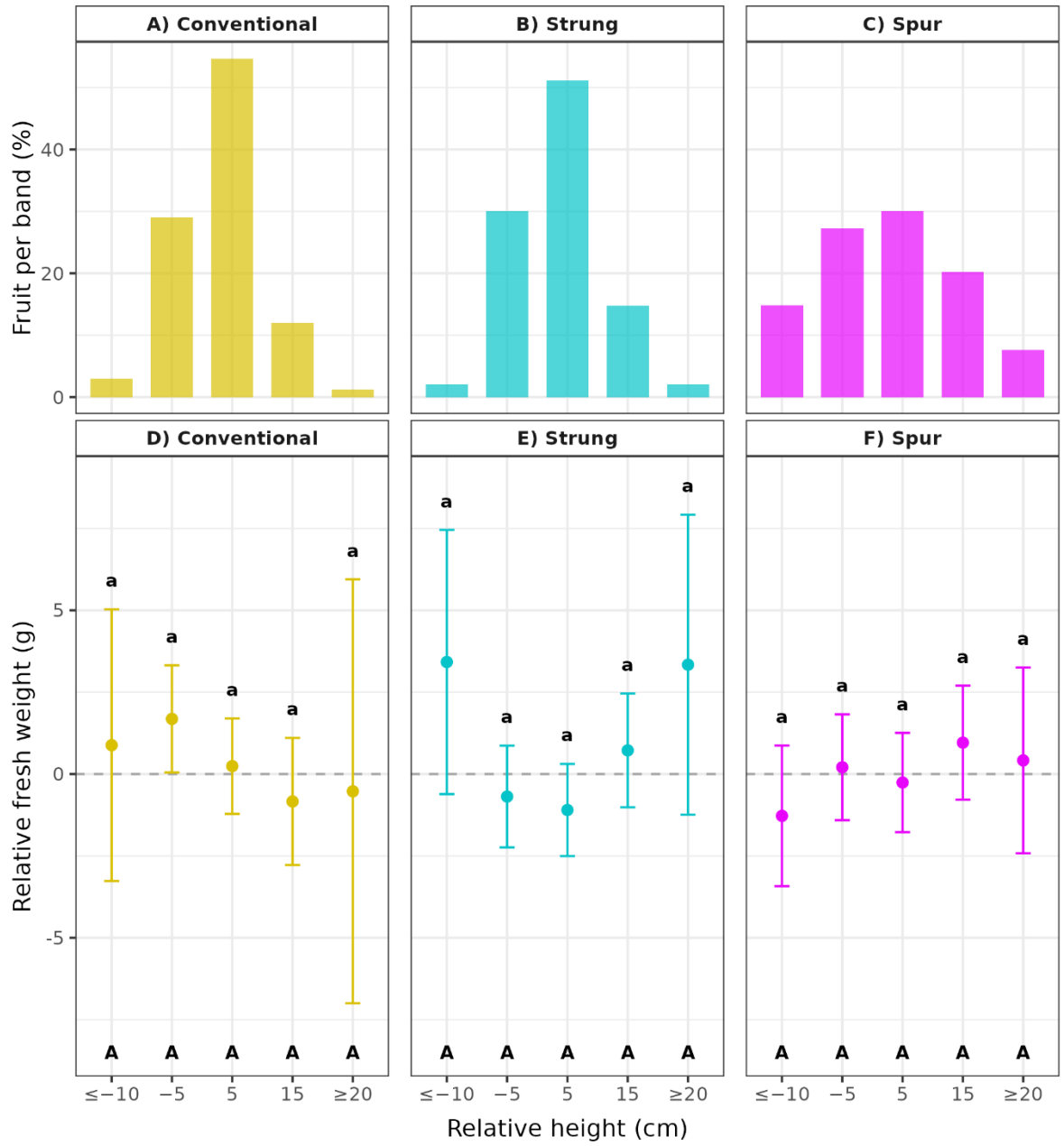


Figure A5. Distribution of relative height in the canopy and model-estimated effects on fruit relative fresh weight in *Actinidia chinensis* 'Zesy002'. Relative height was measured at the stylar end of the fruit and assigned to 10 cm bands (e.g. 5 cm = all fruit whose stylar ends were between 0 and 10 cm above the canopy wire). Fruit more than 10 cm below the canopy wires have been combined, as have all fruit 20 cm above the canopy wires. Panels A–C show the distribution of relative height in the canopy, expressed as the percentage of total fruit within each treatment. Panels D–F display estimated marginal means for fruit fresh weight (centred on the vine mean) at harvest, derived from a linear mixed-effects model that accounts for other measured shoot- and fruit-level covariates. Lowercase letters above points denote statistically significant differences between relative height groups within each treatment panel, while uppercase letters along the x-axis indicate significant differences between treatments for a given height group. Means that do not share a letter were significantly different (Šidák adjusted $\alpha = 0.05$). Error bars represent 95% confidence intervals.

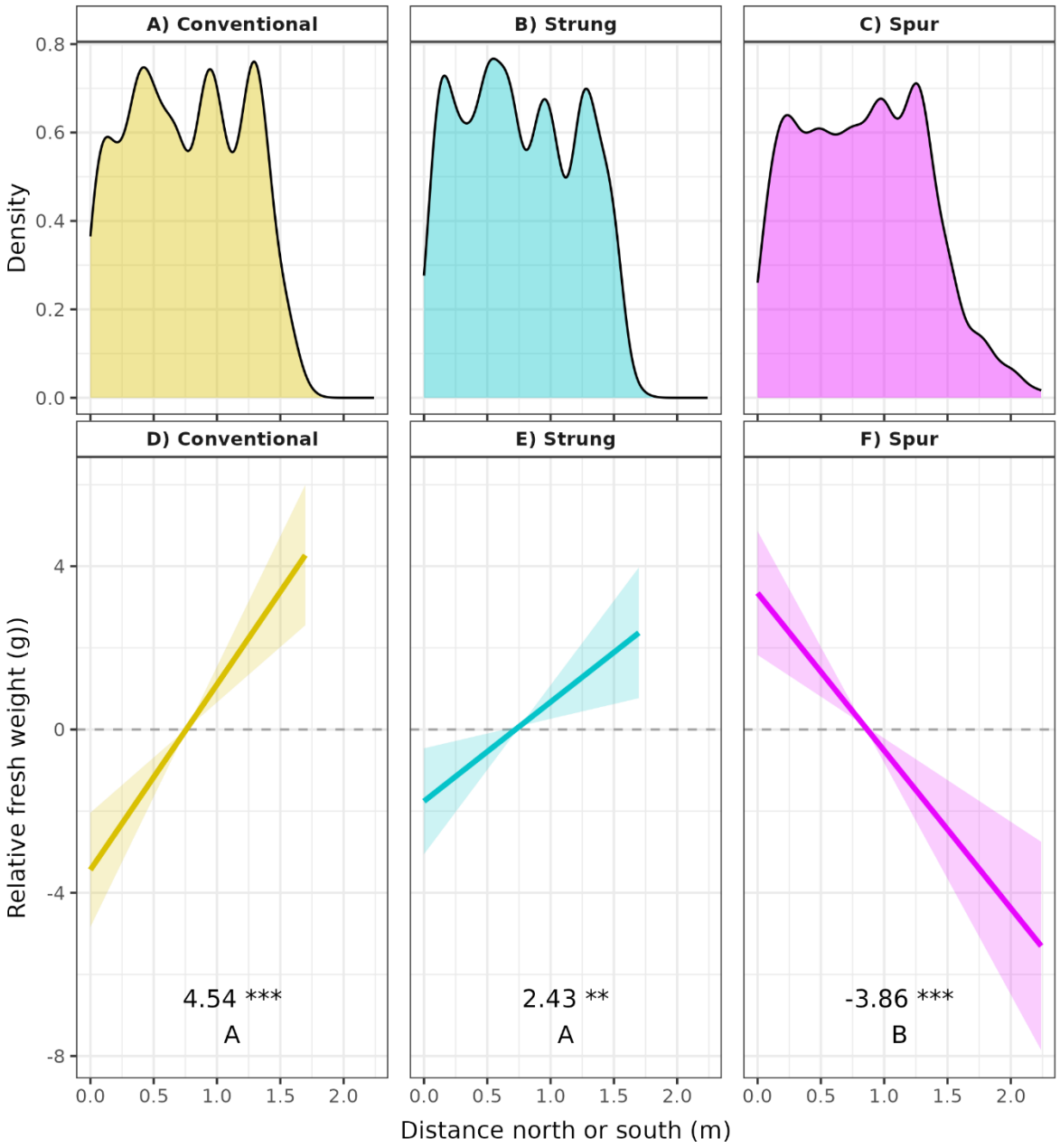


Figure A6. Distribution and model-estimated effect of fruit position along the north–south axis on fruit relative fresh weight in *Actinidia chinensis* 'Zesy002'. Panels A–C show the distribution of fruit across the canopy for each management treatment, expressed as kernel density plots of all measured fruit. Panels D–F display fitted relationships between distance north or south from the vine centre (in metres) and vine-mean centred fruit fresh weight (centred on the vine mean) at harvest, based on estimated marginal trends from a linear mixed-effects model. Slopes represent the expected increase in relative fruit fresh weight per metre north from the vine centre, after adjusting for other covariates in the model. Shaded ribbons indicate 95% confidence intervals. Numeric values within each panel indicate the estimated slope and its significance level (** $p<0.01$, *** $p < 0.001$), while uppercase letters below the slope denote differences in the slope between treatments. Slopes that do not share a letter were significantly different (Šidák adjusted $\alpha = 0.05$).

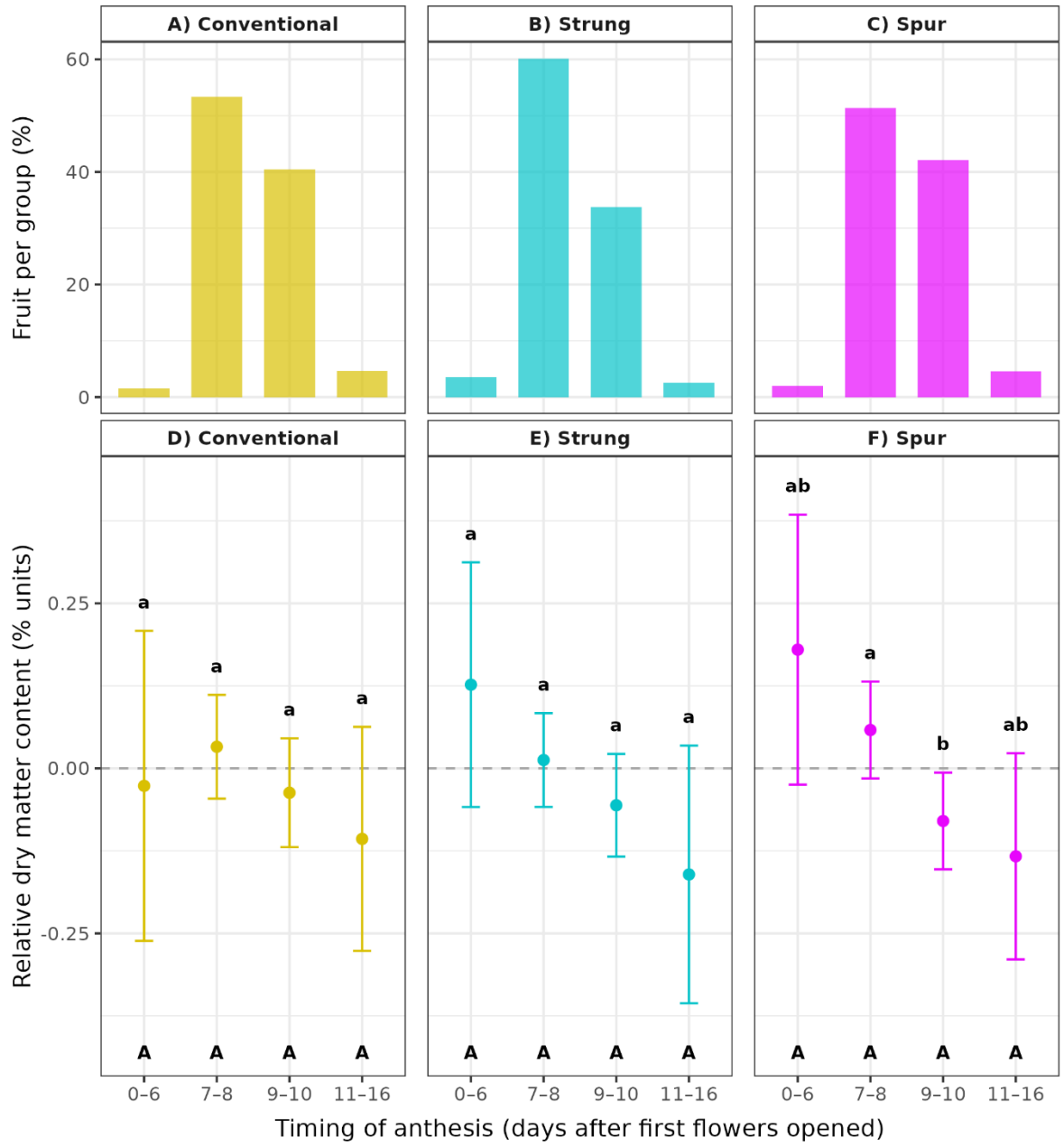


Figure A7. Distribution of anthesis timing and model-estimated effects on fruit relative dry matter content in *Actinidia chinensis* 'Zesy002'. Panels A–C show the distribution of anthesis dates, grouped into four timing bands, expressed as the percentage of total fruit within each treatment. Panels D–F display estimated marginal means for fruit dry matter content (centred on the vine mean) at harvest, derived from a linear mixed-effects model that accounts for other measured shoot- and fruit-level covariates. Lowercase letters above points denote statistically significant differences between anthesis timing bands within each treatment panel, while uppercase letters along the x-axis indicate significant differences between treatments for a given anthesis band. Means that do not share a letter were significantly different (Šidák adjusted ($\alpha = 0.05$). Error bars represent 95% confidence intervals. Day 0 of anthesis was 27/11/2019.

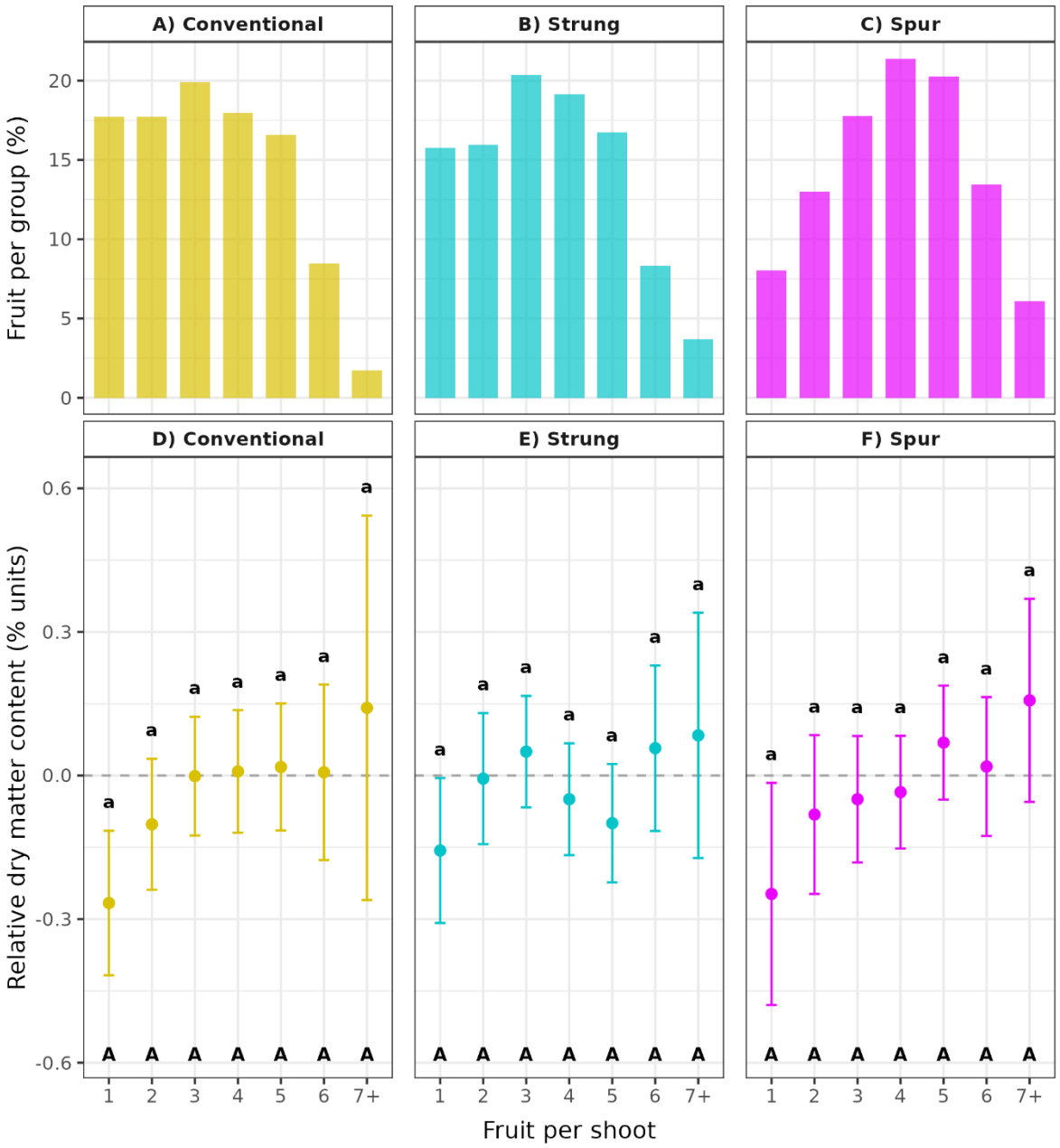


Figure A8. Distribution of fruit per shoot and model-estimated effects on fruit relative dry matter content in *Actinidia chinensis* 'Zesy002'. Panels A–C show the distribution of shoots bearing each number of fruit, expressed as the percentage of total shoots within each treatment. Panels D–F display estimated marginal means for relative fruit dry matter content (centred on the vine mean) at harvest, derived from a linear mixed-effects model that accounts for other measured shoot- and fruit-level covariates. Lowercase letters above points denote statistically significant differences between fruit per shoot categories within treatment panel, while uppercase letters along the x-axis indicate significant differences between treatments for a given fruit per shoot category. Means that do not share a letter were significantly different (Šidák adjusted $\alpha = 0.05$). Error bars represent 95% confidence intervals.

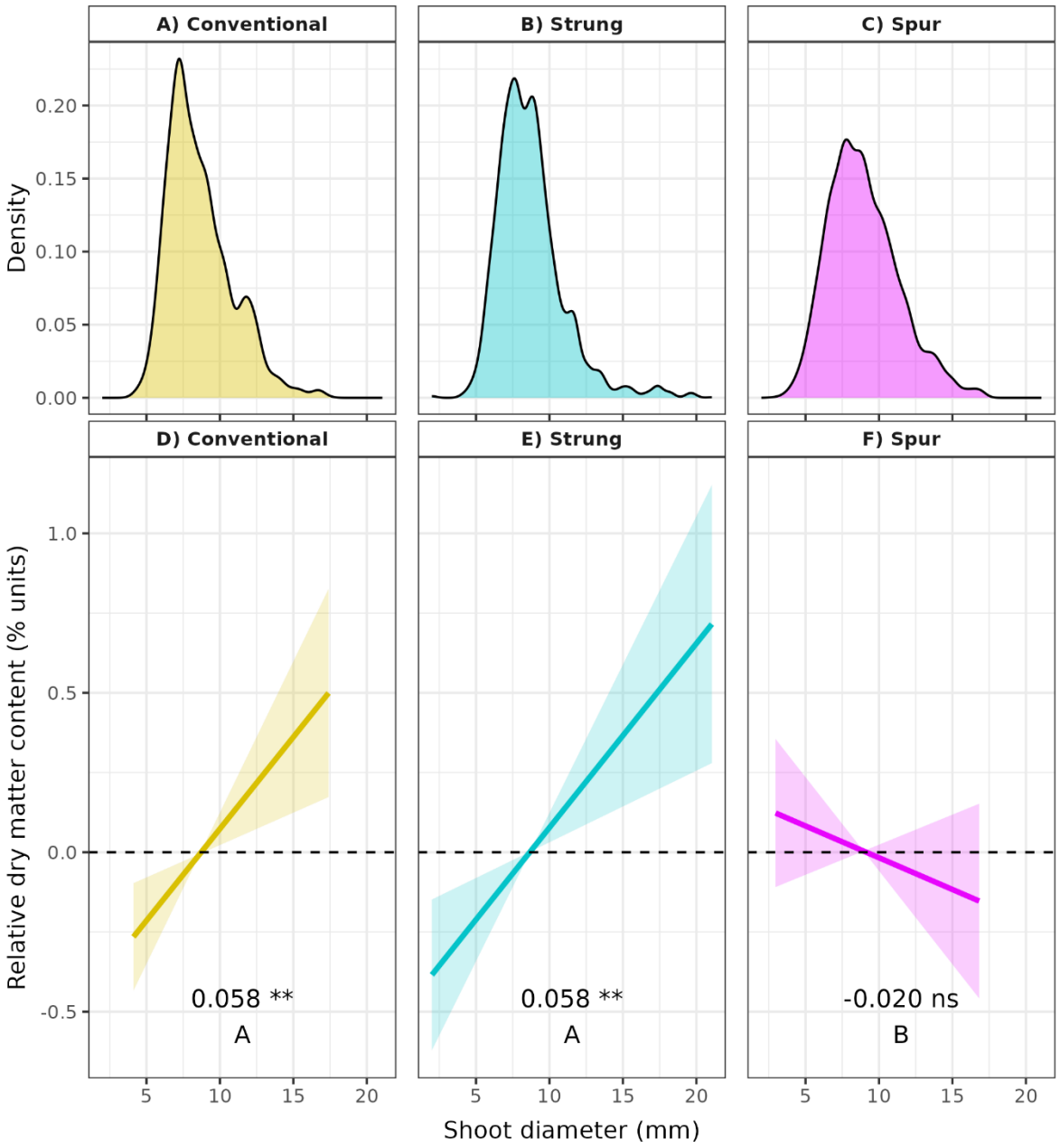


Figure A9. Distribution and model-estimated effect of shoot basal diameter on fruit relative dry matter content in *Actinidia chinensis* 'Zesy002'. Diameters were measured at the base of each shoot, immediately above the tapering region at the cane-shoot junction. Panels A–C show the distribution of shoot diameters for each canopy management treatment, expressed as kernel density plots of all measured fruit. Panels D–F display fitted relationships between shoot diameter (mm) and vine-mean centred fruit dry matter content at harvest, based on estimated marginal trends from a linear mixed-effects model. Slopes represent the expected increase in fruit dry matter content per millimetre increase in shoot diameter, after adjusting for other covariates in the model. Shaded ribbons indicate 95% confidence intervals. Numeric values within each panel indicate the estimated slope and its significance level (ns = non-significant, ** $p < 0.01$), while uppercase letters below the slope denote differences in the slope between treatments. Slopes that do not share a letter were significantly different (Šidák adjusted $\alpha = 0.05$).

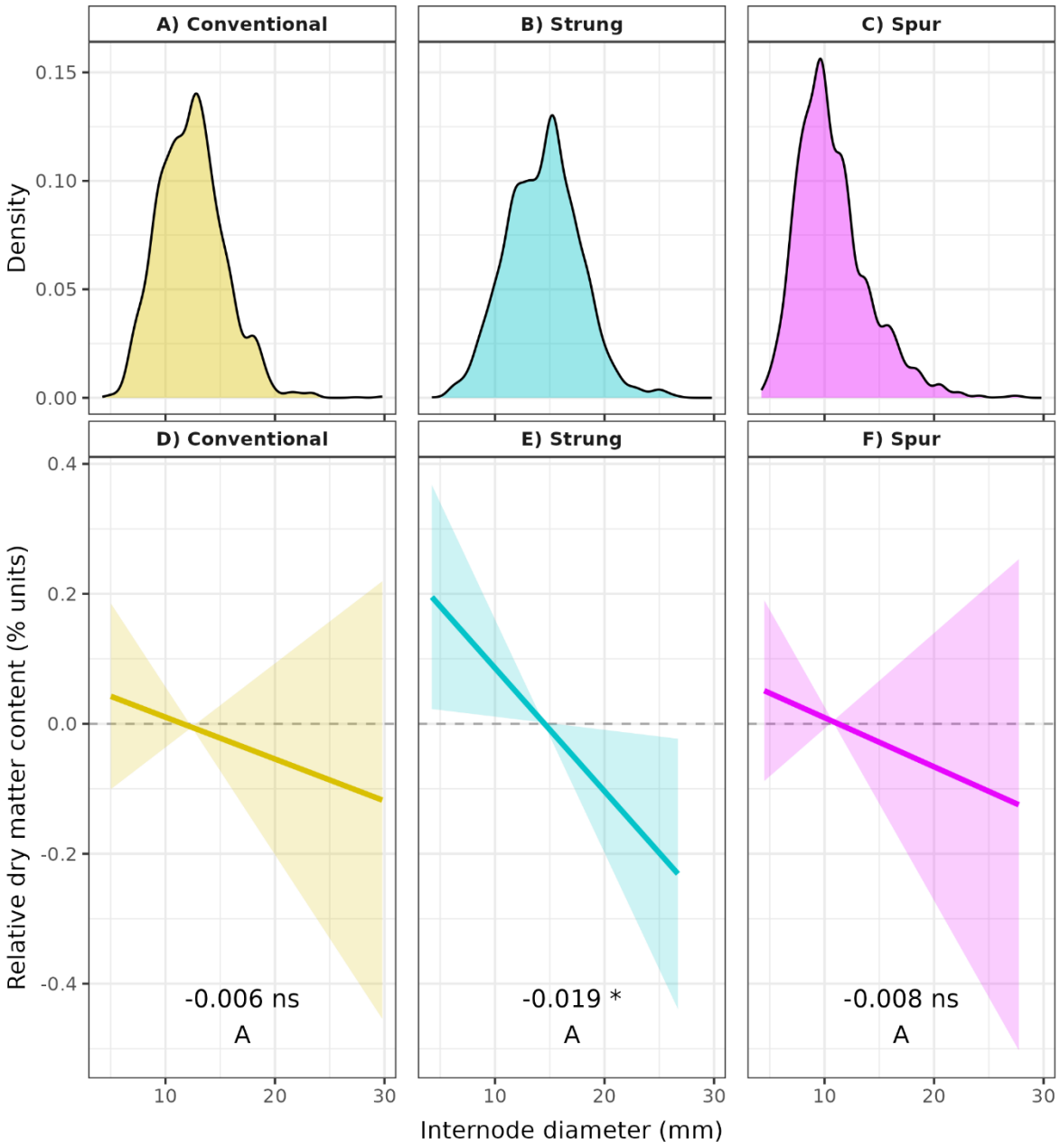


Figure A10. Distribution and model-estimated effect of internode diameter on fruit relative dry matter content in *Actinidia chinensis* 'Zesy002'. Internode diameter was measured at the proximal internode of each shoot (i.e., the internode closest to the trunk). Panels A–C show the distribution of internode basal diameters for each canopy management treatment, expressed as kernel density plots of all measured fruit. Panels D–F display fitted relationships between shoot diameter (mm) and vine-mean centred fruit dry matter content at harvest, based on estimated marginal trends from a linear mixed-effects model. Slopes represent the expected increase in fruit dry matter content per millimetre increase in shoot diameter, after adjusting for other covariates in the model. Shaded ribbons indicate 95% confidence intervals. Numeric values within each panel indicate the estimated slope and its significance level (ns = non-significant, * $p<0.05$;), while uppercase letters below the slope denote differences in the slope between treatments. Slopes that do not share a letter were significantly different (Šidák adjusted $\alpha = 0.05$).

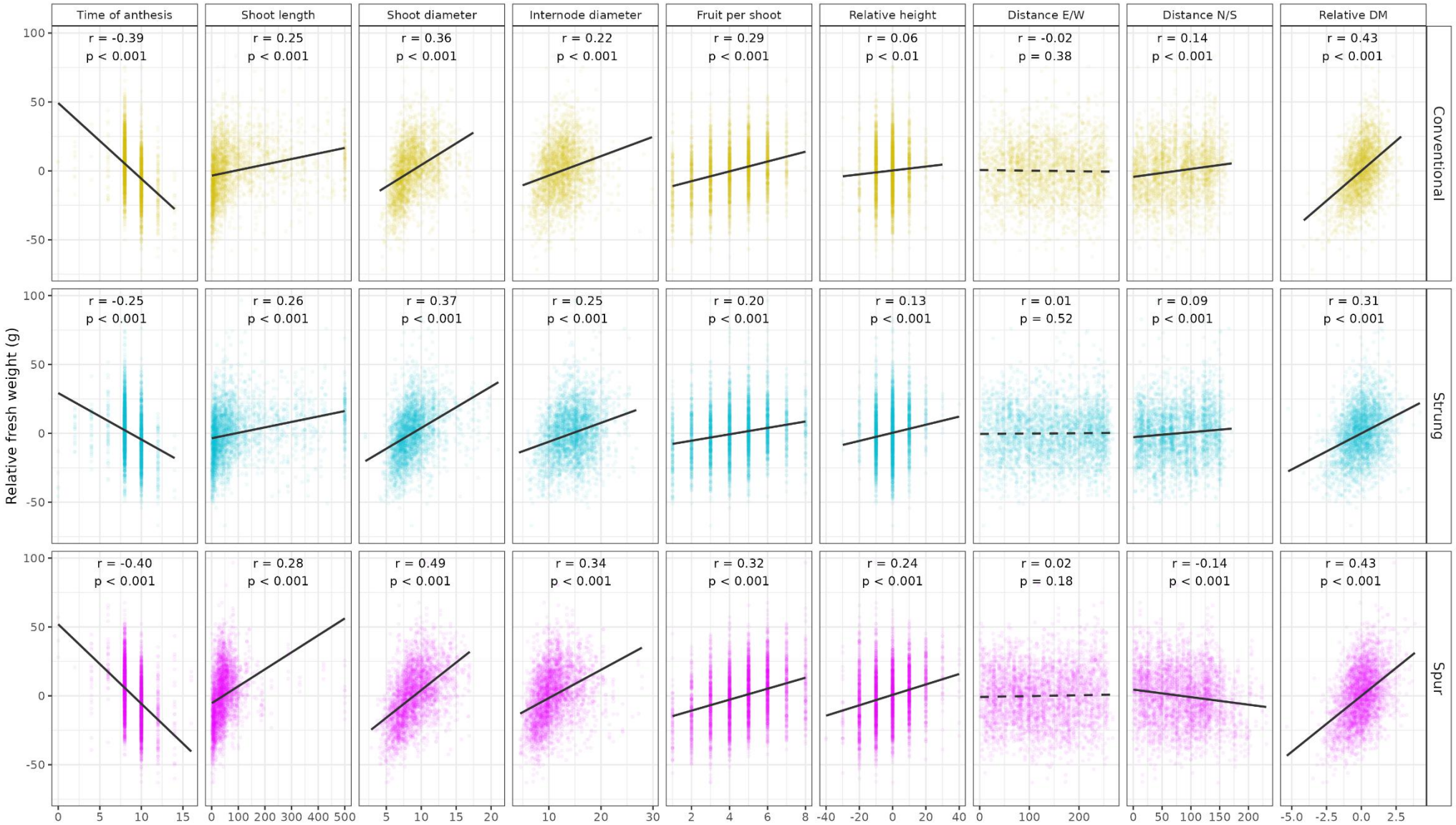


Figure A11. Correlations and linear regressions between fruit relative fresh weight and predictor variables. Fresh weight has been mean-centred within vines. Predictor variables include distance from the centre of the vine east or west (E/W, cm), distance from the centre of the vine north or south (N/S, cm), shoot length (cm), shoot basal diameter (mm), internode diameter (mm), relative fruit height in the canopy (cm), fruit per shoot, and timing of anthesis (days since flowering commenced on 27/11/2019). Each point represents an individual fruit from three whole-vine populations per treatment (conventional, strung, spur). Panels show scatterplots and ordinary least-squares regression lines. Text within each panel show Pearson correlation coefficients (r) and the significance of each correlation under the null hypothesis that there is no linear relationship between the two variables.

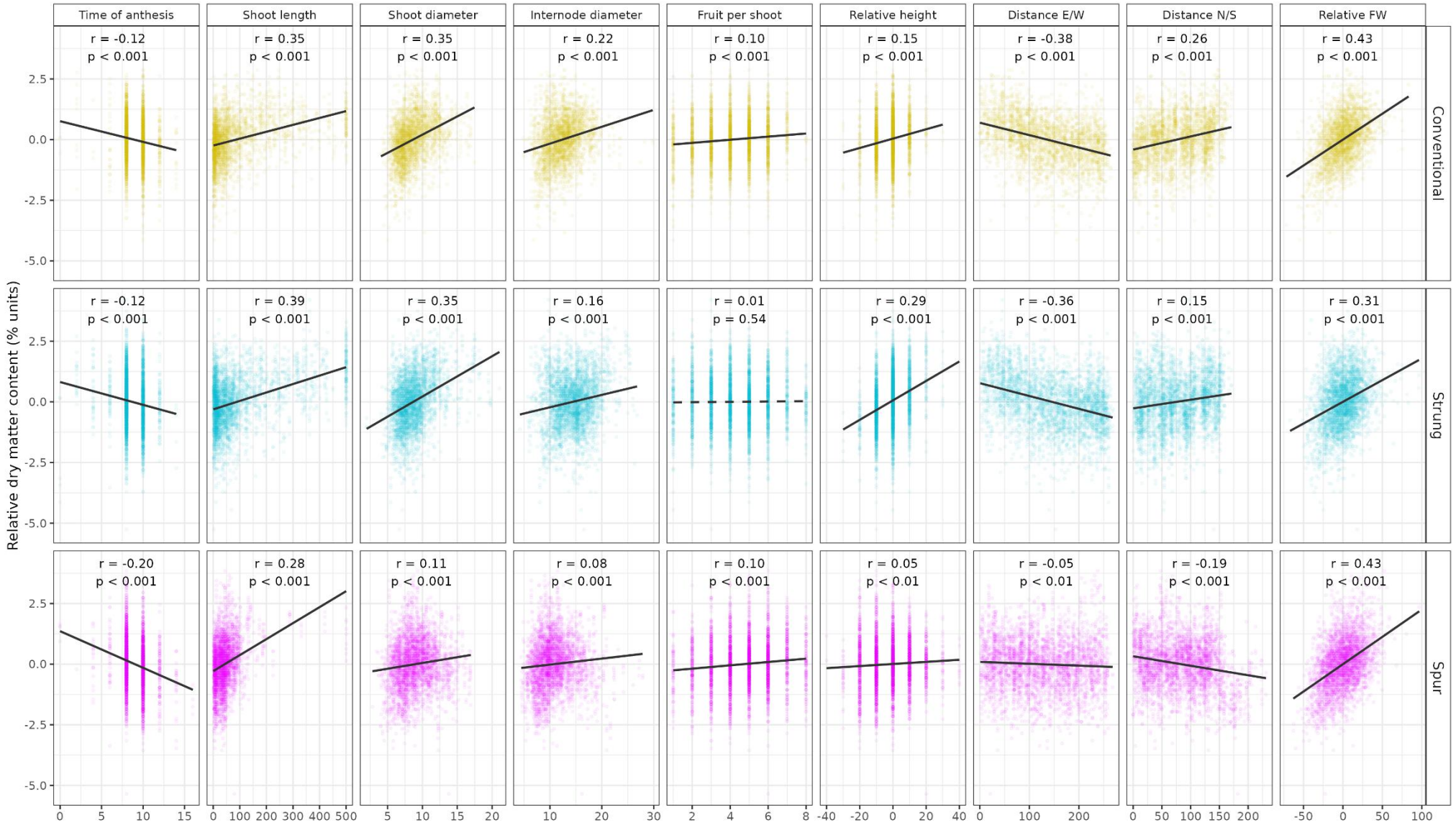


Figure A12. Correlations and linear regressions between fruit relative dry matter content and predictor variables. Dry matter content has been mean-centred within vines. Predictor variables include distance from the centre of the vine east or west (E/W, cm), distance from the centre of the vine north or south (N/S, cm), shoot length (cm), shoot basal diameter (mm), internode diameter (mm), relative fruit height in the canopy (cm), fruit per shoot, and timing of anthesis (days since flowering commenced on 27/11/2019). Each point represents an individual fruit from three whole-vine populations per treatment (conventional, strung, spur). Panels show scatterplots and ordinary least-squares regression lines. Text within each panel show Pearson correlation coefficients (r) and the significance of each correlation under the null hypothesis that there is no linear relationship between the two variables.

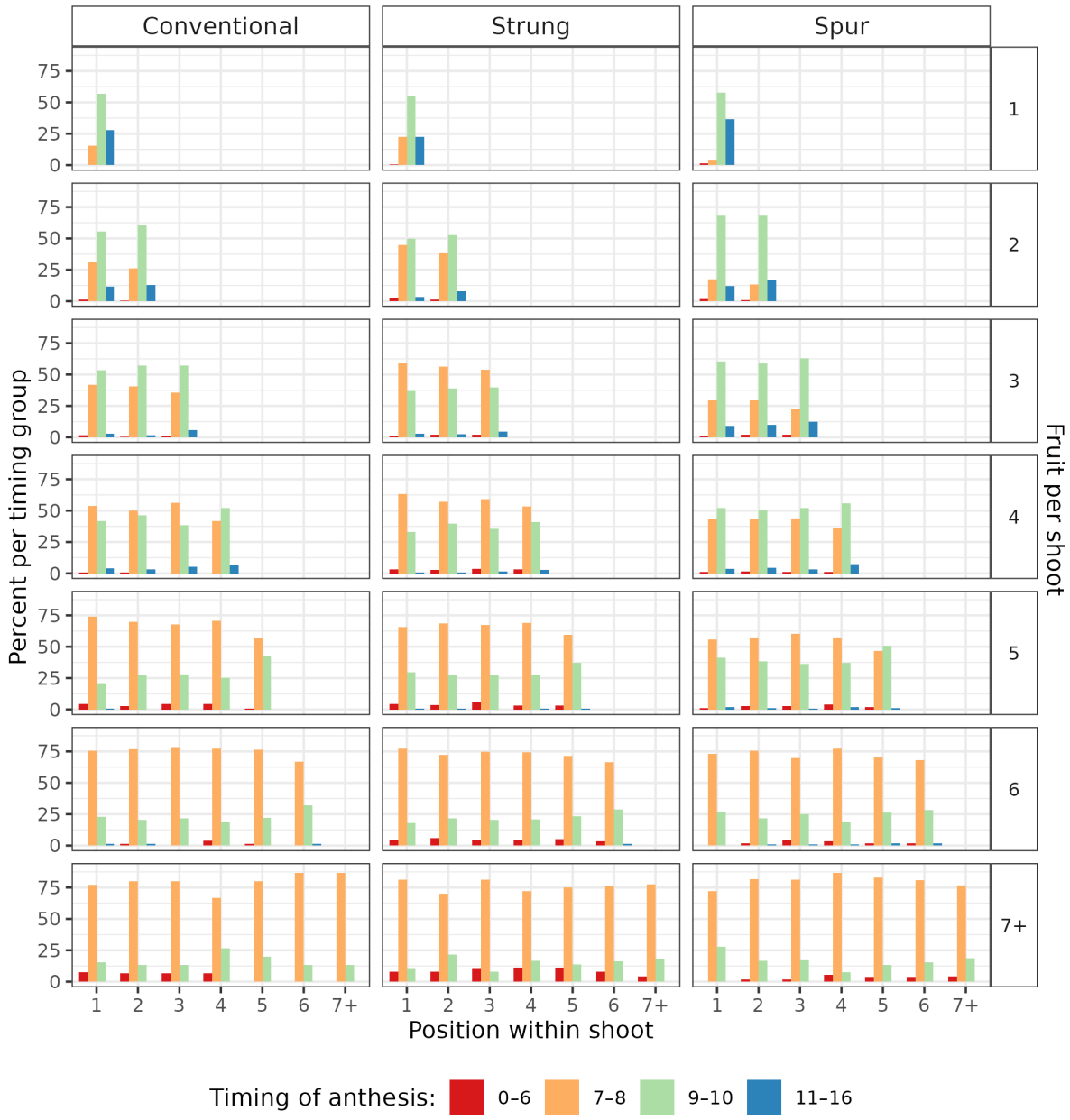


Figure A13. Bar plot of timing of anthesis by fruit position within shoots, number of fruit per shoot and by canopy management treatment. Timing of anthesis groups are days after commencement of flowering. Positions are relative to the order within shoots, where fruit in position 1 were the most basal. Fruit per shoot and positions ≥7 have been pooled due to low replication. Day 0 of anthesis was 27/11/2019

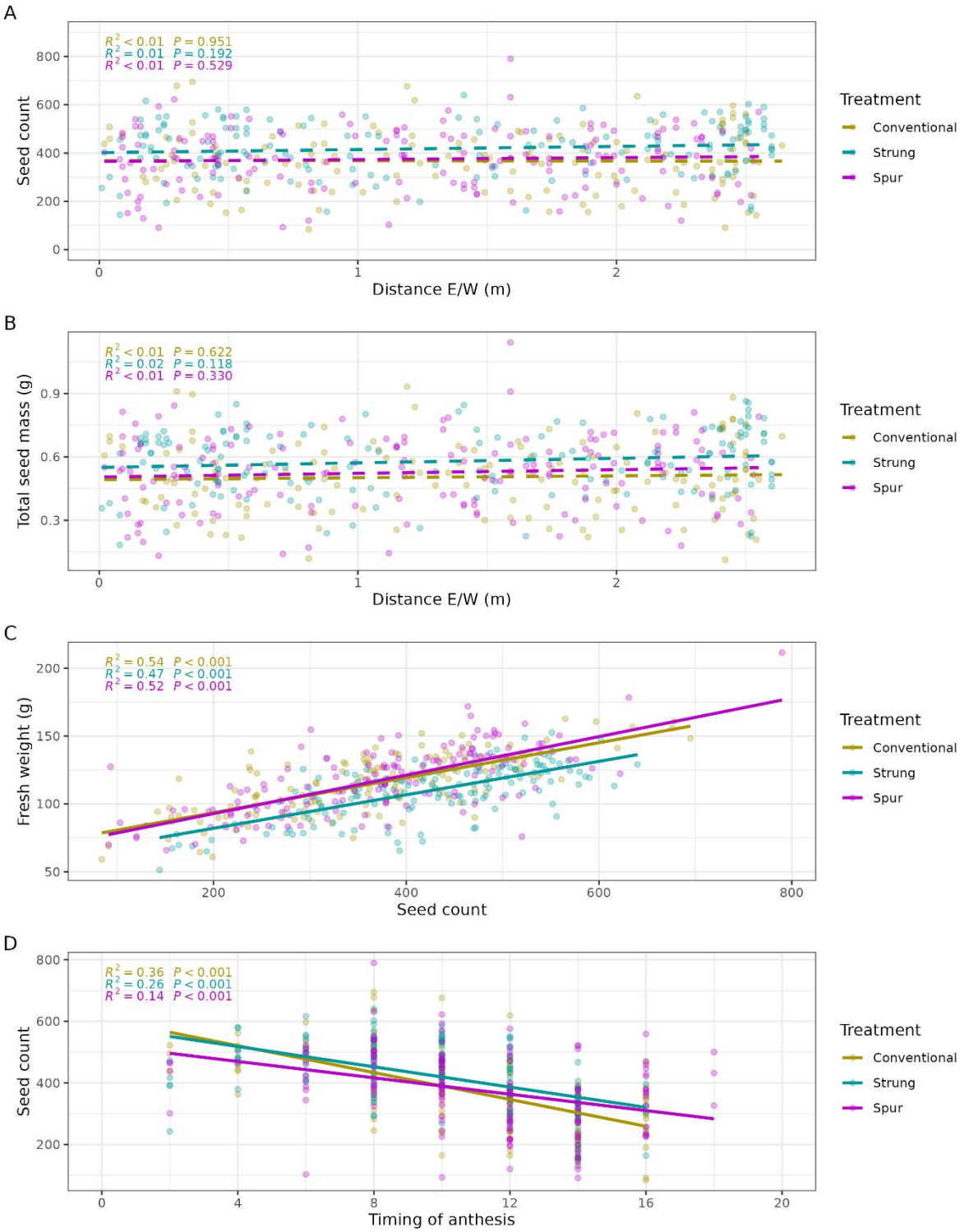


Figure A14. Seed count and seed mass regressions. Fruit were subsampled from the main within-vine populations to ensure similar representation from each timing of anthesis group. A) Seed count vs distance east or west (E/W) in the canopy. B) Total seed mass vs distance E/W. C) Fruit fresh weight vs seed count. D) Seed count vs timing of anthesis (days since first flowers opened on 27/11/2019). Solid lines indicate linear regression slope was significantly different from zero.

# Appendix B

Table B1. Fixed-effect tests from linear mixed-effects model (Wald F tests) summary table for modelled effects on total non-structural carbohydrate concentration of dormant kiwifruit cane internodes. Linear mixed-effects model fitted with random intercepts for cane nested within vine. Num DF = numerator degrees of freedom, Den DF = denominator degrees of freedom.

| Effect | Num DF | Den DF | F-value | p-value |
|---|---|---|---|---|
| Cultivar | 2 | 12 | 7.3 | **0.009** |
| Cane vigour | 2 | 24 | 7.9 | **0.002** |
| Distance from cane base | 1 | 81 | 91.7 | **<0.001** |
| Cultivar : Cane vigour | 4 | 24 | 1.9 | 0.139 |
| Cultivar : Distance | 2 | 81 | 0.9 | 0.402 |
| Cane vigour : Distance | 2 | 81 | 13.3 | **<0.001** |
| Cultivar : Cane vigour : Distance | 4 | 81 | 0.9 | 0.48 |

Table B2. Fixed-effect tests from linear mixed-effects model (Wald F tests) summary table for modelled effects on total non-structural carbohydrate per unit length of dormant kiwifruit cane internodes. Linear mixed-effects model fitted with random intercepts for cane nested within vine. Num DF = numerator degrees of freedom, Den DF = denominator degrees of freedom.

| Effect | Num DF | Den DF | F-value | p-value |
|---|---|---|---|---|
| Cultivar | 2 | 12 | 18.3 | **<0.001** |
| Cane vigour | 2 | 24 | 100.4 | **<0.001** |
| Distance from cane base | 1 | 81 | 162.2 | **<0.001** |
| Cultivar : Cane vigour | 4 | 24 | 1.1 | 0.359 |
| Cultivar : Distance | 2 | 81 | 3.5 | **0.036** |
| Cane vigour : Distance | 2 | 81 | 3.7 | **0.028** |
| Cultivar : Cane vigour : Distance | 4 | 81 | 1.0 | 0.432 |

Table B3. Fixed-effect tests from linear mixed-effects model (Wald F tests) summary table for modelled effects on internode diameter of dormant kiwifruit cane internodes. Linear mixed-effects model fitted with random intercepts for cane nested within vine. Num DF = numerator degrees of freedom, Den DF = denominator degrees of freedom.

| Effect | Num DF | Den DF | F-value | p-value |
|---|---|---|---|---|
| Cultivar | 2 | 12 | 5.9 | **0.016** |
| Cane vigour | 2 | 24 | 159.1 | **<0.001** |
| Distance from cane base | 1 | 81 | 112.8 | **<0.001** |
| Cultivar : Cane vigour | 4 | 24 | 2.7 | 0.053 |
| Cultivar : Distance | 2 | 81 | 10.2 | **<0.001** |
| Cane vigour : Distance | 2 | 81 | 1.9 | 0.155 |
| Cultivar : Cane vigour : Distance | 4 | 81 | 1.5 | 0.197 |

Table B4. Fixed-effect tests from linear mixed-effects model (Wald F tests) summary table for modelled effects on peri-medullary zone to wood area ratio of dormant kiwifruit cane internodes. Linear mixed-effects model fitted with random intercepts for cane nested within vine. Num DF = numerator degrees of freedom, Den DF = denominator degrees of freedom.

| Effect | Num DF | Den DF | F-value | p-value |
|---|---|---|---|---|
| Cultivar | 2 | 12 | 3.2 | 0.079 |
| Cane vigour | 2 | 24 | 6.2 | **0.007** |
| Distance from cane base | 1 | 81 | 218.6 | **<0.001** |
| Cultivar : Cane vigour | 4 | 24 | 2.1 | 0.114 |
| Cultivar : Distance | 2 | 81 | 10.5 | **<0.001** |
| Cane vigour : Distance | 2 | 81 | 5.5 | **0.006** |
| Cultivar : Cane vigour : Distance | 4 | 81 | 3.6 | **0.010** |

Table B5. Fixed-effect tests from linear mixed-effects model (Wald F tests) summary table for modelled effects on soluble sugar concentrations of kiwifruit cane internodes during spring growth. Linear mixed-effects model fitted with random intercepts by vine. Num DF = numerator degrees of freedom, Den DF = denominator degrees of freedom.

| Effect | Num DF | Den DF | F-value | p-value |
|---|---|---|---|---|
| Cultivar | 2 | 12 | 40.2 | **<0.001** |
| Cane vigour | 2 | 168 | 0.4 | 0.647 |
| Time point | 4 | 168 | 57.6 | **<0.001** |
| Cultivar : Cane vigour | 4 | 168 | 0.9 | 0.461 |
| Cultivar : Time | 8 | 168 | 13.3 | **<0.001** |
| Cane vigour : Time | 8 | 168 | 1.5 | 0.179 |
| Cultivar : Cane vigour : Time | 16 | 168 | 1.0 | 0.496 |

Table B6. Fixed-effect tests from linear mixed-effects model (Wald F tests) summary table for modelled effects on starch concentrations of kiwifruit cane internodes during spring growth. Linear mixed-effects model fitted with random intercepts by vine. Num DF = numerator degrees of freedom, Den DF = denominator degrees of freedom.

| Effect | Num DF | Den DF | F-value | p-value |
|---|---|---|---|---|
| Cultivar | 2 | 12 | 37.6 | **<0.001** |
| Cane vigour | 2 | 168 | 2.0 | 0.14 |
| Time point | 4 | 168 | 606.8 | **<0.001** |
| Cultivar : Cane vigour | 4 | 168 | 2.3 | 0.06 |
| Cultivar : Time | 8 | 168 | 24.2 | **<0.001** |
| Cane vigour : Time | 8 | 168 | 1.7 | 0.11 |
| Cultivar : Cane vigour : Time | 16 | 168 | 2.1 | **<0.01** |

Table B7. Fixed-effect tests from linear mixed-effects model (Wald F tests) summary table for modelled effects on total non-structural carbohydrate per unit length of kiwifruit cane internodes during spring growth. Linear mixed-effects model fitted with random intercepts by vine. Num df = numerator degrees of freedom, Den df = denominator degrees of freedom.

| Effect | Num df | Den df | F-value | p-value |
|---|---|---|---|---|
| Cultivar | 1 | 168 | 712.7 | **<0.001** |
| Cane vigour | 2 | 12 | 19.1 | **<0.001** |
| Time round | 2 | 168 | 124.5 | **<0.001** |
| Cultivar : Cane vigour | 4 | 168 | 168.9 | **<0.001** |
| Cultivar : Time | 4 | 168 | 2.2 | 0.074 |
| Cane vigour : Time | 8 | 168 | 8.9 | **<0.001** |
| Cultivar : Cane vigour : Time | 8 | 168 | 26.5 | **<0.001** |

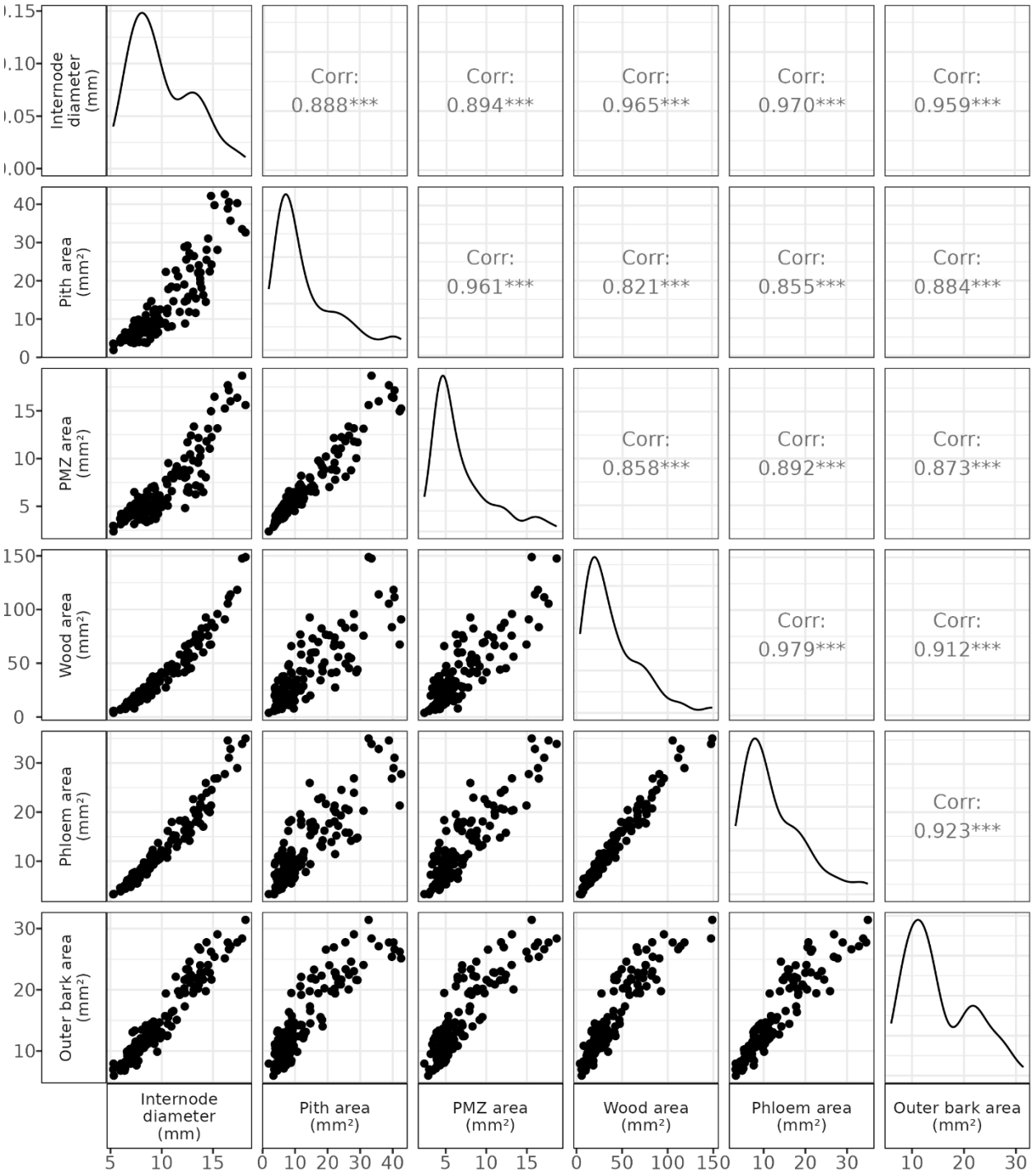


Figure B1. Correlation matrix for cane internode diameter and total tissue layer areas. Wood = secondary xylem. Outer bark includes the epidermis, cortex and bast fibres. PMZ = peri-medullary zone. Diagonal line plots show the probability density for each factor on the x-axis. Corr = Pearson's r correlation coefficient. *** = p <0.001.




Figure B2. Individual sugar concentrations by cultivar for dormant kiwifruit canes and over spring sampling time points. Within cultivars bars are means averaged over low, medium and high vigour canes, error bars are standard error. 'Hayward' = *Actinidia chinensis* var. *deliciosa*, 'Zesy002' and 'Zes008' = *A. chinensis* var. *chinensis*. Suc = sucrose; Glc = glucose; Fru = fructose; Sta = stachyose; Raf = raffinose; Pla = planteose. DABB = days after budbreak.

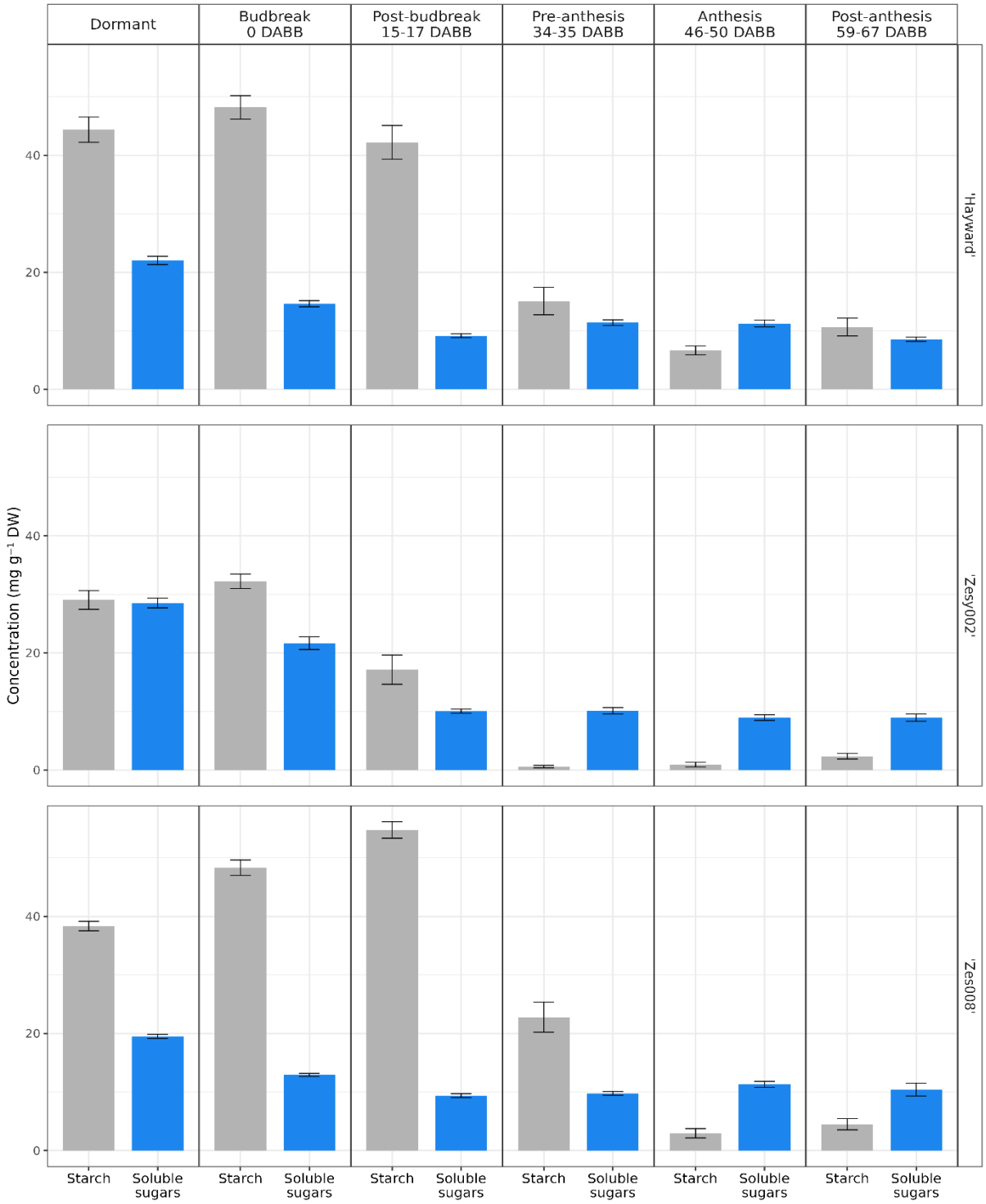


Figure B3. Starch and total soluble sugar concentrations by cultivar for dormant canes and over spring sampling time points. Soluble sugars are the summed concentration of sucrose, glucose, fructose, stachyose, raffinose and planteose. Bars are means averaged over low, medium and high vigour canes within cultivars, error bars are standard error. 'Hayward' = *Actinidia chinensis* var. *deliciosa*, 'Zesy002' and 'Zes008' = *A. chinensis* var. *chinensis*. DABB = days after budbreak.

# Appendix C

Table C1. Summary of heteroscedasticity-robust Wald tests for timing effects for each treatment and analyte in experiment 1. Rows marked with * had non-zero values for pre-injection concentrations so could be included in model comparisons. 'Total' is the combined concentrations of sucrose, glucose, and fructose.

| Treatment | Analyte | DF | F statistic | p value |
|---|---|---|---|---|
| 5% Sucrose | Sucrose | 4* | 483.7 | 0.000 |
| | Glucose | 3 | 1.0 | 0.419 |
| | Fructose | 3 | 4.5 | 0.018 |
| | Total | 4* | 85.4 | 0.000 |
| Water | Sucrose | 3 | 32.2 | 0.000 |
| | Glucose | 3 | 5.3 | 0.008 |
| | Fructose | 3 | 3.8 | 0.031 |
| | Total | 3 | 26.0 | 0.000 |

Table C2. Type II ANOVA table for each tissue and analyte in experiment 2. DF: Numerator degrees of freedom. Soluble sugars are the sum of sucrose, glucose, fructose, planteose, raffinose and stachyose. Total non-structural carbohydrate (TNC) is the sum of soluble sugars and starch.

| Tissue | Analyte | Term | DF | SS | F value | p value |
|---|---|---|---|---|---|---|
| Bark | Soluble sugars | Treatment | 4 | 34196.8 | 50.87 | 0.000 |
| | | Vine | 9 | 822.9 | 0.54 | 0.832 |
| | Starch | Treatment | 4 | 3685.8 | 15.28 | 0.000 |
| | | Vine | 9 | 655 | 1.21 | 0.321 |
| | TNC | Treatment | 4 | 56409.1 | 70.66 | 0.000 |
| | | Vine | 9 | 1895.7 | 1.06 | 0.418 |
| Wood | Soluble sugars | Treatment | 4 | 4307.3 | 20.83 | 0.000 |
| | | Vine | 9 | 440.8 | 0.95 | 0.499 |
| | Starch | Treatment | 4 | 1040.8 | 3.50 | 0.017 |
| | | Vine | 9 | 1073.8 | 1.61 | 0.154 |
| | TNC | Treatment | 4 | 7679.7 | 12.76 | 0.000 |
| | | Vine | 9 | 1506.9 | 1.11 | 0.381 |

Table C3. Type II ANOVA summary table for budbreak percentage, floral shoot percentage and inflorescences per bud in experiment 2. DF: Numerator degrees of freedom. SS: Sums of squares.

| Response | Term | DF | SS | F value | p value |
|---|---|---|---|---|---|
| Budbreak percentage | Treatment | 4 | 1218.3 | 3.730 | 0.010 |
| | Vine | 9 | 581.7 | 0.792 | 0.625 |
| Floral shoot percentage | Treatment | 4 | 1147.6 | 0.229 | 0.921 |
| | Vine | 9 | 3305.0 | 0.293 | 0.973 |
| Inflorescences per bud | Treatment | 4 | 0.006 | 0.261 | 0.901 |
| | Vine | 9 | 0.031 | 0.598 | 0.792 |

Table C4. Mean ± standard error values (mg $g^{-1}$ DW) for individual carbohydrates in bark samples from experiment 2.

**Bark**

| Treatment | Measure | Sucrose | Glucose | Fructose | Planteose | Raffinose | Stachyose | Starch | Total |
|---|---|---|---|---|---|---|---|---|---|
| Control | Start | 39.4 ± 1.2 | 0.9 ± 0.2 | 1.3 ± 0.2 | 9.7 ± 0.8 | 11.7 ± 0.8 | 15.0 ± 0.6 | 20.8 ± 2.8 | 98.8 ± 2.2 |
| Control | End | 43.2 ± 3.4 | 2.3 ± 0.3 | 4.0 ± 0.5 | 6.4 ± 0.7 | 9.4 ± 0.7 | 13.1 ± 0.7 | 8.1 ± 1.1 | 86.5 ± 4.6 |
| Control | Difference | 3.8 ± 3.5 | 1.4 ± 0.4 | 2.7 ± 0.5 | -3.3 ± 0.5 | -2.3 ± 0.5 | -1.9 ± 0.9 | -12.7 ± 2.7 | -12.4 ± 5.1 |
| 0% Suc | Start | 40.3 ± 1.4 | 0.5 ± 0.1 | 0.9 ± 0.1 | 9.3 ± 0.8 | 11.5 ± 0.5 | 15.7 ± 0.6 | 22.9 ± 1.5 | 101.2 ± 1.7 |
| 0% Suc | End | 25.4 ± 1.7 | 0.4 ± 0.1 | 1.6 ± 0.2 | 5.7 ± 0.5 | 4.2 ± 0.4 | 5.2 ± 0.5 | 12.7 ± 1.5 | 55.2 ± 1.7 |
| 0% Suc | Difference | -14.9 ± 1.2 | -0.1 ± 0.1 | 0.7 ± 0.3 | -3.6 ± 0.4 | -7.2 ± 0.5 | -10.6 ± 0.7 | -10.2 ± 1.2 | -46.0 ± 1.5 |
| 5% Suc | Start | 43.0 ± 0.9 | 1.0 ± 0.2 | 1.3 ± 0.2 | 9.8 ± 0.7 | 11.4 ± 0.3 | 15.5 ± 0.4 | 22.4 ± 2.1 | 104.4 ± 2.9 |
| 5% Suc | End | 56.3 ± 1.6 | 1.6 ± 0.3 | 3.4 ± 0.5 | 4.8 ± 0.2 | 4.8 ± 0.5 | 4.8 ± 0.6 | 17.5 ± 2.1 | 93.2 ± 2.5 |
| 5% Suc | Difference | 13.3 ± 1.4 | 0.7 ± 0.3 | 2.1 ± 0.5 | -5.0 ± 0.6 | -6.6 ± 0.5 | -10.7 ± 0.6 | -5.0 ± 2.4 | -11.2 ± 1.8 |
| 10% Suc | Start | 42.3 ± 2.1 | 0.8 ± 0.1 | 1.3 ± 0.1 | 10.6 ± 0.6 | 10.7 ± 0.6 | 15.7 ± 0.6 | 22.6 ± 1.1 | 104.0 ± 3.4 |
| 10% Suc | End | 86.6 ± 3.5 | 3.4 ± 0.5 | 5.7 ± 0.5 | 4.7 ± 0.3 | 4.2 ± 0.2 | 3.8 ± 0.4 | 23.8 ± 1.5 | 132.2 ± 6.0 |
| 10% Suc | Difference | 44.4 ± 3.2 | 2.6 ± 0.5 | 4.4 ± 0.6 | -5.9 ± 0.6 | -6.5 ± 0.5 | -11.9 ± 0.6 | 1.1 ± 1.8 | 28.2 ± 5.6 |
| 15% Suc | Start | 41.5 ± 1.0 | 0.6 ± 0.1 | 1.0 ± 0.1 | 8.7 ± 0.5 | 12.0 ± 0.5 | 15.7 ± 0.6 | 22.8 ± 1.0 | 102.3 ± 1.5 |
| 15% Suc | End | 101.9 ± 3.9 | 2.2 ± 0.2 | 4.8 ± 0.4 | 3.5 ± 0.3 | 3.4 ± 0.4 | 2.1 ± 0.5 | 34.1 ± 3.8 | 152.0 ± 6.6 |
| 15% Suc | Difference | 60.4 ± 3.8 | 1.5 ± 0.2 | 3.8 ± 0.4 | -5.1 ± 0.5 | -8.6 ± 0.6 | -13.6 ± 0.6 | 11.2 ± 3.7 | 49.7 ± 6.2 |

Table C5. Mean ± standard error values (mg $g^{-1}$ DW) for individual carbohydrates in wood samples from experiment 2.

| Wood | | | | | | | | | |
|---|---|---|---|---|---|---|---|---|---|
| **Treatment** | **Measure** | **Sucrose** | **Glucose** | **Fructose** | **Planteose** | **Raffinose** | **Stachyose** | **Starch** | **Total** |
| Control | Start | 9.9 ± 0.5 | 0.1 ± 0.0 | 0.2 ± 0.0 | 2.3 ± 0.2 | 2.6 ± 0.2 | 3.0 ± 0.2 | 64.7 ± 3.1 | 82.8 ± 2.9 |
| Control | End | 12.1 ± 1.2 | 0.5 ± 0.1 | 0.9 ± 0.1 | 1.5 ± 0.2 | 2.3 ± 0.3 | 2.9 ± 0.3 | 58.9 ± 1.3 | 79.0 ± 2.5 |
| Control | Difference | 2.2 ± 1.3 | 0.4 ± 0.1 | 0.7 ± 0.1 | -0.8 ± 0.2 | -0.4 ± 0.2 | -0.2 ± 0.4 | -5.8 ± 4.0 | -3.8 ± 4.8 |
| 0% Suc | Start | 9.6 ± 0.3 | 0.1 ± 0.0 | 0.2 ± 0.0 | 2.1 ± 0.2 | 2.5 ± 0.1 | 3.1 ± 0.2 | 61.0 ± 2.3 | 78.6 ± 2.6 |
| 0% Suc | End | 7.1 ± 0.7 | 0.5 ± 0.0 | 0.8 ± 0.1 | 1.3 ± 0.1 | 1.0 ± 0.2 | 1.4 ± 0.2 | 61.0 ± 3.0 | 73.1 ± 3.7 |
| 0% Suc | Difference | -2.4 ± 0.5 | 0.4 ± 0.0 | 0.6 ± 0.1 | -0.8 ± 0.1 | -1.5 ± 0.2 | -1.7 ± 0.2 | -0.1 ± 2.2 | -5.5 ± 2.8 |
| 5% Suc | Start | 11.2 ± 0.4 | 0.1 ± 0.0 | 0.2 ± 0.0 | 2.3 ± 0.2 | 2.6 ± 0.1 | 3.3 ± 0.1 | 68.5 ± 2.8 | 88.2 ± 3.0 |
| 5% Suc | End | 15.1 ± 1.0 | 2.6 ± 0.3 | 5.1 ± 0.5 | 1.0 ± 0.1 | 0.9 ± 0.1 | 1.0 ± 0.2 | 69.8 ± 2.3 | 95.6 ± 3.4 |
| 5% Suc | Difference | 4.0 ± 1.0 | 2.5 ± 0.3 | 4.9 ± 0.5 | -1.3 ± 0.2 | -1.7 ± 0.2 | -2.2 ± 0.2 | 1.4 ± 2.3 | 7.4 ± 2.7 |
| 10% Suc | Start | 10.2 ± 0.6 | 0.1 ± 0.0 | 0.2 ± 0.0 | 2.5 ± 0.1 | 2.4 ± 0.1 | 3.2 ± 0.2 | 71.9 ± 3.9 | 90.6 ± 4.4 |
| 10% Suc | End | 23.3 ± 1.3 | 4.6 ± 1.4 | 6.9 ± 2.1 | 0.9 ± 0.0 | 0.8 ± 0.0 | 0.8 ± 0.1 | 80.2 ± 2.1 | 117.6 ± 5.6 |
| 10% Suc | Difference | 13.1 ± 1.5 | 4.5 ± 1.4 | 6.7 ± 2.1 | -1.5 ± 0.1 | -1.6 ± 0.1 | -2.5 ± 0.2 | 8.3 ± 3.7 | 27.0 ± 6.1 |
| 15% Suc | Start | 10.2 ± 0.5 | 0.1 ± 0.0 | 0.2 ± 0.0 | 2.0 ± 0.1 | 2.7 ± 0.1 | 3.2 ± 0.2 | 67.1 ± 2.6 | 85.5 ± 2.9 |
| 15% Suc | End | 25.2 ± 1.0 | 3.8 ± 0.6 | 6.9 ± 1.1 | 0.7 ± 0.0 | 0.6 ± 0.1 | 0.4 ± 0.1 | 67.4 ± 1.8 | 105.0 ± 2.9 |
| 15% Suc | Difference | 14.9 ± 0.7 | 3.7 ± 0.6 | 6.8 ± 1.1 | -1.3 ± 0.1 | -2.1 ± 0.1 | -2.8 ± 0.2 | 0.2 ± 2.4 | 19.4 ± 3.4 |

Table C6. Type III ANOVA summary table for soluble sugars in experiment 3. Soluble sugars are the summed concentrations of sucrose, glucose, fructose, planteose, raffinose and stachyose. C: Canopy treatment. I: Injection treatment. C×I: Interaction effect. SS: Sums of squares. All numerator degree of freedom = 1.

**Response: Soluble sugars**

| Tissue | Month | Term | SS | F value | p value |
|---|---|---|---|---|---|
| Bark | March | C | 45.4 | 0.33 | 0.568 |
| | | I | 418.1 | 3.07 | 0.089 |
| | | C×I | 13.7 | 0.10 | 0.753 |
| | May | C | 102.0 | 0.94 | 0.341 |
| | | I | 265.5 | 2.44 | 0.129 |
| | | C×I | 3.3 | 0.03 | 0.862 |
| | June | C | 68.8 | 0.76 | 0.391 |
| | | I | 1459.8 | 16.07 | **0.000** |
| | | C×I | 808.0 | 8.89 | **0.006** |
| Wood | March | C | 34.8 | 1.80 | 0.190 |
| | | I | 54.8 | 2.83 | 0.103 |
| | | C×I | 8.4 | 0.43 | 0.515 |
| | May | C | 5.6 | 0.83 | 0.397 |
| | | I | 1.8 | 0.27 | 0.622 |
| | | C×I | 8.2 | 1.22 | 0.311 |
| | June | C | 3.9 | 0.25 | 0.622 |
| | | I | 288.4 | 18.41 | **0.000** |
| | | C×I | 170.4 | 10.88 | **0.003** |

Table C7. Type III ANOVA summary table for starch concentrations in experiment 3. C: Canopy treatment. I: Injection treatment. C×I: Interaction effect. SS: Sums of squares. All numerator degree of freedom = 1.

**Response: Starch**

| Tissue | Month | Term | SS | F value | p value |
|---|---|---|---|---|---|
| Bark | March | C | 2.4 | 0.3 | 0.580 |
| | | I | 0.4 | 0.0 | 0.832 |
| | | C×I | 8.1 | 1.1 | 0.312 |
| | May | C | 377.7 | 27.3 | **0.002** |
| | | I | 68.4 | 4.9 | 0.068 |
| | | C×I | 8.0 | 0.6 | 0.477 |
| | June | C | 76.1 | 6.5 | **0.034** |
| | | I | 2.3 | 0.2 | 0.671 |
| | | C×I | 0.8 | 0.1 | 0.796 |
| Wood | March | C | 110.2 | 2.8 | 0.107 |
| | | I | 45.5 | 1.1 | 0.294 |
| | | C×I | 9.4 | 0.2 | 0.631 |
| | May | C | 1083.0 | 11.1 | **0.002** |
| | | I | 34.6 | 0.4 | 0.555 |
| | | C×I | 213.7 | 2.2 | 0.148 |
| | June | C | 1033.7 | 10.8 | **0.017** |
| | | I | 39.6 | 0.4 | 0.544 |
| | | C×I | 3.4 | 0.0 | 0.857 |

Table C8. Type III ANOVA summary table for total non-structural carbohydrate concentrations (sum of sucrose, glucose, fructose, planteose, raffinose, stachyose and starch) in experiment 3. C: Canopy treatment. I: Injection treatment. C×I: Interaction effect. SS: Sums of squares. All numerator degree of freedom = 1.

**Response: Total carbohydrates**

| Tissue | Month | Term | SS | F value | p value |
|---|---|---|---|---|---|
| Bark | March | C | 68.6 | 0.45 | 0.505 |
| | | I | 442.8 | 2.93 | 0.097 |
| | | C×I | 0.7 | 0.00 | 0.945 |
| | May | C | 1100.0 | 8.14 | **0.029** |
| | | I | 636.3 | 4.71 | 0.073 |
| | | C×I | 26.5 | 0.20 | 0.673 |
| | June | C | 652.5 | 5.33 | 0.060 |
| | | I | 733.2 | 5.99 | **0.050** |
| | | C×I | 386.2 | 3.16 | 0.126 |
| Wood | March | C | 268.9 | 3.61 | 0.067 |
| | | I | 200.2 | 2.69 | 0.111 |
| | | C×I | 35.6 | 0.48 | 0.494 |
| | May | C | 843.5 | 6.51 | **0.043** |
| | | I | 43.3 | 0.33 | 0.584 |
| | | C×I | 244.3 | 1.88 | 0.219 |
| | June | C | 1117.9 | 8.34 | **0.028** |
| | | I | 310.9 | 2.32 | 0.179 |
| | | C×I | 40.3 | 0.30 | 0.603 |

Table C9. Type III ANOVA summary table for budbreak percentage, floral shoot percentage and inflorescences per bud in experiment 3. C: Canopy treatment. I: Injection treatment. C×I: Interaction effect. SS: Sums of squares.

| Response | Term | SS | F Value | P Value |
|---|---|---|---|---|
| Budbreak percentage | C | 1382.5 | 7.22 | 0.036 |
| | P | 140.6 | 0.73 | 0.424 |
| | C×I | 96.5 | 0.50 | 0.504 |
| Floral shoot percentage | C | 1623.9 | 16.75 | 0.000 |
| | P | 31.0 | 0.32 | 0.575 |
| | C×I | 25.0 | 0.26 | 0.614 |
| Inflorescences per bud | C | 29.1 | 52.02 | 0.000 |
| | P | 0.2 | 0.34 | 0.564 |
| | C×I | 0.7 | 1.31 | 0.258 |

Table C10. Mean ± standard error values for individual carbohydrate concentrations (mg $g^{-1}$ DW) in bark samples from experiment 3.

| Bark | | | | | | | | | | |
|---|---|---|---|---|---|---|---|---|---|---|
| **Sample** | **Canopy** | **Injection** | **Sucrose** | **Glucose** | **Fructose** | **Planteose** | **Raffinose** | **Stachyose** | **Starch** | **Total** |
| March | Intact | No injection | 27.0 ± 3.7 | 0.5 ± 0.2 | 1.1 ± 0.3 | 7.2 ± 1.0 | 0.6 ± 0.1 | 0.3 ± 0.1 | 5.9 ± 1.3 | 42.6 ± 5.0 |
| March | Intact | 10% Sucrose | 30.9 ± 3.1 | 0.5 ± 0.1 | 1.2 ± 0.2 | 8.4 ± 0.8 | 0.8 ± 0.1 | 0.5 ± 0.2 | 7.0 ± 0.8 | 49.4 ± 4.1 |
| March | 3/4 Defoliated | No injection | 23.8 ± 1.5 | 0.4 ± 0.1 | 1.1 ± 0.2 | 7.1 ± 0.6 | 0.6 ± 0.1 | 0.2 ± 0.1 | 6.3 ± 1.0 | 39.6 ± 3.0 |
| March | 3/4 Defoliated | 10% Sucrose | 30.5 ± 3.0 | 0.6 ± 0.1 | 1.4 ± 0.3 | 7.9 ± 0.8 | 0.7 ± 0.1 | 0.4 ± 0.1 | 5.5 ± 1.0 | 46.9 ± 4.1 |
| May | Intact | No injection | 40.1 ± 1.9 | 0.8 ± 0.1 | 1.8 ± 0.2 | 8.3 ± 0.8 | 9.8 ± 0.8 | 17.8 ± 0.5 | 17.1 ± 1.3 | 95.7 ± 3.4 |
| May | Intact | 10% Sucrose | 43.5 ± 2.6 | 0.6 ± 0.1 | 1.5 ± 0.2 | 9.4 ± 1.0 | 11.0 ± 0.7 | 18.8 ± 0.8 | 22.0 ± 1.3 | 106.7 ± 4.7 |
| May | 3/4 Defoliated | No injection | 43.7 ± 1.5 | 1.1 ± 0.2 | 2.1 ± 0.3 | 4.6 ± 0.5 | 9.0 ± 0.5 | 15.4 ± 0.6 | 9.7 ± 1.7 | 85.7 ± 2.9 |
| May | 3/4 Defoliated | 10% Sucrose | 44.8 ± 3.0 | 1.6 ± 0.3 | 2.6 ± 0.4 | 5.8 ± 0.9 | 9.0 ± 0.5 | 16.9 ± 0.7 | 12.1 ± 2.0 | 92.9 ± 4.7 |
| June | Intact | No injection | 48.6 ± 2.2 | 0.7 ± 0.1 | 1.6 ± 0.2 | 7.5 ± 0.7 | 12.9 ± 1.1 | 19.9 ± 1.5 | 17.1 ± 4.2 | 108.4 ± 7.8 |
| June | Intact | 10% Sucrose | 51.9 ± 2.1 | 1.4 ± 0.2 | 2.5 ± 0.3 | 8.4 ± 0.8 | 11.5 ± 0.6 | 18.8 ± 1.1 | 17.9 ± 2.0 | 112.4 ± 4.4 |
| June | 3/4 Defoliated | No injection | 44.1 ± 2.4 | 1.5 ± 0.4 | 2.6 ± 0.5 | 4.0 ± 0.6 | 9.1 ± 0.4 | 17.8 ± 0.9 | 4.9 ± 0.8 | 83.9 ± 4.4 |
| June | 3/4 Defoliated | 10% Sucrose | 60.1 ± 1.6 | 3.9 ± 0.4 | 5.8 ± 0.6 | 4.8 ± 0.4 | 9.0 ± 0.5 | 17.7 ± 0.5 | 8.0 ± 0.8 | 109.2 ± 2.4 |

Table C11. Mean ± standard error values for individual carbohydrate concentrations (mg $g^{-1}$ DW) in wood samples from experiment 3.

| Wood Sample | Canopy | Injection | Sucrose | Glucose | Fructose | Planteose | Raffinose | Stachyose | Starch | Total |
|---|---|---|---|---|---|---|---|---|---|---|
| March | Intact | No injection | 6.2 ± 0.8 | 1.3 ± 0.7 | 1.8 ± 0.8 | 1.2 ± 0.2 | 0.4 ± 0.0 | 0.0 ± 0.0 | 6.5 ± 2.0 | 17.5 ± 4.0 |
| March | Intact | 10% Sucrose | 6.4 ± 0.7 | 0.5 ± 0.1 | 0.8 ± 0.2 | 1.5 ± 0.2 | 0.3 ± 0.0 | 0.1 ± 0.0 | 5.3 ± 1.5 | 14.8 ± 1.9 |
| March | 3/4 Defoliated | No injection | 9.3 ± 0.9 | 0.9 ± 0.3 | 1.0 ± 0.3 | 2.2 ± 0.2 | 0.5 ± 0.1 | 0.1 ± 0.1 | 11.1 ± 2.2 | 25.0 ± 2.4 |
| March | 3/4 Defoliated | 10% Sucrose | 6.6 ± 0.8 | 0.9 ± 0.4 | 1.3 ± 0.5 | 1.4 ± 0.3 | 0.3 ± 0.1 | 0.0 ± 0.0 | 7.8 ± 2.7 | 18.3 ± 3.4 |
| May | Intact | No injection | 10.9 ± 0.9 | 0.1 ± 0.0 | 0.2 ± 0.0 | 2.6 ± 0.3 | 3.1 ± 0.4 | 5.1 ± 0.2 | 46.6 ± 3.6 | 68.5 ± 5.2 |
| May | Intact | 10% Sucrose | 12.0 ± 0.5 | 0.1 ± 0.0 | 0.2 ± 0.0 | 3.0 ± 0.3 | 3.7 ± 0.2 | 5.5 ± 0.2 | 53.4 ± 3.3 | 78.1 ± 4.1 |
| May | 3/4 Defoliated | No injection | 12.2 ± 0.5 | 0.2 ± 0.0 | 0.4 ± 0.1 | 1.5 ± 0.2 | 3.1 ± 0.3 | 4.8 ± 0.3 | 40.5 ± 2.8 | 62.7 ± 3.5 |
| May | 3/4 Defoliated | 10% Sucrose | 11.2 ± 0.6 | 0.3 ± 0.0 | 0.5 ± 0.1 | 1.7 ± 0.3 | 2.7 ± 0.2 | 4.9 ± 0.3 | 37.6 ± 3.7 | 58.8 ± 4.3 |
| June | Intact | No injection | 13.4 ± 0.8 | 0.2 ± 0.1 | 0.4 ± 0.1 | 2.4 ± 0.3 | 4.3 ± 0.5 | 5.7 ± 0.3 | 50.7 ± 3.2 | 77.0 ± 4.0 |
| June | Intact | 10% Sucrose | 14.9 ± 0.8 | 0.2 ± 0.0 | 0.7 ± 0.2 | 2.5 ± 0.2 | 3.8 ± 0.2 | 5.5 ± 0.2 | 55.2 ± 6.6 | 82.9 ± 7.6 |
| June | 3/4 Defoliated | No injection | 12.6 ± 0.6 | 0.3 ± 0.0 | 0.4 ± 0.0 | 1.3 ± 0.2 | 2.8 ± 0.2 | 5.3 ± 0.2 | 33.6 ± 2.6 | 56.2 ± 3.4 |
| June | 3/4 Defoliated | 10% Sucrose | 15.6 ± 0.6 | 1.8 ± 0.4 | 6.2 ± 1.1 | 1.4 ± 0.2 | 2.7 ± 0.3 | 5.0 ± 0.2 | 36.1 ± 2.9 | 68.8 ± 2.9 |